IL
NUOVO CIMENTO
ORGANO DELLA SOCIETÀ ITALIANA DI FISICA
SOTTO GLI AUSPICI DEL CONSIGLIO NAZIONALE DELLE RICERCHE

VOL. XI, N. 2 *Serie decima* 16 Gennaio 1959

Gamma Radiation from ^{63}Zn.

R. W. HAYWARD, E. FARRELLY-PESSOA, D. D. HOPPES
National Bureau of Standards - Washington D.C.

R. VAN LIESHOUT (*)
Nuclear Data Group, National Research Council - Washington D.C.

(ricevuto il 20 Settembre 1958)

Summary. — In the decay of 38 min ^{63}Zn γ-rays are emitted with the following energies: 0.67, 0.96, 1.44, (2.0?), 2.35, 2.55 and 2.75 MeV. There is no 0.29 MeV transition. The 0.67 and 0.96 MeV γ-rays are only strongly coincident with the annihilation radiation, not with each other. The results of the measurement are collected in Table I.

1. – Introduction.

The decay of ^{63}Zn takes place mainly to the ground state of ^{63}Cu, but weak positon and electron capture transitions to levels at 0.97, 1.90 and 2.6 MeV have also been reported ([1,2]). Scattering of protons or neutrons and Coulomb

(*) On leave of absence from the Institute for Nuclear Physics Research, Amsterdam.

([1]) K. WAY, R. W. KING, C. L. MCGINNIS and R. VAN LIESHOUT: *Nucl. Level Schemes*, U.S. Atomic Energy Commission TID-5300 (Washington, 1955).

([2]) O. HUBER, H. MEDICUS, P. PREISWERK and R. STEFFEN: *Helv. Phys. Acta*, **20**, 495 (1947).

excitation experiments with α-particles have revealed the existence of an additional low-lying level at 0.67 MeV, while levels at 1.33, 1.41 and 1.55 MeV are found from inelastic scattering of protons. Other levels at higher excitation energies may also exist [1].

It was thought worth-while to study the γ spectrum of ^{63}Zn by scintillation techniques in order to determine whether a 0.67 MeV transition occurs and to look for the possible existence of additional γ-rays.

2. – Production; experimental procedure.

The ^{63}Zn acitvity was produced by irradiation of pure zinc with the bremsstrahlung spectrum produced by the National Bureau of Standards betatron ($E_{max} = 40$ MeV). In this way very strong sources could be obtained; they also contained 9.4 hour ^{62}Zn, but this does not disturb the γ-ray measurements. No chemical separations were performed.

In most measurements a 3 in. $\times$ 3 in. NaI(Tl) well-type crystal was used, with the source either inside or outside the crystal. The summing technique was applied to identify strong coincident peaks. Some of these were further studied with a conventional fast-slow coincidence set-up, using two 2 in. $\times$ 2 in. NaI(Tl) crystals. The spectra were displayed on a 10 channel analyzer.

3. – Results.

The γ-spectrum shows strong peaks at 0.67 and 0.96 MeV, a weaker one at 1.44 MeV, and peaks at 2.35, 2.55 and 2.75 MeV. There is a doubtful one at 2.0 MeV, while no peak could be found with certainty at 1.9 MeV. There is definitely no strong transition of 0.29 MeV, which might correspond to the stop-over transition between the two lowest excited states of ^{63}Cu. The usual precautions were taken in these measurements to avoid summing peaks.

When the summing technique was applied, the relative intensity of the peak at 1.4 MeV increased strongly, while a bump at 1.2 MeV also showed up. There were also definite peaks at 1.74 and 2.05 MeV. Since all these summing peaks can arise from summing of the annihilation radiation with the two strong γ-rays, coincidences were performed selecting the annihilation radiation and the 0.67 and 0.96 MeV peaks successively. The results are given in Table I.

TABLE I.

^{63}Zn produced by $^{(64)}$Zn(γ, n)		
Energy (MeV)	Rel. int.	
0.67 ± 0.02	st	
0.96 ± 0.03	st	no 0.29 γ, no 1.89 γ
1.44 ± 0.03	m	($\gamma^{\pm}$) (0.67, 0.96 γ)
2.0?	v.w.	no (0.67 γ) (0.96 γ)
2.35 ± 0.05	w	no (0.67 γ) ($1.6 \leqslant E_{\gamma} \leqslant 2.1$)
2.55 ± 0.05	w	no (0.96 γ) (≈ 1.7 γ)
2.75 ± 0.07	w	

4. – Discussion.

From the above measurements it follows that the level at 0.67 MeV in ^{63}Cu is fed directly by positons. There is no γ transition of appreciable intensity going to this level. Neither is there a strong population of the 0.96 level by γ transitions. The γ-ray of 1.44 MeV probably comes from the level of the same energy, but the two levels at 1.33 and 1.55 MeV do not seem to yield such strong ground state transitions. The γ-rays with energies above 2 MeV almost certainly are ground state transitions; in particular the level at 2.6 MeV does not show an appreciable branching to the two lowest excited states. There is no γ-ray with an energy and relative intensity comparable to the reported 1.89 MeV transition ([2]).

* * *

The work reported above was performed during December 1955. One of the authors (R.v.L.) would like to express his sincere thanks for the hospitality at the National Bureau of Standards.

RIASSUNTO

Nel decadimento del ^{63}Zn (38 min) sono emesse radiazioni γ con le seguenti energie: 0.67, 0.96, 1.44, (2.0?), 2.35, 2.55 e 2.75 MeV. Non si è trovata la transizione di 0.29 MeV. Le radiazioni γ di 0.67 e 0.96 MeV sono per la maggior parte in coincidenza con la radiazione di annichilazione e non tra di loro. I risultati sono riassunti nella Tabella I.

IL NUOVO CIMENTO Vol. XI, N. 2 16 Gennaio 1959

The Gamma Ray Spectrum of ^{63}Zn.

R. A. Ricci (*), R. K. Girgis (+) and R. van Lieshout

Instituut voor kernphysisch Onderzoek - Amsterdam

(ricevuto il 20 Settembre 1958)

Summary. — The γ ray spectrum from the decay of ^{63}Zn was measured with scintillation techniques and a complete quantitative analysis was performed. The γ rays found are reported with their relative intensities in Table I and compared with the levels found in ^{63}Cu by the recent inelastic proton scattering experiment reported by Mazari, Buechner and de Figueiredo. The main features of the proposed partial decay scheme of ^{63}Zn are discussed.

1. – Introduction.

A preceding paper (1) summarizes the experimental situation with respect to the decay of ^{63}Zn which seems to show strong population of the ^{63}Cu ground state by positon emission and much weaker population of many excited states by positon and electron capture transitions. The de-excitation of the ^{63}Cu levels seems to take place by ground state γ transitions, mainly by the 0.67, 0.96, 1.44, 2.35 and 2.75 MeV γ-rays. Some of these γ-rays check well with the levels in ^{63}Cu already known at the time the above experiment was performed. Recent work of Mazari *et al.* (2) has established that the excited states in ^{63}Cu, as found from inelastic proton scattering experiments, are very numerous

(*) On leave of absence from the Politecnico di Torino.

(+) On leave of absence from the University of Cairo, Giza.

(1) R. W. Hayward, E. Farrelly-Pessoa, D. D. Hoppes and R. van Lieshout: *Nuovo Cimento*, **11**, 153 (1959).

(2) M. Mazari, W. W. Buechner and R. P. de Figueiredo: *Phys. Rev.*, **108**, 373 (1957).

and the existence of many more γ transitions from the decay of ^{63}Zn can be expected.

Therefore a quantitative analysis of the ^{63}Zn γ spectrum was performed.

2. – Production and measurements.

The sources were prepared by Cu(d, 2n) reactions, bombarding Cu targets with low energy deuterons (14 MeV; this in order to avoid production of ^{62}Zn) from the synchrocyclotron of the Institute; the bombardment lasted for a few minutes in order to reduce the amount of ^{65}Zn produced. (Some ^{65}Zn was always present, its contribution was subtracted.) The chemical procedure consisted of extraction with chloroform of zinc di-β-naphtylthiocarbazone compound ([3]).

The γ spectrum was measured with NaI(Tl) scintillation crystals (2.5 cm $\times$ 2.5 cm) and displayed on the 100 channel RIDL analyzer. The measurements were performed with various sources at different distances from the detector in order to be able to distinguish summing peaks, if present.

3. – Experimental results.

The γ spectra obtained in three different energy regions are shown in Figs. 1, 2, 3; the various γ-rays found in our analysis are indicated. The γ spectrum was analyzed by comparing it with standard peaks and in constructing the unknown peaks by extrapolation and in-

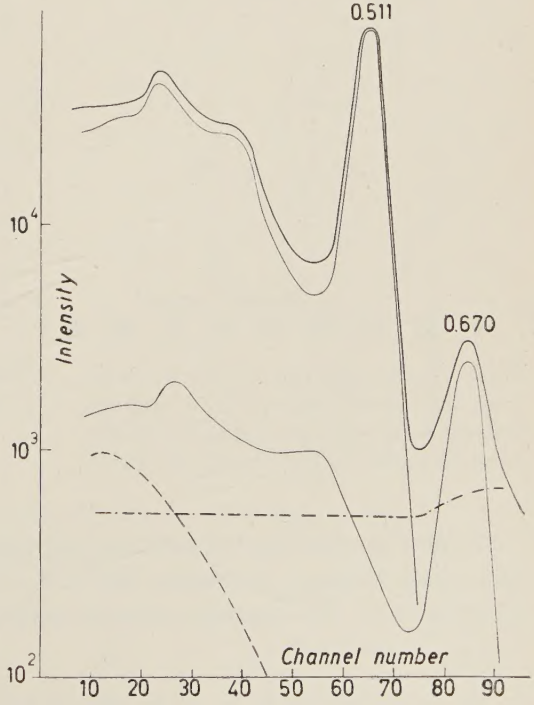

Fig. 1. – γ-ray spectrum of ^{63}Zn in the low energy region. The full line represents the total spectrum, the dot-dashed line the contribution of γ-rays with higher energy, the dashed line the background plus bremsstrahlung contribution. The two analyzed peaks are shown.

([3]) L. Lindner and G. A. Brinkman: *Physica*, **21**, 747 (1955).

terpolation from the standard ones. Compton distributions and pair peak contributions are taken into account [4] (see also [5]).

When weak γ-rays are accompanied by strong positon emission, it is necessary to correct the total γ spectrum for the continuous pulse distribution due to bremsstrahlung radiations and, in particular, to the annihilation of the positons in flight. This correction has been made in the case of ^{63}Zn and the method used in estimating the continuous contribution is reported in more detail in the Appendix.

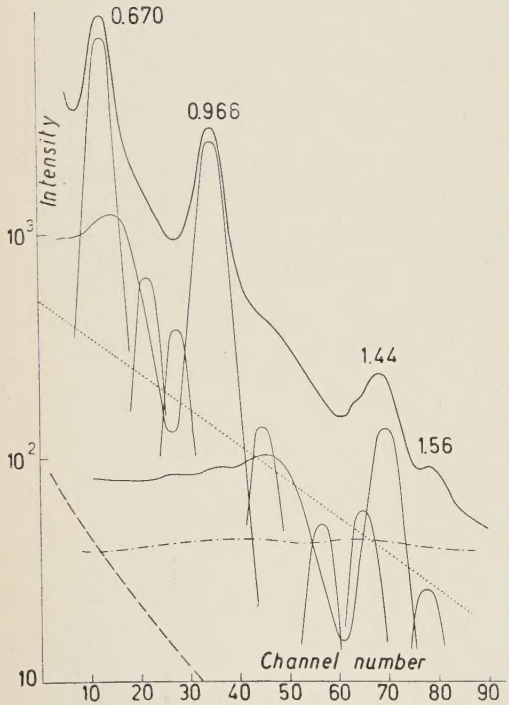

Fig. 2. – γ-ray spectrum of ^{63}Zn in the intermediate energy region. The dotted line represents the contribution due to annihilation in flight; for the others, see Fig. 1.

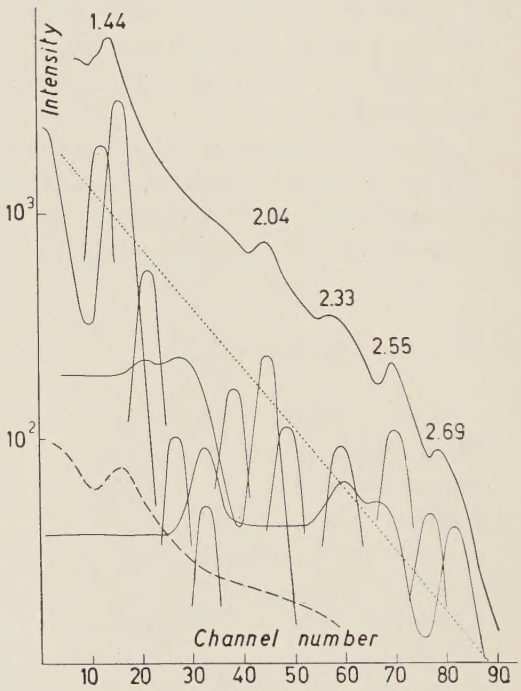

Fig. 3. – γ-ray spectrum of ^{63}Zn in the high energy region. For explanation, see Fig. 1 and 2.

Table I summarizes the results of our analysis; the γ-rays found are reported with their relative intensities and are compared with the actually known levels in ^{63}Cu. The intensity of some peaks was enhanced by summing effects;

---

(4) R. K. GIRGIS, R. A. RICCI and R. VAN LIESHOUT: to be published.

(5) D. MAEDER, A. H. WAPSTRA, G. J. NIJGH and L. TH. M. ORNSTEIN: *Physica*, **20**, 521 (1954).

TABLE I. – ^{63}Zn *produced by* Cu (14 MeV, d, 2n) *chem. Half life*: (38.1 ± 0.3) min.

^{63}Zn γ-rays from scint.				^{63}Cu levels (MAZARI *et al.*)	
Energy (MeV)		Intensity ($\gamma/100\beta^+$)			
0.511	—	200	—	—	—
0.670	*5*	14.0	*8*	0.668	*5*
0.810	*10*	1.8	*1*	—	—
0.875	*10*	1.2	*1*	—	—
0.966	*6*	10.0	*9*	0.961	*5*
1.10	*2*	0.70	*10*	—	—
1.27	*2*	0.30	*5*	—	—
1.35	*2*	0.41	*5*	1.327	*5*
1.44	*3*	0.80	*7*	1.412	*5*
1.56	*3*	0.20	*5*	1.547	*5*
1.67	*3*	0.60	*3*	—	—
1.80	*3*	0.02	*1*	—	—
1.90	*4*	0.08	*1*	1.862	*5*
2.04	*4*	0.12	*1*	2.012 2.063 2.082	*5* *5* *5*
2.14	*4*	0.06	*1*	2.093	*6*
—	—	—	—	2.210	*6*
2.33	*4*	0.05	*1*	2.337	*6*
—	—	—	—	2.405	*6*
2.55	*5*	0.08	*1*	2.497 2.504 2.510 2.535 2.543	*6* *6* *6* *6* *10*
2.69	*5*	0.04	*1*	2.673 2.694 2.716	*8* *8* *8*
2.78	*6*	0.03	*1*	2.761 2.788 2.805 2.831	*8* *8* *8* *8*
—	—	—		2.856	*8*
—	—	—	—	2.869	*8*
—	—	—	—	2.888	*8*
~ 2.9	—	⩽ 0.02	—	2.958	*8*
—	—	—	—	2.974	*8*
—	—	—	—	3.032	*8*
—	—	—	—	etc.	

No $0.29\gamma_{21}$ (< 0.5); no $0.37\gamma_{32}$ (< 0.5); no $0.74\gamma_{41}$ (< 0.6).

Summing peaks

Energy (MeV)		Origin (*)
1.18	*1*	0.570 + 0.511
1.44	*3*	0.966 + 0.511 0.810 + 0.670
1.56	*3*	0.875 + 0.670
1.67	*3*	0.875 + 0.810

(*) Other possibilities have been considered and were found to be incompatible with the experimental results.

this was checked in the usual way and the occurrence of a summing peak is also mentioned in Table I.

The average value of the half life found from all runs is (38.1 ± 0.3) min; all γ-rays mentioned in Table I show the same half life.

4. – Discussion.

The results summarized in Table I confirm that the two γ-rays of 0.670 and 0.966 MeV correspond very well with the two lower levels in ^{63}Cu and are not in cascade with each other. In fact the 1.67 MeV peak cannot be due to the (0.670+0.966) MeV coincidence because in that case its intensity should be much higher, as can be judged from the intensity of the 1.18 MeV summing peak (0.511+0.670). For this reason we have assumed that the part of the 1.67 MeV peak, which is due to summing, arises from the coincidence between the 0.810 and 0.875 MeV γ-rays. From the fact that the 0.670 and 0.966 MeV γ-rays are the most intense ones, it can be inferred that the corresponding levels are strongly populated ([1]). Since the total intensity of all the other γ-rays found is less than 7% and since many of these γ-rays probably represent ground state transitions, we can conclude that the population of these two lower levels is essentially due to positons. Their spins and parities are thereby restricted to $\frac{1}{2}^-$, $\frac{3}{2}^-$ or $\frac{5}{2}^-$.

Recently LAWSON and URETSKY ([6]) have applied the center of gravity theorem to the levels in ^{63}Cu. For the quartet produced by addition of the 29th proton in a $p_{\frac{3}{2}}$ state to the first 2^+ excited state of ^{62}Ni, they find the following level order: 0.668 ($\frac{1}{2}^-$), 0.961 ($\frac{5}{2}^-$), 1.327 ($\frac{7}{2}^-$) and 1.412 ($\frac{3}{2}^-$). From this one might deduce that these levels de-excite mainly by fast $E2$ transitions to the ground state, due to the re-arrangement of the ^{62}Ni core, whereas transitions between members of the quartet would have single particle transition probabilities. This interpretation can be checked in the case of the two lower levels for which the transition probabilities $\varepsilon B(E2)$ for Coulomb excitation have been measured ([7]). By definition $\varepsilon \leqslant 1$ and since internal conversion can be neglected in our case, ε just represents the $E2$-fraction of the transition probability. From the $\varepsilon B(E2)$ one can calculate the reduced $E2$ life time ([8]) according to: $L(E2) = \tau_\gamma(E2) A^{\frac{4}{3}} E^5$, where the partial life time for $E2$ γ emission $\tau_\gamma(E2) = 8.14 E^{-5}(\varepsilon/B)(2J_f+1/2J_i+1)\cdot 10^{-14}$ s. Thus, for the 0.67 and 0.96 MeV transitions: $L(E2) = \varepsilon(9.5 \pm 1.9)\cdot 10^{-10}$ and $\varepsilon(9.8 \pm 1.4)\cdot 10^{-10}$ respectively. Both

([6]) R. D. LAWSON and J. L. URETSKY: *Phys. Rev.*, **108**, 1300 (1957).

([7]) G. M. TEMMER and N. P. HEYDENBURG: *Phys. Rev.*, **104**, 967 (1956).

([8]) M. GOLDHABER and A. W. SUNYAR, in K. SIEGBAHN: *Beta and gamma ray spectroscopy* (Amsterdam, 1955), p. 453.

these values are too small to represent single particle $E2$ transitions, for which the $L(E2)$ value ([8,9]) should be 10^{-8}. Assuming therefore a mixture of collective $E2$ and single particle $M1$ transitions and the theoretical reduced life times given in Table II, we calculate values for both ε and $L(E2)$ for the two transitions. For the 0.67 MeV transition we find: $\varepsilon = 0.4$ and $L(E2) = (4 \pm 1) \cdot 10^{-10}$; for the 0.96 MeV transition: $\varepsilon = 0.6$ and $L(E2) = (6 \pm 1) \cdot 10^{-10}$. The above suppositions therefore seem to represent an internally consistent picture.

TABLE II. – *Transition probabilities and experimental branching ratios.*

^{63}Cu levels ([a]) (MeV)	γ transitions ([b])		Transition probability ([c])			Experimental
			$M1$	$E2_{sp}$	$E2_{coll}$	
0.668	0.670	γ_1	$1.5 \cdot 10^{11}$	$3.3 \cdot 10^{9}$	$1.0 \cdot 10^{11}$	$P = \varepsilon^{-1}(3 \pm 1) \cdot 10^{10}$; $\varepsilon < 1$ ([d])
0.961	0.966	γ_2	$4.4 \cdot 10^{11}$	$2.0 \cdot 10^{10}$	$6.0 \cdot 10^{11}$	$P = \varepsilon^{-1}(2 \pm 1) \cdot 10^{10}$; $\varepsilon < 1$ ([d])
	0.290	γ_{21}	$1.2 \cdot 10^{10}$	$5.3 \cdot 10^{7}$	$1.6 \cdot 10^{9}$	$\gamma_{21}/\gamma_2 < 0.05$
1.327	1.35	γ_3	$1.2 \cdot 10^{12}$	$1.0 \cdot 10^{11}$	$3.0 \cdot 10^{12}$	
	0.37	γ_{32}	$2.5 \cdot 10^{10}$	$1.7 \cdot 10^{8}$	$5.1 \cdot 10^{9}$	$\gamma_{32}/\gamma_3 < 1.2$
1.412	1.44	γ_4	$1.4 \cdot 10^{12}$	$1.4 \cdot 10^{11}$	$4.2 \cdot 10^{12}$	
	0.74	γ_{41}	$2.0 \cdot 10^{11}$	$5.5 \cdot 10^{9}$	$1.7 \cdot 10^{11}$	$\gamma_{41}/\gamma_4 < 0.8$
1.547	1.56	γ_5	$3.7 \cdot 10^{12}$	$2.2 \cdot 10^{11}$	$6.6 \cdot 10^{12}$	
	0.875	γ_{51}	$6.6 \cdot 10^{11}$	$1.2 \cdot 10^{10}$	$3.6 \cdot 10^{11}$	$\gamma_{51}/\gamma_5 = 6 \pm 2$

([a]) Cfr. ref. ([8]).

([b]) Of the possible transitions from a given level only those are reported, which have been found experimentally or for which an upper limit on the intensity could be determined.

([c]) The transition probabilities P have been calculated from average values of reduced life times as given by GOLDHABER and SUNYAR ([8]):

$$L(M1) = 2 \cdot 10^{-12}; \qquad L(E2_{sp}) = 10^{-8}; \qquad L(E2_{coll}) = 3 \cdot 10^{-10}.$$

([d]) Cfr. ref. ([7]).

We have summarized in Table II the transition probabilities for some of the γ transitions from the first five excited states in ^{63}Cu. These probabilities have been calculated from the reduced life times as given by GOLDHABER and SUNYAR ([8]) for $M1$, $E2$ single particle and collective transitions. The experimental branching ratios are reported for comparison. It can be seen

([9]) K. WAY, D. N. KUNDU, C. L. MCGINNIS and R. VAN LIESHOUT: *Ann. Rev. Nucl. Sci.*, **6**, 129 (1956).

that for the 0.961 MeV level the stop over to cross over ratio is compatible with the assumption that the cross over transition is of the collective type.

Of the three levels at 1.327, 1.412 and 1.547 MeV only the lower two give strong ground state transitions, whereas the 1.547 MeV level decays mainly by the 0.875 MeV stop-over transitions. (The placing of the 0.875 MeV γ-ray is based on the presence of the (0.670+0.875) MeV summing peak and on the absence of other summing peaks explainable as due to the 0.875 γ-ray and in agreement with the level order). The possibility that the 1.55 MeV ground state transition is of the collective type is excluded by the experimental stop over to cross over ratio; it follows that this level does not belong to the first quartet.

The branching ratio from the 1.327 MeV level is compatible as well with single particle as with collective character, whereas the 1.412 MeV level seems to be better explained as a collective level. Their assignment to the quartet is then quite acceptable, in agreement with the prediction of Lawson and Uretsky.

The 1.547 MeV level could be interpreted as the $p_{\frac{1}{2}}$ or $f_{\frac{5}{2}}$ single particle level. In this case the relative intensity of the 0.875 MeV stop over to the cross over transition is incompatible with the spin assignment. The branching ratio from the 1.547 MeV level is better explained by postulating that this level belongs to a second quartet formed, for instance, by coupling a $p_{\frac{3}{2}}$ proton to the second excited 2^+ or 4^+ state of the ^{62}Ni core. From this follows that the first single particle level in ^{63}Cu should lie at least at 1.86 MeV ([10]).

A partial decay scheme for ^{63}Zn is reported in Fig. 4, where the other

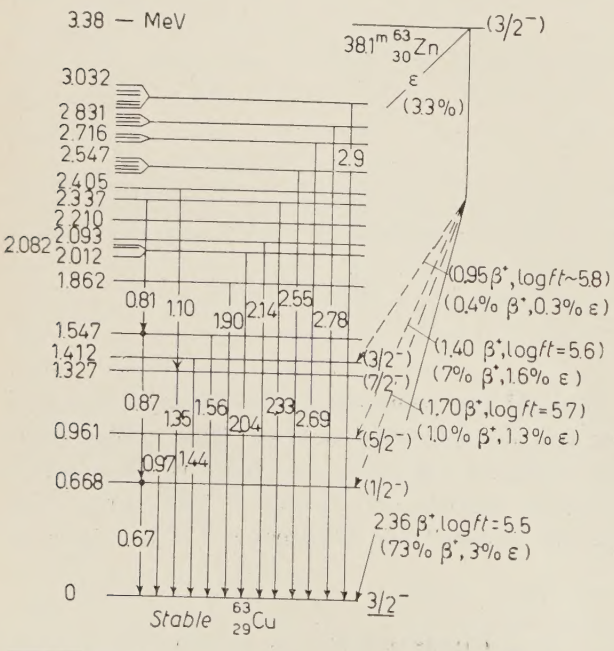

Fig. 4. – Partial decay scheme of ^{63}Zn; the level energies are taken from ref. ([2]), the γ-ray energies are from our work. For a discussion of the calculated intensities of the β branches, see text.

([10]) R. H. NUSSBAUM: *Rev. Mod. Phys.*, **28**, 423 (1956).

γ-rays experimentally found have been placed according to their relative intensities and the level population. The placing of the 1.10 MeV γ-ray is based on the fact that it seems to be the only means of excitation of the 1.327 MeV level, which cannot be populated by positons or electron capture because of its spin ($\frac{7}{2}$). The 1.27, 1.67 and 1.80 MeV γ-rays can be placed at various positions; therefore they have not been shown. Finally it seems reasonable to assume that the higher energy γ-rays are mainly ground state transitions.

Most of our results are in agreement with earlier work ([1,11]), the only important discrepancy being the intensity of the 1.90 MeV γ-ray. HUBER *et al.* ([11]) report an intensity of about 4%, whereas in our case the total intensity of the γ-rays between 1.80 and 2.04 MeV is only 0.22%.

From the proposed decay scheme one can calculate the β branching ratios to the various levels according to the intensity balance. These branching ratios can be expressed in terms of disintegration rates by assuming that the ground state positon group consists of 87% of all positons ([11]). Taking theoretical ε/β^+ ratios the log *ft* values have also been calculated and are reported in Fig. 4.

* * *

Thanks are due to Miss J. C. KAPTEIJN for performing the chemical separations and to the personnel of the cyclotron for the irradiations. The kind interest of Prof. Dr. P. C. GUGELOT, Prof. Dr. A. H. WAPSTRA and of Prof. Dr. A. H. W. ATEN Jr. is gratefully appreciated.

One of the authors (R.K.G.) is indebted to the Egyptian Atomic Energy Commission for a grant.

This work was performed as part of the research program of the « Stichting voor Fundamenteel Onderzoek der Materie » (F.O.M.), which is financially supported by the « Nederlandse Organisatie voor Zuiver Wetenschappelijk Onderzoek » (Z.W.O.).

APPENDIX

Experimental determination of the continuous pulse distribution (bremsstrahlung, annihilation in flight of positons) in a γ scintillation spectrum.

The analysis of a γ scintillation spectrum requires a good knowledge of the effects which may distort the true spectrum, in order to determine with

([11]) O. HUBER, H. MEDICUS, P. PREISWERK and R. STEFFEN: *Helv. Phys. Acta*, **20**, 495 (1947).

sufficient accuracy the energies and the relative intensities of the various γ-rays. This can be an important question in the case of complex γ-spectra especially in the high energy region of the spectrum if weak γ-rays are present.

Various effects will play a role: background pulses, internal and external bremsstrahlung and annihilation of positons in flight. The first contribution can be easily accounted for. Theoretical computation of the other effects is very difficult, due to the many different parameters which must be known ([12]). They can best be studied empirically if care is taken to reproduce the same experimental conditions used for the particular sources under study.

The following experiments have been performed:

a) *Bremsstrahlung.* This is the only continuous contribution in the case of negaton decay. A pure β emitter, *e.g.* ^{90}Sr of ^{32}P, has been used under the standard conditions of geometry and backing, in order to detect a pure bremsstrahlung spectrum. The spectrum was normalized by comparing the intensity of the pure β source and of the source under study with a Geiger-Müller β counter. In general it was found that for all the cases we studied the bremsstrahlung contribution does not distort any γ-ray with a relative intensity higher than 0.01 % of the β disintegration. In the case of ^{63}Zn this was done by means of a ^{90}Sr source ($E_0 = 2.25$ MeV) and the bremsstrahlung spectrum which is shown in Fig. 5, in comparison with the spectrum of annihilation of positons in flight, was found to be neglible except in the low energy region (see Fig. 1).

b) *Annihilation of positons in flight.* For positon decay this is the more important effect. Fig. 5 shows the experimental continuous spectra, obtained under the standard conditions of measurements, for the positon sources ^{62}Cu ($E_0 = 2.92$ MeV), ^{47}V ($E_0 = 1.89$ MeV) and ^{15}O ($E_0 = 1.73$ MeV). In the first case we used ^{62}Cu in equilibrium with ^{62}Zn (^{62}Zn+^{62}Cu); a correction for the contribution of ^{65}Zn (1.112 MeV γ-ray) was applied but no correction was made for possible weak γ-rays due to the decay of ^{62}Cu itself, about which controversy still exists ([13]); they obviously do not seem to distort the spectral shape. In Fig. 5 the (^{62}Zn+^{62}Cu) spectrum is reported with the annihlation peak for normalization. A 0.60 MeV peak is also clearly present and it is due to the ^{62}Zn decay as recently established by BRUN *et al.* ([13]); its relative intensity to the ^{62}Cu positons was estimated about 30 %, which is in agreement with their results.

The ^{47}V source was obtained by Sc(α, 2n) reaction with high enough energy ($\sim$ 30 MeV) to avoid excessive production of ^{48}V ($T_{\frac{1}{2}} = 16.2^{d}$) which is known to have γ-rays of 0.99, 1.33 and 2.22 MeV. Anyway the small ^{48}V contribution was determined after decay of ^{47}V($T_{\frac{1}{2}} = 31^{min}$) and subtracted. ^{47}V itself decays

([12]) H. W. KENDALL and M. DEUTSCH: *Phys. Rev.*, **93**, 932 (1954); R. SHERR and J. B. GERHART: *Phys. Rev.*, **91**, 909 (1953); J. B. GERHART, B. C. CARLSON and R. SHERR: *Phys. Rev.*, **94**, 917 (1954).

([13]) E. BRUN, W. E. MEYERHOF, J. J. KRAUSHAAR and D. HOREN: *Phys. Rev.*, **107**, 1324 (1957); J. W. BUTLER and C. R. GOSSETT: *Bull. Am. Phys. Soc.*, **3**, no. 1, 62 (1958).

by positon emission and no γ rays follow this decay ([14]). The obtained spectrum is also shown in Fig. 5 after normalization to the annihilation peak of ^{62}Cu.

As third calibration source we used ^{15}O from O(n, 2n) reaction. This isotope also decays by pure positon emission ([15]).

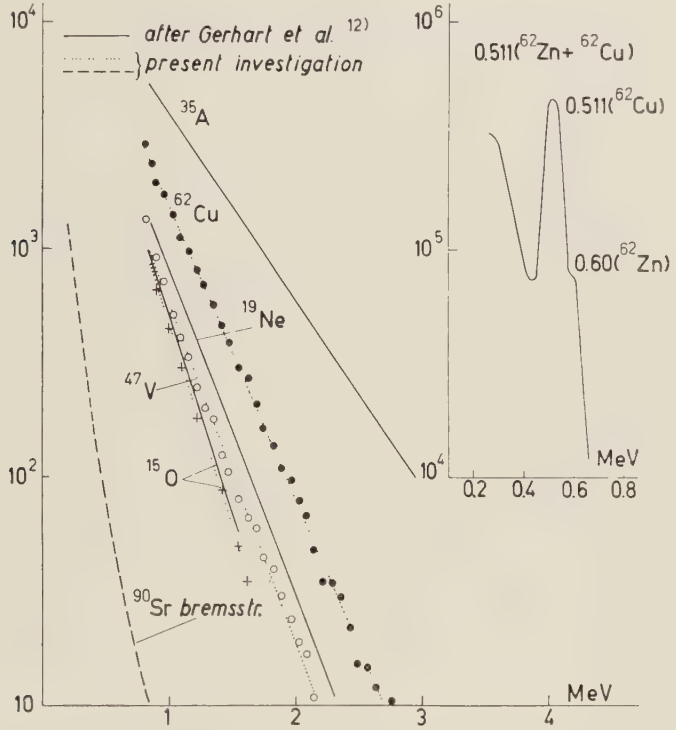

Fig. 5. – The spectral distribution due to annihilation in flight and bremsstrahlung of various positon emitters. All the spectra have been normalized at the annihilation peak of ^{62}Cu (insert). Complete annihilation was ensured with Al absorbers. The pure bremsstrahlung spectrum of ^{90}Sr has been normalized by comparison of the total β disintegrations.

For comparison the spectra obtained by GERHART, CARLSON and SHERR ([12]) for ^{19}Ne ($E_0 = 2.2$ MeV), ^{35}A ($E_0 = 4.4$ MeV) and ^{15}O are reported in Fig. 5 after correction for the difference in crystal efficiencies. The good agreement indicates that the different geometries cause no appreciable distortion.

For ^{63}Zn the continuous spectrum as shown in Fig. 2 and 3 has been obtained by interpolation between the ^{47}V and ^{62}Cu continuous spectra. It should be pointed out that the contribution due to this continuous spectrum is important only in the case of γ-rays with a relative intensity of about 0.1 %. For instance,

([14]) L. J. LIDOFSKY and V. K. FISHER: *Phys. Rev.*, **104**, 759 (1956).
([15]) F. AJZENBERG and T. LAURITSEN: *Rev. Mod. Phys.*, **27**, 77 (1955).

if this contribution is neglected we have found that the increase in the relative intensity of the higher energy γ-rays of ^{63}Zn amounts almost to about 50% when the correct relative intensity is less than 0.05%.

RIASSUNTO

Uno studio completo dello spettro γ associato al decadimento del ^{63}Zn è stato compiuto per mezzo della tecnica a scintillazione. Una dettagliata analisi dello spettro ha permesso di trovare numerosi raggi γ, che sono riportati con le loro intensità relative nella Tabella I. Essi sono in buon accordo con i livelli del ^{63}Cu recentemente trovati per scattering inelastico di protoni da Mazari, Buechner e de Figueiredo. Si discutono le caratteristiche essenziali dello schema di decadimento proposto.

The Internal Conversion Spectra from the Decay of $^{197}Hg^{m}$.

I. J. van Heerden, D. Reitmann and H. Schneider

Nuclear Physics Division of the National Physical Research Laboratory, C.S.I.R. - Pretoria

(ricevuto il 22 Settembre 1958)

Summary. — The relative intensities of a number of internal conversion lines in the decay of ^{197}Hg were determined rather accurately and compared with theoretical values. In general the agreement with static finite size corrected values is very good. It is found, however, that the theoretical M-shell coefficients are too large by about 40% in the cases studied. This is attributed to the neglect of the screening effect in the calculations. For the well-known 77.5 keV ($M1+E2$) transition in ^{197}Au the mixing ratio was found to be $(9.4\pm0.9)\%$ $E2$, and the corrections which have to be applied to the point-nucleus coefficients for $M1$ conversion in the L_{I} and L_{II} shells are 0.75 ± 0.11 and $0.80^{+0.29}_{-0.24}$ respectively. These corrections are exactly those found if the « static » finite nuclear size effect is taken into account, and therefore indicate the absence of any structure dependent (« dynamic ») effect in this case.

1. – Introduction.

The study of relative internal conversion coefficients is a powerful tool in the determination of the multipolarity of a particular transition. In the past it was believed that these coefficients are entirely independent of nuclear size or structure, and the theoretical coefficients were calculated for a point-nucleus. It has now, however, become evident that these coefficients can be influenced by both « static » and « dynamic » finite nuclear size effects. The « static » correction is essentially a correction to the electron wave functions due to the smeared-out nuclear charge distribution [1], whilst the « dynamic » effect is

[1] L. A. Sliv: *Žu. Éksper. Teor. Fiz.*, **21**, 770 (1951); L. A. Sliv and M. Listengarten: *Žu. Éksper. Teor. Fiz.*, **22**, 29 (1952).

related to additional nuclear matrix elements governing γ-emission ([2]). Large dynamic effects are expected to show up only in transitions highly retarded compared with the lifetimes predicted by the single particle model. The static correction to the point-nucleus values is usually small, and is expected to be most important in magnetic dipole transitions for high Z.

The limited amount of reliable experimental data does not yet allow general conclusions to be drawn about the actual presence and size of the above effects. The present paper deals with the internal conversion in the decay

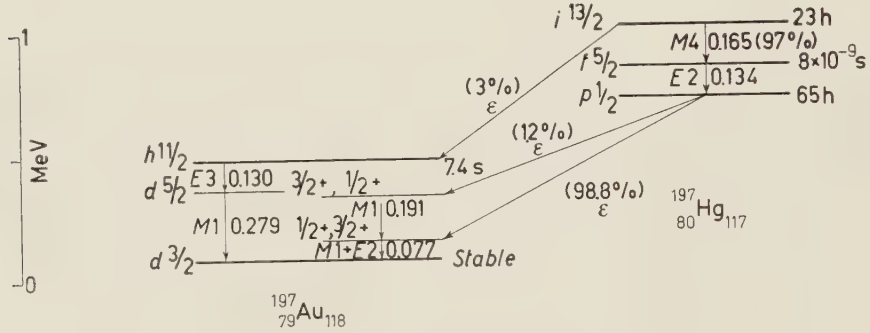

Fig. 1. – Decay scheme of $^{197}Hg^{m}$-$^{197}Au^{m}$.

of $^{197}Hg^{m}$, which offers the possibility of studying a number of transitions of different multipolarity in a region where finite size effects should be measurable. The decay scheme shown in Fig. 1 was suggested by MIHELICH and DE SHALIT ([3]), and is generally accepted as correct.

2. – Experimental procedure.

$^{197}Hg^{m}$ was produced by the $^{197}Au(d, 2n)^{197}Hg$ reaction by bombarding a target of 99.6% pure gold with 15 MeV deuterons in the C.S.I.R. cyclotron. The radioactive mercury was distilled in vacuum on to a 25 μm thick tungsten wire, the front side of which was covered by a thin layer of gold. A thin, almost weightless source of $^{197}Hg^{m}$ was obtained, and was confined to the front side of the wire by a layer of SiO which had been evaporated on to the other side.

The internal conversion spectrum was recorded in a conventional 180° permanent-magnet β spectrograph, using freshly poured Ilford G-5 emulsions,

([2]) E. L. CHURCH and J. WENESER: *Phys. Rev.*, **104**, 1382 (1956).
([3]) J. W. MIHELICH and A. DE SHALIT: *Phys. Rev.*, **91**, 78 (1953).

100 μm thick, as detector. The conversion lines observed are listed in Table I. The resolving power obtained was of the order of 0.05%.

TABLE I.

Transition energy in keV	Conversion lines observed
77.5 (4)	L_{I}, L_{II}, L_{III}, M_{I}, M_{II}, M_{III}, N, O
130.2	L_{II}, L_{III}
134.0	K, L_{I}, L_{II}, L_{III}, M_{I}, M_{II}, M_{III}, N
165.3	K, L_{I}, L_{II}, L_{III}, M_{I}, M_{III}, N
191.6	K

For the determination of the relative intensities of these lines individual electron tracks were counted following a method previously described (5). In all the experimental results given, each point represents the total number of tracks in fifteen adjacent fields of view, each 50 μm × 50 μm. The errors quoted are of a statistical nature only. All the theoretical values given were obtained by interpolation from the tables of ROSE (6).

3. – Results and discussion.

3·1. *The* 165.3 keV *transition.* – The multipolarity of this transition is known to be $M4$ (7). This assignment was made on the basis of lifetime and K/L considerations and agrees well with the shell model. Fig. 2 shows the internal conversion line spectrum of this transition. All values are corrected for transmission relative to the L_{III} line. The results obtained together with the theoretical ratios are given in Table II.

The general agreement with theory is very good. The theoretical K and L values include the correction for the static finite size effect, although it is extremely small in this case (less than 2%). The slight deviation in the K/L

(4) The energy of this transition was determined to be (77.51 ± 0.03) keV, by using values of 134.0 and 165.3 keV for the transitions in ^{197}Hg to calibrate the magnetic field of the spectrograph.

(5) D. REITMANN, H. SCHNEIDER and I. J. VAN HEERDEN: *Phys. Rev.*, **110**, 1093 (1958).

(6) M. E. ROSE: privately distributed tables.

(7) O. HUBER, F. HUMBEL, H. SCHNEIDER, A. DE SHALIT and W. ZÜNTI: *Helv. Phys. Acta*, **24**, 127 (1951).

TABLE II.

Ratios	Experimental results	Theoretical $M4$ values
K/L	0.28 ± 0.01	about 0.33
$L_{\mathrm{I}}/L_{\mathrm{II}}/L_{\mathrm{III}}$	$(0.54 \pm 0.03)/(0.13 \pm 0.01)/(1.00 \pm 0.03)$	0.57/0.13/1.00
$M_{\mathrm{I}}/M_{\mathrm{III}}$	0.40 ± 0.03	0.41
$K/M_{\mathrm{I}}+M_{\mathrm{III}}$	0.79 ± 0.04	0.58
$L/M_{\mathrm{I}}+M_{\mathrm{III}}$	2.81 ± 0.12	1.77
M/N	3.88 ± 0.32	—

value may be attributed to the uncertainty in the determination of the theoretical K coefficient. This transition happens to fall in a region where the K-conversion coefficients follow a strongly non-linear course when plotted against energy on a log-log diagram, and the values given by ROSE are too sparse to allow accurate interpolation. The deviations in the K/M and L/M ratios are probably due to the neglect of the screening effect in the M-shell calculations.

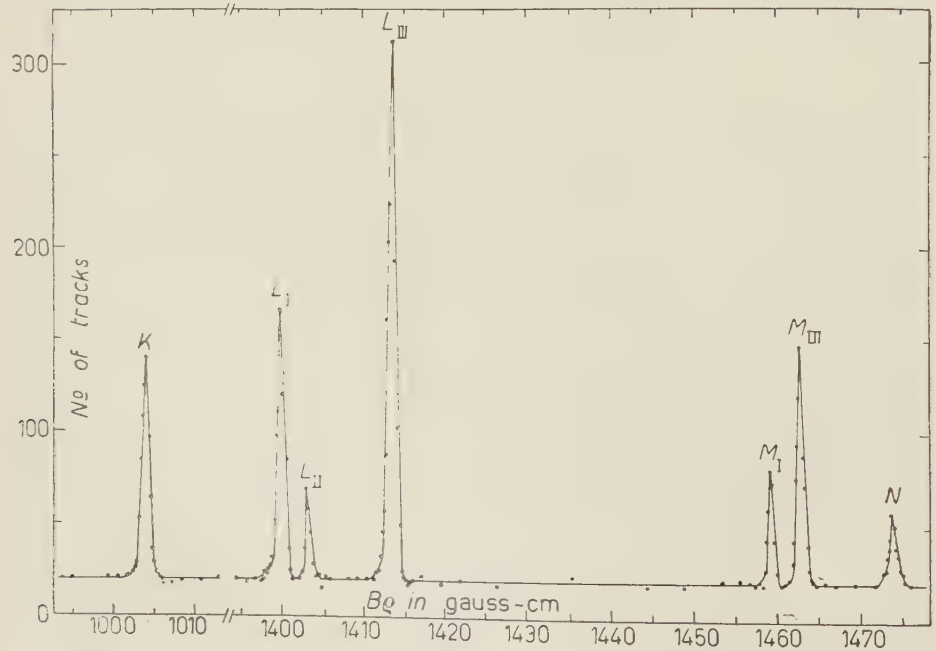

Fig. 2. – Internal conversion lines of the 165.3 keV transition in $^{197}\mathrm{Hg}^{m}$.

They lead to corrections to the theoretical M-shell coefficients of the expected order of magnitude, *viz.*, $f_M = 0.73 \pm 0.04$ and $f_M = 0.63 \pm 0.03$ respectively.

Futhermore, the good agreement in the M_{I}/M_{III} ratio is an indication that the neglect of screening would not affect the relative M-shell conversion coefficients seriously, as mentioned by ROSE.

3·2. *The* 134.0 keV *transition.* – The pure $E2$ assignment of this transition in ^{197}Hg has been well established ([7-9]) on the basis of lifetime and K/L ratio. Fig. 3 shows the measured internal conversion line spectrum of this transition.

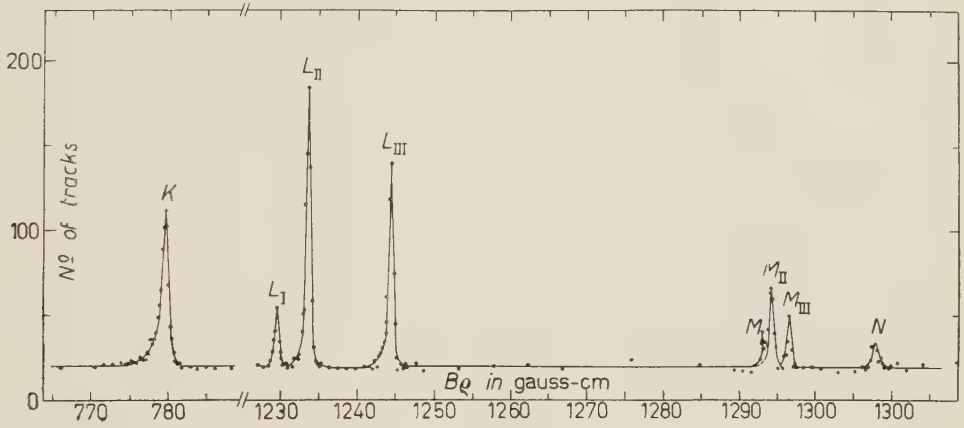

Fig. 3. Internal conversion lines of the 134.0 keV transition in $^{197}Hg^{m}$.

The same exposure as for the 165.3 keV results was used, and the values given were corrected for transmission relative to the M_{III} line. Table III summarizes our results, together with the theoretical values.

Our K/L and L_{II}/L_{III} ratios are in substantial agreement with previous values ([3,7,10]), as well as with theory. The deviation of our L_{I}/L_{III} ratio from theory may be due to the unreliable measurement of such a weak line as the L_{I}. The small difference between the theoretical values for a point nucleus and those corrected for static finite size effects, makes it impossible to decide which give the best representation. The present results, however, indicate that no anomaly is present and that the latest Rose values are probably reliable for $E2$ transitions in this region, as previously mentioned ([5 11]).

The relative intensities of the different M-shell conversion lines have not been reported before. The fair agreement with theory supports the suggestion

([8]) H. H. COBURN, J. V. KANE and S. FRANKEL: *Phys. Rev.*, **105**, 1293 (1957).
([9]) M. GOLDHABER and R. D. HILL: *Rev. Mod. Phys.*, **24**, 179 (1952).
([10]) G. ANDERSSON, E. ARBMAN and B. JUNG: *Ark. f. Fys.*, **11**, 297 (1957).
([11]) G. ANDERSSON and I. BERGSTRÖM: *Nucl. Phys.*, **3**, 506 (1956).

TABLE III.

Ratios	Experimental values	Theoretical $E2$ values (*)
K/L	0.46 ± 0.02	*a*) 0.43 *b*) 0.47
$L_I/L_{II}/L_{III}$	$(0.26 \pm 0.03)/(1.45 \pm 0.09)/(1.00 \pm 0.05)$	*a*) 0.149/1.42/1.0 *b*) 0.144/1.36/1.0
$M_I/M_{II}/M_{III}$	$(0.29 \pm 0.06)/(1.49 \pm 0.19)/(1.00 \pm 0.10)$	*a*) 0.124/1.27/1.0 *b*) —
L/M	4.02 ± 0.27	*a*) 2.24 *b*) 2.19

(*) (*a*) Point-nucleus (*b*) With static finite size corretion.

of ROSE that the finite size- and screening effects, which have been neglected in their calculations would not seriously affect the ratios. The L/M ratio differs considerably from theory, and points to a screening correction, $f_M = 0.54 \pm 0.04$, which is exactly the same as that obtained for another $E2$ transition of about the same energy in mercury ([12]).

3·3. *The* 130.2 keV *transition.* – A measurement of the L_{II}/L_{III} ratio for this transition was carried out in a strongly exposed plate and a value of 1.3 ± 0.1 obtained, with L_I much weaker. This value is in excellent agreement with that of JOLY *et al.* ([13]), *viz.*, 1.31. Comparison with the theoretical ratios definitely excludes the possibility of all multipolarities except $E3$ and $E4$. Unfortunately, in this particular case, one cannot distinguish between these two on the basis of L subshell ratios alone. MIHELICH and DE SHALIT ([3]), however, show that the 130 keV transition should bring about a parity change. It can therefore only be an $E3$, in agreement with their conclusion from the K/L ratio.

3·4. *The* 77.5 keV *transition.* – According to MIHELICH and DE SHALIT ([3]), this transition is an $(M1+E2)$ mixture in the ratio 7:1. The conversion line spectrum obtained in this work is given in Fig. 4. All values are corrected

([12]) G. BACKSTRÖM, O. BERGMAN and J. BURDE: *Nucl. Phys.*, **7**, 263 (1958).

([13]) R. JOLY, J. BRUNNER, J. HALTER and O. HUBER: *Helv. Phys. Acta*, **28**, 403 (1955).

for transmission relative to the M_{111} line. The high resolving power (0.05 %) made it possible to measure the M subshell ratios for the first time. The L_1 and L_{11} lines were over-exposed in the plate that was used for the other measu-

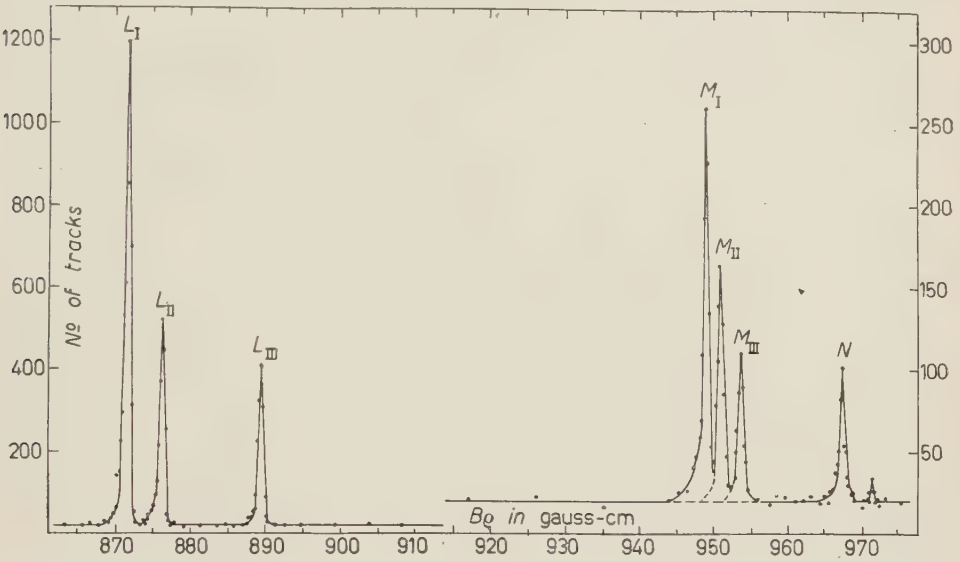

Fig. 4. – Internal conversion lines of the 77.5 keV transition in ^{197}Au.

rements; the three L lines were therefore measured in a plate which was exposed to the same source for about half the time. The values so obtained were then normalized to those of the longer exposure by comparison of the L_{111} areas.

The intensity ratios obtained are listed in Table IV, and the theoretical values in Table V. As is normally the case, the static finite size corrections

TABLE IV.

Ratios	Present work	Previous authors
$L_1/L_{11}/L_{111}$	$(3.06\pm0.13)/(1.35\pm0.07)/(1.00\pm0.04)$	2.94/1.30/1.0 [3] 2.94/1.35/1.0 [13]
$M_1/M_{11}/M_{111}$	$(2.79\pm0.16)/(1.59\pm0.10)/(1.00\pm0.05)$	—
L/M	3.66 ± 0.09	3.6 [7]
M/L_{111}	1.48 ± 0.07	—

to $E2$ coefficients are small, in agreement with our own and other previous results. For $M1$ conversion in the L_1 and L_{11} subshells fairly large corrections

are found when the static finite size effect is taken into account. The extreme sensitivity of the L and M subshell ratios to multipolarity is evident; this may be utilized to determine the mixing ratio with considerable accuracy.

TABLE V.

Theoretical values for		L_{I}	L_{II}	L_{III}	M_{I}	M_{II}	M_{III}
$E2$	uncorrected	0.194	6.15	5.6	0.094	2.60	2.52
	with static correction	0.18	5.95	—	—	—	—
$M1$	uncorrected	2.42	0.213	0.0182	0.84	0.092	0.0082
	with static correction	1.83	0.167	—	—	—	—

For the analysis of the experimental data, a method similar to that of NORDLING *et al.* [14] was used. The following reasonable assumptions are made:

a) The $E2$ conversion coefficients, corrected for static effects only, are reliable.

b) The L_{III} coefficient for an $M1$ transition is unaffected by finite size effects. This is justified by the fact that the wave function of the $p_{\frac{1}{2}}$ electron vanishes inside the nuclear volume [15].

c) The screening correction which has to be applied to the M-shell conversion coefficients is the same for $M1$ and $E2$ transitions, which fact has been justified both theoretically [6] and experimentally [12,16].

Now, from fundamental theoretical considerations it follows that

$$\alpha_{L_i} = r(\alpha 2)_{L_i} + (1-r)\, f_{L_i}(\beta 1)_{L_i}, \qquad i = 1,\ 11 \tag{1}$$

$$\alpha_{L_{\mathrm{III}}} = r(\alpha 2)_{L_{\mathrm{III}}} + (1-r)(\beta 1)_{L_{\mathrm{III}}}, \tag{2}$$

$$\alpha_M = f_M \{ r(\alpha 2)_M + (1-r)(\beta 1)_M \}, \tag{3}$$

where $f_{L_{\mathrm{I}}}$ and $f_{L_{\mathrm{II}}}$ are the corrections to the point-nucleus values for $M1$ conversion in the particular shells, r the fraction of transitions with an $E2$ character and f_M the screening correction for both $M1$ and $E2$ total M-shell conversion coefficients.

[14] C. NORDLING, K. SIEGBAHN, E. SOKOLOWSKI and A. H. WAPSTRA: *Nucl. Phys.*, **1**, 326 (1956).

[15] J. W. MIHELICH, T. J. WARD and K. P. JACOB: *Phys. Rev.*, **103**, 1285 (1956).

[16] P. J. CRESSMAN and R. G. WILKINSON: *Phys. Rev.*, **109**, 872 (1958).

From equations (1)–(3) it follows that:

$$\alpha_{L_{111}}/\alpha_{L_1} = L_{111}/L_1 = \frac{r(\alpha 2)_{L_{111}} + (1-r)(\beta 1)_{L_{111}}}{r(\alpha 2)_{L_1} + (1-r)f_{L_1}(\beta 1)_{L_1}},$$

i.e.

$$r = \frac{(L_{111}/L_1)(\beta 1)_{L_1} f_{L_1} - (\beta 1)_{L_{111}}}{(L_{111}/L_1)(\beta 1)_{L_1} f_{L_1} + (\alpha 2)_{L_{111}} - (L_{111}/L_1)(\alpha 2)_{L_1} - (\beta 1)_{L_{111}}}. \tag{4}$$

Similarly

$$r = \frac{(L_{111}/L_{11})(\beta 1)_{L_{11}} f_{L_{11}} - (\beta 1)_{L_{111}}}{(L_{111}/L_{11})(\beta 1)_{L_{11}} f_{L_{11}} + (\alpha 2)_{L_{111}} - (L_{111}/L_{11})(\alpha 2)_{L_{11}} - (\beta 1)_{L_{111}}}, \tag{5}$$

and also

$$r = \frac{f_M(\beta 1)_M - (\beta 1)_{L_{111}}(M/L_{111})}{M/L_{111}\{(\alpha 2)_{L_{111}} - (\beta 1)_{L_{111}}\} - f_M\{(\alpha 2)_M - (\beta 1)_M\}}. \tag{6}$$

In each of these three equations only r and a single correction factor f_j ($j = L_1, L_{11}, M$) appear as unknowns. Fig. 5 shows the graphical analysis used to determine the mixing ratio r, as well as the corrections, f_j. Allowance for the statistical errors in the experimental ratios gives rise to the error strips indicated.

It is clear that there are four unknowns in the three equations (4)–(6) and one further assumption is hence necessary in order to solve them. Two different methods of approach, yielding the same result, are used:

We may assume f_M to be of the same order of magnitude as the M-shell corrections normally found, *viz.*, about 0.60. From the M/L_{111} curve in Fig. 5, this yields a mixing ratio $r = 0.094$. In this particular case the theoretical L/M ratio is very insensitive to the value chosen for r, and is equal to 2.19 for any mixing ratio within the limits $0.06 < r < 0.13$. Compared with the experimental L/M ratio this yields a true value for f_M of 0.598 ± 0.015. Alternatively one can assume the mixing ratio given by MIHELICH and DE SHALIT, namely $r = 0.125$. This still falls within the limits mentioned above and will therefore yield the same value for f_M.

From this value for f_M and the M/L_{111} curve, a mixing ratio, $r = 0.094 \pm 0.009$ is obtained. It then follows from the other two curves that

$$f_{L_1} = 0.75 \pm 0.11 \quad \text{and} \quad f_{L_{11}} = 0.80^{+0.20}_{-0.24}$$

These corrections are in excellent agreement with those predicted by the new values of ROSE (which were corrected for the static finite size effect only),

namely $f_{L_I} = 0.76$ and $f_{L_{II}} = 0.79$. This indicates the absence of any dynamic finite size effect in this case.

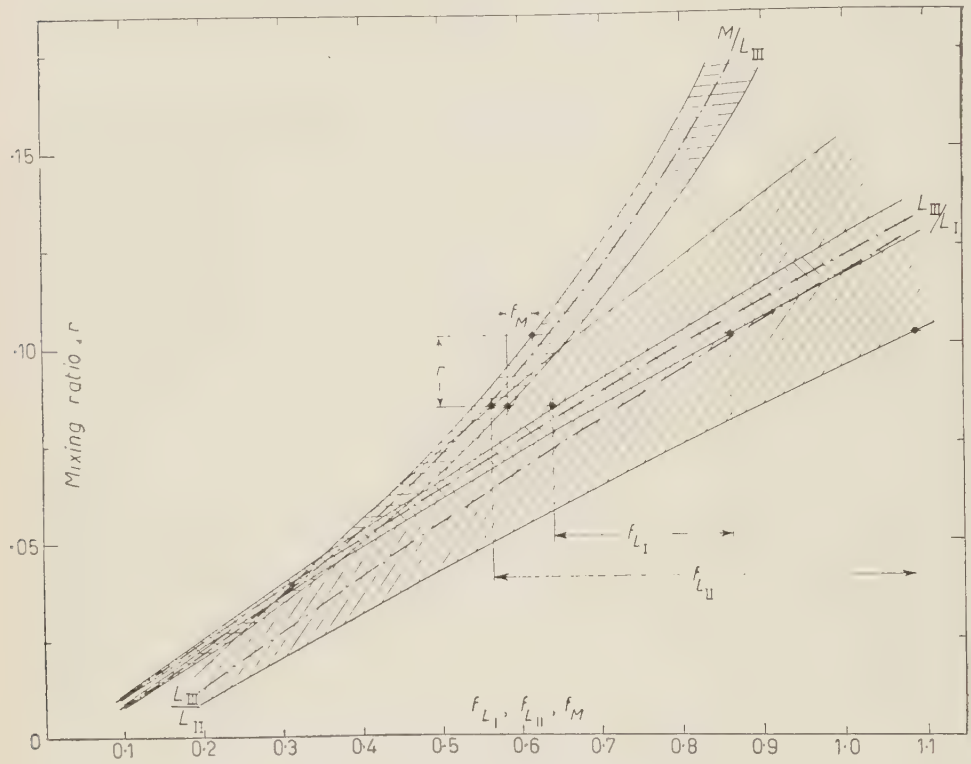

Fig. 5. – Graphical analysis of the relative conversion coefficients of the 77.5 keV transition.

If we further assume that the screening effect would affect the different M subshell coefficients to the same extent, as was inferred by ROSE, we may use

$$f_{M_I} = f_{M_{II}} = f_{M_{III}} = f_M = 0.598 \pm 0.015 .$$

Together with the obtained mixing ratio, the theoretical M-shell ratios then become:

$$M_I/M_{II}/M_{III} = (3.17^{+0.35}_{-0.30}) / (1.34^{+0.04}_{-0.03}) / 1.00 ,$$

in good agreement with the experimental values, *viz.*,

$$M_I/M_{II}/M_{III} = (2.79 \pm 0.16)/(1.59 \pm 0.10)/(1.00 \pm 0.05) .$$

* * *

The authors would like to thank Dr. S. J. DU TOIT, head of the Nuclear Physics Division for his interest in this work, the staff of the C.S.I.R. cyclotron for numerous cyclotron bombardments, and the South African Council for Scientific and Industrial Research for permission to publish this article. One of us (D.R.) would like also to thank the South African Atomic Energy Board for a research scholarship.

RIASSUNTO (*)

Si sono accuratamente determinate e confrontate coi valori teorici le intensità relative di molte righe di conversione interna del decadimento ^{197}Hg. In genere l'accordo coi valori statici finiti corretti è assai buono. Si trova, tuttavia, che i coefficienti teorici dello strato M nei casi esaminati sono eccedenti per circa il 40%. Ciò si attribuisce all'aver trascurato nei calcoli l'effetto di schermo. Per la ben nota transizione ($M1+E2$) di 77.5 keV nel ^{197}Au il rapporto di miscela fu trovato essere $(9.4 \pm .09)\%$ $E3$ e le correzioni da applicare ai coefficienti del nucleo puntiforme per la conversione $M1$ negli strati L_1 e L_{II} sono, rispettivamente, 0.75 ± 0.11 e $0.80^{+0.29}_{-0.24}$. Tali correzioni sono esattamente quelle trovate tenendo conto dell'effetto « statico » della dimensione finita del nucleo e indicano quindi l'assenza in questo caso di ogni effetto dipendente dalla struttura (« dinamico »).

(*) *Traduzione a cura della Redazione.*

Über die Bewegung der rotierenden Satelliten und Doppelsterne nach der Einsteinschen Gravitationstheorie.

N. St. Kalitzin

Bulgarische Akademie der Wissenschaften - Sofia

(ricevuto il 3 Ottobre 1958)

Zusammenfassung. — Es wird die Aufgabe der Apsidendrehung zweier rotierenden Körper mit vergleichbaren Massen auf Grund der Bewegungsgleichungen von Fock in der v^2/c^2 Näherung der Einsteinschen Gravitationstheorie exakt behandelt. Die abgeleitete Formel für die Periastrondrehung enthält als Summanden die Einstein-Focksche Periastrondrehung, die Lense-Thirringsche Periastrondrehung und eine neue Periastrondrehung, welche der Summe der Produkte aus dem spezifischen Drehmoment des einen Körpers und der Masse des anderen Körpers proportional ist.

In unserer Arbeit (1) haben wir die Periheldrehung eines Satelliten mit unendlich kleiner Masse im Felde eines rotierenden Zentralkörpers in der zweiten Näherung nach der Einsteinschen Gravitationstheorie exakt berechnet und nachgewiesen, daß die von Lense und Thirring in (2) abgeleitete Formel auch für endliche Effekte gültig ist.

Hier wollen wir die Bewegung eines rotierenden Satelliten mit endlicher Masse um einen rotierenden Körper nach der Einsteinschen Gravitationstheorie betrachten. Dieses Problem ist von Bedeutung bei den Doppelsternen, deren Komponenten, wie die Spektraluntersuchungen zeigen, oft in rascher Drehbewegung begriffen sind.

Es seien $\boldsymbol{r}_1 = (x_1, y_1, z_1)$, $\boldsymbol{r}_2 = (x_2, y_2, z_2)$ die Lagen der Schwerpunkte beider Körper und m_1 und m_2 ihre Massen. Die Funktion von Lagrange lautet nach (3)

(1) N. St. Kalitzin: *Nuovo Cimento*, **9**, 365 (1958).
(2) J. Lense und H. Thirring: *Phys. Zeits.*, **19**, 156 (1918).
(3) V. A. Fock: *Theorie des Raumes, der Zeit und der Schwere* (Moskau, 1955, russisch).

S. 358 u.a. für diesen Fall folgendermaßen (wir nehmen an, daß die Massenverteilung der Körper sphärische Symmetrie besitzt):

$$(1)\quad L=\frac{1}{2}m_1\dot{\boldsymbol{r}}_1^2+\frac{1}{2}m_2\dot{\boldsymbol{r}}_2^2+\frac{1}{2}\omega_{ik}^{(1)}\omega_{jk}^{(1)}I_{ij}^{(1)}+\frac{1}{2}\omega_{ik}^{(2)}\omega_{jk}^{(2)}I_{ij}^{(2)}+\frac{m_1}{8c^2}(\dot{\boldsymbol{r}}_1^2)^2+\frac{m_2}{8c^2}(\dot{\boldsymbol{r}}_2^2)^2+$$

$$+\frac{1}{2c^2}\frac{fm_1m_2}{|\boldsymbol{r}_1-\boldsymbol{r}_2|}(3\dot{\boldsymbol{r}}_1^2+3\dot{\boldsymbol{r}}_2^2-7\dot{\boldsymbol{r}}_1\dot{\boldsymbol{r}}_2)-\frac{1}{2c^2}fm_1m_2\frac{(\dot{\boldsymbol{r}}_1(\boldsymbol{r}_1-\boldsymbol{r}_2))(\dot{\boldsymbol{r}}_2(\boldsymbol{r}_1-\boldsymbol{r}_2))}{|\boldsymbol{r}_1-\boldsymbol{r}_2|^3}+$$

$$+\left[\frac{f}{c^2}m_1\omega_{si}^{(2)}I_{sj}^{(2)}(3\dot{r}_{2i}-4\dot{r}_{1i})-\frac{f}{c^2}m_2\omega_{si}^{(1)}I_{sj}^{(1)}(3\dot{r}_{1i}-4\dot{r}_{2i})\right]\frac{r_{1j}-r_{2j}}{|\boldsymbol{r}_1-\boldsymbol{r}_2|^3}+$$

$$+f\frac{m_1m_2}{|\boldsymbol{r}_1-\boldsymbol{r}_2|}-\frac{f^2}{2c^2}\frac{m_1m_2(m_1+m_2)}{|\boldsymbol{r}_1-\boldsymbol{r}_2|^2},\qquad i,j=1,2,3.$$

Punkt bedeutet Ableitung nach der Zeit, f, die Newtonsche Gravitationskonstante; $\omega_{si}^{(a)}$ ist der antisymmetrische Tensor der Winkelgeschwindigkeit des a-ten Körpers; $I_{kl}^{(a)}$ ist der durch die Gleichung

$$I_{kl}^{(a)}=\int_{(a)}\varrho(\xi_k-a_k)(\xi_l-a_l)(\mathrm{d}\xi)^3,$$

definierte Tensor des Trägheitsmomentes desgleichen Körpers ($\varrho=$ Massendichte des Körpers). Das Quadrat der Winkelgeschwindigkeit wurde bei der Ableitung von (1) in den Gliedern mit $1/c^2$ vernachläßigt. Dabei ist noch vorausgesetzt, daß die Radien der Körper klein gegenüber ihren Mittelpunktabstand sind, sodaß man die Winkelgeschwindigkeiten als konstant während der Bewegung voraussetzen kann.

Die Bewegungsgrößen der beiden Körper lauten entsprechend

$$(2)\qquad P_{1i}=\frac{\partial L}{\partial\dot{r}_{1i}};\quad P_{2i}=\frac{\partial L}{\partial\dot{r}_{2i}}.$$

Das Energieintegral lautet

$$(3)\qquad \frac{\partial L}{\partial\dot{r}_{1i}}\dot{r}_{1i}+\frac{\partial L}{\partial\dot{r}_{2i}}\dot{r}_{2i}-L=h,$$

h eine Konstante.

Der Drallsatz ergibt in der (xy) Ebene (wir machen die Annahme, daß die Bewegung beider Körper in der Newtonschen Näherung in der (xy) Ebene erfolgt),

$$(4)\qquad x_1P_{1y}-y_1P_{1x}+x_2P_{2y}-y_2P_{2x}=K_{xy},$$

K_{xy} eine Konstante.

Die Integrale der Bewegung des Systemsschwerpunktes lauten (S. [3], S. 373)

$$(5)\qquad r_{1i}\left(m_1+\frac{1}{2c^2}\,m_1\dot{\boldsymbol{r}}_1^2+\frac{1}{2c^2}\,\omega_{sk}^{(1)}\omega_{jk}^{(1)}I_{sj}^{(1)}-\frac{1}{2c^2}\,\frac{fm_1m_2}{|\boldsymbol{r}_1-\boldsymbol{r}_2|}\right)+$$

$$+\,r_{2i}\left(m_2+\frac{1}{2c^2}\,m_2\dot{\boldsymbol{r}}_2^2+\frac{1}{2c^2}\,\omega_{sk}^{(2)}\omega_{jx}^{(2)}I_{sj}^{(2)}-\frac{1}{2c^2}\,\frac{fm_1m_2}{|\boldsymbol{r}_1-\boldsymbol{r}_2|}\right)-(P_{1i}+P_{2i})t=\text{const}\,,$$

t die Zeit.

Wenn wir ein Koordinatensystem verbunden mit dem Schwerpunkt des Systems einführen, dann lassen sich die Schwerpunktsintegrale wie folgt schreiben

$$(6)\qquad m_1\boldsymbol{r}_1\left(1+\frac{1}{2c^2}\,\dot{\boldsymbol{r}}_1^2+\frac{1}{2c^2}\,\omega_{sk}^{(1)}\omega_{jk}^{(1)}I_{sj}^{(1)}\,\frac{1}{m_1}-\frac{1}{2c^2}\,\frac{fm_2}{|\boldsymbol{r}_1-\boldsymbol{r}_2|}\right)+$$

$$+\,m_2\boldsymbol{r}_2\left(1+\frac{1}{2c^2}\,\dot{\boldsymbol{r}}_2^2+\frac{1}{2c^2}\,\omega_{sk}^{(2)}\omega_{jx}^{(2)}I_{sj}^{(2)}\,\frac{1}{m_2}-\frac{1}{2c^2}\,\frac{fm_1}{|\boldsymbol{r}_1-\boldsymbol{r}_2|}\right)=0\,.$$

Wir führen den Schwerpunkt im Newtonschen Sinne

$$(7)\qquad \boldsymbol{r}_0=\frac{m_1\boldsymbol{r}_1+m_2\boldsymbol{r}_2}{m_1+m_2}\,,$$

und die relativen Koordinaten

$$(8)\qquad \boldsymbol{r}=\boldsymbol{r}_1-\boldsymbol{r}_1$$

ein.

Wir führen nach Fock die reduzierte Masse

$$(9)\qquad m^*=\frac{m_1m_2}{m_1+m_2}\,,$$

und die gesamte Masse

$$(10)\qquad m_0=m_1+m_2$$

ein.

Aus Formel (6) folgt, daß der Radiusvektor $\boldsymbol{r}_0$ des Newtonschen Schwerpunktes, wie seine Ableitung nach der Zeit während der Bewegung kleine Größen bleiben. Deswegen können wir in sämtlichen Gliedern, welche c^2 im Nenner enthalten, ansetzen

$$(11)\qquad \begin{cases} \boldsymbol{r}_1=\dfrac{m_2}{m_0}\,\boldsymbol{r}; & \dot{\boldsymbol{r}}_1=\dfrac{m_2}{m_0}\,\dot{\boldsymbol{r}}\,, \\ \boldsymbol{r}_2=-\dfrac{m_1}{m_0}\,\boldsymbol{r}; & \dot{\boldsymbol{r}}_2=-\dfrac{m_1}{m_0}\,\dot{\boldsymbol{r}}\,. \end{cases}$$

Wir schreiben jetzt die Integrale der Energie und des Impulsmomentes bei der Annahme, daß $\boldsymbol{r}_0$ und $\dot{\boldsymbol{r}}_0$ klein sind. Auch in den Newtonschen Gliedern von (3) und (4) können wir $\boldsymbol{r}_0$ und $\dot{\boldsymbol{r}}_0$ vernachlässigen, da sie dort, wie es auch in [1] gezeigt wurde, quadratisch auftreten. Wir können also überall die Werte (11) benutzen. So ergibt das Energieintegral (3), indem wir das Resultat durch m^* teilen

$$h_0 = \frac{1}{2}\dot{\boldsymbol{r}}^2 - f\frac{m_0}{r} + \tag{12}$$
$$+ \frac{1}{c^2}\left\{\frac{3}{8}\left(1 - 3\frac{m^*}{m_0}\right)(\dot{\boldsymbol{r}}^2)^2 + \frac{f}{2r}\dot{\boldsymbol{r}}^2(3m_0 + m^*) + \frac{1}{2}f\frac{m^*}{r^3}(\dot{\boldsymbol{r}}\boldsymbol{r})^2 + \frac{f^2}{2r^2}m_0^2\right\}.$$

h_0 eine Konstante.

Wegen der sphärischsymmetrischen Massenverteilung der Körper können wir ansetzen

$$I_{kl}^{(1)} = I^{(1)}\delta_{kl}\,; \qquad I_{kl}^{(2)} = I^{(2)}\delta_{kl}\,,$$

$$\delta_{kl} = \begin{cases} 1 & \text{für } k = l\,, \\ 0 & \text{für } k \neq l\,. \end{cases} \tag{13}$$

Die Lagrangesche Funktion (1) und die Werte (11) und (13) in Drallintegral (4) eingesetzt ergeben

$$\mu + \sigma\frac{1}{r} = \left\{1 + \frac{1}{2c^2}\left(1 - 3\frac{m^*}{m_0}\right)\dot{\boldsymbol{r}}^2 + \frac{1}{c^2}\frac{f}{r}(3m_0 + m^*)\right\}(x\dot{y} - y\dot{x}) = \tag{13}$$
$$= \left\{1 + \frac{1}{2c^2}\left(1 - 3\frac{m^*}{m_0}\right)v^2 + \frac{1}{c^2}\frac{f}{r}(3m_0 + m^*)\right\}r^2\dot{\varphi}\,,$$

wobei

$$\sigma = \frac{4}{c^2}f(I^{(1)}\omega_{12}^{(1)} + I^{(2)}\omega_{12}^{(2)}) + \frac{3}{c^2}f\left(\frac{m_2}{m_1}I^{(1)}\omega_{12}^{(1)} + \frac{m_1}{m_2}I^{(2)}\omega_{12}^{(2)}\right), \tag{14}$$

μ eine Konstante.

Wenn wir ansetzen

$$u = \frac{1}{r}, \tag{15}$$

dann haben wir die Identität

$$\dot{\boldsymbol{r}}^2 = v^2 = \left(r^2\frac{\mathrm{d}\varphi}{\mathrm{d}t}\right)^2\left[\left(\frac{\mathrm{d}u}{\mathrm{d}\varphi}\right)^2 + u^2\right], \tag{16}$$

woraus sich durch Erheben von (13) ins Quadrat ergibt

$$(17)\qquad \left(\mu^2+2\mu\sigma\frac{1}{r}\right)\left[\left(\frac{\mathrm{d}u}{\mathrm{d}\varphi}\right)^2+u^2\right]=\left\{1+\frac{v^2}{c^2}\left(1-3\frac{m^*}{m_0}\right)+\frac{2f}{c^2r}\,(3m_0+m^*)\right\}\cdot v^2\,.$$

In die rechte Seite von (17) setzen wir v^2 aus dem Energieintegral (12) ein, in welchem wir $(\dot{\boldsymbol{r}}\boldsymbol{r})^2$ durch den Ausdruck

$$(18)\qquad (\dot{\boldsymbol{r}}\boldsymbol{r})^2=r^2v^2-\mu^2$$

ersetzen. Die Formel (12) für h_0 läßt sich dann so schreiben

$$(19)\qquad h_0=\frac{1}{2}\,v^2-f\frac{m_0}{r}+\frac{3}{8c^2}\left(1-3\frac{m^*}{m_0}\right)v^4+$$
$$+\frac{f}{2c^2r}\,(3m_0+2m^*)\,v^2+\frac{f^2}{2c^2r^2}\,m_0^2-\frac{fm^*}{2c^2r^3}\,\mu^2\,.$$

Wir lösen diese Gleichung in der betrachteten Näherung nach r^2 und setzen die gefundene Lösung in (17) ein. Dann erhalten wir indem wir $1/r$ durch u ersetzen

$$(20)\qquad \mu^2\left(1+2\frac{\sigma}{\mu}u\right)\left[\left(\frac{\mathrm{d}u}{\mathrm{d}\varphi}\right)^2+u^2\right]=2h_0+\frac{h_0^2}{c^2}\left(1-3\frac{m^*}{m_0}\right)+$$
$$+2fm_0\left[1+\frac{h_0}{c^2}\left(4-3\frac{m^*}{m_0}\right)\right]u+\frac{3f^2m_0^2}{c^2}\left(2-\frac{m^*}{m_0}\right)u^2+\frac{fm^*}{c^2}\,\mu^2u^3\,.$$

Wenn wir $1/(1+2(\sigma/\mu)u)$ in Potenzreihe entwickeln, so ergibt sich aus (20)

$$(21)\qquad \mu^2\left[\left(\frac{\mathrm{d}u}{\mathrm{d}q}\right)^2+u^2\right]=2h_0+\frac{h_0^2}{c^2}\left(1-3\frac{m^*}{m_0}\right)+\left\{2fm_0\left[1+\frac{h_0}{c^2}\left(4-3\frac{m^*}{m_0}\right)\right]-4h_0\frac{\sigma}{\mu}\right\}u+$$
$$+\left[\frac{3f^2m_0^2}{c^2}\left(2-\frac{m^*}{m_0}\right)-4fm_0\frac{\sigma}{\mu}\right]u^2+\frac{fm^*}{c^2}\,\mu^2u^3\,.$$

Gleichung (21) nach p differenziert und durch $2\mu^2(\mathrm{d}u/\mathrm{d}q)$ dividiert ergibt

$$(22)\qquad \frac{\mathrm{d}^2u}{\mathrm{d}\varphi^2}+u=\frac{1}{\mu^2}\left\{fm_0\left[1+\frac{h_0}{c^2}\left(4-3\frac{m^*}{m_0}\right)-2h_0\frac{\sigma}{\mu}\right]+\right.$$
$$\left.+\left[\frac{3f^2m_0^2}{\mu^2c^2}\left(2-\frac{m^*}{m_0}\right)-4fm_0\frac{\sigma}{\mu^3}\right]u+\frac{3fm^*}{2c^2}\,u^2\right.\,.$$

Die Gleichung (21) für die relative Bewegung des einen Körpers um den anderen läßt sich mit Hilfe von elliptischen Funktionen integrieren. Wir

erhalten aber astronomisch wichtige Resultate direkter mit Hilfe der Methode der sukzessiven Approximationen. In erster Näherung haben wir

$$\frac{\mathrm{d}^2u}{\mathrm{d}\varphi^2} + u = \frac{fm_0}{\mu^2}. \tag{23}$$

Die Lösung dieser Differentialgleichung lautet

$$u = \frac{1 + e\cos(\varphi - \varepsilon)}{p}, \tag{24}$$

wobei e und ε beliebige Konstanten sind. Durch Einsetzen von (24) in (23) erhalten wir

$$\mu^2 = fm_0 p\,. \tag{25}$$

Die Lösung ist in dieser Näherung eine Ellipse ($e < 1$)

$$p = a(1 - e^2)\,, \tag{26}$$

a – die große Halbachse der Ellipse, e – Exzentrizität.

Um die zweite Näherung zu finden setzen wir die Lösung (24) in die rechte Seite von Gleichung (22) ein und erhalten

$$\begin{aligned}\frac{\mathrm{d}^2u}{\mathrm{d}\varphi^2} + u = \frac{1}{\mu^2}\left\{fm_0\left[1 + \frac{h_0}{c^2}\left(4 - 3\frac{m^*}{m_0}\right)\right] - 2h_0\frac{\sigma}{\mu}\right\} + \\ + \left[\frac{3f^2m_0^2}{\mu^2c^2}\left(2 - \frac{m^*}{m_0}\right) - 4fm_0\frac{\sigma}{\mu^3}\right]\frac{1 + e\cos(\varphi - \varepsilon)}{p} + \\ - \frac{3fm^*}{2c^2}\,\frac{1 + 2e\cos(\varphi - \varepsilon) + e^2\cos^2(\varphi - \varepsilon)}{p^2}.\end{aligned} \tag{27}$$

Von den hinzukommenden Gliedern ist das Glied in $\cos(\varphi - \varepsilon)$ das einzige, das einen Einfluß infolge von Resonanz innerhalb der Beobachtungsgrenzen haben kann. Da

$$u = \tfrac{1}{2}A\varphi\sin\varphi$$

ein partikulares Integral von

$$\frac{\mathrm{d}^2u}{\mathrm{d}\varphi^2} + u = A\cos\varphi\,,$$

ist, so liefert jenes Glied die folgende zum Integral (24) hinzukommende Korrektur

$$u_1 = \frac{1}{2}\frac{e}{p}\left\{\frac{3f^2m_0^2}{\mu^2c^2}\left(2-\frac{m^*}{m_0}\right)-4fm_0\frac{\sigma}{\mu^3}+\frac{3fm^*}{c^2p}\right\}\varphi\sin(\varphi-\varepsilon)\,. \tag{28}$$

So erhalten wir als zweite Näherung

$$u = \frac{1}{p}(1+e\cos(\varphi-\varepsilon))+\frac{1}{2}\frac{e}{p}\left\{\frac{3f^2m_0^2}{\mu^2c^2}\left(2-\frac{m^*}{m_0}\right)-4fm_0\frac{\sigma}{\mu^3}+\right. \tag{29}$$

$$\left.+\frac{3fm^*}{c^2p}\right\}\varphi\sin(\varphi-\varepsilon)=\frac{1}{p}(1+e\cos(\varphi-\varepsilon-\delta\varepsilon))\,,$$

wobei

$$\delta\varepsilon=\frac{1}{2}\left\{\frac{3f^2m_0^2}{\mu^2c^2}\left(2-\frac{m^*}{m_0}\right)-4fm_0\frac{\sigma}{\mu^3}+\frac{3fm^*}{c^2p}\right\}\varphi\,, \tag{30}$$

ist und $(\delta\varepsilon)^2$ vernachläßigt wurde.

Die Periheldrehung (Periastrondrehung) für einen Umlauf des einen Körpers mit der Masse m_1 um den anderen ist

$$\delta\varepsilon=\frac{6\pi fm_0}{pc^2}-\frac{4\pi\sigma}{p\sqrt{fm_0p}}\,. \tag{31}$$

Die gleiche Periheldrehung erhalten wir, wenn wir die Näherungslösung

$$u=\frac{1+e\cos(\lambda\varphi-\varepsilon)}{p}\,, \tag{32}$$

in Gl. (22) einführen und dadurch die Konstanten λ und p bestimmen. Wir setzen an

$$\omega^{(1)}=\sqrt{(\omega_{23}^{(1)})^2+(\omega_{31}^{(1)})^2+(\omega_{12}^{(1)})^2}\,,$$

$$\omega^{(2)}=\sqrt{(\omega_{23}^{(2)})^2+(\omega_{31}^{(2)})^2+(\omega_{12}^{(2)})^2}\,,$$

und

$$\omega_{12}^{(1)}=\omega^{(1)}\cos i_1\;;\qquad \omega_{12}^{(2)}=\omega^{(2)}\cos i_2\,. \tag{33}$$

i_1 und i_2 bedeuten die Winkel zwischen der Bahnebene und den Äquatorebenen der beiden Körper. Dann läßt sich die Formel (31) folgendermaßen schreiben

$$\delta\varepsilon=\frac{6\pi fm_0}{a(1-e^2)c^2}-16\,\frac{\pi f(I^{(1)}\omega^{(1)}\cos i_1+I^{(2)}\omega^{(2)}\cos i_2)}{c^2a^{\frac{3}{2}}(1-e^2)^{\frac{3}{2}}\sqrt{fm_0}}- \tag{34}$$

$$-12\,\frac{\pi f((m_2/m_1)I^{(1)}\omega^{(1)}\cos i_1+(m_1/m_2)I^{(2)}\omega^{(2)}\cos i_2)}{c^2a^{\frac{3}{2}}(1-e^2)^{\frac{3}{2}}\sqrt{fm_0}}\,.$$

Wenn beide Körper homogen sind, dann können wir ansetzen

$$I^{(1)} = \tfrac{1}{5} m_1 r_1^2 \,; \qquad I^{(2)} = \tfrac{1}{5} m_2 r_2^2 \,. \tag{35}$$

r_1 und r_2 sind die Radien der Körper. Also

$$\delta\varepsilon = \frac{6\pi f m_0}{a(1-e^2)c^2} - 16\,\frac{\pi f(m_1 r_1^2 \omega^{(1)} \cos i_1 + m_2 r_2^2 \omega^{(2)} \cos i_2)}{5c^2 a^{\frac{3}{2}}(1-e^2)^{\frac{3}{2}}\sqrt{f m_0}} - \tag{36}$$

$$- 12\,\frac{\pi f(m_2 r_1^2 \omega^{(1)} \cos i_1 + m_1 r_2^2 \omega^{(2)} \cos i_2)}{5c^2 a^{\frac{3}{2}}(1-e^2)^{\frac{3}{2}}\sqrt{f m_0}} \,.$$

Das erste Glied auf der rechten Seiten von (36) entspricht der Einsteinschen Periheldrehung, nur die hier auftretende Konstante m_0 hat einen anderen Sinn. Bei gegebenen a und e hängt die Periastrondrehung nur von der Summe der Massen der beiden Komponenten ab. Diese Periastrondrehung ist von Fock in seinem Buche ([3]), S. 381 abgeleitet worden.

Das zweite Glied entspricht der Lense-Thirringschen Periheldrehung, welche in ([2]) abgeleitet ist (vergl. auch ([1])). Hier kommen die Massen und die Winkelgeschwindigkeiten der beiden Komponenten des Systems vor.

Das dritte Glied ergibt eine neuartige Periastrondrehung, welche, grob gesprochen, durch die gegenseitige Wechselwirkung der Massen und der Drehmomente der beiden Körper zustande kommt.

Die Formeln (34) und (36) können von Bedeutung werden bei der Betrachtung der Bewegung der rotierenden künstlichen Satelliten mit unendlich kleiner oder endlicher Masse. Sie können auch nützlich sein bei der Deutung der Apsidendrehung der Doppelsterne, deren Komponenten um ihre Schwerpunkte rotieren.

RIASSUNTO (*)

In base alle equazioni di moto di Fock si tratta in modo esatto, nell'approssimazione v^2/c^2 della teoria gravitazionale di Einstein, il problema della rotazione absidale di due corpi rotanti di masse confrontabili. La formola ottenuta per la rotazione del periastro contiene come sommandi la rotazione del periastro di Einstein-Fock, la rotazione del periastro di Lense-Thirring e una nuova rotazione del periastro proporzionale alla somma dei prodotti del momento di rotazione specifico dell'un corpo e della massa dell'altro.

(*) *Traduzione a cura della Redazione.*

On the Overhauser Stationary Effect in Paramagnetic Salts and Semiconductors.

G. R. Khutsishvili

Physical Institute of the Georgian Academy of Sciences - Tbilissi

(ricevuto il 4 Ottobre 1958)

Summary. — The expressions of the parameters f_K characterizing the degree of nuclei stationary orientation are obtained for the partial saturation of one of the hyperfine structure components in a paramagnetic salt (in case of the effective spin $\frac{1}{2}$ for the electron shell) or in silicon or in germanium with a pentavalent donor or trivalent acceptor impurity. The expressions of the parameters f_K are also obtained for the same partial saturation of all the hyperfine structure components. The contribution of the non-contact terms in the nuclei relaxation is taken into account for spin $\frac{1}{2}$. The methods for measuring the parameters f_K are also considered.

1. – During the past few years there appeared some papers suggesting some modifications of Overhauser's method for the polarization of nuclei in paramagnetic salts and semiconductors ([1-6]). Most of them deal with the problem of obtaining non-stationary dynamic polarization of the nuclei.

([1]) A. Abragam: *Phys. Rev.*, **98**, 1729 (1955).

([2]) A. Abragam: *Compt. Rend.*, **242**, 1720 (1956); A. Abragam and J. Combrisson: *Compt. Rend.*, **243**, 650 (1956); *Suppl. Nuovo Cimento*, **6**, 1197 (1957); A. Abragam, J. Combrisson and I. Solomon: *Compt. Rend.*, **245**, 157 (1957); A. Abragam and W. G. Proctor: *Compt. Rend.*, **246**, 2253 (1957).

([3]) G. Feher: *Phys. Rev.*, **103**, 500 (1956); G. Feher and E. A. Gere: *Phys. Rev.*, **103**, 501 (1956).

([4]) C. D. Jeffries: *Phys. Rev.*, **106**, 164 (1957); M. Abraham, R. W. Kedzie and C. D. Jeffries: *Phys. Rev.*, **106**, 165 (1957).

([5]) D. Pines, J. Bardeen and C. P. Slichter: *Phys. Rev.*, **106**, 489 (1957).

([6]) F. M. Pipkin and J. W. Culvahouse: *Phys. Rev.*, **106**, 1102 (1957); **109**, 319 (1958); **109**, 1423 (1958).

In this paper we deal with the problem of obtaining stationary nuclear polarization in non-metals by means of a complete or partial saturation of one or more components of the paramagnetic resonance hyperfine structure.

2. – Let us consider the system consisting of the electron shell with effective spin $S = \frac{1}{2}$ and the nucleus with spin J, placed in an external magnetic field H (this includes the cases of trivalent acceptor or pentavalent donor impurity and also the cases of many paramagnetic salts). The Hamiltonian of the system is ([7]) (we neglect the quadrupole effects and the direct influence of the external field on the nuclear spin and treat the case of axial symmetry),

$$\mathcal{H} = \beta [g_{\parallel} H_z S_z + g_{\perp} (H_x S_x + H_y S_y)] + [A S_z J_z + B(S_x J_x + S_y J_y)] . \tag{1}$$

We restrict ourselves to the case of a strong field

$$\beta H \gg A , \qquad \beta H \gg B .$$

If M and m are the projections on the direction of the external field of the electron shell spin and the nuclear spin respectively than we have for the energy levels (with an accuracy up to terms of order A and B)

$$E_{Mm} = Mg\beta H + KMm , \tag{2}$$

where

$$g = \sqrt{g_{\parallel}^2 \cos^2 \vartheta + g_{\perp}^2 \sin^2 \vartheta} , \tag{3}$$

$$Kg = \sqrt{(Ag_{\parallel})^2 \cos^2 \vartheta + (Bg_{\perp})^2 \sin^2 \vartheta} \quad (*). \tag{4}$$

The alternating fields of the corresponding frequencies induce the resonance transitions between the levels (2). In particular, transitions $\Delta M = \pm 1$ $\Delta m = 0$ give the paramagnetic resonance, and transitions $\Delta M = 0$, $\Delta m = \pm 1$ give the nuclear magnetic resonance. The spectrum of the paramagnetic resonance is

$$\beta g H + Km ,$$

i.e. we get $2J+1$ equally spaced (with an accuracy up to terms of order A and B) components of the hyperfine structure.

([7]) B. BLEANEY: *Phil. Mag.*, **42**, 441 (1951).

(*) In the case of the pentavalent donor or trivalent acceptor impurity in silicon or germanium we have $g_{\parallel} = g_{\perp} = g = 2$, $K = A = B$.

In the calculation of the Boltzmann populations of the energy levels we neglect the spin-spin interaction. With such an approximation we have $2J+1$ pairs of levels which have the same energy, the energy difference of the components of each pair being $g\beta H$ (see Fig. 1).

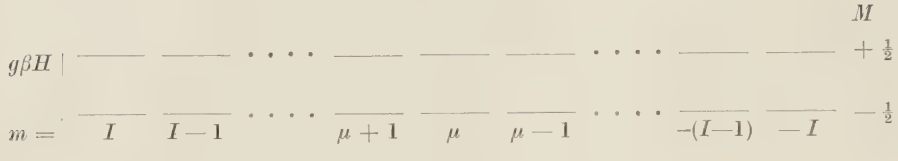

Fig. 1.

We have four types of relaxation transitions:

I. $\Delta M = \pm 1$, $\Delta m = 0$ are « vertical » transitions. They induce the relaxation of the electronic spin.

II. $\Delta M = -\Delta m = \pm 1$ are « flip-flop » transitions. Such transitions are induced, in particular, by the hyperfine (contact) interaction.

III. $\Delta M = \Delta m = \pm 1$ are « flip-flop » transitions.

IV. $\Delta m = 0$, $\Delta m = \pm 1$ are « horizontal » transitions (+).

Relaxations III and IV are not important in comparison with relaxation II if the electron wave function (more accurately the wave-function of the shell with $S = \frac{1}{2}$) at the position of the nucleus is great, in other words if the part « s » of the electron wave function is not small ([8]). This condition is fulfilled in the case of pentavalent donor or trivalent acceptor impurity in silicon or germanium. One is led to believe that this condition is fulfilled also in the case of many paramagnetic salts (indeed according to ([9]), the great value of the hyperfine structure of the paramagnetic resonance shows that the hyperfine interaction in a paramagnetic salt is due to the mixing of the excited state which has the unpaired s electron with the ground state of the paramagnetic ion).

3. – First we consider the case of the complete saturation of one of the components of the paramagnetic resonance hyperfine structure for an arbi-

(+) The quadrupole relaxation of the nuclei which we neglect is also possible, *i.e.* the transitions with $\Delta M = 0$, $\Delta m = \pm 2$. This relaxation is weak as it is not associated with the interaction of the nuclear and the electronic spins.

([8]) J. Korringa: *Physica*, **16**, 601 (1950).

([9]) A. Abragam and M. H. L. Pryce: *Proc. Roy. Soc.*, A **205**, 135 (1951).

trary J. We suggest at the same time that only relaxations I and II occur.

Let us carry out the complete saturation of the hyperfine structure component of the paramagnetic resonance corresponding to the transition between the two states with the nuclear spin projections equal to μ (Fig. 1). In the stationary state the populations of the states shown in Fig. 1 are the following

$$\begin{array}{cccccccccccc|c} & & & & & & & & & & & & M \\ L, & L & \ldots\ldots & L, & L, & Le^{-2\delta} & \ldots\ldots & & Le^{-2\delta}, & Le^{-2\delta} & & & +\frac{1}{2} \\ Le^{2\delta}, & Le^{2\delta}, & \ldots\ldots & Le^{2\delta}, & L, & L & \ldots\ldots & & L, & L & & & -\frac{1}{2} \\ \hline m=J, & J-1 & \ldots\ldots & \mu+1, & \mu, & \mu-1 & \ldots\ldots & & -(J-1), & -J & & & \end{array}$$

where

$$2\delta = \frac{g\beta H}{kT} \tag{5}$$

and L is determined by the normalization condition. It is easy to get (the line means an average on the types of the nuclei in sample)

$$\overline{m^K} = \frac{2\mu^K + (1+e^{2\delta})\sum_{\mu+1}^{J} m^K + (1+e^{-2\delta})\sum_{\mu-1}^{-J} m^K}{2 + (1+e^{2\delta})(J-\mu) + (1+e^{-2\delta})(J+\mu)}\,. \tag{6}$$

It is well known (see ([10]), for example) that with axial symmetry of quantization the degree of orientation of the nuclei is described by $2J$ parameters f_K. The most important parameters are, in particular, f_1 and f_2.

$$f_1 = \frac{\overline{m}}{J}\,, \tag{7}$$

$$f_2 = \frac{3}{J(2J-1)}\left[\overline{m^2} - \frac{1}{3}(J+1)\right]. \tag{8}$$

Using (6) one can easily show that in the case considered

$$f_1(\mu) = \frac{1}{J}\cdot\frac{2\mu + \frac{1}{2}[J(J+1)-\mu(\mu+1)](1+e^{2\delta}) - \frac{1}{2}[J(J+1)-\mu(\mu-1)](1+e^{-2\delta})}{2+(J-\mu)(1+e^{2\delta})+(J+\mu)(1+e^{-2\delta})} \tag{9}$$

$$f_2(\mu) = \frac{3}{J(2J-1)}\cdot \tag{10}$$

$$\cdot\frac{2[\mu^2 - \frac{1}{3}J(J+1)] + \frac{1}{6}[J(J+1)-\mu(\mu+1)](2\mu+1)(1+e^{2\delta}) - \frac{1}{6}[J(J+1)-\mu(\mu-1)](2\mu-1)(1+e^{-2\delta})}{2+(J-\mu)(1+e^{2\delta})+(J+\mu)(1+e^{-2\delta})}$$

Let us consider the extreme cases.

([10]) G. R. Khutsishvili: *Žu. Ėksp. Teor. Fiz.*, **28**, 496 (1955).

For $\delta \ll 1$

$$f_1(\mu) = \delta \frac{J(J+1) - \mu^2}{J(2J+1)}, \tag{9a}$$

$$f_2(\mu) = \delta \frac{\mu[2J(J+1) - 2\mu^2 - 1]}{J(2J-1)(2J+1)}. \tag{10a}$$

For $\delta \ll 1$

$$f_1(\mu) = \frac{J+1+\mu}{2J} \qquad \text{if} \quad \mu \neq J, \tag{9b}$$

$$f_1(J) = \frac{1}{2(J+1)}, \tag{9c}$$

$$f_2(\mu) = \frac{(J+1+\mu)(2\mu+1)}{2J(2J-1)} \qquad \text{if} \quad \mu \neq J. \tag{10b}$$

$$f_2(J) = \frac{1}{2(J+1)}. \tag{10c}$$

It is seen that for $\delta \gg 1$ the saturation of the line with $m = J-1$ is the most profitable. Then $f_1 = f_2 = 1$. This result is easy to understand: in the case considered the only level populated is the level with $M = -\frac{1}{2}$, $m = J$.

4. – Let us consider then the case of partial saturation of one of the hyperfine structure components of the paramagnetic resonance. To be more concrete we consider the case with $J = \frac{3}{2}$. Then we have four pairs of levels (Fig. 2).

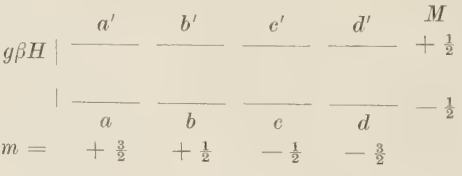

Fig. 2.

The probability of the transition $a \leftrightarrow a'$ per unit time induced by an alternating field perpendicular to the ground field and with the frequency corresponding to this transition is $W(a)$. It is well known that [11]

$$W(a) = \frac{\pi}{2} (\gamma_e H_1)^2 \varphi_a(\omega), \tag{11}$$

[11] N. Bloembergen, E. M. Purcell and R. V. Pound: *Phys. Rev.*, **73**, 679 (1948).

where γ_e is a gyromagnetic ratio of the electron shell spin, $2H_1$ is the amplitude of the alternating field, ω is its frequency (circular) and $\varphi_a(\omega)$ is a function which gives the shape of the transition line $a \leftrightarrow a'$ (here $\int_0^\infty \varphi_a(\omega)\,\mathrm{d}\omega = 1$).

In a similar way we introduce the probabilities $W(b)$, $W(c)$ and $W(d)$. The corresponding frequencies of these four alternating fields are $(\beta g H + Km)/\hbar$ (where $m = +\frac{3}{2}$, $+\frac{1}{2}$, $-\frac{1}{2}$ and $-\frac{3}{2}$).

We suggest again that only relaxations I and II occur.

The probability of the transition $a \to a'$ per unit time induced by the interaction with the lattice is $W(aa')$. In a similar way we introduce $W(a'a)$, $W(bb')$, etc., we have

$$W(aa') = W(bb') = W(cc') = W(dd') = We^{-\delta}, \tag{12a}$$

$$W(a'a) = W(b'b) = W(c'c) = W(d'd) = We^{\delta}, \tag{12b}$$

where W is some function of the temperature. If $N(a)$, $N(a')$, $N(b)$, etc., are the populations of the corresponding levels and $N^0(a)$, $N^0(a')$, $N^0(b)$, etc., are the equilibrium populations, and N is the total number of systems considered we have

$$N(a) + N(a') + N(b) + N(b') + N(c) + N(c') + N(d) + N(d') = N, \tag{13}$$

$$N^0(a) - N^0(a') = N^0(b) - N^0(b') = N^0(c) - N^0(c') = N^0(d) - N^0(d') = \frac{N}{4}\operatorname{tgh}\delta. \tag{14}$$

In the stationary case we have

$$\begin{cases} \dfrac{N(a)}{N(a')} = \dfrac{W(a) + We^{\delta}}{W(a) + We^{-\delta}}, & \dfrac{N(b)}{N(b')} = \dfrac{W(b) + We^{\delta}}{W(b) + We^{-\delta}}, \\ \dfrac{N(c)}{N(c')} = \dfrac{W(c) + We^{\delta}}{W(c) + We^{-\delta}}, & \dfrac{N(d)}{N(d')} = \dfrac{W(d) + We^{\delta}}{W(d) + We^{-\delta}}, \end{cases} \tag{15}$$

$$\frac{N(a)}{N(b')} = \frac{N(b)}{N(c')} = \frac{N(c)}{N(d')} = e^{2\delta}. \tag{16}$$

(16) means that the hyperfine interaction establishes the equilibrium between the levels a and b', b and c', c and d'.

If the partial saturation of only $b \leftrightarrow b'$ is carried out then $W(a) = W(c) = W(d) = 0$ and the solution of equations (13), (15) and (16) gives

$$N(b) = N(c) = N(d) = \frac{N[W(b) + We^{\delta}]}{(5 + e^{2\delta} + 2e^{-2\delta})W(b) + 4W(e^{\delta} + e^{-\delta})}, \tag{17a}$$

$$N(c') = N(d') = \frac{Ne^{-2\delta}[W(b) + We^{\delta}]}{(5 + e^{2\delta} + 2e^{-2\delta})W(b) + 4W(e^{\delta} + e^{-\delta})}, \tag{17b}$$

$$N(a') = N(b') = \frac{N[W(b) + We^{-\delta}]}{(5 + e^{2\delta} + 2e^{-2\delta})W(b) + 4W(e^{\delta} + e^{-\delta})}, \tag{17c}$$

$$N(a) = \frac{Ne^{2\delta}[W(b) + We^{-\delta}]}{(5 + e^{2\delta} + 2e^{-2\delta})W(b) + 4W(e^{\delta} + e^{-\delta})}. \tag{17d}$$

The parameter of the resonance saturation $s(b)$ is introduced in the following way

$$N(b) - N(b') = [1 - s(b)][N^0(b) - N^0(b')]. \tag{18}$$

It is easy to get

$$s(b) = \frac{(5 + e^{2\delta} + 2e^{-2\delta})W(b)}{(5 + e^{2\delta} + 2e^{-2\delta})W(b) + 4W(e^{\delta} + e^{-\delta})}. \tag{19}$$

We get for the parameters f_1 and f_2

$$f_1(b) = s(b)\frac{\frac{1}{3} + e^{2\delta} - \frac{4}{3}e^{-2\delta}}{5 + e^{2\delta} + 2e^{-2\delta}}, \tag{20}$$

$$f_2(b) = s(b)\frac{e^{2\delta} - 1}{5 + e^{2\delta} + 2e^{-2\delta}}. \tag{21}$$

Quite similarly one can consider the cases of the partial saturation for the resonances $a \leftrightarrow a'$, $c \leftrightarrow c'$, and $d \leftrightarrow d'$.

5. – The results obtained are easily generalized if J is arbitrary. If the partial saturation of the transition between two states with nuclear spin projections μ is carried out, then the saturation parameter of this resonance is

$$s(\mu) = \frac{[2 + (J - \mu)(1 + e^{2\delta}) + (J + \mu)(1 + e^{-2\delta}]W(\mu)}{[2 + (J - \mu)(1 + e^{2\delta}) + (J + \mu)(1 + e^{-2\delta})]W(\mu) + (2J + 1)W(e^{\delta} + e^{-\delta})}, \tag{22}$$

where $W(\mu)$ is the probability of the transition (per unit time) between these two states due to the alternating field of the corresponding frequency.

We have for the parameters f_K

$$f_K[s(\mu)] = f_K[s(\mu) = 1] \cdot s(\mu)$$

and the values of $f_K[s(\mu) = 1]$ are given by formulas (9) and (10).

The results obtained show in particular that the condition $W(J) \gg We^{\delta}$ is required for the complete saturation of the paramagnetic resonance cor-

responding to the transition between the levels with nuclear spin projections equal to J. A weaker condition $W(\mu) \gg We^{-\delta}$ is required for the saturation of all the other transitions.

The physical meaning of this difference is easy to understand. To be concrete we consider the case $J = \frac{3}{2}$ (Fig. 2). The saturation of the transition $b \leftrightarrow b'$ induces an increase of the population of the level b' and a decrease of the population of the level b. But as the population of the level b' increases the hyperfine interaction induces the transition $b' \rightarrow a$. Thus the hyperfine interaction will favour the transition of the system from the states b and b' into the states a and a' and this in its turn makes the saturation of the transition $b \leftrightarrow b'$ easier. The same results are obtained at the saturation of resonances $c \leftrightarrow c'$ and $d \leftrightarrow d'$. When resonance $a \leftrightarrow a'$ is saturated there will be no such effect, for the level a' is not connected with the other levels by the hyperfine interaction.

6. – Let us consider now, for an arbitrary J, the case of the same partial saturation of all the $2J+1$ components of the paramagnetic resonance. It is suggested again that only relaxations I and II occur. $N(m)$ and $N(m')$ be the populations of the states with nuclear spin projections m, m' the projections of the shell spin being $-\frac{1}{2}$ and $+\frac{1}{2}$ respectively. In the stationary case we have

$$\frac{N(m)}{N(m')} = \frac{W(m) + We^{\delta}}{W(m) + We^{-\delta}}.$$

Then we get

$$N(m) - N(m') = \frac{N(m)}{W(m) + We^{\delta}} W(e^{\delta} - e^{-\delta}) = \frac{N(m')}{W(m) + We^{-\delta}} W(e^{\delta} - e^{-\delta}) \tag{24}$$

or, as according to the condition imposed all the resonances are equally saturated

$$\frac{N(m)}{W(m) + We^{\delta}} = \frac{N(m')}{W(m) + We^{-\delta}} = \text{const}.$$

The constant does not depend on m.

The hyperfine interaction establishes the equilibrium between the levels $m+1$ and m'. Thus $(m \neq J)$

$$\frac{N(m+1)}{N(m')} = \frac{W(m+1) + We^{\delta}}{W(m) + We^{-\delta}} = e^{2\delta}.$$

Therefore if all the resonances must be equally saturated we need that

$$W(m) = qe^{2m\delta} . \tag{25}$$

q does not depend on m. Let us introduce the parameter of saturation which is the same for all the resonances. We have

$$N(m) - N(m') = (1 - s)[N^0(m) - N^0(m')] = (1 - s)\frac{N}{2J+1}\operatorname{tgh}\delta . \tag{26}$$

Thus according to (24) we have

$$\frac{N(m)}{W(m) + We^{\delta}} = \frac{N(m')}{W(m) + We^{-\delta}} = \frac{N}{2J+1}\cdot\frac{1-s}{W(e^{\delta} + e^{-\delta})} . \tag{27}$$

From (27) we get

$$N(m) + N(m') = (1 - s)\frac{N}{2J+1}\left[1 + \frac{2W(m)}{W(e^{\delta} + e^{-\delta})}\right] .$$

Using the normalization condition we establish the relation between q and s

$$2\frac{1-s}{s}q = (2J+1)W(e^{\delta} + e^{-\delta})\frac{\sinh\delta}{\sinh(2J+1)\delta} , \tag{28}$$

and thus

$$N(m) + N(m') = \frac{N}{2J+1}(1 - s) + sNe^{im\delta}\frac{\sinh\delta}{\sinh(2J+1)\delta} . \tag{29}$$

From (29) it is easy to determine f_1. We get

$$f_1 = dB_J(2J\delta) . \tag{30}$$

It is also easy to write the expressions of f_2, f_3 and f_4. To do this one must substitute x with 2δ in formulas (8), (9) and (10) of paper [10] and multiply these expressions by the factor s.

For $s = 1$ we get the well known Overhauser result: at the complete saturation of all the components of the paramagnetic resonance the effective gyromagnetic ratio of the nucleus is equal to the gyromagnetic ratio of the electron.

7. – At last let us consider the effects induced by relaxations III and IV in the case $J = \frac{1}{2}$. We can write (Fig. 3) for the probabilities of the tran-

sitions induced by the interaction with the lattice

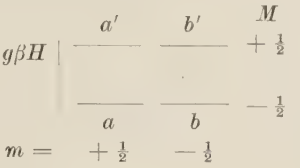

Fig. 3.

(31a) $$W(a'a) = W(b'b) = We^{\delta} \qquad W(aa') = W(bb') = We^{-\delta}$$

(31b) $$W(b'a) = \lambda We^{\delta} \qquad W(ab') = \lambda We^{-\delta}$$

(31c) $$W(a'b) = \lambda_1 We^{\delta} \qquad W(ba') = \lambda_1 We^{-\delta}$$

(31d) $$W(ab) = W(ba) = W(a'b') = W(b'a') = \lambda_2 W\,,$$

where λ, λ_1, λ_2, W are functions of the temperature.

For the stationary case we obtain

(32a) $$N(a')(\lambda_1 e^{\delta} + \lambda_2) + N(a)(\lambda e^{-\delta} + \lambda_2) = N(b')(\lambda e^{\delta} + \lambda_2) + N(b)(\lambda_1 e^{-\delta} + \lambda_2)\,,$$

(32b) $$N(a')[W(a) + We^{\delta}] + N(b')\lambda We^{\delta} + N(b)\lambda_2 W = \\ = N(a)[W(a) + W(1+\lambda)e^{-\delta} + \lambda_2 W]\,,$$

(32c) $$N(b)[W(b) + We^{-\delta}] + N(a)\lambda We^{-\delta} + N(a')\lambda_2 W = \\ = N(b')[W(b) + W(1+\lambda)e^{\delta} + \lambda_2 W]\,.$$

We have still the normalization condition

(32d) $$N(a) + N(a') + N(b) + N(b') = N\,.$$

First let us consider the case of complete saturation of both the paramagnetic resonance components. Then $N(a) = N(a')$, $N(b) = N(b')$ and we get

(33) $$\frac{N(a)}{N(b)} = \frac{\lambda e^{\delta} + \lambda_1 e^{-\delta} + 2\lambda_2}{\lambda e^{-\delta} + \lambda_1 e^{\delta} + 2\lambda_2}\,,$$

(34) $$f_1 = \frac{(\lambda - \lambda_1)\sinh\delta}{(\lambda + \lambda_1)\cosh\delta + 2\lambda_2}\,.$$

If only resonance $a \leftrightarrow a'$ is saturated (completely) we get for f_1 the following expression

(35) $$f_1 = \frac{\lambda_2(\lambda-\lambda_1)(e^{\delta}-e^{-\delta})+(\lambda+\lambda_1+2\lambda\lambda_1)-\lambda_1(1+\lambda)e^{2\delta}-\lambda(1+\lambda_1)e^{-2\delta}}{\lambda_2(1+\lambda)(3e^{\delta}+e^{-\delta})+\lambda_2(1+\lambda_1)(e^{\delta}+3e^{-\delta})+(3\lambda+3\lambda_1+2\lambda\lambda_1+4\lambda_2^2)+\lambda_1(1+\lambda)e^{2\delta}+\lambda(1+\lambda_1)e^{-2\delta}}.$$

8. – To conclude let us consider the problem of the possibility of direct experimental determination of the parameters which characterize the degree of nuclei orientation in the above mentioned effects. Here desirable means of methods would be those by which one could determine f_K without using the theoretical results obtained above.

Let us consider the case $J = \frac{3}{2}$. It is easy to get

(36) $$f_1 = \frac{1}{3N}\langle 3[N(a)-N(b)]+3[N(a')-N(b')]+4[N(b)-N(c)]+ \\ +4[N(b')-N(c')]+3[N(c)-N(d)]+3[N(c')-N(d')]\rangle,$$

(37) $$f_2 = \frac{1}{N}\langle [N(a)-N(b)]+[N(a')-N(b')]-[N(c)-N(d)]-[N(c')-N(d')]\rangle.$$

If one measures experimentally, for example, the value of the signal of the nuclear resonance $a \leftrightarrow b$ one can obtain $N(a)-N(b)$ from the value of the signal. Thus measuring the nuclear resonances $a \leftrightarrow b$, $a' \leftrightarrow b'$, $b \leftrightarrow c$, etc., one can obtain experimentally the values of f_K.

Let us note too that some of the differences $N(a)-N(b)$, $N(a')-N(b')$, $N(b)-N(c)$, etc., must increase greatly with the saturation of at least one of the hyperfine structure components of the paramagnetic resonance, even if $\delta \ll 1$ (this can be seen from formulae (17)). Thus one could verify the validity of the theoretical results obtained above by measuring the nuclear magnetic resonance.

However, the situation is in fact much more complicated. According to (2) the energies of all the transitions are the same with an accuracy up to terms of order A and B and are $K/2$. The next approximation gives a difference in the terms of the order $B^2/g\beta H$. To avoid overlapping of these separate nuclear resonance components the experiments are to be carried with comparatively weak fields.

Besides according to [12] the experiments on the nuclear magnetic resonance in paramagnetic salts are likely to be successful only at helium temperatures. Let us note that these experiments are very interesting by themselves.

[12] K. A. Valieff: *Žu. Èksp. Teor. Fiz.* (in the press).

It follows from formulae (36) and (37) that at the saturation of one of the paramagnetic resonance components, it is impossible to determine the values of f_K directly by measuring the paramagnetic resonance of unsaturated components.

However one can make such measurements with the aim of verifying the theoretical results. For example, according to (17) at the complete saturation of the resonance $b \leftrightarrow b'$

$$N(a) - N(a') = \frac{N(e^{2\delta} - 1)}{5 + e^{2\delta} + 2e^{-2\delta}},$$

while in absence of saturation

$$N^0(a) - N^0(a') = \frac{N}{4} \operatorname{tgh} \delta,$$

thus if only δ is of the order of the unity or more then at the complete saturation of the resonance $b \leftrightarrow b'$, the signal of the resonance $a \leftrightarrow a'$ must increase accordingly (four times more in particular if $\delta \gg 1$).

At last let us note that in the case of the polarization of radioactive nuclei, the parameters f_K with even k can be determined directly from the angular anisotropy of the γ radiation.

RIASSUNTO (*)

Le espressioni dei parametri f_K che caratterizzano il grado di orientamento dei nuclei stazionari si ottengono per la saturazione parziale di uno dei componenti della struttura iperfine in un sale paramagnetico (nel caso di spin effettivo $\frac{1}{2}$ per lo strato elettronico), o in silicio o in germanio con una impurità di donatore pentavalente o di accettore trivalente. Le espressioni pei parametri f_K si ottengono anche per la stessa saturazione parziale di tutti i componenti della struttura iperfine. Si tiene conto del contributo dei termini di non-contatto nel rilassamento nucleare per lo spin $\frac{1}{2}$. Si esaminano anche i metodi per la misura dei parametri f_K.

(*) *Traduzione a cura della Redazione.*

Zur Bestimmung des Isotopengehaltverhältnisses $^{238}U/^{234}U$ mit Alphaspektrometern.

F. I. Havliček

J. Stefan Institut - Ljubljana

(ricevuto il 13 Ottobre 1958)

Zusammenfassung. — Es wird ein Alphaspektrometer für Elektronensammlung zur Bestimmung des Isotopengehaltverhältnisses $^{238}U/^{234}U$ beschrieben und seine Genauigkeit im Falle der Bestimmung des Konzentrationsverhältnisses der Uranisotope nach Verdampfung von Uranhexafluorid gezeigt.

Wegen der nur geringfügigen Menge der Isotope ^{235}U und ^{234}U neben ^{238}U im natürlichen Uran, sind zur Bestimmung schwacher Anreicherungen nur sehr hochentwickelte Massenspektrometer geeignet. Begnügt man sich hingegen mit der Bestimmung der Zusammensetzungsverschiebung in Bezug auf nur eines der Isotope d.i. des ^{234}U gegen ^{238}U, so kann man dies tun, wenn man statt des Massenverhältnisses, die ev. Verschiebung der Intensität der Radioaktivität bestimmt.

Da ^{238}U und ^{234}U im natürlichen Uran in radioaktivem Gleichgewicht stehen, wird eine, wenn auch kleine Verschiebung des Mengenverhältnisses dieser Isotope hier voll zum Ausdruck kommen und nicht so leicht, wie bei der Massenspektrometrie, durch die relativ sehr kleinen Mengenanteile der Nebenisotope verdeckt werden.

Cassignol [1] verwendet Alphaspektrometer zur Bestimmung der Mengenverschiebung des ^{235}U. (Dies geht aus kurzen Bemerkungen hervor, doch ist damit zu rechnen, daß wegen der Nähe der Energien der anderen Isotope im

[1] Ch. Cassignol: *Proc. Intern. Symp. Isotope Separation* (Amsterdam, 1958), p. 631

Abb. 1. – Ionisationskammer zur Bestimmung der Verschiebung des Mengenverhältnisses $^{238}U/^{233}U$.

Spektrum, man nur sehr dünne Präparate verwenden kann, was bei der Bestimmung von nur kleinen Isotopenzusammensetzungsverschiebungen außerordentlich lange Meßzeiten bedingt.) Auch sonst werden Alphaspektrometer, soweit es sich um entsprechend radioaktive Stoffe handelt, mit Erfolg z. B. von FACCHINI und seinen Mittarbeitern zur Bestimmung von kleinen Mengen schwerer Elemente verwendet ([2,3]).

Die im Folgenden beschriebene Apparatur ist in erster Linie zur Bestimmung möglichst kleiner Isotopenverschiebungen ^{234}U gegen ^{238}U entwickelt worden. Sie besteht aus einer Ionisationskammer für Elektronensammlung, einem Vorverstärker, einem linearen Verstärker, einem Einkanalanalysator und Dekadenzählern, sowie Kontrolleinrichtungen zur Überwachung, d.i. einem Pulsgenerator und einem Oszillographen. Als Präparate dienen dünne elektrolytisch hergestellte Schichten.

1. – Die Ionisationskammer.

Der Zylinder der Ionisationskammer (Abb. 1) hat einen Durchmesser von 120 mm. Ein Teflon-Durchführungsisolator trägt die Kollektorplatte von 70 mm Durchmesser. Der Teflonisolator sitzt in einem Schutzring, der auf einem Isolator aus Plexiglas montiert ist. Der Isolationswiderstand zwischen Kollektor und Schutzring ist ca. $10^{14}\ \Omega$. 25 mm unter dem Kollektor ist das Frisch'sche Schutzgitter ([1]), das praktisch den ganzen Querschnitt des Zylinders ausfüllt; es ist durch Polyvinyl-Isolatoren abgestützt. Kollektor und Schutzgitter lassen sich mit dem Deckel der Kammer abheben. Durch diesen Deckel geht auch der Isolator, durch den die Spannungszuführung für das Schutzgitter geht.

Die Kapazität des Kollektors beträgt ca 8 pF. Die Kapazität des Gittereingangs des Vorverstärkers beträgt auch ca 8 pF, insgesammt also rund 16 pF. Im Falle von Alphateilchen eines ^{210}Po Präparats, mit einer Energie von 5.3 MeV erhält man in Argon, mit einer Ionisationsspannung von 29 V, ~180000 Ionenpaare: dies gibt am Kollektor eine Spannungsänderung von 1.8 mV für ein Alphateilchen. Der Verstärkungsfaktor des Vorverstärkers war 7, der des linearen Verstärkers 5000, insgesammt also 35000. Bei kleiner Integration im linearen Verstärker lag die Spitze des Spektrums entsprechend bei 65 V.

Das Schutzgitter, das 55 mm über der Ebene des Präparats liegt, hat eine Teilung von 5 mm und einen Drahtdurchmesser von 0.1 mm. Man kann

([2]) U. FACCHINI, M. FORLE, A. MALVICINI und T. ROSSINI: *Nucleonics*, **14**, 126 (1956).

([3]) R. DUGNANI, U. FACCHINI, I. IORI, F. G. HOUTERMANS und E. TONGIORGI: *Study on Alpharadioactivity in low concentration* (Publ. CISE, Milano, 1957).

demnach mit einem Sigma der Gauß'schen Verteilung um die Spitze der Spektren von $\sim 0.6\%$, wegen der Influenz durch die Ionenladungen durch das Schutzgitter rechnen ([4]). Dies ist für die vorliegenden Zwecke der Ionisationskammer ausreichend. Die Spannung am Kollektor lag bei den Messungen zwischen 1 600 und 1 400 V, die am Schutzgitter zwischen 600 und 350 V.

Am Zylinder der Ionisationskammer sind auch zwei Stutzen für die Gaszufuhr vorgesehen, sowie eine Einrichtung zur Gasreinigung, die aus einer Kammer mit geheiztem Kupfer besteht. Diese wurde aber bei den Messungen nicht verwendet (Siehe unten). Der Füllgasdruck betrug rund 1 ata. Die Ionisationskammer sitzt exzentrisch auf einer flachen Kammer in der sich ein Drehteller mit vier Abteilungen zur Aufnahme der Präparate befindet. Zwischen den Abteilungen sind Stege vorgesehen um Strahlungen von einer Kammer in die andere hinüber zu vermeiden. Die einzelnen Abteilungen haben Zentriervertiefungen und können Präparate bis zu einem Durchmesser von 110 mm aufnehmen. Gegenüber der Ionisationskammer ist die Einsatzöffnung der flachen Kammer für die Präparate. Die Lage des Drehtellers kann von außen nach einer Gradeinteilung auf einer Scheibe eingestellt werden. Die einzelnen Teile sind Vakuumdicht mit normalisierten Ringen aus synthetischem Gummi miteinander verschraubt. Die Einrichtung wird vor der Füllung mit Argon mehrere Stunden lang auf 0.1 bis 0.05 Torr evakuiert.

2. – Das Füllgas.

Als Füllgas kommt in erster Linie wegen seiner niedrigen Ionisationsspannung Argon in Frage. Geeignet ist oft normaler, besser nachgereinigter Schweißargon. Nach Facchini und Malvicini ([5]) ist ein Zusatz von 2% Stickstoff vorteilhaft. Ein derartiges Gemisch verträgt, ohne merklichen Einfluß negativer Ionen zu zeigen bis zu 0.25% Sauerstoff. Da Luft nur 20% Sauerstoff enthält, konnte diese Erfahrung bestätigt werden, indem vor der Füllung mit Argon etwas Luft in die Kammer eingelassen wurde. Außerdem wird nach Valladas ([6]) ein Zusatz von etwa 1.5% Kohlensäure vorgeschlagen. Versuche zeigten, daß man im Stande ist, durch Vorfüllung der Kammer mit hinreichend reiner Kohlensäure, die Kammer in etwa 12 Stunden zu reinigen; die Verunreinigungen normaler Industriekohlensäure machen jedoch oft Schwierigkeiten. Verwendet man diese Kohlensäure als Füllgas, so wird Kohlensäure und deren Verunreinigungen an den Präparaten stark adsorbiert und die Spektren werden sehr stark verbreitert. Bei porösen Uranpräparaten kann es sogar dazu kommen,

([4]) O. Bunemann, T. E. Cranshaw und I. A. Harvey: *Can. Journ. Res.*, A **27**, 192 (1949).

([5]) U. Facchini und A. Malvicini: *Nucleonics*, **13**, no. 4, 36 (1955).

([6]) G. Valladas: *These-Rapport C.E.Aa.*, no. 483 (Saclay, 1955).

dass die gesamte Alphradioaktivität praktisch bis auf einen breiten Hintergrund ausgelöscht wird. Evakuiert man aber mehrere Stunden, so erhält man nacher mit Argon die zu erwartenden Spektren.

Die Kohlensäure als Reinugungsgas läßt auch ohne weiteres die Verwendung von Gummidichtungen zu, die sonst oft sehr langes Ausgasen verlangen.

Die Wirkung der Kohlensäure, läßt sich durch die Annahme, daß sich metastabile Molekülkomplexe zwischen der Kohlensäure und den Verunreinigungen bilden erklären, die in die Kohlensäurefüllung, in die Kammer hinein, gelöst werden. Die Reinigung mit Kohlensäure erübrigte auch die Verwendung der Gasreinigungseinrichtung mit geheiztem Kupfer.

Bei den Versuchen wurde stets anfangs Argon oder Argonstickstoffgemisch durch die Kammer durchgeblasen. Es flossen hiebei etwa 100 cm^3/min durch. Auf diese Weise wurde in den ersten Stunden etwa jede halbe Stunde die Kammerfüllung erneuert. Dann ließ man das Durchströmen von selbst aufhören, was bei geringen Mengen fast immer eintritt, wenn das Reduzierventil nicht nachreguliert wird. Die strömende Menge wurde kontrolliert, indem man sie durch Wasser durchperlen ließ und von Zeit zu Zeit das Gas in einem umgestülpten Becherglas auffing und die Füllzeit maß. (Versuche mit einem Argon, 2% Sickstoff, 2% Kohlensäuregemisch sind beabsichtigt.)

3. – Die Uranpräparate.

Quantitativ reproduzierbare dünne Uranschichten, lassen sich am besten elektrolytisch ([7-9]) herstellen. Als Unterlage wird hiebei insbesondere Platinblech vorgeschlagen. Weiter kommt Nickel u.a. in Betracht. Um die Platten gründlich mit Salpetersäure reinigen zu können, wurde widerstandsfähiger nichtrostender Stahl gewählt. Die Schwierigkeiten liegen in der Herstellung einer gut haftenden und möglichst gleichmäßigen, sowie verhältnismäßig dicken Schicht. Angeätzte Platten nehmen die Schicht sehr gut an, führen aber wegen der unebenen Unterlage zu schlechter Geometrie der Schicht und in deren Folge zu verbreiterten Spektren. Weiter ist durch das Anätzen die Möglichkeit der quantitativen Reproduzierbarkeit der Schichten herabgesetzt.

Der Vorgang bei der Herstellung der Schichten war wie folgt:

1) Platten eines Durchmessers von 105 mm wurden genau eben gedreht und vorgeschliffen. Hierauf wurden sie optisch fein in Öl nachgeschliffen und mit Polierrot und Öl auf Pech poliert.

([7]) D. E. Hull: Decl. Doc. Manhattan Proj. P.B.-54219 (1946).
([8]) C. C. Casto: *Nat. Nucl. Energy*, Ser, VIII, vol. **1** (New York, 1950), p. 523.
([9]) E. Würger, K. P. Meyer und P. Huber: *Helv. Phys. Acta*, **30**, 157 (1957).

2) Gereinigt wurden sie zuerst 30 min in konzentrierter Salpetersäure. Nachden sie gründlich in destilliertem Wasser gespült wurden, wurden sie mit feuchtem Berlinerkalk abgerieben. Beim Abreiben wird ausschließlich Zellstoffwatte verwendet, da Baumwollwatte Fett enthält. Hierauf wird mit destilliertem Wasser und Zellstoffwatte die Platte vom Berlinerkalk gereinigt und nachbespült; zum Schluß wird die Platte mit etwas Azeton P.A. übergossen. Die Rückseite kann mit Lack gespritzt werden.

3) Eine Reihe von Versuchen ergab als geeignete Elektrolytlösung Folgendes: Die Lösung A besteht aus 500 cm^3 destilliertem Wasser 5.41 g Ammonoxalat P.A. der Ammoniak zugesetzt wird bis die Lösung ein pH 9 hat. Die Lösung B erhält man durch Zusatz von 30 mg Uranylnitrat und Zugeben von Ammoniak bis bie Lösung wieder pH 9 hat.

4) Die Einrichtung zum Aufbringen der elektrolytischen Schicht besteht aus einer elektrischen Heizplatte von 600 W auf der ein Becherglas von 2 l steht. Hierin schwimmt in Wasser ein zweites Becherglas von 1.5 l, auf dessen Grund die Stahlplatte liegt. Die elektrische Zuleitung des Minuspols eines 12 V Akkumulators geht durch einen Stahldraht, der mit einem Polytenschlauch isoliert ist. Die andere Elektrode ist eine Platinplatte von $\sim$ 50 mm Durchmesser, die mit 500 Umdrehungen/min drehbar, 55 mm über der Stahlplatte montiert ist. Ihre elektrische Zuleitung ist ein Platindraht. Um die Wirbelbildung herabzusetzen, ganz vermeidbar ist sie nicht, ist quer über die Platte, in einem Polytenschlauch isoliert, ein Stahldraht in einer Höhe von 15 mm angebracht.

5) Das Aufbringen der elektrolytischen Schicht erfolgt, indem das Bad A auf 80 °C geheizt wird und 20 min Strom durchgelassen wird. Hierauf erfolgt der Zusatz von Uranylnitrat und Ammoniak B und der Strom wird auf 40 mA/cm^2 genau einreguliert. Ein Amperestundenzähler dient zur Kontrolle. Auf diese Weise erhält man nach 40 min Schichten mit $\sim$ 0.12 mg Uran/cm^2 die etwa 75 Alphateilchen/cm^2 min geben. Dünnere oder dickere Schichten erhält man indem man die Zeiten ändert und hiebei ev., auch die Menge von Uranylnitrat entsprechend, aber nicht zu sehr ändert. Bei den Versuchen wird der immer etwas ungleichmäßige Rand durch einen zentrierten Ring von 85 mm Durchmesser verdeckt.

Es lassen sich so Schichten bis 0.18 mg Uran/cm^2 herstellen. Die Schichten über 0.12 mg Uran/cm^2 halten nicht mehr gut, insbesondere zerfallen sie bald in Kohlensäureatmosphäre in kleine Plättchen.

Kontrolliert wird die Dicke der Schichten durch die Interferenzfarben der konzentrischen Ringe auf den Schichten, wobei die Dicke auf Wellenlängen in Luft bezogen wird (Siehe Abb. 2).

Abb. 3 zeigt die Abhängigkeit der Schichtdicke von der spezifisch aufgebrachten Uranmenge. Es zeigt sich, daß der lineare Verlauf des Diagramms hinter 0.12 mg/cm² abbricht. Wie oben angeführt, ist dies auch die Grenze für die gute Haftfähigkeit der Schicht.

Die Umrechnung der Teilchenzahl/cm² min auf die entsprechende Uranmenge/cm² erfolgt nach den Angaben von HULL (⁷).

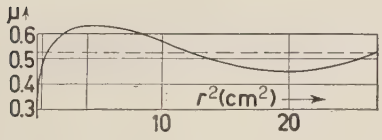

Abb. 2. – Profil einer elektrolytischen Schicht von ca 0.116 mg Uran/cm², bezogen auf Wellenlängen in Luft.

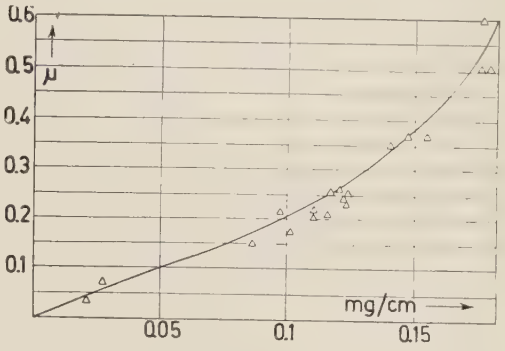

Abb. 3. – Abhängigkeit der Schichtdicken bezogen auf Luft von der aufgebrachten Uranmenge.

Eine elektronenoptische Prüfung der Oberfläche der Schichten unter 0.12 mg Uran/cm² zeigte die gleiche Struktur wie die optisch fein polierten Platten. Ausserdem wurde versucht durch Elektronenbeugung die Molekularstruktur der Schichten zu bestimmen. Neben wenig UO_2 konnte ein größerer Anteil U_3O_8 neben noch Ungeklärtem festgestellt werden.

Das Uranspektrum läßt sich wie Abb. 4 zeigt, in seinen wesentlichen Zügen nachrechnen, wenn der Einfluß der Schichtdicke berücksichtigt wird.

Nimmt man genähert eine lineare Energie E-Reichweite d Abhängigkeit für die Alphateilchen an, und bezieht die Energie auf die, am Einkanalanalysator gemessenen Spannung in volt, so ist für Uran im Mittel, wenn man auf das mittlere

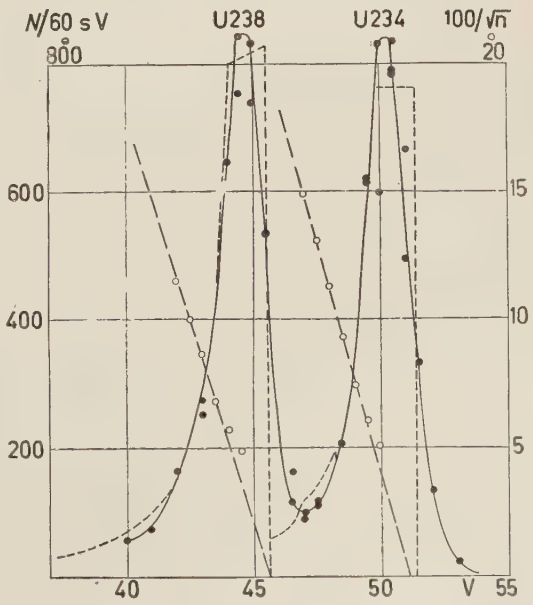

Abb. 4. – Vergleich gemessener und gerechneter Uranspektren.

Isotop ^{235}U sich bezieht, z.B.

$$E/d = 44.4/2.93 = 15.1 \text{ V/cm} .$$

Bezieht man weiter die Luftdichte auf die Dichte von U_3O_8 und danach die entsprechenden Dicken der Schichten gemäß einem Verhältnis 8.3/0.00129 also 6430, so folgt der Umrechnungsfaktor K für U_3O_8 mit

$$K = 0.97 \cdot 10^5 \text{ V/cm} .$$

Aus den Daten für den Zerfall der Uranisotope, kann man weiter die Teilchenzahl R für ^{238}U und ^{234}U sowie für ^{235}U errechnen, die in einer Schicht von 1 cm/Dicke/cm² in der Minute bei natürlicher Uranzusammensetzung entstehen. Es ist

$$R = 5.20 \cdot 10^6/\text{cm}^3 \text{ min } ^{238}U \text{ oder } ^{234}U .$$

Ist nun D die Dicke der Schicht, E_0 die Zerfallsenergie der Teilchen, so erhält man eine Verteilungsfunktion φE als Funktion der Energie mit

$$\varphi = R/4K ,$$

für Energien E zwischen $E = E_0$ und $E \geqslant E_0 - DK$. Für Energien $E \geqslant E_0 - DK$ ist die Verteilungsfunktion

$$\varphi = RD^2K/4(E_0 - E)^2 .$$

Für den Fall des Spektrums nach Abb. 4 gab die Schicht der Oberfläche F 57 cm², 68.5 Teilchen/cm² min, entsprechend 0.128 mg U_3O_8/cm². Die Schichtdicke D ist also $1.56 \cdot 10^{-5}$ cm und das DK 1.52 V.

Danach ist also für den konstanten Teil der Verteilungsfunktion

$$FR/4K = 763 \text{ Teilchen/min V}; \; ^{238}U \text{ oder } ^{234}U .$$

Die Konstante des zweiten Teils der Verteilungsfunktion ist

$$FRD^2K/4 = 1\,750 .$$

Mit diesen Werten sind die Spektren, idealisiert für die Abb. 4 gerechnet worden. Bezogen wurde auf $E_{0\,^{238}U} = 41{,}8$ V; $E_{0\,^{234}U} = 47{,}6$ V; sowie $E_{0\,^{235}U} = 44.4$ V (4.1 % der Höhe der Spektren von ^{234}U und ^{238}U). Die gerechneten Spektren wurden superponiert und über die gemessenen Spektren geschoben, wobei sich die kurz gestrichelte Linie ergab.

Die Meßwerte des Spektrums, volle Kreise, wurden durch einen glatten Linienzug ausgeglichen und für die linken Flanken die hundertfachen Werte der reziproken Werte der Wurzeln der Teilchenzahlen aufgetragen; leere Kreise. Gemäß der Verteilungsfunktion haben diese Punkte auf Geraden zu liegen, lang gestrichelte Geraden, deren Neigung die Konstanten des zweiten Teils der Verteilungsfunktionen sind und deren Schnittpunkte mit der Abszisse, auf den nicht durch Absorbtion verringerten Energiewerten der entsprechenden Alphateilchen zu liegen haben. Die sich hier ergebenden Konstanten sind für ^{238}U, 1940 und für ^{234}U, 1534.

Diese Untersuchung ist im Hinblick auf die Bestimmung des Verhältnisses der Isotopengehalte von Interesse. Einerseits zeigt es sich, daß die wirklich gemessenen Spektren, die wohl hauptsächlich durch die Influenz der Ionen in der Kammer durch das Frisch'sche Gitter und durch die Störungen am ersten Röhrengitter des Vorverstärkers diffus verbreitert sind im Wesentlichen den erwarteten Verlauf haben und weiter läßt sich im Voraus das Verhältnis der Teilchenzahlen errechnen das zu erwarten ist, wenn man die Zahl der Teilchen mißt mit Energien die größer sind als die, der die Lage des Sattels entspricht und diese Teilchenzahl mit der gesammten Teilchenzahl vergleicht.

Für die Flächen der gerechneten Verteilungen, die den gemessenen Teilchenzahlen entsprechen, ist für das konstante DK Gebiet

$$FDK \cdot R/4K ,$$

und für das Gebiet zwischen der DK Grenze und einer bestimmten Energie, E, hier der Sattelenergie

$$FRD^2K/4 \cdot (1/DK - 1/(E_0 - E)) .$$

Addiert ergibt sich

$$RD/2 - RD^2K/4(E_0 - E) .$$

Für Schichten von D $1.5 \cdot 10^{-5}$ cm Dicke ist bei einer Sattelenergie von 43 V das Verhältnis, wenn man den Anteil des ^{235}U hier vernachlässigt 0.421.

Weiter ist es auch möglich, den Einfluß einer Änderung der Dicke der Schicht um ΔD auf das obige Verhältnis zu errechnen. Es folgt hiebei der Korrekturfaktor

$$1 - (\Delta D/D)(2(E_0 - E)/DK - 1) .$$

Diese Formel ließ sich quantitativ nur schlecht bestätigen. Der Grund dafür ist neben der vereinfachenden Annahme E/d = konst vor allem darin,

daß die Struktur der elektrolytischen Schicht nicht genügend geklärt ist und eine erste Näherung mit der Annahme von homogenem U_3O_8 sicher nicht ausreicht um Feinheiten quantitativ darzustellen. (Weitere elektronenoptische Untersuchungen der Schichten sind im Gange).

4. – Der elektronische Anschluß.

Die Elektronensammlung am Kollektor erzeugt negative Spannungsänderungen von etwas weniger als 2 mV für ein Alphateilchen. Diese werden auf das Eingangsgitter des Vorverstärkers, vom hohen Potential des Kollektors über einen Teflonkondensator übertragen. Dieser Kondensator wurde auf 0.25 mm starke Teflonfolien mit Kupferblech, bei einem Durchmesser von ~ 10 mm und einer Länge von 77 mm gewickelt. Seine Kapazität ist etwa 400 pF, sein Isolationswiderstand rund $10^{14}\ \Omega$.

Die Auslegung wurde nach den Gillespie'schen Richtlinien ([10]) durchgeführt; zwecks Einstellung auf ein optimales Eingangsstörung-Vorverstärkerverhältnis wurde nach Valladas ([6-11]) der Heizstrom der ersten Röhre fein reguliert. Günstig hat sich bei der Röhre EF 36 ein Vorschaltwiderstand von 30 Ω erwiesen. Es fließt dann ein Anodenstrom von ca 30 mA, die im Anodenkreis liegenden Widerstände reduzieren die Anodenspannung der ersten Röhre auf etwa 30 V und der Verstärkungsfaktor ist knapp über 7. In diesem Gebiet ist die Verstärkung auch am wenigsten vom Anodenstrom, bzw. Heizstrom abhängig. Die Köpfe der Röhren wurden mit Azeton P.A. sorgfältig gereinigt und der Widerstand am Steuergitter beträgt etwa 10^{12} V (die erste Röhre soll durch eine besondere Elektrometerröhre ersetzt werden).

Wie das Schema, Abb. 5 zeigt ist besondere Aufmerksamkeit einer gründlichen Filterung gegeben worden. Um wahlweise positive oder negative Pulse zur Verfügung zu haben, ist am Ausgang ein Permalloy-Transformator vorgesehen, der auch die Eingangsgeräusche bei der Übertragung zur linearen Verstärkung hinüber herabsetzt. Der gesamte elektronische Anschluß ist sorgfältig abgeschirmt und geerdet. Seine Anordnung ist aus Abb. 1 ersichtlich.

Zur Kontrolle dient ein Pulsgenerator, der über eine kleine Antenne seine Signale auf den Leiter zum Kollektor der Ionisationskammer überträgt; er kann so auch während der Messung zur schnellen Überprüfung eingeschaltet werden. Seine Frequenz ist etwa 100 Hz. Hiedurch sind scharfe Pulse möglich,

([10]) A. B. Gillespie: *Signal, Noise and Resolution in Nuclear Counteramplifiers* (London, 1953).

([11]) G. Valladas: *Onde Electrique*, **33**, 615 (1953).

wenn ein Permalloy-Transformator die Pulse der Glimmröhre OA3 überträgt; es wird so nur das scharfe Abreissen übertragen.

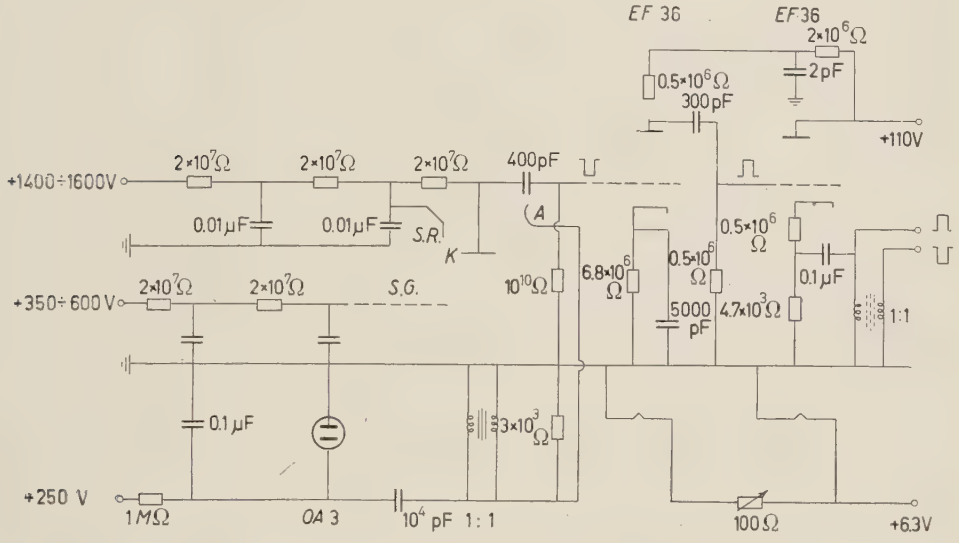

Abb. 5. – Schema des elektronischen Anschlusses. *K*, Kollektor; *SG*, Schutzgitter; *A*, Antenne; *SR*, Schutzring.

Alle Anschlußspannungen sind stabilisiert, die Heizung der Röhren geschieht durch eine Akkumulatorenbatterie die dauernd nachgeladen wird.

5. – Die Durchführung der Messungen.

Gleichzeitig mit dem Beginn des Evakuierens der Ionisationskammer, werden Vorverstärker, linearer Verstärker und Einkanalanalysator eingeschaltet. Nach drei Stunden wird die Kammer gefüllt und mit den Kontrollmessungen begonnen. Zuerst wird die Lage der Pulse des Pulsgenerators gemessen und diese weiter von Zeit zu Zeit überprüft, bis sie sich nicht mehr ändert. Dann werden die Spektren der beiden Uranpräparate gemessen die verglichen werden sollen und hiebei kontrolliert, ob sie sich überdecken; insbesondere im Sattelpunkt. Allenfalls wird auch ein Polonium 210 Präparat zur Kontrolle des Füllgases gemessen. Sind diese Messungen befriedigend ausgefallen, wird ein Diagramm der Pulszahlen über Niveaus die von Volt zu Volt gestuft sind für eines der Uranpräparate gemessen. Die Nähe des Sattelpunkts wird hiebei besonders sorgfältig untersucht um den Inflexionspunkt des Diagramms zu bestimmen, auf den hierauf der Analysator eingestellt wird. Diese Messungen

dauern etwa zwei Stunden und danach ist auch gewöhnlich der Temperaturausgleich der elektrischen Einrichtungen hinreichend erfolgt. Siehe Abb. 6.

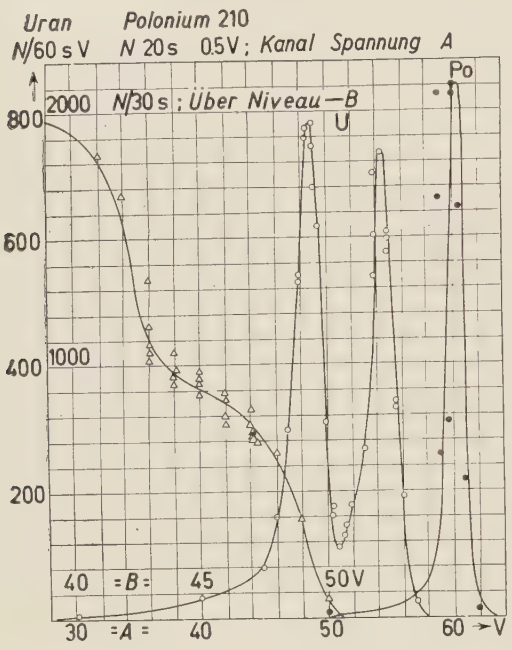

Abb. 6. – Diagramm der Kontrollmessungen für die Bestimmungen der Mengenverhältnisse.

Die eigentlichen Messungen erfolgen so, daß abwechselnd je fünf Minuten lang für beide Präparate die verglichen werden sollen, die Pulszahlen über dem eingestellten Analysatorniveau einerseits, meist um 8400/5 min und die Gesamtzahl der Pulse, das sind die, welche direkt nach der linearen Verstärkung von einem Dekadenzähler (seine Schwelle liegt bei 15 V) andererseits, etwa 20000/5 min gemessen werden.

Für diese Messungen wird der Quotient der gezählten Pulse gerechnet der um 0.42 liegt. Um nun die langsamen Änderungen in der Apparatur auszugleichen (eine Temperaturstabilisierung des Meßraumes ist beabsichtigt) wird weiter der Mittelwert zweier konsekutiver Messungen eines Präparats berechnet und dieser mit der Messung am anderen Präparat, deren Wert zwischen den beiden genannten liegt verglichen.

Wurden so zwei Präparate von natürlichem Uran verglichen, so ergab sich gemäß den, den Pulszahlen entsprechenden Statistiken ein Verhältnis der Quotiente um eins.

Zum Beispiel wurden zwei Präparate von natürlichem Uran verglichen, wobei bei der zweiten Hälfte der Messungen am andern Tag die Lage der Präparate in den Kammern alterniert wurde. Für 2·28 Messungen zu je 5 min, also bei einer Gesamtstatistik von rund einer Viertelmillion Pulsen, folgte statt eins, ein Verhältnis von

$$0.9967 \pm 0.0023 .$$

6. – Messungen an destilliertem Uranhexafluorid.

Da keinerlei Angaben über Messungen einer ev. Isotopenseparation beim Verdampfen und bei fraktionierter Destillation von Uranhexafluorid vorliegen,

und nach der Clausius-Clapeyron-Sackur-Tetrode'schen Formel für das Druckverhältnis der Dämpfe der Uranisotope nach dem Massenverhältnis allein, ein Trennfaktor von größenordnungsweise 1 % zu erwarten ist, wurden Abdampfversuche in bewegten Behältern und Destillationsversuche in üblichen Laboratoriumskolonnen, thermisch etwas über dem Tripelpunkt gemacht. (Der Einfluß des Ganges der spezifischen Wärmen, soweit sie sich nach den bekannten Schwingungsspektren für Uranhexafluoridgas [12] errechnen lassen, liegen wesentlich unter dem Masseneffekt und auch die nach der neuen Baertschi-Kuhn'schen Theorie [13] gerechnete Korrektur beträgt nur etwa 20%, wenn man neben den sonst nötigen Angaben [12] noch das Verhältnis der Molekülpolarisationen für das Ultraviolette und das infrarote Gebiet auf 1:10 schätzt. Die Unsicherheit eines großen Teils der Konstanten, z.B. der Schwingungsspektren im festen Uranhexafluorid — die Debye'sche Theorie führt nur zu sehr unvollkommenen Resultaten — ermöglicht für den vorliegenden Zweck keine bessere Diskussion).

Die einzelnen Vergleichsmessungen, die mit verschiedenen Abdampf und Destillationfraktionen durchgeführt wurden, ergaben ähnliche Resultate wie die oben angeführten mit natürlichem Uran in den beiden Kammern. Ein Separationseffekt kann deshalb nach solchen Einzelmessungen nicht besser als 0.25% sein.

Stellt man wie folgt, die Messungen an einzelnen Fraktionen zusammen, so zeigt es sich, daß man bestenfalls mit einem noch kleineren Separationsfaktor rechnen muß. Es ergab sich im einzelnen:

1) Vergleich einer kleinen abgedampften Menge mit natürlichem Uran gab den Faktor 1.000 ± 0.005.

2) Vergleich einer kleinen abgedampften Menge mit einer rund auf ein Viertel eingedampften Menge gab den Faktor 0.998 ± 0.002.

3) Vergleich einer kleinen Fraktion aus einer Destillationskolonne einer Länge von 600 mm und einem Durchmesser von 10 mm mit natürlichem Uran gab den Faktor 1.000 ± 0.0017.

4) Vergleich einer kleinen Fraktion aus einer Destillationskolonne von 120 mm Länge und 15 mm Durchmesser mit natürlichem Uran gab den Faktor 1.002 ± 0.002.

Die Fraktionen wurden etwa zehn Stunden nach erfolgter Inbetriebsetzung der Einrichtungen entnommen. Die Temperatur betrug 75 °C.

---

[12] I. I. Katz und E. Rabinowitch: *Nat. Nucl. Energy*, Ser. VIII, vol. 5 (New York, 1951), p. 396.

[13] P. Baertschi und W. Kuhn: *Helv. Chim. Acta*, 40, 1084 (1957).

Stellt man aus den Verhältnissen konsekutiver Einzelmessungen gemäß den unter 1) bis 4) angeführten Versuchen eine Statistik zusammen, so folgt nach einer Gauß'schen Darstellung, siehe Abb. 7 das Verhältnis 1.001 ± 0.001. (Die gestrichelte Gerade gilt für das Verhältnis eins — insgesamt sind es 87 gerechnete Verhältnisse.) Danach läßt sich also kein Trennfaktor über 1.001 erwarten.

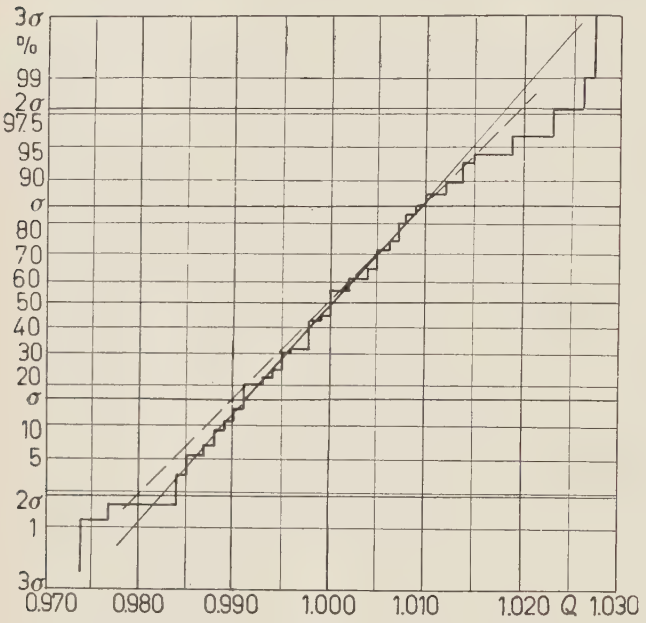

Abb. 7. – Gesamtstatistik der Messungen nach einfachem Abdampfen. (87 gerechnete Verhältnisse); Mittelwert 1.001 ± 0.001.

Ferner wurde ausgehend von einer Menge von ~300 g Uranhexafluorid in der 600 mm Kolonne die Hälfte abgedampft. Mit dieser Hälfte wurde die Kolonne neu gefüllt und wieder die Hälfte abgedampft. Von dieser Hälfte wurde aus einem bewegten Behälter abermals die Hälfte abgedampft und schließlich davon noch einmal ein Teil, ~7 g abgedampft. Mit der so erhaltenen Fraktion wurden zwei Meßreihen durchgeführt, die ein Verhältnis von $1.002 \pm 0.001\,33$ ergaben; siehe Abb. 8. Die Statistik umfaßt hier 57 gerechnete Verhältnisse. Diese Messungen deuten bestenfalls auf einen Trennfaktor um 1,000 5 hin.

Man kann noch, wenn man dem Wert 1.001 ± 0.001 einfaches Gewicht und dem Wert

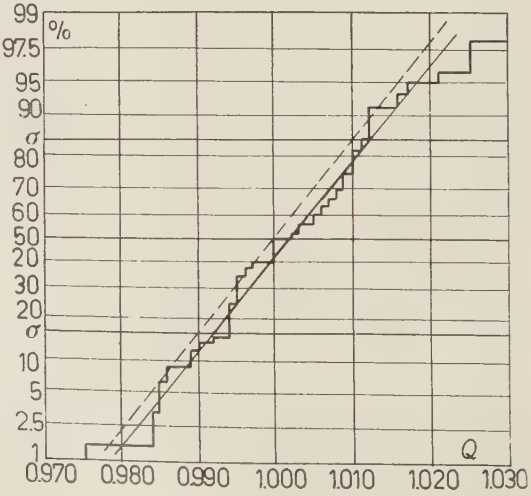

Abb. 8. – Gesamtstatistik der Messungen nach viermaligem Abdampfen. (57 gerechnete Verhältnisse); Mittelwert 1.002 ± 0.001.

$1.0005 \pm 0{,}000308$ vierfaches Gewicht zuteilt — die Statistiken haben ungefähr gleiche Mengen von gemessenen bezw. gerechneten Verhältnissen — ein Mittel rechnen und erhält

$$1.0006 \pm 0.0002 .$$

Die Untersuchungen an Uranhexafluorid ergaben also, daß der theoretisch zu erwartende Trenneffekt nicht eintrat, daß auch sonst in den Kolonnen keinerlei Vervielfachen eines primären Effekts auftrat, und daß wahrscheinlich ein eventueller Trenneffekt nicht größer als 0.05% pro Stufe ist, der für praktische Anreicherung wohl zu klein ist.

* * *

Herr K. Cotman der Elektronischen Abteilung des Instituts hat den Linearen Verstärker und die Dekadenzähler gebaut und sich auch um ein einwandfreies Arbeiten der schon vorher im Institut gebauten Einkanalanalysatoren bemüht. Das Uranhexafluorid wurde in Laboratorium des Herrn Prof. Dr. B. Brčić im Institut hergestellt. Herr Dipl. Ing. V. Marinković besorgte die elektronenoptischen Untersuchungen.

Fräulein M. Modesto hat wesentlich zur Herstellung der elektrolytischen Schichten beigetragen, sie leistete auch die gesamte chemisch-präparative Arbeit und von ihr und Herrn J. Sterle, der auch alle Instandhaltungsarbeiten der Apparaturen besorgte, wurden die Destillationsversuche durchgeführt. Herr S. Sterbal war anfangs am Projektieren und bei der Aufstellung des Alphaspektrometers beteiligt. Alle Metallarbeiten wurden von der mechanischen Werkstätte des Instituts unter der Leitung des Herrn R. Petkovšek durchgeführt.

Herr Prof. Dr. U. Facchini der CISE, Mailand gestattete eine eingehende Besichtigung der von ihm gebauten Alphaspektrometer. Herr Prof. Dr. W. Kuhn, Basel korrespondierte bereitwillig über theoretische Destillationsfragen. Herr Prof. Dr. Ch. Cassignol, Saclay stellte freundlicher Weise Separata der von seinen Mitarbeitern veröffentlichten Arbeiten über Alphaspektrometer zur Verfügung.

Allen oben genannten ist herzlich zu danken.

RIASSUNTO (*)

Si descrive uno spettrometro α raccoglitore di elettroni per la determinazione del rapporto $^{238}U/^{234}U$ fra gli isotopi dell'uranio e se ne dimostra l'esattezza per la determinazione del rapporto di concentrazione degli isotopi dell'uranio dopo l'evaporazione di esafluoruro di uranio.

(*) *Traduzione a cura della Redazione.*

IL NUOVO CIMENTO Vol. XI, N. 2 16 Gennaio 1959

Investigation of Accumulation and Persistence Time of Ultrasonic Striation Grating of Starch Suspensions in Liquids.

B. Ramachandra Rao and C. Krishnamurty

Department of Physics, Andhra University - Waltair

(ricevuto il 20 Ottobre 1958)

Summary. — A quantitative study of the phenomena of accumulation of particles in stationary ultrasonic fields and the persistence of striation grating after stopping the ultrasonic waves, has been made with reference to its dependence on the particle size and the nature of the suspension employed. Observations of the variation of accumulation time with grain size are shown to be in agreement with the theoretical deductions from King's investigations of acoustic radiation pressure on spheres. The variation of persistence time with viscosity in Agar Agar sol as it sets to a gel and finally the formation of a permanent striation grating of starch suspensions in Agar Agar gel is also studied.

1. – Introduction.

The best known ponderomotive effect of sound waves is the accumulation of solid particles in the nodal or antinodal planes of a field of stationary sound waves in liquid systems. Accumulation occurs at the nodes of pressure if the dispersed substance is less dense than the medium of dispersion; and at the antinodes if it is denser. This effect has been investigated carefully by Boyle and his collaborators [1] who have shown that the particles take a finite time to get accumulated at the planes of the nodes or antinodes. Söllner and Bondy [2] have studied the dependence of the rate of accumulation of dispersed substances at the nodes or antinodes on the size of the particles and found qualitatively that the time for the accumulation increases with decreasing

(1) R. W. Boyle: *Nature*, **120**, 476 (1927).

(2) K. Söllner and C. Bondy: *Trans. Far. Soc.*, **32**, 616 (1936).

size of the particles. They have used a horizontal narrow tube containing the suspension with the ultrasonic waves propagated along the lengthwise direction when it is found that the particles settling in the liquid accumulate in equidistant planes which are half wavelengths apart. We have taken up for investigation the more interesting case of formation of striations in a horizontal plane due to a vertical sound beam. In this investigation the dependence of accumulation time on size of the grains and also the viscosity of the liquid is studied quantitatively as no detailed investigation has so far been made on this aspect.

In addition to this phenomena of finite time of accumulation of microscopic suspended particles at the antinodes in case of starch suspensions in liquids, it is observed that the striation grating so formed will persist for a few seconds after stopping the ultrasonic waves. This phenomenon was studied by CARRELLI and PORRECA ([3]) in a different way by observing the persistence of even diffraction lines after stopping the ultrasonic waves. A detailed investigation of this phenomena of persistence of starch striation grating after stopping the ultrasonic waves has also been taken up with a view to study the dependence of persistence time on the size of the grains and the viscosity of the medium. An interesting feature of this investigation is the study of the variation of persistence time in Agar Agar sol as it sets to a gel and finally the formation of permanent striation grating of starch suspensions in the Agar Agar gel.

2. – Theoretical considerations.

The ponderomotive effects of sound waves were discussed by KING ([4]) from a theoretical analysis of the acoustic radiation pressure on spheres. It explained Boyle's observations and confirmed that radiation pressure is chiefly responsible for the accumulation of particles at the antinodal planes and that the higher the radiation pressure the more quickly the particles are driven to the antinodal planes. In this case the influence of supersonic waves to bring about accumulation must be sufficiently large so as to overcome the effect of gravity acting on the particles. Such a possibility will now be considered in detail following KING's analysis.

According to KING, the mean radiation pressure $\overline{P}$ on a sphere with radius « a » in a stationary ultrasonic field is given by

$$\overline{P} = \frac{4\pi^2 E a^3}{\lambda} \sin 2kz F(\varrho_0, \varrho_1) , \tag{1}$$

([3]) A. CARRELLI and F. PORRECA: *Nuovo Cimento*, **10**, 98, 883, 1466 (1953).
([4]) L. V. KING: *Proc. Roy. Soc.*, A **147**, 212 (1934).

where

$$F(\varrho_0, \varrho_1) = \frac{1 + \frac{2}{3}(1 - \varrho_0/\varrho_1)}{2/\varrho_0 + 1/\varrho_1},$$

ϱ_0 and ϱ_1 are the densities of the liquid and particles respectively, λ the wavelength of sound in the liquid, E the average energy density of the sound field, k is $2\pi/\lambda$ and z is the distance of the sphere from the nodal planes of pressure. This expression is valid for particles of very small size such that $ka \ll 1$. In this investigation, the maximum size of the starch grains is about 4 μm and the wavelength is about 1 mm so that this is fully satisfied.

The equation of motion of the spherical particle under the influence of the mean radiation pressure due to the sound beam alone can be written as

$$(M + M')\ddot{z} + \mu\dot{z} = \frac{4\pi^2 E a^3}{\lambda} F(\varrho_0, \varrho_1) \sin 2kz, \tag{2}$$

where M is the mass of the particle, M' is $(2/3)\mathrm{p}a^3\varrho_0$ and μ is the coefficient of frictional force due to viscosity of the medium. Using the Stokes formula

$$\mu\dot{z} = 6\pi\eta a\dot{z} \tag{3}$$

it can be easily shown that μ is much greater than $(M+M')$ for the small size of starch grains used in this investigation. Equation (2) therefore reduces to the simple form,

$$\mu\dot{z}_p = \frac{4\pi^2 E a^3}{\lambda} F(\varrho_0, \varrho_1) \sin 2kz. \tag{4}$$

The equation of motion of the particles under the influence of gravity alone can be written as

$$\mu\dot{z}_g = \tfrac{4}{3}\pi a^3(\varrho_1 - \varrho_0)g. \tag{5}$$

Dividing (4) by (5) we get

$$\frac{\dot{z}_p}{\dot{z}_g} = \frac{3\pi E}{\lambda} \frac{F(\varrho_0, \varrho_1) \sin 2kz}{(\varrho_1 - \varrho_0)g}. \tag{6}$$

This relation enables us to compare the velocities of particles due to the effects of sound pressure and gravity separately. For the case of starch grains in water $F(\varrho_0, \varrho_1)$ has a value of 0.6. For a wavelength of 1 mm and for low sound powers E of order of 200 ergs per second per cm it is found that the ratio of $\dot{z}_p/\dot{z}_g$ is sufficiently high for almost all the values of z except those corresponding to the nodes and antinodes. Though the value of this ratio is zero

in the vicinity of nodes, when once the particle goes down by gravity it comes into the field of the ultrasonic wave and will be drawn to the antinodes. We shall now consider the treatment of the equilibrium of the particles collected at antinodes neglecting gravity effect in order to simplify the treatment.

The accumulation time may be taken as the time taken by the particles near the nodal planes to arrive at the antinodal planes. Integrating the equation (4) between the limits z_1 and z_2 we get the relation

$$\frac{\mu}{2k} \log \frac{\operatorname{tg} kz_2}{\operatorname{tg} kz_1} = \frac{4\pi E a^3}{\lambda} F(\varrho_0, \varrho_1) t , \tag{7}$$

where t is the time taken for the migration of particles from z_1 to z_2 planes. As the time t becomes infinity for values of z_1 and z_2 exactly corresponding to the node and antinode respectively, we shall take $z_1 = \delta$ and $z_2 = (\lambda/4) - \delta$ the equation reducing then to

$$t = \frac{3\eta^2 \lambda^2 \log (1/k\delta)}{4\pi^2 E a^2 F(\varrho_0, \varrho_1)} , \tag{8}$$

where δ is a very small fraction of the wavelength.

It is obvious from this relation that the accumulation time varies inversely as the square of the radius of the particle and the mean energy density and directly as the square of the wavelength and the viscosity of the medium.

3. – Experimental details.

The ultrasonic generator used in this investigation is a conventional shunt-fed Hartley type of oscillator delivering an R.F. power of 10 W with an X-cut quartz crystal connected across the tank circuit. The oscillator covers a continuous frequency range of 1 to 12 MHz in three bands. The piezoelectric vibrator is mounted horizontally in a crystal holder of conventional design. A transparent hollow glass cube containg the liquid with starch suspension is placed underneath the crystal and the crystal holder height is so adjusted that the bottom surface of the crystal is just in contact with the surface of the liquid.

The set up used here is different from that of Sollner and Bondy in that the striation grating of starch suspension is formed in a vertical beam of ultrasonic waves. The particles remain in the antinodal planes overcoming the pull of gravity acting on them. The determination of the accumulation and persistence time of this suspension grating is made by a visual observation of the grating and noting the times with a stop watch. The observations are

repeated a large number of times to reduce the personal error in estimating the short time intervals.

For the study of the dependence of persistence and accumulation time on grain size, suspensions of different grain sizes are obtained by using the method of fractional floatation. Suspensions of fairly uniform size are obtained by this method and the average grain size is determined by using a high power Leica microscope with photographic arrangement. Samples of the liquid containing the suspensions are placed on a slide with a cover glass slip and the grains are photographed after high magnification on a 35 mm film along with a standard 2 mm transparent scale divided into 200 divisions. Using this cale, the diameters of the grains are determined by taking measurements of the photographs under a microfilm reader. As the grains are not perfectly spherical the mean diameter for each grain is measured and the average for all the grains is taken for the purpose of this study.

4. – Results and discussion.

4·1. *Effect of size of the grains.* – In order to study the grain size effect five different samples containing starch suspensions of different sizes in water are obtained by the method of fractional floatation and their accumulation and persistence times are determined. Table I gives the values thus obtained along with the values of mean radius a and $1/a^2$. The frequency of ultrasonic waves (1.4 MHz) and the power are maintained constant for throughout observation.

TABLE I.

Accumulation times in s	Persistence time in s	Mean radius of the grains in μm (a)	$1/a^2$
3.0	2.0	4.31	0.054
4.0	3.5	3.76	0.071
7.0	5.0	3.15	0.101
8.0	6.0	2.88	0.120
10.0	8.0	2.29	0.195

It may be noted that the accumulation time bears a linear relationship with the reciprocal of the square of the average radius of the grains in agreement with the theoretical deduction from equation (8). It may also be noted that the persistence time varies linearly as $1/a^2$, just as the accumulation time but no simple theoretical explanation could be given as this phenomenon depends in a complicated way on various factors. According to King's analysis, the particles which gather at the antinodes will oscillate across the

antinodal plane at a low frequency. Soon after switching off the ultrasonic waves the particles will cease to oscillate and the entire striation grating collapses and becomes a uniform suspension due to the combined effect of diffusion and gravity.

4·2. *Results in different suspensions.* – The formation and persistence of striations are studied in starch suspensions in different liquids in addition to starch in water at the same frequency of 1.4 MHz and the results are presented in Table II.

TABLE II.

Liquid	Density (g/cm^3)	Viscosity C.G.S. units	Accumulation time in s	Persistence time in s
Water	1.00	0.008	4	3
Nitrobenzene	1.26	0.02	7	6
Glycerine	1.26	3.5	120	30
Toluene	0.86	0.006	—	—
Benzene	0.87	0.007	—	—

Here, it may be emphasized that the essential requirement for the accumulation and persistence to occur is that the starch particles should form a good suspension in the liquid. Further, the ratio of the densities should be nearer the optimum value $= 10/13$. In cases of starch in Benzene and Toluene, no striation grating could be formed as the grains do not form a good suspension in the liquid. In case of starch in nitrobenzene the striations are as sharp as for the case of starch in water while for the case of starch in glycerine, the effect of viscosity being predominant the striation grating is formed very slowly. The dependence of accumulation time and persistence time on viscosity is obvious from the results presented in Table II, the effect being very predominant in the case of glycerine. The results for the case of accumulation time do not obey the linear dependence on viscosity shown in relation (8) possibly due to the grain size in this case being not quite uniform. No theoretical explanation was possible to explain the variation of persistence time with viscosity.

4·3. *Persistence of striation grating in Agar Agar sol.* – As viscosity plays an important role in the formation and disappearance of a striation grating in an ultrasonic field, a more detailed study of persistence and its dependence on viscosity is undertaken using Agar Agar sol whose viscosity increases while it sets to a gel. Persistence times are determined at different stages of gelatinization using starch as the suspension. To avoid fluctuations due to thermal

agitation observations were made after the Agar Agar sol has cooled down to nearly room temperature.

The Agar Agar sol is prepared by swelling a known amount of E. Merck Agar Agar fine powder, in water for 24 hours and it is then boiled and afterwards filtered through glass wool while hot. The Ostwald viscosimeter is used for the determination of viscosity at each stage of gelatinization.

The time of persistence of the striation grating and the viscosity of the sol are determined simultaneously at each state of gelatinization of the Agar Agar sol as it sets to a gel and the results are presented in Table III. The sol is formed by dissolving 2 g of Agar Agar in 400 cm^3 of water.

Table III.

Viscosity $\times 10^{-3}$ C.G.S. units	Persistence time in case (h)
8	3
10	5
11	7
13	180
20	> 1 hour

It is clear that the values of persistence time first increase slowly and then rapidly with the increase of viscosity. As the ratio of variation of persistence is much more rapid than the viscosity during sol-gel transformation, the latter part of the variation may not be due to viscosity but to gelation. The persistence time is very large in the gelatinized state, as the starch particles once driven to the antinodes by the ultrasonic beam are restricted to fall off even after removing the sound beam.

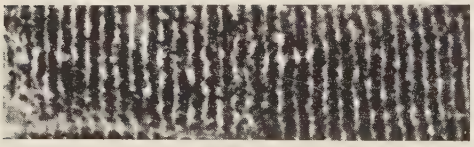

Plate 1.

It is interesting to note that the starch striation grating formed in an Agar Agar sol of high concentration just before setting, remains intact even if the ultrasonic beam is removed after the gel formation. Thus a permanent pattern of the striation grating of starch suspensions in Agar Agar gel is formed. A number of such patterns have been easily obtained at various frequencies. A very thin slice of one of these gels containing the permanent grating taken from the ultrasonic cell is placed on a glass plate and a magnified print of the same is obtained by placing it in an enlarger directly. A photograph of the starch striation grating thus obtained with a magnification of 4 is reproduced in Plate 1.

* * *

Our thanks are due to Prof. C. Venkata Rao, Head of the Department of Technology for kindly providing facilities to take microphotographs of starch grains.

RIASSUNTO (*)

In questo lavoro viene trattato il fenomeno dell'accumulazione di particelle solide in sospensione nelle posizioni dei nodi o dei ventri dei campi ultrasonori nei liquidi. Viene studiato in particolare il caso (finora trascurato) della formazione di piani di accumulazione orizzontali, in un campo di onde ultrasonore che si propagano verticalmente. Gli AA. determinano il tempo di accumulazione delle particelle nei piani nodali o ventrali e quello di permanenza dopo l'interruzione della sorgente ultrasonora, in funzione delle dimensioni delle particelle, della viscosità del mezzo e della densità del mezzo e delle particelle per una frequenza ed una intensità degli ultrasuoni tenute costanti. Precede uno studio analitico del problema, basato sull'impostazione data da King ed i risultati di tale studio teorico vengono confrontati con i dati sperimentali, mettendo in evidenza con chiarezza i limiti dell'accordo fra teoria ed esperienza.

(*) *A cura del prof.* I. Barducci.

Polarization Phenomena in Photoelectric Effect and One Quantum Annihilation of Positrons in the K-shell.

H. Banerjee

Department of Physics, Indian Institute of Technology - Kharagpur

(ricevuto il 21 Ottobre 1958)

Summary. — Polarization effects in the cross sections for both the photoelectric and the positron annihilation processes in the K-shell have been investigated by the Stokes parameter method for arbitrary polarization of the incident particles. The scattering states of the electron and the positron have been approximated by Sommerfeld-Maue wave functions. Results have been obtained correctly up to terms of $O(a)$ and neglecting terms of $O(a/\varepsilon)$, where $a=Z/137$ and ε is the energy of the scattering state in units of mc^2. It has been found for either case that in the first approximation there is correlation only between the circular polarization of the photon and the component of the polarization vector of the free Dirac particle in the plane of scattering. In the high energy limit, the ratio of the degree of circular polarization of the incident (emitted) radiation and the degree of longitudinal polarization of the photoelectron (positron) tends to unity.

1. – Introduction.

Effects of circular polarization of the incident photon in the photoelectric effect and longitudinal polarization of the positron in the one quantum annihilation process have been considered by McVoy [1]. The present work is intended to remove certain limitations in McVoy's paper, which have their origin in the assumptions made by him for simplifying the problem. The most serious of these limitations consists in the plane wave approximation of the scattering states of electron and positron. As has been pointed out in an earlier paper [2],

[1] K. W. McVoy: *Phys. Rev.*, **108**, 365 (1957).

[2] H. Banerjee: *Nuovo Cimento*. **10**, 863 (1958) Hereafter referred to as A.

this simplification gives rise to errors even in the approximation up to which Sauter's ([3]) results are valid. It is only in the extreme relativistic limit that the results of McVoy's calculations may be expected to agree with those of Sauter. This difficulty may be removed and at the same time polarization effects may very conveniently be included in our consideration by employing the Sommerfeld-Maue wave functions for the representation of the scattering states of electron and positron. In fact, following the calculations in A, one may proceed further and obtain the contributions to the polarization dependent parts of the cross sections from terms of relative order a, neglecting, of course, terms of relative $O(a/\varepsilon)$.

In view of recent works ([4-7]) on polarisation in different scattering processes, where the Stokes parameter technique has been successfully employed, it will be interesting to consider the polarization of the charged particles and radiation in the most general context. Besides furnishing us with formulae from which the results corresponding to longitudinally polarized electron or positron and circularly polarized radiation can be readily obtained, such general treatment would also enable us to compare our results with those of similar scattering processes. This may also help us in understanding the mechanism of the interaction between the spin angular momenta of different particles.

The Stokes parameter method of describing the polarization of electron, positron, and photon, which has been followed in the present work, has been briefly outlined in the following section with special reference to some points which are not very clear from earlier works. In section 3 the differential cross sections for photoelectric effect and one quantum annihilation of positrons have been given in terms of these parameters.

The notations employed in the following is that of A and a natural system of units has been adopted in which $m = c = \hbar = 1$.

2. – Polarization formalism.

As in eq. (5) of A, one may write the matrix element for the photoelectric effect in the K-shell in the form

$$M = C\bar{u}(p)Qw\,, \tag{1}$$

([3]) F. Sauter: *Ann. Phys.*, **11**, 454 (1931).

([4]) F. W. Lipps and H. A. Tolhoek: *Physica*, **20**, 85, 395 (1954); G. Böbel: *Nuovo Cimento*, **6**, 1241 (1957) and others.

([5]) W. H. McMaster: *Am. Journ. Phys.*, **22**, 351 (1954).

([6]) H. A. Tolhoek: *Rev. Mod. Phys.*, **28**, 277 (1956).

([7]) H. Banerjee: *Phys. Rev.*, **111**, 532 (1958).

where

$$Q = (\boldsymbol{e}\cdot\boldsymbol{\gamma})I_0 + (\boldsymbol{e}\cdot\boldsymbol{\gamma})(\boldsymbol{I}_1\cdot\boldsymbol{\gamma}) + (\boldsymbol{I}_2\cdot\boldsymbol{\alpha})(\boldsymbol{e}\cdot\boldsymbol{\gamma}) + I_3 \,. \tag{2}$$

The integrals I_0, $\boldsymbol{I}_1$, $\boldsymbol{I}_2$, and I_3 have been defined in eqs. (8) of A. The polarization vector $\boldsymbol{e}$, characterising the filter through which the incident radiation has been transmitted, may be conveniently represented in terms of the two perpendicular unit vectors $\boldsymbol{e}_1$ and $\boldsymbol{e}_2$ as

$$\boldsymbol{e} = a_1\boldsymbol{e}_1 + a_2\boldsymbol{e}_2 \,. \tag{3}$$

$|M|^2$, which is proportional to the transition probability, may now be written as follows:

$$|M|^2 = |C|^2 \,\mathrm{Tr}\,[u(p)\bar{u}(p)Qw\bar{w}\bar{Q}] = \tfrac{1}{4}\,\mathrm{Tr}\,[(\xi_0 + \boldsymbol{\xi}\cdot\boldsymbol{\omega})(\Sigma_0 + \boldsymbol{\Sigma}\cdot\boldsymbol{\omega})] \,, \tag{4}$$

where ω's are 2×2 Pauli matrices with ω_1 diagonal, and $(\xi_0, \boldsymbol{\xi})$ and $(\Sigma_0, \boldsymbol{\Sigma})$ are defined by

$$\begin{cases} \xi_0 = |a_1|^2 + |a_2|^2; & \xi_r = |a_1|^2 - |a_2|^2 \,, \\ \xi_1 = a_1^* a_2 + a_2 a_1^*; & \xi_3 = i(a_1 a_2^* - a_2 a_1^*) \,, \end{cases} \tag{5}$$

and

$$\begin{cases} \Sigma_0 = |M_1|^2 + |M_2|^2; & \Sigma_1 = |M_1|^2 - |M_2|^2 \,, \\ \Sigma_2 = M_1^* M_2 + M_2^* M_1; & \Sigma_3 = i(M_1^* M_2 - M_2^* M_1) \,. \end{cases} \tag{6}$$

In the above M_r is obtained from M in (1) with $\boldsymbol{e}$ replaced by $\boldsymbol{e}_r\,(r=1, 2)$. Following McMaster (5), the physical significance of the set of parameters $(\xi_0, \boldsymbol{\xi})$, which are the Stokes parameters (*) of the polarization filter, may be explained as follows: ξ_0 is a measure of total intensity trasmitted, and ξ_1, ξ_2, ξ_3 are the « orientation coefficients » with respect to three basic sets of vectors viz., (*a*) $\boldsymbol{e}_1$ and $\boldsymbol{e}_2$; (*b*) $(\boldsymbol{e}_1+\boldsymbol{e}_2)/\sqrt{2}$ and $(\boldsymbol{e}_1-\boldsymbol{e}_2)/\sqrt{2}$; and (*c*) $(\boldsymbol{e}_1+i\boldsymbol{e}_2)\sqrt{2}$ and $(\boldsymbol{e}_1 - i\boldsymbol{e}_2)/\sqrt{2}$, respectively. From (4) it is apparent that for maximum response $(\xi_0, \boldsymbol{\xi})$ must be proportional to $(\Sigma_0, \boldsymbol{\Sigma})$.

The matrix element for the positron annihilation process, in which a photon is created, may also be expressed by equations of the form of (1) and (2) with the only difference that in (2) one now writes $\boldsymbol{e}^*$ instead of $\boldsymbol{e}$, where $\boldsymbol{e}$, now the polarisation vector characterising the analyser of the emitted radiation, may be represented by (3). As a consequence, the eqs. (4), (5), and (6) remain valid here also with the sole exception that for Σ_3 one now writes

$$\Sigma_3 = -\,i(M_1^* M_2 - M_2^* M_1) \,.$$

(*) We have adopted the convention that for right circularly polarized photons $\boldsymbol{e} = (\boldsymbol{e}_1 + i\boldsymbol{e}_2)/\sqrt{2}$.

For the description of the polarization of the electron, one makes use of the matrix $u(p)\,u(p)$ in (4) which is the projection operator in the four dimensional spinor space. Following TOLHOEK (6) this operator can be decomposed into a product of two projection operators, each of which separates the four dimensional space into two dimensional subspaces, as follows:

$$u(p)\,u(p) = \tfrac{1}{4}\,(1 - ip^{\mu}\gamma_{\mu})(1 - s^{\nu}\gamma_{\nu}\gamma_5)\,, \tag{7}$$

where

$$s = (s^0, \boldsymbol{s}) = \left(\boldsymbol{\zeta}\cdot\boldsymbol{p},\ \boldsymbol{\zeta} + \frac{(\boldsymbol{\zeta}\cdot\boldsymbol{p})\boldsymbol{p}}{\varepsilon + 1}\right), \tag{8}$$

with $\boldsymbol{\zeta}$, the direction of the spin angular momentum of the electron, in its rest system. The first of these two operators corresponds to energy projection and the second to spin projection. For positron moving with momentum $\boldsymbol{p}$ and energy ε, the spin projection operator remains unaltered, whereas the energy projection operator may be obtained from that in the case of electron by the well known substitution law. The validity of this statement may be realized if one regards the operator $u(p)\,u(p)$ as the result of transformation of the projection operator in the rest system so that

$$u(p)\,\bar{u}(p) = \tfrac{1}{4}\,S(1 + i\gamma^0)(1 + \boldsymbol{\zeta}\cdot\boldsymbol{\sigma})S^{-1} = \tfrac{1}{4}\,S(1 + i\gamma^0)\left[1 - (\boldsymbol{\zeta}\cdot\boldsymbol{\gamma})\gamma_5\right]S^{-1}\,,$$

where S is the representation in the spinor space of the Lorentz transformation L from the rest system of the electron to the system in which it is moving with momentum $\boldsymbol{p}$. The projection operator $v(p)v(p)$ for the positron may, therefore, be written as

$$\begin{aligned} v(p)\,\bar{v}(p) &= -\tfrac{1}{4}\,S(1 - i\gamma^0)(1 - \boldsymbol{\zeta}\cdot\boldsymbol{\sigma})S^{-1} = \\ &= -\tfrac{1}{4}\,S(1 - i\gamma^0)\left[1 - (\boldsymbol{\zeta}\cdot\boldsymbol{\gamma})\gamma_5\right]S^{-1} = -\tfrac{1}{4}\,(1 + ip^{\mu}\gamma_{\mu})(1 - s^{\nu}\gamma_{\nu}\gamma_5)\,, \end{aligned} \tag{9}$$

where s is given by eq. (8) (*). The substitution law may be shown to be true

(*) *Note added in proof*: Our derivation of eq. (9) is based on Dirac's hole theory according to which there is an one to one correspondence between a positron and a negative energy electron with opposite spin and momentum to whose absence from the vacuum state the presence of the positron may be attributed. Alternatively, one may perform the charge conjugation transformation on the projection operator of the electron. This will also lead to the same result because under the charge conjugation transformation the energy momentum 4-vector changes sign, whereas, the spin angular momentum which is a pseudovector remains unaltered A. PAIS and R. JOST: *Phys. Rev.*, **87**, 871 (1952).

for the spin projection operator also if one writes the four vector s in the form

$$s = (\beta\varepsilon\zeta_3,\ \zeta_1\boldsymbol{n}_1 + \zeta_2\boldsymbol{n}_2 + \varepsilon\zeta_3\hat{\boldsymbol{p}})\,. \tag{10}$$

where $\hat{\boldsymbol{p}}$ is the unit vector in the direction of the momentum $\boldsymbol{p}$ and $\boldsymbol{n}_1$, $\boldsymbol{n}_2$ are mutually perpendicular unit vectors transverse to p. One may, therefore, expect that just as in the case of polarization independent parts, the polarization dependent parts of the positron annihilation cross section can be directly obtained from the corresponding results for photoelectric effect by making use of the substitution law. From eq. (10) it is further evident that unless ζ is exactly perpendicular to $\boldsymbol{p}$, the coefficient of the longitudinal component in the system in which the particle is moving would increase with increasing velocity. This, of course, is a direct consequence of the Lorentz transformation.

3. – Differential cross section.

As has been indicated in the preceding section the differential cross sections for both the photoelectric effect and the one quantum annihilation of positron which are proportional to $|M|^2$ in (4) will be presented in the form

$$|M|^2 = \tfrac{1}{2}\,(\xi_0\Sigma_0 + \xi_1\Sigma_1 + \xi_2\Sigma_2 + \xi_3\Sigma_3)\,. \tag{11}$$

where $(\xi_0, \boldsymbol{\xi})$ are the Stokes parameters of the polarization filter in the case of the photoelectric effect, or of the polarization analyser for the positron annihilation process. The Stokes parameters for the scattered electron and the incoming positron will be specified by $(1, \boldsymbol{\zeta})$ where the longitudinal component is represented by ζ_3, and the trasverse components by ζ_1, ζ_2 as in (10). The unit vector $\boldsymbol{n}_1$ is taken in the $\boldsymbol{p} - \boldsymbol{k}$ plane so that $(\boldsymbol{k}\cdot\boldsymbol{n}_1) = -k\sin\theta$ and $\boldsymbol{n}_1$, $\boldsymbol{n}_2$, $\boldsymbol{p}$ are so chosen as to form a righthanded system of rectangular axes. In view of the random relative phase between the wave functions of the two K-electrons, we have to average over the polarization of the bound electron and write for $w\bar{w}$ in $|M|^2$ in (4)

$$w\bar{w} = \tfrac{1}{4}\,(1+\beta)\,, \tag{12}$$

in terms of Dirac's β-matrix. It may be pointed out here that so far as the trace calculations are concerned much simplification would result if one adopts the standard representation of the k-matrices viz.,

$$\boldsymbol{\gamma} = \begin{pmatrix} 0 & \boldsymbol{\sigma} \\ \boldsymbol{\sigma} & 0 \end{pmatrix}, \qquad \text{and} \qquad \gamma^0 = -i\beta\,, \tag{13}$$

where σ's are the well known two dimensional Pauli matrices.

3·1. *Photoelectric effect.* – Expressions for the integrals I_0, $\boldsymbol{I}_1$, and $\boldsymbol{I}_2$ in (2) may be directly obtained from eqs. (24) and (29) of A as follows:

$$I_0 = C' J_0 \frac{a(1-ia)}{(\varepsilon-1)} \left\{ \frac{1}{\varepsilon(1-\beta\cos\theta)} - \varepsilon + \frac{\pi a}{4\sqrt{2}(1-\beta\cos\theta)^{\frac{1}{2}}} \right\} \tag{14a}$$

$$\boldsymbol{I}_1 = iC' J_0 \frac{a(1-ia)}{2(\varepsilon-1)(1-\frac{1}{2}\delta)} \left\{ \frac{1}{\varepsilon(1-\beta\cos\theta)} \boldsymbol{q} - ia\boldsymbol{k} \right\}, \tag{15a}$$

$$\boldsymbol{I}_2 = C' J_0 \frac{a(1-ia)}{2(\varepsilon-1)} \boldsymbol{q}, \tag{16a}$$

where

$$J_0 = \frac{4\pi(a^2+q^2)^{ia_1-1}}{\{(a-ip)^2+(\boldsymbol{p}+\boldsymbol{q})^2\}^{ia_1}}. \tag{17a}$$

The undefined symbols used in the above have the same meanings as in A. I_3, which has been shown in A to be of relative $O(a/\varepsilon)$, will be neglected.

From (11) and (6) one then gets

$$\Sigma_0 = \eta \frac{1}{\varepsilon^2(\varepsilon-1)^5} \left[\frac{\beta^2\sin^2\theta}{\Delta^3} \left(\varepsilon^2 - 3\varepsilon + 2 + \frac{2}{\varepsilon\Delta} \right) - \frac{\sqrt{2}\pi a\beta\varepsilon\sin^2\theta/2}{\Delta^{7/2}} \right]. \tag{18a}$$

$$\Sigma_1 = \eta \frac{1}{\varepsilon^2(\varepsilon-1)^5} \left[\frac{\beta^2\sin^2\theta\cos 2\varphi}{\Delta^3} \left(\frac{2}{\varepsilon\Delta} - \varepsilon + 1 \right) + \right.$$
$$\left. + \zeta_1 \frac{a\beta\varepsilon\sin\theta\sin 2\varphi}{\Delta^3} - \zeta_2 \frac{a\beta\varepsilon\sin\theta\cos 2\varphi}{\Delta^3} \right], \tag{19a}$$

$$\Sigma_2 = \eta \frac{1}{\varepsilon^2(\varepsilon-1)^5} \left[\frac{\beta^2\sin^2\theta\sin 2\varphi}{\Delta^3} \left(\frac{2}{\varepsilon\Delta} - \varepsilon + 1 \right) - \right.$$
$$\left. - \zeta_1 \frac{a\beta\varepsilon\sin\theta\cos 2\varphi}{\Delta^3} + \zeta_2 \frac{a\beta\varepsilon\sin\theta\sin 2\varphi}{\Delta^3} \right], \tag{20a}$$

$$\Sigma_3 = \eta \frac{1}{\varepsilon^2(\varepsilon-1)^5} \left[\beta\zeta_3 \left\{ \frac{(\varepsilon-1)\sin^2\theta}{\varepsilon\Delta^3} \left(\varepsilon^2 - 2\varepsilon - 1 + \frac{2}{\varepsilon\Delta} \right) - \right. \right.$$
$$\left. \left. - \frac{\sqrt{2}\pi a\beta\varepsilon\sin^2\theta/2}{\Delta^{7/2}} \right\} - \zeta_1 \frac{2(\varepsilon-1)\beta^2\sin^3\theta}{\varepsilon\Delta^4} \right]. \tag{21a}$$

where

$$\eta = \frac{Z^5\alpha^6}{8\pi^2} \cdot \frac{\exp\left[-\pi a + 2a\,\mathrm{tg}^{-1}\dfrac{a}{1-\delta} \right]}{a^{2\delta}\left(1 - \dfrac{33-2\pi^2}{6}\delta \right)}, \tag{22}$$

and $\Delta = 1 - \beta\cos\theta$.

In the first approximation, *i.e.*, if we neglect terms of relative $O(a)$, the coefficient of ζ_2 vanishes; so that the polarization vector of the photoelectron would lie in the scattering plane. It may be further noticed that in the high energy region, where the scattering angles for most of the photoelectrons are of $O(1/\varepsilon)$, the coefficient of ζ_1 in Σ_3 is of order $1/\varepsilon$ relative to that of ζ_3. One may, therefore, conclude that in the high energy region most of the photoelectrons will be longitudinally polarized. It is thus apparent that in these respects the polarization phenomenon in the photoelectric effect is similar to that in the bremsstrahlung (7). The probability $P(\zeta_3)$ of obtaining longitudinally polarized photoelectrons for right circularly polarized incident photons, which has the same significance as the asymmetry ratio in McVoy's paper (1), is given by

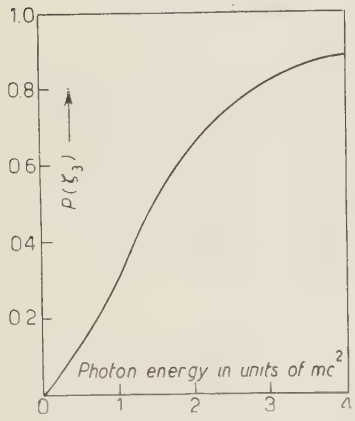

Fig. 1. – Probability $P(\zeta_3)$ of obtaining longitudinally polarized photoelectrons from an iron converter ($Z=26$) when the incident photon is right circularly polarised.

$$P(\zeta_3) = \frac{\beta F + G}{F + H}, \tag{23a}$$

where

$$\begin{cases} F = 1 - \dfrac{4\pi a}{15} - \dfrac{2}{3\varepsilon} + \dfrac{1}{2\beta\varepsilon^2} \ln \dfrac{1-\beta}{1+\beta}, \\ G = -\dfrac{1}{\beta\varepsilon^3}\left(2 + \dfrac{1}{\beta} \ln \dfrac{1-\beta}{1+\beta}\right), \end{cases} \tag{24a}$$

and

$$H = \frac{4}{3\varepsilon^2} - \frac{1}{\beta\varepsilon^3} \ln \frac{1-\beta}{1+\beta}.$$

In Fig. 1 $P(\zeta_3)$ has been plotted against the photon energy, neglecting the binding energy of the K-electron. It may be observed that although in the high energy region the curve given by McVoy (1) asymptotically tends to unity, as it should, for lower energy the rise is much more rapid in his curve than shown by the curve in Fig. 1. This difference is due to the fact that in McVoy's calculation the integral $\boldsymbol{I}_2$ in (16*a*), which is of $O(1/\varepsilon)$ relative to I_0, and $\boldsymbol{I}_1$ does not occur and hence our results must necessarily differ from that of McVoy in the lower energy region.

3·2. *Positron annihilation.* – For positron annihilation process the integrals I_0, $\boldsymbol{I}_1$, and $\boldsymbol{I}_2$ are given by

$$I_0 = C' J_0' \frac{a(1+ia)}{(\varepsilon+1)} \left\{ \frac{1}{\varepsilon(1-\beta\cos\theta)} - \varepsilon + \frac{\pi a}{4\sqrt{2}(1-\beta\cos\theta)^{\frac{1}{2}}} \right\}, \tag{14b}$$

(15)*b* $$\boldsymbol{I}_1 = -iC'J_0' \frac{a(1+ia)}{2(\varepsilon+1)(1-\frac{1}{2}\delta)} \left\{ \frac{1}{\varepsilon(1-\beta\cos\theta)} \boldsymbol{q} - ia\boldsymbol{k} \right\},$$

(16*b*) $$\boldsymbol{I}_2 = C'J_0' \frac{a(1+ia)}{2(\varepsilon+1)} \boldsymbol{q},$$

with

(17*b*) $$J_0 = \frac{4\pi(a^2+q^2)^{-ia_1-1}}{\{(a-ip)^2+(\boldsymbol{p}+\boldsymbol{q})^2\}^{-ia_1}}.$$

The undefined symbols which appear in the above equations have the same significance as in the case of photoeffect. Remembering that Σ_3, in this case is given by $\Sigma_3 = -i(M_1^* M_2 - M_2^* M_1)$, we get for the Stokes parameters (Σ_3, $\boldsymbol{\Sigma}$) of the emitted radiation

(18*b*) $$\Sigma_0 = \eta \frac{1}{\varepsilon^2(\varepsilon+1)^5} \left[\frac{\beta^2 \sin^2\theta}{\Delta^3} \left(\varepsilon^2 + 3\varepsilon + 2 - \frac{2}{\varepsilon\Delta} \right) - \frac{\sqrt{2}\pi a\beta\varepsilon \sin^2\theta/2}{\Delta^{7/2}} \right],$$

(19*b*) $$\Sigma_1 = \eta \frac{1}{\varepsilon^2(\varepsilon+1)^5} \left[\frac{\beta^2 \sin^2\theta\cos 2\varphi}{\Delta^3} \left(-\frac{2}{\varepsilon\Delta} + \varepsilon + 1 \right) + \right.$$
$$\left. + \zeta_1 \frac{a\beta\varepsilon \sin\theta \sin 2\varphi}{\Delta^3} - \zeta_2 \frac{a\beta\varepsilon \sin\theta\cos 2\varphi}{\Delta^3} \right],$$

(20*b*) $$\Sigma_2 = \eta \frac{1}{\varepsilon^2(\varepsilon+1)^5} \left[\frac{\beta^2 \sin^2\theta \sin 2\varphi}{\Delta^3} \cdot \right.$$
$$\left. \cdot \left(-\frac{2}{\varepsilon\Delta} + \varepsilon + 1 \right) - \zeta_1 \frac{a\beta\varepsilon \sin\theta\cos^2\varphi}{\Delta^3} + \zeta_2 \frac{a\beta\varepsilon \sin\theta \sin 2\varphi}{\Delta^3} \right],$$

(21*b*) $$\Sigma_3 = \eta \frac{1}{\varepsilon^2(\varepsilon+1)^5} \left[\beta\zeta_3 \left\{ \frac{(\varepsilon+1)\sin^2\theta}{\varepsilon\Delta^3} \left(\varepsilon^2 + 2\varepsilon - 1 - \frac{2}{\varepsilon\Delta} \right) - \frac{\sqrt{2}\pi a\beta\varepsilon \sin^2\theta/2}{\Delta^{7/2}} \right\} + \right.$$
$$\left. + \zeta_1 \frac{2(\varepsilon+1)\beta^2 \sin^3\theta}{\varepsilon\Delta^4} \right],$$

where η is given by eq. (22). We thus find that the circular polarization of the radiation has the same sense as that of the longitudinal polarization of the annihilated positron, *i.e.*, the radiation will be right or left circularly polarized according as the longitudinal polarization of the annihilated positron is parallel or antiparallel to its momentum. One again finds for the degree $P'(\zeta_3)$ of circular polarization of the radiation emitted due to the annihilation of longitudinally polarized positron

(23*b*) $$P'(\zeta_3) = \frac{\beta F' + G'}{F' + H'},$$

where

$$(24b) \qquad \begin{cases} F' = 1 - \dfrac{4\pi a}{15} + \dfrac{2}{3\varepsilon} + \dfrac{1}{2\beta\varepsilon^2} \ln \dfrac{1-\beta}{1+\beta}, \\ G' = \dfrac{1}{\beta\varepsilon^2}\left(2 + \dfrac{1}{\beta} \ln \dfrac{1-\beta}{1+\beta}\right), \end{cases}$$

and

$$H' = \frac{4}{3\varepsilon^2} + \frac{1}{\beta\varepsilon^2} \ln \frac{1-\beta}{1+\beta}.$$

* * *

I wish to thank Prof. S. Gupta for his constant encouragement and keen interest in this work and Mr. T. Majumdar for checking a part of the calculations.

RIASSUNTO (*)

Gli effetti della polarizzazione sulle sezioni d'urto per i processi di annichilamento fotoelettrico e positonico nello strato K sono stati studiati col metodo del parametro di Stokes per polarizzazione arbitraria delle particelle incidenti. Gli stati di scattering dell'elettrone e del positone sono stati approssimati con funzioni d'onda di Sommerfeld-Maue. Si sono ottenuti risultati corretti fino a termini di ordine a e negligendo termini di ordine a/ε, dove $a = Z/137$ ed ε è l'energia dello stato di scattering in unità mc^2. Per ambo i casi si è trovato che in prima approssimazione si ha correlazione solo tra la polarizzazione circolare del fotone e la componente del vettore di polarizzazione della particella libera di Dirac nel piano di scattering. Al limite delle alte energie il rapporto del grado di polarizzazione circolare della radiazione incidente (emessa) e il grado di polarizzazione longitudinale del fotoelettrone (positone) tende all'unità.

(*) *Traduzione a cura della Redazione.*

IL NUOVO CIMENTO Vol. XI, N. 2 16 Gennaio 1959

Dispersion Relations for Pion Production in a Pion-Nucleon Collision.

G. R. Screaton (*)

Tait Institute of Mathematical Physics, University of Edinburgh - Edimburgh

(ricevuto il 30 Ottobre 1958)

Summary. — The dispersion relations for pion production are written down in terms of sixteen invariant functions and it is shown that the bound state terms can be evaluated from a knowledge of the dispersive part of pion-nucleon scattering.

Introduction.

Considerable use has been made of the pion-nucleon dispersion relations, not only to the scattering problem by Goldberger *et al.*, Chew *et al.* [1] and many others, but also to other problems such as the electromagnetic structure of the nucleon by Chew *et al.* [2]. It is desirable to derive the dispersion relations for more complicated meson processes. In this paper the relations for pion production in a pion-nucleon collision are considered. Kibble [3] has already shown that a rigorous proof can be given for the dispersion relations written down by Polkinghorne [4] for the production of any number of mesons in a meson nucleon collision. We therefore concentrate on deriving the bound state contributions and expressing the relations in terms of invariant functions.

Sects. **1** and **2** are devoted to defining a series of amplitudes which will be required in subsequent considerations; amongst these are the retarded and

(*) Present address: Emmanuel College, Cambridge.

(1) M. L. Goldberger, M. Miyazawa and R. Oehme: *Phys. Rev.*, **99**, 986 (1955); G. F. Chew, M. L. Goldberger, F. E. Low and Y. Nambu: *Phys. Rev.*, **106**, 1337 (1957).

(2) G. F. Chew, R. Karplus and S. Gasiorowicz: *Phys. Rev.*, **110**, 265 (1958).

(3) T. W. B. Kibble: *Proc. Roy. Soc.*, A **244**, 355 (1958).

(4) J. C. Polkinghorne: *Nuovo Cimento*, **4**, 216 (1956).

advanced amplitudes T_R and T_A, and the dispersive and absorptive parts D and A. In Sect. **3** we deduce from isotopic and Lorentz space considerations, that these amplitudes can be expressed as the product of matrix elements of isotopic and Lorentz functions $\mathcal{I}^i$ and $\mathcal{L}_j$, and invariant functions F_j^i of the four momenta. The kinematics of the process can be formulated in terms of five scalar parameters. To obtain the dispersion relations it is necessary to single out one of these, ω, for special consideration; this is done in Sect. **4**. By considering the effects of Hermitian conjugation and time reversal, Sect. **5**, we are able to show that $D_j^i(\omega)$ and $A_j^i(\omega)$ are real functions of ω, which are equal to the real and imaginary parts of $T_{Rj}^i(\omega)$ for real ω, and that there is a simple connection between the amplitudes at ω and those at $-\omega$. The dispersion relations in terms of D_j^i and A_j^i are then written down. In Sect. **6** the structure of $A(\omega)$ is discussed using a resolution of unity, in terms of intermediate states, and in particular δ-functions of ω are shown to exist, corresponding to nucleon intermediate states (the bound states). In Sect. **7** the bound states are evaluated in terms of the coupling constant and the dispersive part of the pion-nucleon scattering amplitude. Finally, in Sect. **8** the results of Sects. **6** and **7** are put into the dispersion relations to express them in a physically useful form and some of their features discussed.

1. – Causal amplitudes.

We consider the process in which a pion-nucleon collision produces a pion. The initial state is taken to consist of a nucleon Prs and a pion $p\beta$. P denotes the four momentum, r and s the charge and spin states respectively, of the nucleon. p is the meson four momentum and β its isotopic component. With the same notation the final state is taken to consist of the pions $q\alpha$, $q'\alpha'$, and the nucleon $Q\varrho\sigma$. The matrix element for the process is

$$(1)\quad S_{\sigma s}^{\varrho r}(Q, q\alpha, q'\alpha'; P, p\beta) = \left\{(2\pi)^9(2p_0)(2q_0)(2q_0')\right\}^{-\frac{1}{2}}(-i)^3\int \mathrm{d}x\,\mathrm{d}x'\,\mathrm{d}y\cdot$$
$$\cdot\langle Q\varrho\sigma\,|\,T(j_\alpha(x)j_{\alpha'}(x')j_\beta(y))\,|\,Prs\rangle\exp\left[iq\cdot x\right]\exp\left[iq'\cdot x'\right]\exp\left[-ip\cdot y\right],$$

where $j_\nu(x)$ is the meson current in the Heisenberg representation. S, as defined here, is the probability amplitude normalized in three dimensional momentum space. Using translational invariance we obtain the δ-function corresponding to energy momentum conservation

$$(2)\quad S_{\sigma s}^{\varrho r}(Q, q\alpha, q'\alpha'; P, p\beta) = (2\pi)^4\,\delta(Q+q+q'-P-p)\left\{(2\pi)^9(2p_0)(2q_0)(2q_0')\right\}^{-\frac{1}{2}}\cdot$$
$$\cdot(-i)^3\int \mathrm{d}x\,\mathrm{d}x'\langle Q\varrho\sigma\,|\,T(j_\alpha(x)j_{\alpha'}(x')j_\beta\,(0))\,|\,Prs\rangle\exp\left[iq\cdot x\right]\exp\left[iq'\cdot x'\right].$$

Certain normalization factors can be extracted from S to obtain an amplitude invariant under proper Lorentz rotations. It is also convenient at this stage to extract the δ-function. We define the resulting amplitude, T_F by

$$(3)\quad T^{\varrho r}_{F\sigma s}(Q, q\alpha, q'\alpha'; P, p\beta) \equiv$$

$$\equiv \Omega \int \mathrm{d}x\, \mathrm{d}x' \langle Q\varrho\sigma | T(j_\alpha(x) j_{\alpha'}(x') j_\beta(0)) | Prs\rangle \exp[iq\cdot x] \exp[iq'\cdot x'],$$

with

$$(4)\quad \Omega = (-i)^2 \sqrt{\frac{(2\pi)^3 P_0}{M}} \sqrt{\frac{(2\pi)^3 Q_0}{M}},$$

and

$$(5)\quad Q + q + q' = P + p\,.$$

As p does not occur on the r.h.s. of (3) the last equation is to be regarded as defining it. It is easily seen that T_F is invariant under proper Lorentz rotations, as the j's are pseudo-scalar, and Ω provides the factor necessary to change the normalization of $|Q\varrho\sigma\rangle$ and $|Prs\rangle$ from that in three dimensional momentum space to an invariant one.

With T_F are associated the retarded and advanced amplitudes, T_R and T_A

$$(6)\ (*)\quad T^{\varrho r}_{R\sigma s}(Q, q\alpha, q'\alpha'; P, p\beta) \equiv$$

$$\equiv \Omega \int \mathrm{d}x\, \mathrm{d}x' \langle Q\varrho\sigma | \theta[j_\alpha(x) j_{\alpha'}(x') : j_\beta(0)] | Prs\rangle \exp[iq\cdot x] \exp[iq'\cdot x'],$$

$$(7)\ (*)\quad T^{\varrho r}_{A\sigma s}(Q, q\alpha, q'\alpha'; P, p\beta) \equiv$$

$$\equiv \Omega \int \mathrm{d}x\, \mathrm{d}x' \langle Q\varrho\sigma | \theta[j_\beta(0) : j_\alpha(x) j_{\alpha'}(x')] | Prs\rangle \exp[iq\cdot x] \exp[iq'\cdot x'].$$

In these definitions (5) has again been used to give a meaning to p. We have previously shown ([5]) that the θ product together with local causality, requires that x and x' should lie in the future light cone of 0 to contribute to the retarded amplitude; similarly only those x and x' in the past light cone of 0 will contribute to the advanced amplitude. It was also shown that for all physical values of the momenta T_R and T_F are equal. Thus, as far as the physics is concerned, it is irrelevant which we work with, but as in the scattering case the dispersion relations follow from the analytic structure of T_R implied by the causality condition.

(*) The θ products are as defined in ([5]),

$$\theta[j(x)j(x') : j(0)] = \sum \theta(x > x' > 0)[j(x), [j(x'), j(0)]],$$

$$\theta[j(0) : j(x)j(x')] = \sum \theta(0 > x' > x)[[j(0), j(x')], j(x)],$$

the sum is over permutations of x and x'.

([5]) G. R. Screaton: *Nuovo Cimento*, **5**, 1398 (1957).

2. – Dispersive and absorptive parts.

In the course of obtaining the dispersion relations it will be necessary to split T_R into real and imaginary components. To this end we define the dispersive and absorptive parts D and A,

$$\left\{\begin{aligned} D &\equiv \frac{1}{2}(T_R + T_A)\,, \\ A &\equiv \frac{1}{2i}(T_R - T_A)\,, \end{aligned}\right. \tag{8}$$

thus

$$T_R = D + iA\,. \tag{9}$$

As in the scattering case the value of D at given values of a set of invariant parameters will be related to an integral over A. To find the form of the bound state term and the range of integration we have to look at the operator structure of A. This will be greatly facilitated by splitting it into a series of terms, between which we shall subsequently establish simple relationships (Sect. 5). From (6), (7) and (8) we see that the operator occuring in A is

$$\begin{aligned} &\frac{1}{2i}\left(\theta(x > x' > 0) - \theta(0 > x' > x)\right)\left[j_\alpha(x), [j_{\alpha'}(x'), j_\beta(0)]\right] + \\ &\qquad + \frac{1}{2i}\left(\theta(x' > x > 0) - \theta(0 > x > x')\right)\left[j_{\alpha'}(x'), [j_\alpha(x), j_\beta(0)]\right], \end{aligned} \tag{10}$$

but

$$\theta(x > x' > 0) - \theta(0 > x' > x) = \tfrac{1}{2}\varepsilon(x - x') + \tfrac{1}{2}\varepsilon(x')$$

and so it can be written as the sum of three operators O, O' and $\bar{O}$, with

$$\left\{\begin{aligned} O &= \frac{1}{4i}\,\varepsilon(x)\left[j_{\alpha'}(x'), [j_\alpha(x), j_\beta(0)]\right], \\ O' &= \frac{1}{4i}\,\varepsilon(x')\left[j_\alpha(x), [j_{\alpha'}(x'), j_\beta(0)]\right], \\ \bar{O} &= \frac{1}{4i}\,\varepsilon(x - x')\left\{\left[j_\alpha(x), [j_{\alpha'}(x'), j_\beta(0)]\right] - \left[j_{\alpha'}(x'), [j_\alpha(x), j_\beta(0)]\right]\right\} = \\ &\qquad = \frac{1}{4i}\,\varepsilon(x - x')\left[[j_\alpha(x), j_{\alpha'}(x')], j_\beta(0)\right]. \end{aligned}\right. \tag{11}$$

We break the operators down yet one step further by expanding the outside

of the two commutators

$$O = O_{\mathrm{I}} - O_{\mathrm{II}}\,, \quad \text{etc.} \tag{12}$$

with

$$\left\{\begin{aligned} O_{\mathrm{I}} &= \frac{1}{4i}\, j_{\alpha'}(x')\varepsilon(x)\,[j_{\alpha}(x), j_{\beta}(0)]\,, \\ O_{\mathrm{II}} &= \frac{1}{4i}\,\varepsilon(x)\,[j_{\alpha}(x), j_{\beta}(0)]j_{\alpha'}(x')\,, \\ \bar{O}_{\mathrm{I}} &= \frac{1}{4i}\,\varepsilon(x-x')\,[j_{\alpha}(x), j_{\alpha'}(x')]j_{\beta}(0)\,, \\ \bar{O}_{\mathrm{II}} &= \frac{1}{4i}\, j_{\beta}(0)\varepsilon(x-x')\,[j_{\alpha}(x), j_{\alpha'}(x')]\,, \end{aligned}\right. \tag{13}$$

the expressions for O'_{I} and O'_{II} being obtained by interchanging $x\alpha$ and $x'\alpha'$. Corresponding to this splitting of the operator we define a splitting of the amplitude A

$$A = \mathcal{A} + \mathcal{A}' + \bar{\mathcal{A}}\,, \tag{14}$$

$$\mathcal{A} = \mathcal{A}_{\mathrm{I}} - \mathcal{A}_{\mathrm{II}}\,, \quad \text{etc.} \tag{15}$$

with

$$\mathcal{A}^{\varrho r}_{\sigma s}(Q, q\alpha, q'\alpha'; P, p\beta) = \tag{16}$$

$$= \Omega \int \mathrm{d}x\, \mathrm{d}x' \langle Q\varrho\sigma \,|\, O \,|\, Prs\rangle \exp\,[iq\cdot x] \exp\,[iq'\cdot x']\,, \quad \text{etc.}\,.$$

3. – Isotopic and Lorentz space.

In the previous two sections we have defined a series of amplitudes; we now wish to see what information we can obtain from charge independence and Lorentz invariance. We first of all deal with charge independence.

We write any one of our previously defined amplitudes, exhibiting only the isotopic variables, as $F^{\varrho r}(\alpha, \alpha'; \beta)$. Neglecting the effects of interactions which do not conserve isotopic spin (*e.g.* electromagnetic and weak interactions) as being small, $F^{\varrho r}(\alpha, \alpha'; \beta)$ when multiplied by the isotopic wave functions will be invariant under all three dimensional rotations in this space. Thus it can be expressed as the matrix element of the homogeneous products of τ_{α}, $\tau_{\alpha'}$ and τ_{β}. Using the commutation relations between the τ's, the six products can be reduced to four independent ones, which we take to be

$$\left\{\begin{aligned} \mathcal{T}^1 &= \tfrac{1}{2}[\delta_{\alpha'\beta}\tau_{\alpha} + \delta_{\alpha\beta}\tau_{\alpha'}]\,, \qquad \mathcal{T}^3 = \delta_{\alpha\alpha'}\tau_{\beta}\,, \\ \mathcal{T}^2 &= \tfrac{1}{2}[\delta_{\alpha'\beta}\tau_{\alpha} - \delta_{\alpha\beta}\tau_{\alpha'}]\,; \qquad \mathcal{T}^4 = i\varepsilon_{\alpha\alpha'\beta}\,. \end{aligned}\right. \tag{17}$$

Thus

$$F^{\varrho r}(\alpha, \alpha'; \beta) = \sum_i (\mathcal{T}^i)^{\varrho r} F^i , \tag{18}$$

with F^i now independent of the isotopic variables.

In Sect. **1** we extracted from S certain normalization factors, to obtain the amplitude T_F which is invariant under all proper Lorentz rotations. It will be noticed that all the amplitudes defined in Sects. **1** and **2** have this property. We use $F^{\varrho r}_{\sigma s}(Q, q\alpha, q'\alpha'; P, p\beta)$ to denote any one of these. The reference to isotopic spin will be dropped whenever this dependence is irrelevant. From the structure of the amplitudes, we see that not only are they invariant under proper Lorentz rotations, but they are also pseudo-scalar under rotations of the homogeneous Lorentz group. F can be written in the form

$$F_{\sigma s}(Q, q, q'; P, p) = \overline{u}^{\sigma}(Q) K(Q, q, q'; P, p) u^s(P) , \tag{19} (*)$$

where K is to be constructed from the γ matrices and the independent vectors P, Q, p and $(q - q')/2$. Taking into account the Dirac equation for the nucleons and the pseudo-scalarity of F, K can be expressed in terms of the independent matrices

$$\begin{cases} \Gamma_1 = \gamma_5 , & \Gamma_3 = \gamma \cdot p \gamma_5 , \\ \Gamma_2 = \gamma \cdot \delta \gamma_5 , & \Gamma_4 = \tfrac{1}{2}(\gamma \cdot p \gamma \cdot \delta - \gamma \cdot \delta \gamma \cdot p)\gamma_5 , \end{cases} \tag{20}$$

with

$$\delta = \frac{q - q'}{2} , \tag{21}$$

multiplied by scalar functions of the four momenta. Thus

$$F^{\varrho r}_{\sigma s}(Q, q\alpha, q'\alpha'; P, p\beta) = \sum_{ij} (\mathcal{T}^i)^{\varrho r} (\mathcal{L}_j)_{\sigma s} F^i_j(Q, q, q'; P, p) , \tag{22}$$

with

$$\mathcal{L}_j = \overline{u}(Q) \Gamma_j u(P) \tag{23}$$

and F^i_j a scalar function of its four vector arguments, *i.e.* each of our amplitudes can be decomposed into sixteen independent invariant functions of the four momenta.

(*) $u^s(P)$ is the s-th column of $(\gamma \cdot P + M)/\sqrt{2M(P_0 + M)}$ $s = 1, 2$.

4. – Kinematics.

The invariant functions F_j^i, can be expressed in terms of the scalar products of its four vector arguments. Taking into account energy momentum conservation (5) and the mass shell conditions, we find that there are five independent scalar products. To obtain the dispersion relations we must fix four of these, and be left with what is effectively an energy variable. This we do by using the prescription of POLKINGHORNE [4].

For all physically realizable processes there exists a Lorentz transformation to a Breit frame for the nucleons,

$$\text{(24)} \qquad \begin{cases} P = (\sqrt{M^2 + \Delta^2},\, 0,\, 0,\, \Delta) & Q = (\sqrt{M^2 + \Delta^2},\, 0,\, 0,\, -\Delta)\,, \\ p = (\omega, \boldsymbol{p})\,, & q = (\nu\omega, \boldsymbol{q})\,, \\ & q' = (\nu'\omega, \boldsymbol{q}')\,. \end{cases}$$

The conservation of energy and momentum requires

$$\text{(25)} \qquad \begin{cases} \nu + \nu' = 1\,, \\ \boldsymbol{q} + \boldsymbol{q}' = \boldsymbol{p} + 2\boldsymbol{\Delta}\,, \qquad \dfrac{P - Q}{2} = (0, \boldsymbol{\Delta})\,. \end{cases}$$

From the vectors p, q and q' we can construct the vectors ξ and ξ', with zero energy component,

$$\text{(26)} \qquad \xi = \nu p - q\,, \qquad \xi' = \nu' p - q'$$

from (25)

$$\text{(27)} \qquad \boldsymbol{\xi} + \boldsymbol{\xi}' + 2\boldsymbol{\Delta} = 0\,.$$

We choose the Lorentz frame so that

$$\text{(28)} \qquad \boldsymbol{\xi} = (0, -d, -(\Delta + c))\,, \qquad \boldsymbol{\xi}' = (0, d, -(\Delta - c))\,.$$

The kinematic description is completed by fixing the magnitudes of the vectors ξ and ξ', and this we do by taking c and d as fixed. It only remains to specify p, q and q' in terms of the constants Δ, c, d, ν and the only variable ω. This is achieved by requiring these vectors to lie on the meson mass shell. Using

(24), (26) and (28) we obtain

$$(29)\quad \begin{cases} p_1 = \lambda(\omega) = \sqrt{\omega^2 - \varepsilon^2}\,, \qquad \varepsilon = \sqrt{\mu^2 + p_2^2 + p_3^2}\,, \\ p_2 = \dfrac{1}{4\nu\nu' \Delta}\big\{(\nu - \nu')\Delta\,[(1 + \nu\nu')\,\mu^2 + d^2 + \Delta^2 - c^2] + \\ \qquad\qquad + c[(1 - \nu\nu')\mu^2 + d^2 + c^2 - \Delta^2]\big\}, \\ p_3 = \dfrac{-1}{4\nu\nu' \Delta}\big\{\nu(\Delta - c)^2 + \nu'(\Delta + c)^2 + (1 - \nu\nu')\mu^2 + d^2\big\}. \end{cases}$$

Summarizing: in the special frame

$$(30)\quad \begin{cases} P = (\sqrt{M^2 + \Delta^2},\, 0,\, 0,\, \Delta)\,, & Q = (\sqrt{M^2 + \Delta^2},\, 0,\, 0,\, -\Delta)\,, \\ p = (\omega,\, \lambda(\omega),\, p_2,\, p_3)\,, & q = (\nu\omega,\, \nu\lambda(\omega),\, \nu p_2 + d,\, \nu p_3 + \Delta + c)\,, \\ & q' = (\nu'\omega, \nu'\lambda(\omega), \nu' p_2 - d,\, \nu' p_3 + \Delta - c)\,, \end{cases}$$

and these expressions are real if ω lies in the physical region, $\omega \geqslant \varepsilon$. The five parameters can be expressed in terms of invariants,

$$(31)\quad \begin{cases} \Delta^2 = -\tfrac{1}{4}(P - Q)^2\,, & \Delta^2 + \Delta c = \tfrac{1}{2}(\nu p - q)\cdot(P - Q)\,, \\ \sqrt{M^2 + \Delta^2}\,\omega = \tfrac{1}{2} p\cdot(P + Q)\,, & \sqrt{M^2 + \Delta^2}\,\nu\omega = \tfrac{1}{2} q\cdot(P + Q)\,, \\ d^2 + c^2 - \Delta^2 = (\nu p - q)\cdot(\nu' p - q')\,. \end{cases}$$

We could take the point of view that the parameters are defined by the above equations but we will find it convenient to work with the special frame at the back of our mind.

The invariant functions can now be written in terms of these parameters

$$(32)\qquad F_j^i(Q, q, q';\, P, p) = F_j^i(\omega, \Delta^2, \nu, \Delta c, d^2 + c^2)\,.$$

It will be noticed that $\lambda(\omega)$ only occurs in the form $\lambda^2(\omega)$; as this is an analytic function in the whole ω plane, F_j^i will not depend on how the cuts for $\lambda(\omega)$ are defined. As we are interested in the ω dependence of the functions, for real fixed values of the other parameters we will in future drop the reference to these.

5. – Symmetry properties.

In this section we establish some simple symmetry properties of the amplitudes which will enable us to show that $D_j^i(\omega)$ and $A_j^i(\omega)$ are real for real values of ω. These symmetry properties are the result of the operator structure of the amplitudes.

5·1. *Complex conjugation.* – Consider the effect of complex conjugation on T_R,

$$T^{*\,\varrho r}_{R\,\sigma s}(Q, q\alpha, q'\alpha'; P, p\beta) = \tag{33}$$

$$= \Omega \int \mathrm{d}x\, \mathrm{d}x' \langle Prs \,|\, \theta\,[j_\alpha(x) j_{\alpha'}(x') : j_\beta(0)]\,|\, Q\varrho\sigma\rangle \exp[-iq^*\cdot x] \exp[-iq'^*\cdot x'] .$$

Comparing the r.h.s. with the definition of T_R, (6), we see that

$$T^{*\varrho r}_{R\sigma s}(Q, q\alpha, q'\alpha'; P, p\beta) = T_{Rs\sigma}{}^{r\varrho}(P, -q^*\alpha, -q'^*\alpha'; Q, -p^*\beta) , \tag{34}$$

similarly

$$T^{*\varrho r}_{A\sigma s}(Q, q\alpha, q'\alpha'; P, p\beta) = T_{As\sigma}{}^{r\varrho}(P, -q^*\alpha, -q'^*\alpha'; Q, -p^*\beta) . \tag{35}$$

Both sides of these equations can be expressed in terms of invariant functions. The parameters defined in (31) are the same for both, except that ω must be changed to $-\omega^*$ for the r.h.s. Thus for T_R and T_A

$$\sum_{ij} (\mathcal{T}^{*i})^{\varrho r} (\mathcal{L}^*_j(Q, q, q'; P, p))_{\sigma s} T^{*i}_j(\omega) = \tag{36}$$

$$= \sum_{ij} (\mathcal{T}^i)^{r\varrho} (\mathcal{L}_j(P, -q^*, -q'^*; Q, -p^*))_{s\sigma} T^i_j(-\omega^*) .$$

From (17)

$$\mathcal{T}^{i\dagger} = \zeta^i \mathcal{T}^i , \tag{37}$$

with

$$\begin{cases} \zeta^i = 1 , & i = 1, 2, 3 \\ \quad = -1 , & i = 4 \end{cases} \tag{38}$$

and from (20) and (23)

$$\mathcal{L}^\dagger_j(Q, q, q'; P, p) = -\zeta_j \mathcal{L}_j(P, -q^*, -q'^*; Q, -p^*) \tag{39}$$

with

$$\begin{cases} \zeta_j = 1 , & j = 4, \\ \quad = -1 , & j = 1, 2, 3. \end{cases} \tag{40}$$

As the $\mathcal{T}$'s and $\mathcal{L}$'s are independent we have, on substituting into (36), a relation between invariant functions

$$T^{*i}_j(\omega) = -\zeta^i_j T^i_j(-\omega^*) \qquad \text{for } T_R \text{ and } T_A , \tag{41}$$

with

$$\zeta^i_j = \zeta^i \zeta_j . \tag{42}$$

Expanding D and A in terms of invariant functions and putting in (41) we have

$$D^{*i}_j(\omega) = -\zeta^i_j D^i_j(-\omega^*)\,, \tag{43}$$

$$A^{*i}_j(\omega) = \zeta^i_j A^i_j(-\omega^*)\,. \tag{44}$$

We find it useful to have the corresponding results for the component parts of A. Carrying through the above arguments for them, we find

$$\mathcal{A}^{*i}_{\mathrm{I}j}(\omega) = -\zeta^i_j \mathcal{A}^i_{\mathrm{II}j}(-\omega^*) \qquad \text{for } \mathcal{A},\ \mathcal{A}' \text{ and } \overline{\mathcal{A}}\,. \tag{45}$$

5·2. *Time reversal.* – The other symmetry property that we require follows from applying time reversal to our amplitudes. It is shown in Appendix I that this yields for the invariant functions, (A.19) and (A.20),

$$T^{\ i}_{Bj}(\omega) = -\zeta^i_j T^{\ i}_{Aj}(-\omega) \tag{46}$$

$$T^{\ i}_{Aj}(\omega) = -\zeta^i_j T^{\ i}_{Bj}(-\omega) \tag{47}$$

and putting these results into the definitions of D and A,

$$D^i_j(\omega) = -\zeta^i_j D^i_j(-\omega)\,, \tag{48}$$

$$A^i_j(\omega) = \zeta^i_j A^i_j(-\omega)\,. \tag{49}$$

We again state the results for the component parts of A,

$$\mathcal{A}^{\ i}_{\mathrm{I}j}(\omega) = -\zeta^i_j \mathcal{A}^{\ i}_{\mathrm{II}j}(-\omega) \qquad \text{for } \mathcal{A},\ \mathcal{A}' \text{ and } \overline{\mathcal{A}}. \tag{50}$$

As there is no symmetry between the number of mesons in the initial and final states we do not have the conventional meson crossing relations. We can however consider nucleon crossing on T_F, this leads to the same symmetry as does time reversal.

Combining (43) and (44) with (48) and (49) we find

$$D^{*i}_j(\omega) = D^i_j(\omega^*)\,, \tag{51}$$

$$A^{*i}_j(\omega) = A^i_j(\omega^*)\,, \tag{52}$$

thus $D^i_j(\omega)$ and $A^i_j(\omega)$ are real functions of ω. In particular when ω is real, $D^i_j(\omega)$ and $A^i_j(\omega)$ are real and from (9), equal to the real and imaginary parts of $T^{\ i}_{Bj}(\omega)$, respectively. From (45) and (50) we see that the component parts of A are also real functions of ω.

We conclude this section by writing down the dispersion relations in terms of $D_j^i(\omega)$ and $A_j^i(\omega)$. A formal proof of the dispersion relations for this process suggested by POLKINGHORNE [4] has been given by KIBBLE [3]. Using techniques similar to those employed by BOGOLJUBOV *et al.* [6] for the scattering case, he has reduced the proof to the requirement of a single theorem. Consequently we will be content to state the results. The Lorentz functions $\mathcal{L}_j$ are easily seen to be analytic in ω and so for each $T_{Rj}^i(\omega)$ we have the dispersion relation

$$\text{Re } T_{Rj}^i(\omega) = \frac{1}{\pi} P\int_{-\infty}^{\infty} \mathrm{d}\omega' \frac{\text{Im } (T_{Rj}^i(\omega'))}{\omega' - \omega}, \tag{53}$$

or in terms of D and A,

$$D_j^i(\omega) = \frac{1}{\pi} P\int_{-\infty}^{\infty} \mathrm{d}\omega' \frac{A_j^i(\omega')}{\omega' - \omega}. \tag{54}$$

If the principal value integral is not convergent then in the usual way we subtract off terms until it is.

6. – Structure of the absorptive part.

The integral in (54) extends from $-\infty$ to ∞ and only the region $\omega \geqslant \varepsilon$ is physically realizable; even with the relation (49) we are still left with the region $-\varepsilon < \omega < \varepsilon$. In this section we find how the various components of A contribute to the integral. It will only be necessary to consider the $\mathcal{A}_{\text{I}}$'s, the behaviour of the $\mathcal{A}_{\text{II}}$'s following from (50).

We first of all consider $\mathcal{A}_{\text{I}}$, from (13) and (16)

$$\mathcal{A}_{1\sigma s}^{qr}(Q, q\alpha, q'\alpha'; P, p\beta) = \tag{55}$$
$$= \frac{\Omega}{4i}\int \mathrm{d}x\, \mathrm{d}x' \langle Q\varrho\sigma | j_{x'}(x')\varepsilon(x)[j_\alpha(x), j_\beta(0)] | Prs\rangle \exp[iq\cdot x] \exp[iq'\cdot x'].$$

Introducing a resolution of unity in terms of intermediate state $|n\rangle$, with four momenta n, normalized in three dimensional momentum space

$$I = \int \mathrm{d}n\, \mathrm{d}m^2 \varrho(m^2) \delta(n_0 - \sqrt{m^2 + \boldsymbol{n}^2}) |n\rangle\langle n|, \tag{56}$$

---

[6] N. N. BOGOLJUBOV, B. V. MEDVEDEV and M. K. POLIVANOV: *Lecture Notes* (Princeton, 1956).

with an implied sum over the other quantum numbers necessary to specify the state, and performing the x' and n integrations, we obtain

$$(57)\quad \mathscr{A}_1(\omega) = \frac{\Omega}{4i}\int \mathrm{d}x\,\mathrm{d}m^2\varrho(m^2)\langle Q\varrho\sigma|j_\lambda(0)|Q+q' \quad Q+q'|\varepsilon(x)[j_\alpha(x), j_\beta(0)]|Prs\rangle\cdot$$
$$\cdot\exp[iq\cdot x](2\pi)^4\delta(Q_0+q'_0-\sqrt{m^2+(\boldsymbol{Q}+\boldsymbol{q}')^2}) .$$

The δ-function requires

$$(58)\qquad m^2 = (Q+q')^2$$

but from (30)

$$(59)\qquad (Q+q'(\omega))^2 = 2\sqrt{M^2+\Delta^2}\,\nu'(\omega-\omega_0) ,$$

with

$$(60)\qquad \omega_0 = \frac{-M^2-\mu^2-2\Delta(\nu' p_3+\Delta-c)}{2\sqrt{M^2+\Delta^2}\nu'} .$$

Now performing the m^2 integration, we have

$$(61)\quad \mathscr{A}_1(\omega) = \frac{\Omega}{4i}\int \mathrm{d}x\langle Q\varrho\sigma|j_\alpha(0)|Q+q'\rangle\cdot$$
$$\cdot\langle Q+q'|\varepsilon(x)[j_\alpha(x), j_\beta(0)]|Prs\rangle\exp[iq\cdot x](2\pi)^4 2(Q_0+q'_0)\varrho((Q+q')^2) .$$

The meson current j_α conserves heavy particle number and so our intermediate state must contain at least one heavy particle. Taking this into account there will be a δ-function in the mass spectrum of intermediate states at the nucleon mass, and a continuum for masses greater than the sum of the nucleon and meson masses. Thus we can effectively write

$$(62)\qquad \varrho(m^2) = \varrho^B(m^2)+\varrho^C(m^2) ,$$

with

$$(63)\qquad \begin{cases} \varrho^B(m^2) = \delta(m^2-M^2) , \\ \varrho^C(m^2) = 0 , \qquad m^2 < (M+\mu)^2 . \end{cases}$$

The integral in (56) is only over states with real four momenta and consequently (61) is only applicable to the physical region. The problem in proving dispersion relations is to show that it is possible to continue into the non-physical region. If this continuation exists then it will be implicit in our representation in terms of intermediate states and our subsequent manipulations will be justified ([3,6]). Putting (63) into (61) we see from (59), that the δ-function

or bound state contributes at $\omega = \omega_B$,

$$\omega_B = \omega_0 + \frac{M^2}{2\sqrt{M^2+\Delta^2}\,\nu'} = \frac{-\mu^2 - 2\Delta(\nu' p_3 + \Delta - c)}{2\sqrt{M^2+\Delta^2}\,\nu'}, \tag{64}$$

and the continuum for $\omega \geqslant \omega_c$,

$$\omega_c = \omega_0 + \frac{(M+\mu)^2}{2\sqrt{M^2+\Delta^2}\,\nu'} = \frac{M\mu - \Delta(\nu' p_3 + \Delta - c)}{\sqrt{M^2+\Delta^2}\,\nu'}. \tag{65}$$

It is easily verified that

$$-\varepsilon < \omega_B < \omega_c \leqslant \varepsilon \tag{66}$$

the bound state is always in the non-physical region and the beginning of the continuum is either in it, or coincident with the beginning of the physical region.

We split $\mathscr{A}_1(\omega)$ into the sum of two terms $\mathscr{A}_1^B(\omega)$ and $\mathscr{A}_1^C(\omega)$, corresponding to the splitting of $\varrho(m^2)$ into $\varrho^B(m^2)$ and $\varrho^C(m^2)$. Then we have shown

$$\begin{cases} \mathscr{A}_1(\omega) = \mathscr{A}_1^B(\omega) + \mathscr{A}_1^C(\omega), \\ \mathscr{A}_1^B(\omega) = 0, \qquad \omega \neq \omega_B, \\ \mathscr{A}_1^C(\omega) = 0, \qquad \omega < \omega_c. \end{cases} \tag{67}$$

Similar results hold for $\mathscr{A}_1'(\omega)$, the bound state now occuring at ω_B' and the continuum at ω_c'.

$$\omega_B' = \frac{-\mu^2 - 2\Delta(\nu p_3 + \Delta + c)}{2\sqrt{M^2+\Delta^2}\,\nu}, \tag{68}$$

$$\omega_c' = \frac{M\mu - \Delta(\nu p_3 + \Delta + c)}{\sqrt{M^2+\Delta^2}\,\nu}. \tag{69}$$

Finally we consider $\overline{\mathscr{A}}(\omega)$, from (13) and (16)

$$\overline{\mathscr{A}}_1(\omega) = \tag{70}$$

$$= \frac{\Omega}{4i}\int \mathrm{d}x\,\mathrm{d}x' \langle Q\varrho\sigma\,|\,\varepsilon(x-x')[j_\alpha(x), j_{\alpha'}(x')]j_\beta(0)\,|\,Prs\rangle \exp[iq\cdot x]\exp[iq'\cdot x'].$$

Introducing (56), and changing the variable of integration x to $x+x'$ and then

performing the x', n and m^2 integrations,

$$(71)\quad \overline{\mathcal{A}}_{\mathrm{I}}(\omega) = \frac{\Omega}{4i}\int \mathrm{d}x \langle Q\varrho\sigma | \varepsilon(x)\,[j_\alpha(x), j_{\alpha'}(0)] | P+p\rangle \cdot \\ \cdot \langle P+p | j_\beta(0) | Prs\rangle \exp[iq\cdot x]\,(2\pi)^4 2(P_0+p_0)\,\varrho((P+p)^2)\,.$$

But

$$(72)\quad (P+p(\omega))^2 = 2\sqrt{M^2+\Delta^2}\,(\omega-\overline{\omega}_0)\,,$$

with

$$(73)\quad \overline{\omega}_0 = \frac{-M^2-\mu^2+2\Delta p_3}{2\sqrt{M^2+\Delta^2}}\,,$$

and so from (63) the bound state occurs at $\omega = \overline{\omega}_B$,

$$(74)\quad \overline{\omega}_B = \overline{\omega}_0 + \frac{M^2}{2\sqrt{M^2+\Delta^2}} = \frac{-\mu^2+2\Delta p_3}{2\sqrt{M^2+\Delta^2}}\,,$$

and the continuum $\omega \geqslant \overline{\omega}_C$,

$$(75)\quad \overline{\omega}_C = \overline{\omega}_0 + \frac{(M+\mu)^2}{2\sqrt{M^2+\Delta^2}} = \frac{M\mu+\Delta p_3}{\sqrt{M^2+\Delta^2}}\,.$$

In this case we also give the value of ω, $\overline{\omega}_{2C}$, at which intermediate states with two mesons begin to contribute

$$(76)\quad \overline{\omega}_{2C} = \overline{\omega}_0 + \frac{(M+2\mu)^2}{2\sqrt{M^2+\Delta^2}} = \frac{4M\mu+3\mu^2+2\Delta p_3}{2\sqrt{M^2+\Delta^2}}\,.$$

Again it can be easily verified that

$$(77)\quad -\varepsilon < \overline{\omega}_B < \overline{\omega}_C < \overline{\omega}_{2C} \leqslant \varepsilon$$

the bound state and the beginning of the continuum both lie in the non-physical region. Thus we have shown that

$$(78)\quad \begin{cases} \overline{\mathcal{A}}_{\mathrm{I}}(\omega) = \overline{\mathcal{A}}^B_{\mathrm{I}}(\omega) + \overline{\mathcal{A}}^C_{\mathrm{I}}(\omega) \\ \overline{\mathcal{A}}^B_{\mathrm{I}}(\omega) = 0 \qquad \omega \neq \overline{\omega}_B \\ \overline{\mathcal{A}}^C_{\mathrm{I}}(\omega) = 0 \qquad \omega \leqslant \overline{\omega}_C \end{cases}$$

with $\overline{\mathcal{A}}^B_{\mathrm{I}}$ and $\overline{\mathcal{A}}^C_{\mathrm{I}}$ defined as for $\mathcal{A}_{\mathrm{I}}$.

7. – Evaluation of the bound state terms.

When we have a nucleon intermediate state our amplitudes $\mathscr{A}_1$, $\mathscr{A}'_1$ and $\overline{\mathscr{A}}_1$ are split into the product of two matrix elements involving one and two mesons. Consequently we can express $\mathscr{A}_1^B$, $\mathscr{A}'^B_1$ and $\overline{\mathscr{A}}_1^B$ in terms of these processes of lower order.

Putting $\varrho^B(m^2)$ from (63) into (61), and using the definition of ω_B, (64), we have

$$(79)\quad \mathscr{A}_1^B(\omega) = \frac{\Omega}{4i}\langle Q\varrho\sigma\,|\,j_{\alpha'}(0)\,|\,Q+q'\rangle\cdot$$

$$\cdot\int \mathrm{d}x\langle Q+q'\,|\,\varepsilon(x)[j_\alpha(x),\,j_\beta(0)]\,|\,Prs\rangle\exp[iq\cdot x](2\pi)^4\frac{(Q_0+q'_0)}{\sqrt{M^2+\Delta^2}\,\nu'}\,\delta(\omega-\omega_B)\,.$$

Comparing the matrix element after the integral sign with (A.25) we see that it is simply related to the dispersive part of the pion-nucleon scattering amplitude. In fact

$$(80)\quad \int \mathrm{d}x\langle Q+q'vw\,|\,\varepsilon(x)[j_\alpha(x),\,j_\beta(0)]\,|\,Prs\rangle\exp[iq\cdot x] =$$

$$= 2i\sqrt{\frac{M^2}{(2\pi)^6 P_0(Q_0+q'_0)}}\,d^{vr}_{ws}(Q+q',\,q\alpha;\,P,\,p\beta)\,,\qquad \omega=\omega_B,$$

but we can write

$$(81)\qquad \mathrm{d}(Q+q',\,q\alpha;\,P,\,p\beta) = \sum_{ij} I^i(\alpha,\beta)L_j(Q+q',\,q;\,P,\,p)d^i_j(z\,\chi^2)\,,\qquad \omega=\omega_B,$$

I^i and L_j being defined in (A.28) and (A.29), and with

$$(82)\qquad \begin{cases} \chi^2 = -\tfrac{1}{4}(P-Q-q')^2 = \dfrac{(\Delta+c)^2+d^2+\nu'^2\mu^2}{4\nu}\,, \\ \sqrt{M^2+\chi^2}\,z = \tfrac{1}{2}q\cdot(Q+P+q')\,, \qquad \omega=\omega_B. \end{cases}$$

Whether this value of z lies in the physical or non-physical region will depend on the values of the parameters ν, Δ, c and d. The matrix element before the integral sign can be evaluated using the Lepore definition of the coupling constant,

$$(83)\quad \langle Q\,|\,j_{\alpha'}(0)\,|\,Q+q'\rangle = \sqrt{\frac{M^2}{(2\pi)^6 Q_0(Q_0+q'_0)}}\,G\,\bar{u}(Q)\gamma_5\tau_{\alpha'}u(Q+q')\,,\qquad \omega=\omega_B.$$

Putting these expressions into (80), and using

$$\sum_w u^w(n)\,\overline{u}^w(n) = \frac{\gamma\cdot n + M}{2M}, \tag{84}$$

we find for the invariant functions, after algebraic manipulation

$$\mathscr{A}^{Bi}_{1\,j}(\omega) = -\frac{G\pi\,\delta(\omega-\omega_B)}{2\nu'\sqrt{M^2+\Delta^2}}\sum_{lk}\alpha^{il}\beta_{jk}d^l_k(z,\chi^2), \tag{85}$$

with

$$\alpha^{il} = \begin{pmatrix} 1 & -1 \\ -1 & -1 \\ 0 & 1 \\ 0 & -1 \end{pmatrix}, \qquad \beta_{jk} = \begin{pmatrix} M & \beta_{12} \\ 1 & 0 \\ -\frac{1}{2} & 0 \\ 0 & 1 \end{pmatrix}, \tag{86}$$

$$\beta_{12} = (P\cdot p - \delta\cdot p + \tfrac{1}{2}\mu^2)_{\omega=\omega_B} = \sqrt{M^2+\Delta^2}\,(\nu\omega_B + \nu\omega'_B - \overline{\omega}_B).$$

$\mathscr{A}'^{Bi}_{1\,j}(\omega)$ can be obtained from $\mathscr{A}^{Bi}_{1\,j}(\omega)$ by interchanging $q\,\varkappa$ and $q'\alpha'$. Thus

$$\begin{cases} \chi'^2 = -\dfrac{1}{4}(P-Q-q)^2 = \dfrac{(\Delta-c)^2+d^2+\nu^2\mu^2}{4\nu'}, \\ \sqrt{M^2+\chi'^2}\,z' = \tfrac{1}{2}\,q'\cdot(P+Q+q), \qquad \omega=\omega'_B, \end{cases} \tag{87}$$

and so

$$\mathscr{A}'^{Bi}_{1\,j}(\omega) = -\frac{G\pi\delta(\omega-\omega'_B)}{2\nu\sqrt{M^2+\Delta^2}}\sum_{lk}\alpha'^{il}\beta'_{jk}d^l_k(z',\chi'^2), \tag{88}$$

with

$$\alpha'^{il} = \begin{pmatrix} 1 & -1 \\ 1 & 1 \\ 0 & 1 \\ 0 & 1 \end{pmatrix}, \qquad \beta'_{jk} = \begin{pmatrix} M & \beta'_{12} \\ -1 & 0 \\ -\frac{1}{2} & 0 \\ 0 & -1 \end{pmatrix}, \tag{89}$$

$$\beta'_{12} = (P\cdot p + \delta\cdot p + \tfrac{1}{2}\mu^2)_{\omega=\omega'_B} = \sqrt{M^2+\Delta^2}\,(\nu'\omega_B + \nu'\omega'_B - \overline{\omega}_B).$$

We carry through a similar analysis for $\overline{\mathscr{A}}^{\gamma}_1(\omega)$. Substituting (63) into (71)

$$\overline{\mathscr{A}}^{B}_1(\omega) = \frac{\Omega}{4i}\int \mathrm{d}x\,\langle Q\varrho\sigma\,|\,\varepsilon(x)[j_\alpha(x), j_{\alpha'}(0)]\,|\,P+p\rangle\cdot \tag{90}$$

$$\cdot\,\langle P+p\,|\,j_\beta(0)\,|\,Prs\rangle\,\exp[iq\cdot x](2\pi)^4\,\frac{(P_0+p_0)}{\sqrt{M^2+\Delta^2}}\,\delta(\omega-\overline{\omega}_B).$$

This can again be split into the product of the dispersive part for pion-nucleon scattering and a coupling constant term.

$$(91)\quad \int \mathrm{d}x \langle Q\varrho\sigma | \varepsilon(x)[j_\alpha(x), j_{\alpha'}(0)] | P + pvw \rangle \exp[iq\cdot x] =$$

$$= 2i \sqrt{\frac{M^2}{(2\pi)^6 Q_0 (P_0 + p_0)}}\, d^{\varrho v}_{\sigma w}(Q, q\alpha; P + p, -q'\alpha'), \qquad \omega = \bar{\omega}_B,$$

and

$$(92)\quad d(Q, q\alpha; P+p, -q'\alpha') = \sum_{ij} I^i(\alpha, \alpha')\, L_i(Q, q; P+p, -q')\, d^i_j(\bar{z}, \bar{\chi}^2), \quad \omega = \bar{\omega}_B$$

with

$$(93)\quad \begin{cases} \bar{\chi}^2 = -\dfrac{1}{4}(Q - P - p)^2 = -\dfrac{[\nu'(\Delta + c) - \nu(\Delta - c)]^2 + d^2 + \mu^2}{4\nu\nu'}, \\ \sqrt{M^2 + \bar{\chi}^2}\,\bar{z} = -\tfrac{1}{2} q'\cdot(Q + P + p), \end{cases} \qquad \omega = \bar{\omega}_B;$$

and

$$(94)\quad \langle P + p | j_\beta(0) | P \rangle = \sqrt{\frac{M^2}{(2\pi)^6 P_0 (P_0 + p_0)}}\, G\bar{u}(P + p)\gamma_5 \tau_\beta u(P), \qquad \omega = \omega_B.$$

Substituting these expressions into (90), and using (84), we find for the invariant functions

$$(95)\quad \bar{\mathcal{A}}^{B\,i}_{\mathrm{I}\,j}(\omega) = \frac{-\pi G \delta(\omega - \bar{\omega}_B)}{2\sqrt{M^2 + \Delta^2}} \sum_{lk} \bar{\alpha}^{il} \bar{\beta}_{jk}\, d^l_k(\bar{z}, \bar{\chi}^2),$$

with

$$(96)\quad \bar{\alpha}^{il} = \begin{pmatrix} 0 & 0 \\ 0 & 2 \\ 1 & 0 \\ 0 & 1 \end{pmatrix}, \qquad \bar{\beta}_{jk} = \begin{pmatrix} 0 & \bar{\beta}_{12} \\ 0 & 0 \\ 1 & 0 \\ 0 & -1 \end{pmatrix},$$

$$\bar{\beta}_{12} = (-P\cdot p - \tfrac{1}{2}\mu^2 + \delta\cdot p)_{\omega = \bar{\omega}_B} = \sqrt{M^2 + \Delta^2}\,(\nu'\omega_B - \nu\omega'_B).$$

8. – The dispersion relations.

The dispersion relations, (54), can be written in terms of the $\mathcal{A}_{\mathrm{I}}$'s and $\mathcal{A}_{\mathrm{II}}$'s; if use is then made of the relations (50) to get rid of the $\mathcal{A}_{\mathrm{II}}$'s, we have

$$(97)\quad D^i_j(\omega) = \frac{2}{\pi} P \int_{-\infty}^{\infty} \mathrm{d}\omega' \frac{(\mathcal{A}^i_{\mathrm{I}\,j}(\omega') + \mathcal{A}'^i_{\mathrm{I}\,j}(\omega') + \bar{\mathcal{A}}^i_{\mathrm{I}\,j}(\omega'))}{\omega'^2 - \omega^2} \left\{ \omega' \cdot \frac{1 - \zeta^i_j}{2} + \omega \cdot \frac{1 + \zeta^i_j}{2} \right\}.$$

Looking back to equations (67) and (78), we see that the $\mathscr{A}_{\mathrm{I}}$'s are zero over large portions of the real axis, and if we substitute from (85), (88) and (95) for the bound state contributions, the relations become

$$(98)\qquad D^i_j(\omega) = B^i_j(\omega) + \frac{2}{\pi} P\int_{\omega_c}^{\infty} \mathrm{d}\omega' \frac{\mathscr{A}^{\ i}_{1j}(\omega')}{\omega'^2 - \omega^2} \zeta^i_j(\omega, \omega') +$$

$$+ B'^i_j(\omega) + \frac{2}{\pi} P\int_{\omega'_c}^{\infty} \mathrm{d}\omega' \frac{\mathscr{A}'^{\ i}_{1j}(\omega')}{\omega'^2 - \omega^2} \zeta^i_j(\omega, \omega') + \overline{B}^i_j(\omega) + \frac{2}{\pi} P\int_{\overline{\omega}_c}^{\infty} \mathrm{d}\omega' \frac{\overline{\mathscr{A}}^{\ i}_{1j}(\omega')}{\omega'^2 - \omega^2} \zeta^i_j(\omega, \omega') ,$$

with

$$(99)\qquad \begin{cases} \zeta^i_j(\omega, \omega') = \omega & \zeta^i_j = \ \ 1 \\ \qquad\qquad = \omega', & \ \ = -1 \end{cases}$$

and

$$(100)\qquad \begin{cases} B^i_j(\omega) = \dfrac{G}{\nu'\sqrt{M^2 + \Delta^2}} \dfrac{\zeta^i_j(\omega, \omega_B)}{\omega^2 - \omega_B^2} \sum\limits_{lk} \alpha^{il}\beta_{jk} d^l_k(z, \chi^2) , \\ B'^i_j(\omega) = \dfrac{G}{\nu\sqrt{M^2 + \Delta^2}} \dfrac{\zeta^i_j(\omega, \omega'_B)}{\omega^2 - \omega'^2_B} \sum\limits_{lk} \alpha'^{il}\beta'_{jk} d'^l_k(z', \chi'^2), \\ \overline{B}^i_j(\omega) = \dfrac{G}{\sqrt{M^2 + \Delta^2}} \dfrac{\zeta^i_j(\omega, \overline{\omega}_B)}{\omega^2 - \overline{\omega}_B^2} \sum\limits_{lk} \overline{\alpha}^{il}\overline{\beta}_{jk} d^l_k(\overline{z}, \overline{\chi}^2) . \end{cases}$$

Defining ω_m as the minimum of ω_c, ω'_c and $\overline{\omega}_c$ and explicitly ignoring the bound states, (98) can be written

$$(101)\qquad D^i_j(\omega) = B^i_j(\omega) + B'^i_j(\omega) + \overline{B}^i_j(\omega) + \frac{2}{\pi}\int_{\omega_m}^{\infty} \mathrm{d}\omega' \frac{A^{\ i}_{1j}(\omega')}{\omega'^2 - \omega^2} \zeta^i_j(\omega, \omega') ,$$

with

$$(102)\qquad A_{\mathrm{I}}(\omega) = \mathscr{A}_{\mathrm{I}}(\omega) + \mathscr{A}'_{\mathrm{I}}(\omega) + \overline{\mathscr{A}}_{\mathrm{I}}(\omega) .$$

For that part of the integral in the physical region, $A_{\mathrm{I}}(\omega)$ is equal to $A(\omega)$, as in Sect. **6** it was shown that $-\omega_c$, $-\omega'_c$, $-\overline{\omega}_c \leqslant \varepsilon$, and so the $\mathscr{A}_{\mathrm{II}}$'s are zero, $\omega \geqslant \varepsilon$. In any case the $\mathscr{A}_{\mathrm{I}}(\omega)$'s in the non-physical region are to be regarded as the continuations of the $\mathscr{A}(\omega)$'s from the physical region: in fact a certain amount of continuation will always be necessary as $\overline{\omega}_c < \overline{\omega}_{2c} \leqslant \varepsilon$. For the set of parameters which correspond to threshold in the centre of

mass (*) the part of the non-physical region for which the $\mathcal{A}_l$'s are non zero is a minimum, *i.e.* $\omega_c = \omega'_c = \overline{\omega}_{2c} = \varepsilon$. This is reminiscent of the forward scattering case, for this also is threshold in the centre of mass, and further the contribution of the non-physical region to the absorptive integral is a minimum, as only the bound states lie in it.

The bound state terms, $B^i_j(\omega)$, are expressed in terms of the dispersive part of the pion-nucleon scattering amplitude. From (82) and (87) we see that χ^2 and χ'^2 are positive, and consequently the momentum transfer is real. As pointed out in Sect. **7**, z and z' may or may not lie in the physical region. In substituting for the dispersive parts we will if necessary, continue from the physical region, and use the crossing relations implicit in (A.32). For $B^i_j(\omega)$ the situation is slightly different, as from (93) $\overline{\chi}^2$ is negative, and so we will certainly have to continue in this variable ([7]). From the practical point of view these continuations are probably best done in terms of a phase shift expansion ([7]).

As in the case of the scattering relations there is a simple connection between the bound state terms and the Born approximation. In fact the Born approximation is equal to what one may call the strict bound state term, *i.e.* the term obtained by taking the bound state term only (or the Born approximation to the dispersive part) of the scattering relations, (A.32), in evaluating (100). After the bound states have been ignored, $A^i_j(\omega)$ is zero in this approximation, and so the system of dispersion relation equations (A.32) and (98), are satisfied by the Born approximation.

Using arguments similar to those presented here, it is possible to obtain dispersion relations for the photo-production of two pions on a nucleon. The situation is algebraically more complicated as we only have rotational symmetry about the third axis in isotopic space, leading to six $\mathcal{T}^i$ functions, and in Lorentz space we have fourteen functions $\mathcal{L}_j$, on introducing the polarization vector and taking into account gauge invariance. Otherwise the argument goes through exactly as before, with two bound state terms expressed in terms of the dispersive part for photo-production of one pion, and the other in terms of the dispersive part for pion scattering.

(*) $P_c = (\sqrt{M^2 + \Delta_c^2}\ 0, 0, \Delta_c)$, $\quad Q_c = (M, 0, 0, 0)$;

$p_c = (\sqrt{\mu^2 + \Delta_c^2}\ 0, 0, -\Delta_c)$, $\quad q_c = q'_c = (\mu, 0, 0, 0)$;

$\Delta^2 = \dfrac{3M\mu}{4(M + 2\mu)}$, $\quad \nu = \nu' = \dfrac{1}{2}$, $\quad c = d = 0$, $\quad \omega = \varepsilon$.

([7]) H. LEHMAN: *Analytic properties of scattering amplitudes as functions of momentum transfer* (preprint).

The application of the relations to experimental data is by no means trivial, for unlike the forward scattering case we do not have the optical theorem to enable us to express our amplitudes in terms of physically observable quantities. Instead one might try the one meson approximation to evaluate the absorptive part. This results in an integral equation with the absorptive and dispersive parts of the production amplitude appearing with the elastic scattering amplitudes in the integral. The solution of such an equation presents obvious difficulties. An alternative approach would be the use of an isobar model for the real intermediate states in A.

* * *

The author wishes to thank Dr. J. C. Polkinghorne for many stimulating discussions and useful suggestions, and Prof. N. Kemmer for the hospitality of the Tait Institute.

Appendix I

Time reversal.

In this appendix we consider the effects of the unitary time reversal operator, $\mathcal{T}$, on our amplitudes, to obtain the results stated in Sect. 5·2. The time reversal operator that we use is essentially the same as that defined by Jauch and Rohrlich [8].

$\mathcal{T}$ operating on the nucleon field, $\psi(x)$, produces the time reversed field, $\psi^t(x)$,

$$\mathcal{T}\psi(x)\mathcal{T}^\dagger = \psi^t(x)\,, \tag{A.1}$$

with

$$\psi^t(x^t) = D\psi^*(x)\,, \qquad x^t = (-x_0, \boldsymbol{x})\,, \tag{A.2}$$ (+)

and D satisfies

$$D\gamma^{\mu *}D^{-1} = (\gamma^0, -\gamma^i)\,, \qquad D^*D = -1\,, \tag{A.3}$$

$\mathcal{T}$ operating on the pion field gives

$$\mathcal{T}\varphi_\alpha(x)\mathcal{T}^\dagger = \varphi^t_\alpha(x)\,, \tag{A.4}$$

with

$$\varphi^t_\alpha(x^t) = (-)^\alpha \varphi^*_\alpha(x)\,. \tag{A.5}$$

[8] J. M. Jauch and F. Rohrlich: *The theory of photons and electrons* (Cambridge, Mass. 1955),

(+) * on an operator denotes the complex conjugate (without transposition) in Hilbert space.

As the nucleon states are steady states, they can be represented by an operator $\Psi(x)$, which satisfies the free field Dirac equation, and under time reversal behaves as the nucleon field. Expanding in terms of positive and negative frequency parts

$$\text{(A.6)} \qquad \Psi(x) = \int \mathrm{d}\boldsymbol{p} \sqrt{\frac{M}{(2\pi)^3 p_0}} \cdot \cdot \left\{ A_{\varrho\sigma}(\boldsymbol{p}) u^{\sigma}(\boldsymbol{p}) \eta^{\varrho} \exp\left[-ip\cdot x\right] + B^{\dagger}_{\varrho\sigma}(\boldsymbol{p}) v^{\sigma}(\boldsymbol{p}) \eta^{\varrho} \exp\left[ip\cdot x\right] \right\}.$$

Thus

$$\text{(A.7)} \qquad D\Psi^*(x) = \int \mathrm{d}\boldsymbol{p} \sqrt{\frac{M}{(2\pi)^3 p_0}} \left\{ A^*_{\varrho\sigma}(-\bar{\boldsymbol{p}}) u^{\sigma'}(\bar{\boldsymbol{p}}) D^{\sigma'\sigma} \eta^{\varrho} \exp\left[-i\bar{\boldsymbol{p}}\cdot x^t\right] + \ldots \right\},$$

with

$$\bar{p} = -p^t = (p_0, -\boldsymbol{p}),$$

as

$$\text{(A.8)} \qquad Du^{*\sigma}(\boldsymbol{p}) = D^{\sigma'\sigma} u^{\sigma'}(-\boldsymbol{p}).$$

From the equation corresponding to (A.2)

$$\text{(A.9)} \qquad A^{t}_{\varrho\sigma}(\boldsymbol{p}) = D^{\sigma\sigma'} A^*_{\varrho\sigma'}(-\boldsymbol{p}).$$

Consider the effect of time reversal on T_R,

$$\text{(A.10)} \quad T^{\varrho\tau}_{R\sigma s}(Q, q\alpha, q'\alpha'; P, p\beta) = -\Omega \int \mathrm{d}x\, \mathrm{d}x' \langle 0 | A^{t}_{\varrho\sigma}(\boldsymbol{Q}) \theta[j^{t}_{\lambda}(x) j^{t}_{\lambda'}(x') : j^{t}_{\beta}(0)] A^{tt}_{rs}(\boldsymbol{P}) | 0 \rangle \exp\left[iq\cdot x\right] \exp\left[iq'\cdot x'\right].$$

From (A.2) and (A.5), $j^{t}_{\lambda}(x') = (-)^{\lambda} j^{*}_{\lambda}(x)$; using this and the hermiticity of the j's

$$\text{(A.11)} \ (*) \qquad \theta[j^{t}_{\alpha}(x) j^{t}_{\alpha'}(x') : j^{t}_{\beta}(0)] = (-)^{\alpha+\alpha'+\beta} \theta[j_{\beta}(0) : j_{\alpha}(x^t) j_{\alpha'}(x'^t)]^{\sim}.$$

Substituting this together with (A.9), we have for the r.h.s. of (A.10)

$$\text{(A.12)} \quad (-)^{\alpha+\alpha'+\beta} D^{\sigma\sigma'} D^{*ss'} \Omega \int \mathrm{d}x\, \mathrm{d}x' \cdot \cdot \langle 0 | \left\{ A_{rs'}(-\boldsymbol{P}) \theta[j_{\beta}(0) : j_{\lambda}(x') j_{\lambda'}(x'^t)] A^{\dagger}_{\varrho\sigma'}(-\boldsymbol{Q}) \right\}^{\sim} | 0 \rangle \exp\left[iq\cdot x\right] \exp\left[iq'\cdot x'\right].$$

As this is a diagonal matrix element in Hilbert space we can drop the trans-

(*) $\sim$ denotes the transpose in Hilbert space.

pose and upon changing the variables of integration, this becomes

$$(A.13)\quad (-)^{\lambda+\lambda'+\beta} D^{\sigma\sigma'} D^{*ss'} \cdot \Omega \int \mathrm{d}x\, \mathrm{d}x' \langle -P^t{}_{rs'} | \theta[j_\beta(0) : j_\lambda(x) j_{\alpha'}(x')] | -Q^t{}_{\varrho\sigma'} \rangle \exp[iq^t \cdot x] \exp[iq'^t \cdot x'] .$$

Comparing this with the definition of T_A, (7), we see that

$$(A.14)\quad T^{\varrho r}_{R\alpha s}(Q, q\alpha, q'\alpha'; P, p\beta) = (-)^{\lambda+\lambda'+\beta} D^{\sigma\sigma'} D^{*ss'} T^{r\varrho}_{As'\sigma'}(-P^t, q^t\alpha, q'\alpha'^t; -Q^t, p^t\beta) .$$

Similarly

$$(A.15)\quad T^{\varrho r}_{A\alpha s}(Q, q\alpha, q'\alpha'; P, p\beta) = (-)^{\lambda+\lambda'+\beta} D^{\sigma\sigma'} D^{*ss'} T^{r\varrho}_{Rs'\sigma'}(-P^t, q^t\alpha, q'^t\alpha'; -Q^t, p^t\beta) ,$$

$$(A.16)\quad T^{\varrho r}_{F\alpha s}(Q, q\alpha, q'\alpha'; P, p\beta) = (-)^{\lambda+\lambda'+\beta} D^{\sigma\sigma'} D^{*ss'} T^{r\varrho}_{Fs\sigma'}(-P^t, q^t\alpha, q'^t\alpha'; -Q^t, p^t\beta) .$$

For the isotopic functions,

$$(A.17)\qquad (-)^{\alpha+\alpha'+\beta} \mathcal{T}^{iT} = -\zeta^i \mathcal{T}^i ,$$

and for the Lorentz functions,

$$(A.18)\qquad D^{\sigma\sigma'} D^{*ss'} \mathcal{L}^{s'\sigma'}_j(-P^t, q^t, q'^t; -Q^t, p^t) = \zeta_j \mathcal{L}^{\sigma s}_j(Q, q, q'; P, p) ,$$

with ζ^i and ζ_j as defined in (38) and (40). The equations (A.14), (A.15) and (A.16) can be expressed in terms of invariant functions, the parameters defined in (31) are the same for both sides, except ω must be changed to $-\omega$ for the r.h.s. Making use of (A.17) and (A.18), we have

$$(A.19)\qquad T^i_{Rj}(\omega) = -\zeta^i_j T^i_{Aj}(-\omega) ,$$

$$(A.20)\qquad T^i_{Aj}(\omega) = -\zeta^i_j T^i_{Rj}(-\omega) ,$$

$$(A.21)\qquad T^i_{Fj}(\omega) = -\zeta^i_j T^i_{Fj}(-\omega) .$$

Appendix II

Pion nucleon scattering.

Both in evaluating the contribution of the bound states for the production process and in our subsequent discussion, we find it convenient to have the dispersion relations for pion-nucleon scattering. These have been derived by many authors [9]. We state their results in a form which will be most useful to us.

---

[9] M. L. Goldberger: *Phys. Rev.*, **99**, 979 (1955); A. Salam: *Nuovo Cimento*, **3**, 424 (1956); A. Salam and W. Gilbert: *Nuovo Cimento*, **3**, 607 (1956); R. Oehme: *Phys. Rev.*, **100**, 1503 (1955) and **102**, 1174 (1956); R. H. Kapps and G. Takeda: *Phys. Rev.*, **103**, 1877 (1956).

We define the amplitudes t_F, t_R and t_A for the scattering of a pion $p\beta$ and a nucleon Prs into a nucleon $Q\varrho\sigma$ and a pion $q\alpha$, by

$$t_{F\sigma s}^{\varrho r}(Q, q\alpha; P, p\beta) \equiv -i\varkappa\int \mathrm{d}x \langle Q\varrho\sigma | T(j_\alpha(x) : j_\beta(0)) | Prs\rangle \exp[iq\cdot x], \tag{A.19}$$

$$t_{R\sigma s}^{\varrho r}(Q, q\alpha; P, p\beta) \equiv -i\varkappa\int \mathrm{d}x \langle Q\varrho\sigma | \theta[j_\alpha(x) : j_\beta(0)] | Prs\rangle \exp[iq\cdot x], \tag{A.20}$$

$$t_{A\sigma s}^{\varrho r}(Q, q\alpha; P, p\beta) \equiv -i\varkappa\int \mathrm{d}x \langle Q\varrho\sigma | \theta[j_\beta(0) : j_\alpha(x)] | Prs\rangle \exp[iq\cdot x], \tag{A.21}$$

with

$$\varkappa = \sqrt{\frac{(2\pi)^3 P_0}{M}}\ \sqrt{\frac{(2\pi)^3 Q_0}{M}}, \tag{A.22}$$

and

$$Q + q = P + p. \tag{A.23}$$

t_F and t_R are equal for all physical four momenta. The dispersive and absorptive parts are given by

$$d = \frac{1}{2}(t_R + t_A), \qquad a = \frac{1}{2i}(t_R - t_A). \tag{A.24}$$

Thus

$$d_{\sigma s}^{\varrho r}(Q, q\alpha; P, p\beta) = \frac{-i\varkappa}{2}\int \mathrm{d}x \langle Q\varrho\sigma | \varepsilon(x)[j_\alpha(x), j_\beta(0)] | Prs\rangle \exp[iq\cdot x], \tag{A.25}$$

and

$$a = a_{\mathrm{I}} - a_{\mathrm{II}}, \tag{A.26}$$

with

$$\begin{cases} a_{\mathrm{I}\sigma s}^{\varrho r}(Q, q\alpha; P, p\beta) = \dfrac{-\varkappa}{2}\displaystyle\int \mathrm{d}x \langle Q\varrho\sigma | j_\alpha(x) j_\beta(0) | Prs\rangle \exp[iq\cdot x], \\ a_{\mathrm{II}\sigma s}^{\varrho r}(Q, q\alpha; P, p\beta) = \dfrac{-\varkappa}{2}\displaystyle\int \mathrm{d}x \langle Q\varrho\sigma | j_\beta(0) j_\alpha(x) | Prs\rangle \exp[iq\cdot x]. \end{cases} \tag{A.27}$$

Using

$$I^1 = \delta_{\alpha\beta}, \qquad I^2 = i\varepsilon_{\alpha\beta\gamma}\tau_\gamma, \tag{A.28}$$

and

$$L_1 = \overline{u}(Q)u(P), \qquad L_2 = \overline{u}(Q)\gamma\cdot p u(P), \tag{A.29}$$

all the above amplitudes can be expressed in terms of invariant functions, *i.e.*

$$f_{\sigma s}^{\varrho r}(Q, q\alpha; P, p\beta) = \sum_{ij} (I^i)^{\varrho r} (L_j)_{\sigma s} f_j^i(Q, q; P, p), \tag{A.30}$$

where f_j^i is an invariant function. In the scattering case there are two independent scalar products

$$\chi^2 = -\tfrac{1}{4}(P-Q)^2\,, \qquad \sqrt{M^2+\chi^2}\,z = \tfrac{1}{2}p\cdot(P+Q)\,, \tag{A.31}$$

and so $f_j^i(Q, q; P, p) = f_j^i(z, \chi^2)$.

By considering the effects of complex conjugation and meson crossing, it is found that $d_j^i(z)$ and $a_j^i(z)$ are the real and imaginary parts of $t_{Rj}^i(z)$, when z is real. The dispersion relations are

$$d_j^i(z) = b_j^i(z) + \frac{2}{\pi}P\int_{z_c}^{\infty} \mathrm{d}z'\,\frac{a_{1j}^i(z')}{z'^2 - z^2}\,\xi_j^i(z, z')\,, \tag{A.32}$$

where

$$b_2^i(z) = \frac{G^2}{\sqrt{M^2+\chi^2}}\,\frac{\xi_2^i(z, z_B)}{z^2 - z_B^2}\,, \qquad b_1^i(z) = 0\,, \tag{A.33}$$

and

$$z_B = \frac{-\mu^2 - 2\chi^2}{2\sqrt{M^2+\chi^2}}\,, \quad z_C = \frac{M\mu - \chi^2}{\sqrt{M^2+\chi^2}}\,, \quad -\sqrt{\mu^2+\chi^2} < z_B < z_C \leqslant \sqrt{\mu^2+\chi^2}\,, \tag{A.34}$$

$$\xi_j^i(z, z') = \begin{pmatrix} z' & z \\ z & z' \end{pmatrix}_{ij}. \tag{A.35}$$

In the physical region $z \geqslant \sqrt{\mu^2+\chi^2}$, $a_1(z)$ can be replaced by $a(z)$ and in any case $a_1(z)$ is to be regarded as the continuation of $a(z)$ into the non physical region.

RIASSUNTO (*)

Si scrivono le relazioni di dispersione per la produzione di pioni in termini di 16 funzioni invarianti e si dimostra che i termini dovuti agli stati legati si possono calcolare conoscendo la parte dispersiva dello scattering pione-nucleone.

(*) *Traduzione a cura della Redazione.*

IL NUOVO CIMENTO Vol. XI, N. 2 16 Gennaio 1959

Longitudinal Polarization of the Fast Neutrons from μ^- Absorption by Nuclei.

M. Cini and R. Gatto

Istituto di Fisica e Scuola di Perfezionamento - Università di Roma
Istituto Nazionale di Fisica Nucleare - Sezione di Roma

(ricevuto il 10 Novembre 1958)

Summary. — The longitudinal polarization of the fast neutron emitted in the absorption of a negative muon by a nucleus is calculated for the $A \pm V$ interaction using a Fermi model for the nucleus. It is shown that, as long as this model can be applied to describe the process, the emitted neutron has an appreciable longitudinal polarization if the interaction is $A—V$. Rescattering corrections are estimated using an optical model and it is found that they do not alter this conclusions for the neutrons in the upper part of the spectrum.

1. – The absorption process $\mu^- + p \to n + \nu$ has been recently discussed by different authors [1]. It is indeed very important to obtain direct experimental information on the interaction responsible for such a process. Experiments in hydrogen are unfortunately very difficult because of the very low rate expected for the absorption process as compared to the μ-decay rate, and also because of the expected frequent formation of the μ-H_2 complex and possible spurious effects due to small deuterium contaminations. Experiments on complex nuclei are certainly possible, though their interpretation is complicated by the intricacy of the nuclear dynamics. It has been suggested that a measurement of the difference between the lifetimes of the two hyperfine states of a μ^- captured in the K-orbit may provide information on the absorption pro-

(1) I. S. Shapiro, E. L. Dolinsky and L. D. Blohinčev: *Nucl. Phys.*, **4**, 273 (1951). K. Huang, C. N. Yang and T. D. Lee: *Phys. Rev.*, **108**, 1304 (1957); L. Wolfenstein: *Nuovo Cimento*, **7**, 706 (1958).

cess (2). A second possibility would be offered by a measurement of the asymmetry of the fast neutron produced in the absorption process with respect to the μ^- spin direction. There are two difficulties however with regard to such a possibility. First, for a coupling of the form $A \pm V$, which is very strongly recommended by the recent theoretical and experimental developments in weak interactions (3), the asymmetry in $\mu^- + p \to n + \nu$ at rest with μ^- completely polarized is expected to be very small. Indeed the asymmetry parameter is exactly zero for $A - V$, and (v/c) for $A + V$, where v is the neutron velocity, if the radiative pion corrections are neglected. When such corrections are estimated and taken into account in the effective Hamiltonian the asymmetry parameter changes to $-.21$ for $A - V$ and to $-.11$ for $A + V$ (4). A second difficulty is that by cascading through the atomic orbits the μ^- gets appreciably depolarized as can be seen from the smaller asymmetry of $\mu^- \to e^- + \nu + \bar{\nu}$ as compared to the large asymmetry in μ^+ decay. We shall try to estimate here the amount of longitudinal polarization of the fast neutron which is emitted in the absorption process with unpolarized muons, assuming an $A - V$, or $A + V$ interaction. We find that such neutrons are expected to have an appreciable longitudinal polarization if the interaction is $A - V$, and essentially no polarization if the interaction is an $A + V$, at least to the extent that we can apply a Fermi model to describe the nucleus. For absorption at rest of unpolarized μ^- the longitudinal polarization of the emitted neutron is maximum, equal to -1, for $A - V$ and v/c for $A + V$, again neglecting effects due to virtual pion corrections. It may be instructive to give an intuitive argument for both the lack of asymmetry and the maximum polarization in the physically relevant $A - V$ case. In the non-relativistic limit for such an interaction one finds that the non-spin flip term and the spin-flip term of the transition matrix are equal but with opposite sign. Thus there can be no absorption from the triplet state, but only from the singlet state of the system. Since such a state has zero spin no asymmetry can occur and furthermore since the emitted neutrino is lefthanded also the neutron must be lefthanded.

2. – The calculation of the neutron polarization is most easily performed in covariant notations. Call q_λ, P_λ, p_λ and k_λ the four-moments of μ^-, p, n and ν, which satisfy $q^2 = -\mu^2$, $P^2 = -m'^2$, $p^2 = -m^2$ and $k^2 = 0$ (to make use of the symmetries of the Feynman, Gell-Mann, Marshak, Sudarshan Hamil-

---

(2) J. BERNSTEIN, T. D. LEE, C. N. YANG and H. PRIMAKOFF: *Phys. Rev.*, **111**, 313 (1958).

(3) R. P. FEYNMAN and M. GELL-MANN: *Phys. Rev.*, **109**, 193 (1958); E. SUDARSHAN and R. MARSHAK: *Proc. of the Padua-Venice Conf.* (Sept. 1957).

(4) L. WOLFENSTEIN: *Nuovo Cimento*, **8**, 882 (1958).

tonian we denote differently the masses of p and of n). Call S_λ and s_λ the polarization four-vectors of μ^- and n respectively, with s_λ, for instance, defined as $s_\lambda = (\boldsymbol{\zeta} + m^{-1}(E+m^{-1})(\boldsymbol{\zeta}\cdot\boldsymbol{p})\boldsymbol{p},\ im^{-1}(\boldsymbol{\zeta}\cdot\boldsymbol{p}))$, where $\boldsymbol{\zeta}$ is the unit vector along the neutron spin direction in the neutron's rest system. The distribution will then be proportional to the product $\Omega^{\pm}_{\varrho\sigma}\Omega^{L}_{\varrho\sigma}$, where

$$\Omega^{\pm}_{\varrho\sigma} = \mathrm{Sp}\left\{\gamma_\varrho(1\pm\gamma_5)(-i\gamma P + m')(1\mp\gamma_5)\,\gamma_\sigma(-i\gamma p + m)(1 + i\gamma_5\gamma s)\right\}$$

and $\Omega^{L}_{\varrho\sigma}$ is obtained from $\Omega^{+}_{\varrho\sigma}$ by the substitutions $\varrho \rightleftarrows \sigma$, $P_\lambda \to k_\lambda$, $m' \to 0$, $p_\lambda \to q_\lambda$, $m \to \mu$, $s_\lambda \to S_\lambda$ expressing the substitution $\mathrm{p} \to \nu$ and $\mathrm{n} \to \mu^-$. Here $\pm$ stands for the two choices $\frac{1}{2}(1+\gamma_5)$ or $\frac{1}{2}(1-\gamma_5)$, for the projection operator in front of the nucleon field. Universal interaction and the experiments on β^- decay of polarized neutrons suggest the « plus » sign.

One finds $\Omega^{\pm}_{\varrho\sigma} = 2^3 P_\alpha(-p_\beta + m s_\beta)\lambda^{\pm}_{\varrho\alpha\sigma\beta}$, where the tensor $\lambda^{\pm}_{\varrho\alpha\sigma\beta}$ is $\delta_{\varrho\alpha}\delta_{\sigma\beta} - \delta_{\varrho\sigma}\delta_{\alpha\beta} + \delta_{\varrho\beta}\delta_{\alpha\sigma} \mp \varepsilon_{\varrho\alpha\sigma\beta}$. After contracting with $\Omega^{L}_{\varrho\sigma}$ one finds $\Omega^{+}_{\varrho\sigma}\Omega^{L}_{\varrho\sigma} = 2^8(-(Pq)+\mu(PS))(-(pk)+m(ks))$ and $\Omega^{-}_{\varrho\sigma}\Omega^{L}_{\varrho\sigma} = 2^8(Pk)((pq) - \mu(PS) + m(qs) - \mu m(sS))$.

Let us specialize our results to the case of unpolarized μ^- absorbed at rest by a moving proton. We call $P_\lambda \equiv (\boldsymbol{P}\boldsymbol{e}, i\mathcal{E})$ and $p_\lambda \equiv (p\boldsymbol{n}, iE)$. The distributions can be written in the form $(\mathcal{E}E\mu k)^{-1}W_\pm$ with

$$W_\pm = W^{(0)}_\pm + (\boldsymbol{e}\boldsymbol{\zeta})W^{(1)}_\pm + (\boldsymbol{n}\boldsymbol{\zeta})W^{(2)}_\pm . \tag{1}$$

Here $W_+ = -(Pq)[-(kp) + m(ks)]$ and $W_- = (Pk)[(pq) + m(qs)]$. Calling ξ the cosine of the angle between $\boldsymbol{e}$ and $\boldsymbol{n}$, one finds

$$W^{(0)}_+ = \mu\mathcal{E}[E(\mu+\mathcal{E}) - m^2 + Pp\xi] , \tag{2}$$

$$W^{(1)}_+ = \mu\mathcal{E}mP , \tag{2'}$$

$$W^{(2)}_+ = \mu\mathcal{E}[-p(\mu+\mathcal{E}) + P(E-m)\xi] , \tag{2''}$$

$$W^{(0)}_- = \mu E[\mathcal{E}(\mu - E) + m^2 + Pp\xi] , \tag{3}$$

$$W^{(1)}_- = 0 , \tag{3'}$$

$$W^{(2)}_- = \mu p[\mathcal{E}(\mu - E) + m^2 + Pp\xi] . \tag{3''}$$

To obtain the neutron spectrum and polarization we write the integral

$$\int \delta(\mu + \mathcal{E} - E - k)\,\delta(\boldsymbol{P} - \boldsymbol{p} - \boldsymbol{k})(\mathcal{E}E\mu k)^{-1} W_\pm \,\mathrm{d}\boldsymbol{P} f(\mathcal{E})\,\mathrm{d}\boldsymbol{p}[1 - f(E)]\,\mathrm{d}\boldsymbol{k} ,$$

where $f(\mathcal{E}) = 1$ for $\mathcal{E} < F$ and $= 0$ for $\mathcal{E} > F$ (F = Fermi energy), in the form

$$\int \mathrm{d}E\, \mathrm{d}\boldsymbol{n}[1 - f(E)]\mathrm{d}\mathcal{E} f(\mathcal{E})\mathrm{d}\boldsymbol{e}\, \delta(\xi - \xi_0)\, W_{\pm}\,, \tag{4}$$

where ξ_0 is the solution of

$$\mu + \mathcal{E} - E - \sqrt{P^2 + p^2 - 2Pp}\xi_0 = 0\,. \tag{5}$$

Using (1) and performing the angular integration one can write (4) as

$$\int \mathrm{d}E\, \mathrm{d}\boldsymbol{n}[\, U^{(0)}_{\pm}(E) + (\boldsymbol{\zeta}\cdot\boldsymbol{n})\, U^{(1)}_{\pm}(E)]\,, \tag{6}$$

where

$$U^{(0)}_{\pm}(E) = [1 - f(E)]\int \mathrm{d}\mathcal{E} f(\mathcal{E})\, U(\xi_0)\, W^{(0)}_{\pm}\,, \tag{7}$$

$$U^{(1)}_{\pm}(E) = [1 - f(E)]\int \mathrm{d}\mathcal{E} f(\mathcal{E})\, U(\xi_0)[\, W^{(1)}_{\pm}(\xi_0) + W^{(2)}_{\pm}]\,. \tag{7'}$$

Here $U(\xi_0)$ is a step function $= 1$ for $-1 \leqslant \xi_0 \leqslant 1$, $= 0$ elsewhere. From (6) it is now evident that the spectrum is given by

$$U^{(0)}_{\pm}(E)\, \mathrm{d}E\,, \tag{8}$$

while the neutron polarization is only longitudinal and given by

$$P_L = \frac{U^{(1)}_{\pm}(E)}{U^{(0)}_{\pm}(E)}\,. \tag{8'}$$

Note from (7) and (7') how, after averaging over the Fermi motion, the component of the neutron polarization along the proton momentum gives rise to an additional longitudinal contribution. In Eqs. (7) and (7') ξ_0 has to be expressed as a function of E and $\mathcal{E}$ through (5). Furthermore, the step function $U(\xi_0)$ requires for each E that a certain quadratic form of $\mathcal{E}$, that can be derived from (5), be $\geqslant 0$, thus limiting the possible values of $\mathcal{E}$ to those between the two roots $\mathcal{E}_-(E)$ and $\mathcal{E}_+(E)$ of the quadratic form. We do not report here the expressions for $\mathcal{E}_-(E)$ and $\mathcal{E}_+(E)$, since it turns out that by combining this limitation on $\mathcal{E}$ with that imposed by the other step function $f(\mathcal{E})$, the resulting limitation is $\mathcal{E}_-(E) \leqslant \mathcal{E} \leqslant F$ for all the allowed values of E, *i.e.* $F + \Delta < E \leqslant E_{\max}$, where Δ is the binding energy for the last neutron, about 8 MeV. The energy $E_{\max}$ is that energy for which the neutron distri-

bution falls to zero, namely for which $\mathcal{E}(E_{max}) = F$. Performing the integrations we find for the choice « plus » in the coupling

$$m^{-4}U_{+}^{(0)} = \frac{1}{4}a^2(f^2 - u^2) + \frac{1}{3}a(f^3 - u^3)\,, \tag{9}$$

$$m^{-4}U_{+}^{(1)} = \frac{1}{2}\frac{m}{p}\left(a - \frac{E}{m} - \frac{1}{2}a^2\frac{E}{m}\right)(f^2 - u^2) + \frac{1}{3}\frac{m}{p}\left(1 - a\frac{E}{m}\right)(f^3 - m^3)\,, \tag{9'}$$

where we have put for brevity $(\mu/m) = a$, $(F/m) = f$ and $(\mathcal{E}_{-}/m) = u$. For allowed values of E, u is found numerically to be accurately given by

$$u = 0.987 + 0.791t\,, \tag{10}$$

where t is the neutron kinetic energy in units of m, $t = (E - m)/m$. For the choice « minus » in the coupling the spectrum turns out to be given by

$$m^{-4}U_{-}^{(0)} = a\frac{E}{m}\left(-\frac{1}{2}a + \frac{E}{m}\right)(f - u)\,, \tag{11}$$

and the polarization is $P_L = p/E = r/c$ at any energy E, as evident from (3) and (3″). The energy E of the neutron inside the nucleus is related to the measured kinetic energy outside the nucleus by $T = E - m - F - \Delta$.

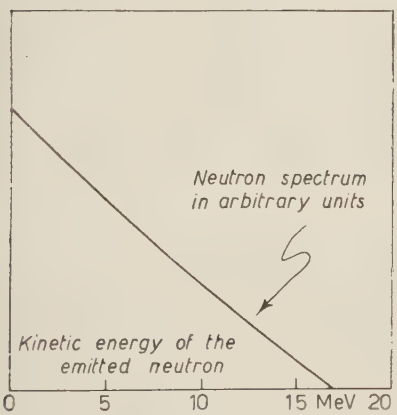

Fig. 1.

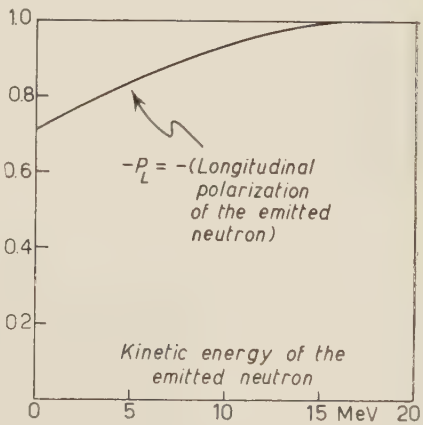

Fig. 2.

In Fig. 1 we plot the neutron spectrum as given by (8), (9) and (10) for the choice « plus ». The spectrum turns out to be essentially linear since most of the energy variation in (9) comes from the factor $(f - u)$. In Fig. 2 we report the longitudinal polarization P_L, for the choice « plus », as given by

(8′), (9), (9′) and (10). It is seen that the polarization is indeed large. A discussion of the limitations of this result is given in the next section. For the choice « minus » the shape of the spectrum would again be essentially linear, and the polarization negligible.

3. – The longitudinal polarization of neutrons has been calculated with a Fermi gas model of the nucleus. Nevertheless, once the polarized neutron is produced, it has to travel in the nuclear matter before escaping from the nucleus. In traversing the nuclear matter the neutron is subject to an average potential due to the presence of other nucleons.

In order to evaluate the depolarization suffered by the neutron in the nuclear matter we will make the assumption that the neutron is first produced in a plane wave state with a definite momentum and polarization, and then scattered by the whole nucleus. This is approximately equivalent to evaluate the rescattering corrections in an impulse approximation.

Let

$$T = A + i\boldsymbol{\sigma}\cdot\boldsymbol{p}\times\boldsymbol{q}\,\frac{B}{pq},$$

be the scattering matrix of a nucleon of initial momentum $\boldsymbol{p}$ and final momentum $\boldsymbol{q}$. If the initial state χ_i is completely polarized along $\boldsymbol{p}$, then

$$(\boldsymbol{\sigma}\boldsymbol{p}/p)\chi_i = \chi_i\,.$$

We want to find the probability that in the final state the neutron has spin opposite to the momentum q for all directions of the initial momentum $\boldsymbol{p}$, since we only detect the direction of the neutron after it has been scattered, without knowing the momentum of production. Clearly the longitudinal polarization of the escaping neutron will be

$$P'_L = 1 - 2\,w, \tag{12}$$

since $1 - w$ is the probability that the spin is parallel to $\boldsymbol{q}$ in the final state. Then

$$w = \frac{1}{\sigma_t}\int \chi_i^*\left(A^* - i\boldsymbol{\sigma}\cdot\boldsymbol{p}\times\boldsymbol{q}\,\frac{B^*}{pq}\right)\frac{1}{2}\left(1 - \frac{\boldsymbol{\sigma}\boldsymbol{q}}{q}\right)\left(A + i\boldsymbol{\sigma}\cdot\boldsymbol{p}\times\boldsymbol{q}\,\frac{B}{pq}\right)\chi_i\,\mathrm{d}\Omega_p. \tag{13}$$

The total cross-section σ_t is given by the well known formula

$$\sigma_t = \int (A^*A + B^*B\sin^2\vartheta)\,\mathrm{d}(\cos\vartheta)\,\mathrm{d}\varphi\,,$$

where ϑ is the scattering angle between $\boldsymbol{p}$ and $\boldsymbol{q}$.

From Eqs. (12) and (13) it is easy to obtain:

$$P'_L = \frac{1}{\sigma_t}\int[(A^*A - B^*B\sin^2\vartheta)\cos\vartheta - (A^*B + B^*A)\sin^2\vartheta]\,\mathrm{d}(\cos\vartheta)\,\mathrm{d}\varphi\,. \tag{14}$$

If the scattering matrix of neutrons against the target nucleus is known, the residual polarization is easily calculated by means of Eq. (14). As an example we assume the μ^- capture to take place in ^{12}C. Neutrons at the high energy tail of the spectrum are, according to our previous calculations, completely polarized at production. Therefore we evaluate the residual polarization of 14 MeV neutrons. For our calculations we assume a nuclear potential given by the optical model of Bjorklund and Fernbach ([5]):

$$V = (V_{CR} + iV_{CI})\varrho(r) + V_{SR}\frac{1}{\mu^2}\frac{1}{r}\frac{\mathrm{d}\varrho(r)}{\mathrm{d}r}\boldsymbol{\sigma}\cdot\boldsymbol{l}\,,$$

with $V_{CR} = 45$ MeV, $V_{CI} = 11$ MeV, $V_{SR} = 8.3$ MeV.

Since the differential cross-section is strongly peaked in the forward direction (at 60° its magnitude is 1/100 of the one in the forward direction and it remains of this order also in the backward direction) we can use in our integrals the Born approximation for A and B. We stress that in spite of the fact that usually the Born approximation does not give correctly the polarization at large angles, we can safely use it because to our integrals only the contributions below, say, 40° are important. Then

$$A = \frac{1}{2\pi}E(V_{CR} + iV_{CI})v(\boldsymbol{p} - \boldsymbol{q}), \tag{15}$$

$$B = \frac{1}{2\pi}EV_{SR}\frac{p^2}{\mu^2}v(\boldsymbol{p} - \boldsymbol{q})\,, \tag{15'}$$

whe $v(\boldsymbol{p} - \boldsymbol{q})$ is the Fourier transform of $\varrho(r)$. Now we point out that the differential cross-section below 60° is practically proportional to $v^2(\boldsymbol{p} - \boldsymbol{q})$, because the term $B^*B\sin^2\vartheta$ is negligible compared to A^*A. Therefore we simply replace $v^2(\boldsymbol{p} - \boldsymbol{q})$ in our integrals with the experimental differential cross-section (in this way one can check that in fact the term $B^*B\sin^2\vartheta$ is negligible), since the angle-independent proportionality coefficient drops out. We easily obtain then, by substitution of Eqs. (15) and (15') in Eq. (14):

$$P'_L = 0.79\,.$$

([5]) F. Bjørklund and S. Fernbach: *Phys. Rev.*, **109**, 1295 (1958).

We conclude therefore that depolarization of the high energy tail of the neutron spectrum due to rescattering by the nucleus is reasonably small (~ 0.2).

On the contrary we expect the depolarization to be very high at low energies since we know from scattering experiments of 3 MeV neutrons on Carbon that the cross-section is approximately symmetrical around 90° and the transverse polarization of unpolarized neutrons very high.

Finally, as a partial justification of the model that we have employed, we want to remark that, on the basis of the optical model, the calculated mean free path for neutrons of the energy considered here is always greater than the nuclear radius for all light nuclei. We therefore do not expect a large probability of reabsorption for the emitted neutrons, such as to give rise to compound nucleus formation.

4. – The calculation of the polarization was based on a form $A - V$ for the μ-capture interaction. It is known however that even when the primary weak interaction is exactly $A - V$, virtual pion effects in the μ-capture will modify it and produce an effective interaction which in addition to A and V, with coefficients now in general different, may also contain other forms of coupling. The problem has been recently discussed by GOLDBERGER and TREIMAN ([6]) and by WOLFENSTEIN ([4]). GOLDBERGER and TREIMAN find that the S-matrix for μ-capture contains in addition to A and V also a PS coupling and a term involving derivatives of the lepton fields. The coupling constants for A and V in the effective interaction are found however to be essentially the same as the corresponding renormalized coupling constants for β-decay, in spite of the larger momentum transfer involved. The error that one makes by identifying the A and V effective coupling constants for μ-capture with the corresponding effective coupling constants for β-decay is estimated to be of the order of 4% for the A term and perhaps less, of the order of 0.1% for the V term. However the effective coupling for β-decay is known experimentally to have almost the same amount of A and V, so we are justified, in view of the other approximations, to take the effective coupling constants for A and V in μ-capture of the same magnitude. The effective PS coupling in μ-capture is found by GOLDBERGER and TREIMAN and by WOLFENSTEIN ([4]) to be $\sim 8 g_A$ ([7]). Its contribution to the various measurable effects in μ-capture in hydrogen has been discussed by WOLFENSTEIN ([4]). For the relevant case of a coupling $g_P = -g_A$ it is found that the longitudinal polarization of the neutron is reduced from the value -1 to -0.93. Thus we expect a reduction of the values that we have obtained here for the longitudinal polarization if the effective

([6]) M. L. GOLDBERGER and S. B. TREIMAN: *Phys. Rev.*, **111**, 354 (1958).

([7]) A first estimate was given by LOPES. I. L. LOPES: *Phys. Rev.*, **109**, 509 (1958).

PS interaction is included in the effective Hamiltonian. The reduction may possibly be greater than 10% because the absorbing protons are here considered in motion. Finally the derivative term, which is also expected to be present on the basis of invariance arguments, should give negligible contribution if only the $A - V$ four fermion interaction exists. It may give appreciable contributions if a direct pion-lepton interaction also exists, as postulated by FEYNMAN and GELL-MANN in order to have non-renormalization of the V part ([8]).

([8]) R. P. FEYNMAN and M. GELL-MANN: *Phys. Rev.*, **109**, 193 (1958).

RIASSUNTO

La polarizzazione longitudinale del neutrone veloce emesso nell'assorbimento di un muone negativo da parte di un nucleo viene calcolato per una interazione $A \pm V$ ed usando un modello di Fermi per il nucleo. Si fa vedere come, nei limiti in cui tale modello può venire usato per descrivere il processo, il neutrone emesso ha un'apprezzabile polarizzazione longitudinale nel caso di accoppiamento $A - V$. Il calcolo delle correzioni dovute al rescattering dentro il nucleo mostra che questa conclusione resta valida per i neutroni emessi nella porzione superiore dello spettro.

On the Mechanical Moment of Rotation of Mixtures of Liquids in Rotating Electric Fields.

A. Carrelli and M. Marinaro

Istituto di Fisica dell'Università - Napoli

(ricevuto il 18 Novembre 1958)

Summary. — In this paper the behaviour of some mixtures of liquids in rotating electric fields at low frequencies has been studied. It was found that the mechanical moment produced, even taking into account the electric conductivity variation, is about 10^3 greater than that foreseen by Lampa's theory.

In this work the behaviour of some mixtures of liquids in rotating electric fields at low frequencies ($\nu = 50$, 150 and 840 Hz), and also for $\nu = 1500$ kHz, has been studied. In such a frequency range a bridge system, as shown in Fig. 1, has been used. The alternating voltage produced by an oscillator is sent to the vertexes of a bridge composed of resistances and capacitors; if we take for R and C such values as to satisfy the condition:

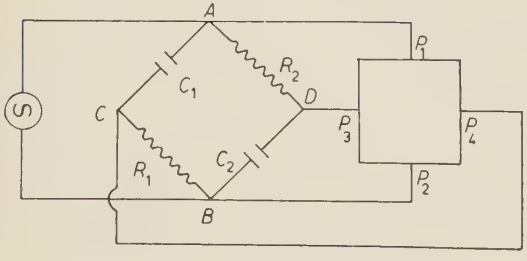

Fig. 1.

$$R_1 = R_2 = \frac{1}{C_1\omega} = \frac{1}{C_2\omega},$$

where ω is the pulsation of the rotating electric field, we obtain on the plates P_1, P_2, P_3, P_4 alternate voltages of the same intensity and by 90° out of phase with each other, and, therefore, inside them, a rotating and uniform electric field. In the middle of the plates a cylindrical vessel made of teflon

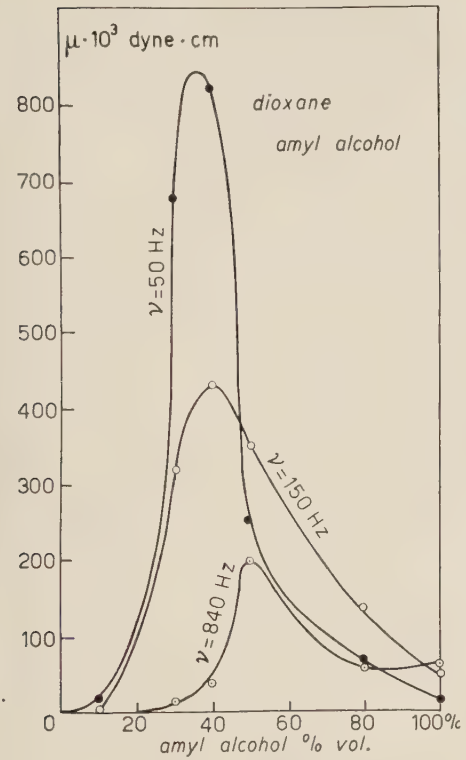

g. 2.

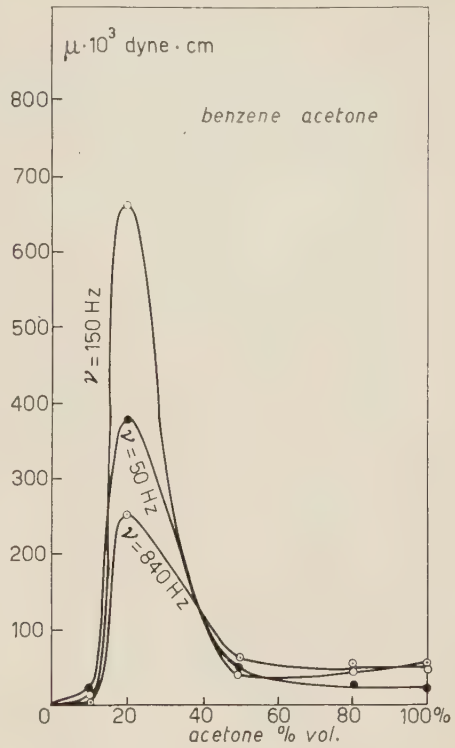

Fig. 3.

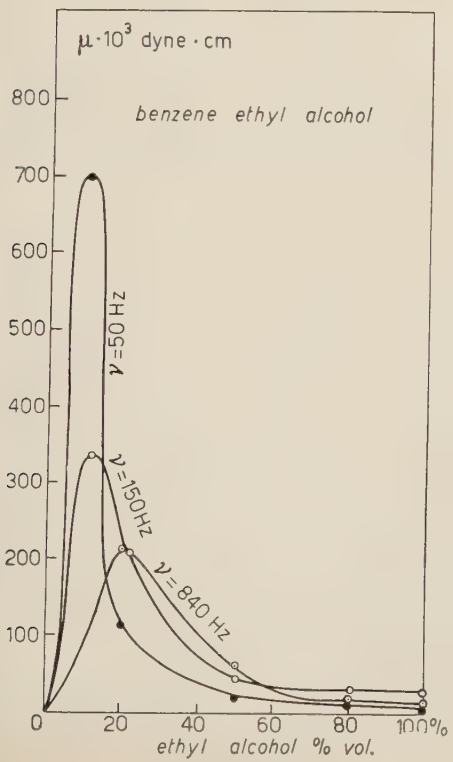

4.

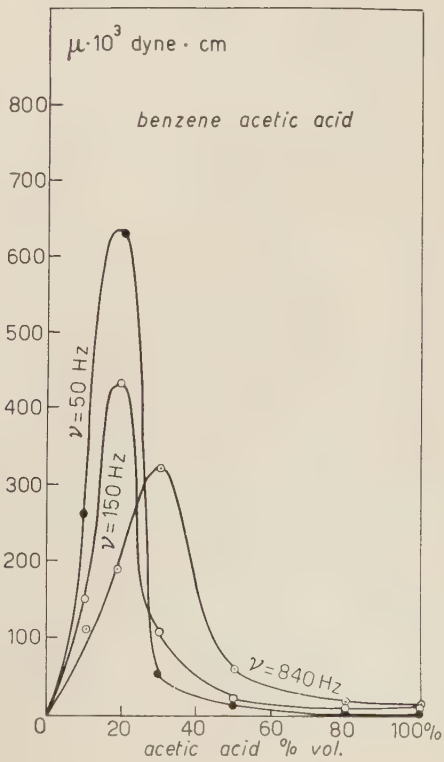

Fig. 5.

(external radius 2.5 cm, internal radius 2.2 cm, height 3.5 cm), containing the tested liquid, is overhung by means of a copper wire with diamete 0.01 cm. By means of such an apparatus it is possible to measure the moments of rotation in a range of 10^{-3} dyne·cm. The mixtures are formed of non-polar

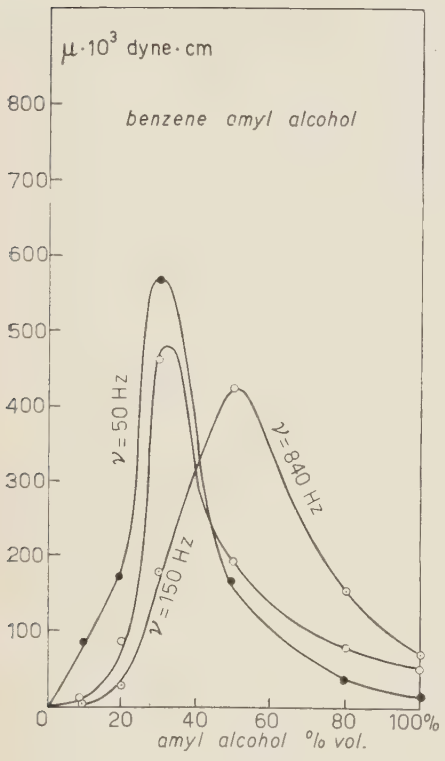

Fig. 6.

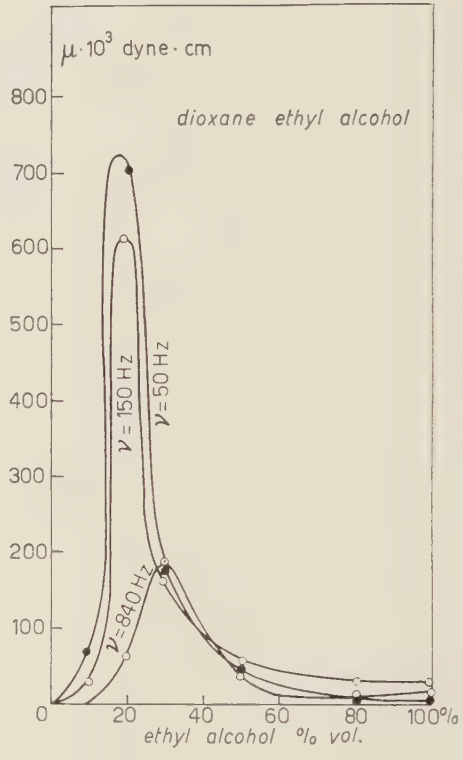

Fig. 7.

liquids (benzene or dioxane) and polar liquids (ethyl alcohol, amyl alcohol, acetic acid, nitrobenzene, acetone). Figs. 2, 3, 4, 5, 6, 7, 8 refer to the results we obtained: the moments of rotation are plotted against the volumetric concentrations; the acting electric field is 0.35 u.e.s. As we can deduce from the graphs, the moments of rotation show a very high maximum which, except in the case of the mixture benzene-acetone, decreases with increasing frequency shifting towards concentrations with larger percentage of polar liquid. Now, according to a theory developed by A. LAMPA [1], a liquid with dielectric

[1] A. LAMPA: *Wien. Ber.*, **115** (2*a*), 1659 (1906).

constant ε_i and electric conductivity λ_i, placed in a rotating electric field, on account of the phase displacement between the charge arrangement on the surfaces dividing the different dielectrics (liquid, vessel, air) and the electric field, feels the action of a mechanical moment M given by:

$$M = 36\pi E^2 R^3 \frac{\lambda_i \omega}{16\lambda_i^2 + \omega^2(2+\varepsilon_i)^2},$$

E = intensity of the electric field,
R = internal radius of the vessel.

In order to compare the experimental data with such a moment, it is necessary to know the values of ε_i and λ_i for the different mixtures. We must notice

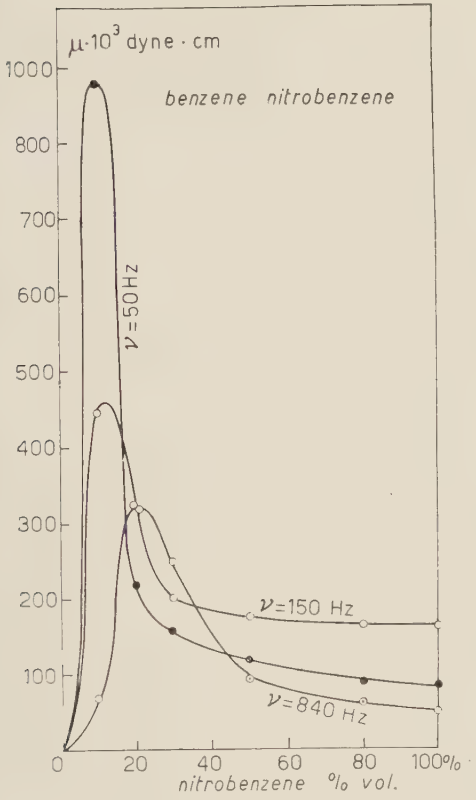

Fig. 8.

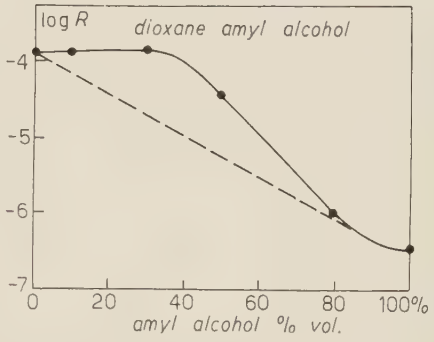

Fig. 9.

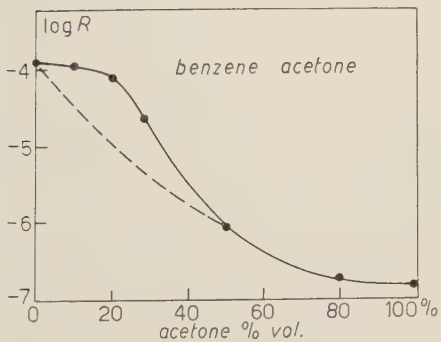

Fig. 10.

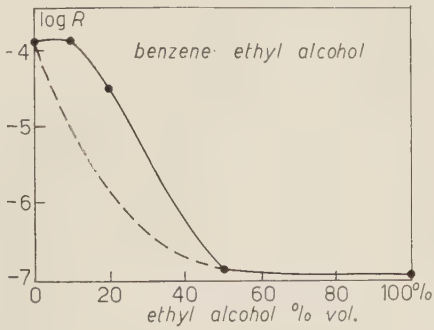

Fig. 11.

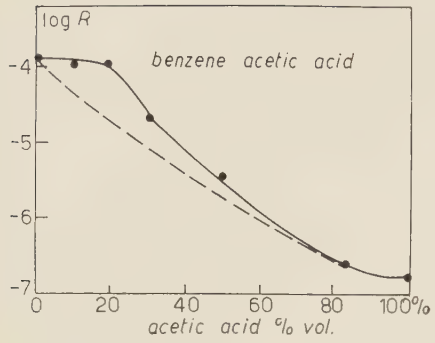

Fig. 12.

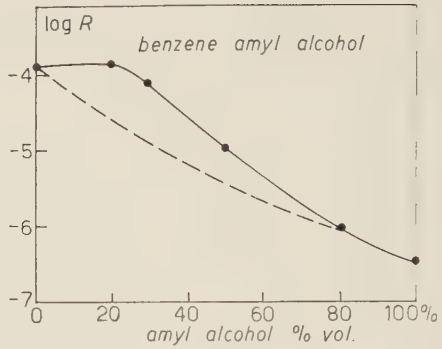

Fig. 13.

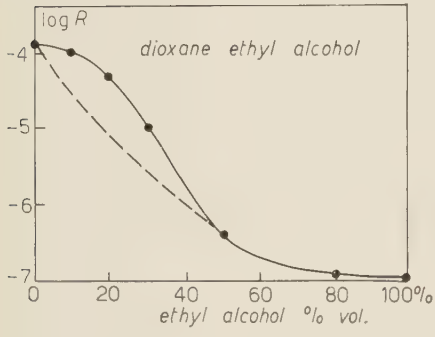

Fig. 14.

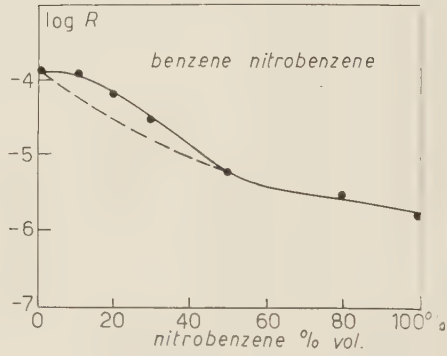

Fig. 15.

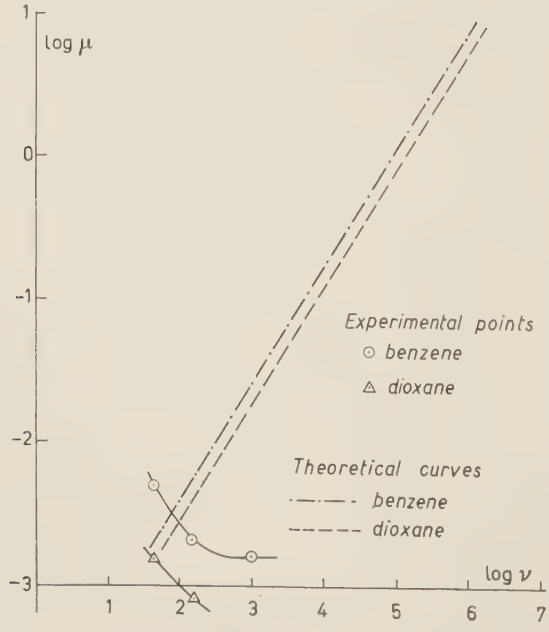

Fig. 16.

that at the frequencies used by us the term in which ε_i appears is negligible in respect of the one with λ_i, and therefore the formula is simplified as follows:

$$(1) \qquad M = 36\pi E^2 R^3 \frac{\omega}{16\lambda_i}.$$

Measurements of λ_i for our mixtures have been done with the method of the discharge through a capacitor; the values we obtained are reproduced in a logarithmic scale (Figs. 9, 10, 11, 12, 13, 14, 15). According to the formula (1) M should have very small values, in a range of 10^{-3} dyne·cm, and even smaller, and therefore beyond the limits of the sensibility of the apparatus used by us.

The values of M we measured are much larger, and therefore the experimental curves show a completely different behaviour from the theoretical one; really, whilst the resistivity only shows a very low maximum, in respect of the regular behaviour, and such a maximum should produce only a very small increase in the moment of rotation, we found experimentally a much larger value.

In Figs. 16 and 17 the theoretical curves of the moments of rotation of pure liquids foreseen by LAMPA are compared with the experimental ones.

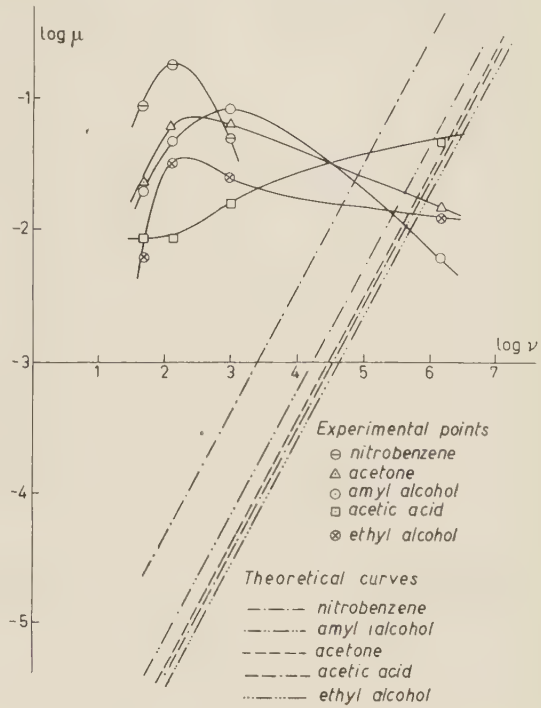

Fig. 17.

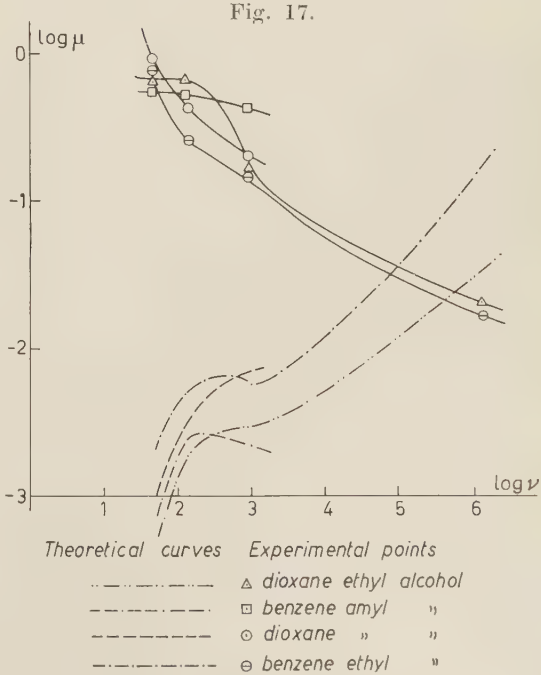

Fig. 18.

As we can see, at high frequency ($\nu = 1500$ kHz) the moments are the same size, whilst, at low frequencies, they are also 10^3 times larger; in Figs. 17 and 18 the same comparison for the theoretical and for the experimental moments is made at the concentrations for which there is a maximum for such a moment of rotation.

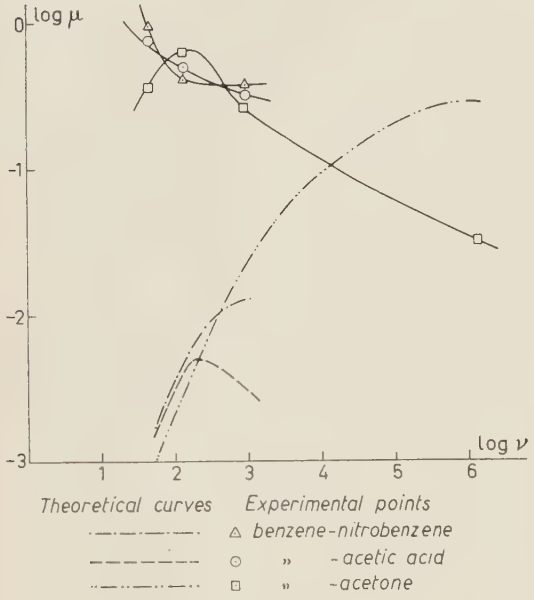

Fig. 19.

The experimental results obtained by us at such low frequencies may be interpreted thinking that for the mixtures we used there is, at special concentrations, a remarkable decrease of the conductivity due to the formation of complexes which must also be considered very unstable because they appear to be very sensitive to the frequency change of the rotating field. It should also be noted that the measurements of conductivity made by us and reproduced in Figs. 9, 10, 11, 12 13, 14 and 15 have been done at $\nu = 0$ and for this reason, probably, it is not possible to notice a variation of λ_i. The variation of the conductivity, put indirectly in evidence by us, is confirmed by testing the diffraction of the X-rays in these mixtures. In fact, as it results from other researches (*), the intensity of the ring of diffraction shows a maximum due to the formation of complexes just at the concentrations for which there is the maximum of rotation.

(*) To be published in *Nuovo Cimento*.

RIASSUNTO

In questo lavoro si è studiato il comportamento di alcune soluzioni di liquidi posti in campi elettrici ruotanti a basse frequenze (50, 150, 840 Hz). Si è trovato che il momento meccanico che così si genera, pur tenendo conto della variazione della conducibilità elettrica, è circa 10^3 volte maggiore di quello previsto dalla teoria di Lampa.

IL NUOVO CIMENTO Vol. XI, N. 2 16 Gennaio 1959

On the Renormalization of the Axial Vector β-Decay Coupling.

K. Symanzik

Max-Planck-Institut für Physik - München

(ricevuto il 18 Novembre 1958)

Summary. — A formula expressing the ratio g_A/g_V in β-decay on the basis of equality of the corresponding bare coupling constants is proposed and proved in perturbation theory with cut-off, provided electromagnetic interactions are neglected. The physical background of a formula of this type is discussed and illustrated by comparison with recent work by Goldberger and Treiman on π-μ decay.

The question of whether the ratio g_A/g_V could be determined on the basis of the assumption that the corresponding bare coupling constants are equal has recently been raised [1]. In fact, unless this ratio can be determined from a knowledge of the interactions responsible for the «renormalization» alone and goes to one if these interactions go to zero, the statement that μ-decay suggests that the bare coupling constants are equal could not be based simply on the smallness of the fine structure constant. Moreover, the equality of the bare coupling constants would remain a meaningless concept unless it leads to predictable consequences for the ratio g_A/g_V [2]. In this note we propose a formula that expresses this ratio, provided electromagnetic interactions are neglected, and discuss the physical background of this formula at some length.

[1] Cfr. *Proc. of the Annual International Conference on High Energy Physics at CERN* (1958), p. 258.

[2] The author is grateful to Prof. W. Pauli for a stimulating letter in which this was pointed out. Of course, one thinks here always in terms of the first order of the weak coupling constant. It might be remarked here that higher orders are not necessarily untractable since their non-renormalizability refers to a power development also in the strong couplings.

In the notation of GOLDBERGER and TREIMAN [3] we have

$$A_\mu(x) \equiv GZ_2 \overline{\psi}_p(x) i\gamma_5 \gamma_\mu \psi_n(x) , \tag{1}$$

$$V_\mu(x) \equiv GZ_2 \overline{\psi}_p(x) \gamma_\mu \psi_n(x) , \tag{2}$$

with $\psi(x)$ etc., being the renormalized operators. The quantities in question are

$$\langle p | A_\mu(0) | n \rangle = \overline{U}(p)[a i\gamma_5 \gamma_\mu - ib(p-n)_\mu \gamma_5] U(n) ,$$

$$\langle p | V_\mu(0) | n \rangle = \overline{U}(p)[c\gamma_\mu - id\sigma_{\mu\nu}(p-n)^\nu] U(n) ,$$

where a, b, c and d are real functions, the momentum transfer variable $(p-n)^2 \leqslant 0$ and, by definition, under neglect of the electron mass, $a(0) = g_A$ and $c(0) = g_V$. g_A/g_V is to be found. In all of the following, electromagnetic corrections will be neglected.

If the pion mass were larger than $\sqrt{2}-1$ times the nucleon mass it could be proven [4] that a, b, c and d are analytic in the complex $(p-n)^2 \equiv z$-plane with cuts from $9\mu^2$, $9\mu^2$, $4\mu^2$, $4\mu^2$, respectively to $+\infty$, with b having an additional pole at μ^2. It is, however, probable that this restriction comes from the present unsufficient techniques only, and we shall assume this analytic property to hold.

Consider now the difference $a(z) - c(z)$. When $|z| \to \infty$, $a(z)$ and $c(z)$ can be expected to approach each other. This would follow from a result [5] of Källén's in quantum electrodynamics and generalized by him to the conjecture [6] that in the limit of infinite energies the Born approximation becomes valid. We shall come back to this later. In our case the Born approximations to $a(\infty)$ and $c(\infty)$ are GZ_2 and this cancels in the difference. Therefore we expect

$$g_A - g_V = \frac{1}{\pi} \int_{4\mu^2}^{\infty} \frac{\operatorname{Im}\,(a(\xi) - c(\xi))}{\xi} \, d\xi . \tag{3}$$

Since $a(\xi) = g_A \alpha(\xi)$ and $c(\xi) = g_V \gamma(\xi)$ with α and γ depending only on the

[3] M. L. GOLDBERGER and S. B. TREIMAN: *Phys. Rev.*, **111**, 354 (1958). We prefer to use in the present article the notation of BETHE, SCHWEBER and DE HOFFMAN: *Mesons and fields*, vol. **1**.

[4] H. J. BREMERMANN, R. OEHME and J. G. TAYLOR: *Phys. Rev.*, **109**, 2178 (1958).

[5] G. KÄLLÉN: *Quantum electrodynamics*, in: *Encyclopedia of Physics*, vol. **5**, part I, pp. 362-363.

[6] G. KÄLLÉN: *Consistency problems in quantum electrodynamics*, CERN 57-43, and *CERN Symposium*, vol. **2** (1956), p. 187.

strong interactions, we obtain

$$\frac{g_A}{g_V} = \frac{1 - (1/\pi)\int_{4\mu^2}^{\infty} (\operatorname{Im} \gamma(\xi)/\xi)\, \mathrm{d}\xi}{1 - (1/\pi)\int_{9\mu^2}^{\infty} (\operatorname{Im} \alpha(\xi)/\xi)\, \mathrm{d}\xi}. \tag{4}$$

This ratio goes, at least formally, to one if the « renormalizing » interactions go to zero, as it should be, and can be evaluated for instance with such approximation methods as Goldberger and Treiman's [3] where only one type of intermediate states is taken into account.

If the integrals in the denominator and numerator in (4) converge too slowly, the relation (3) would be more useful for numerical checks. If they would be divergent, this would mean that $GZ_2 = \infty$, and the assumption that the cancellation of the leading term in the difference $a(z) - b(z)$ leads to $a(z) - b(z) \to 0$ at infinity would appear less justified. Rather we would have, in this case,

$$\frac{g_A}{g_V} = \lim_{|z|\to\infty} \frac{\gamma(z)}{\alpha(z)}.$$

The dispersion treatment of the ratio $[a(z) - c(z)]/c(z)$ seems impracticable because of the unknown zeros of $c(z)$.

In the case of divergence-free vector coupling [7] one adds to $V_\mu(x)$ in (2) the requisite terms and shows easily, for instance by the method of the appendix, that $g_V = G$. So G is finite and, since $0 \leqslant Z_2 < 1$, the reasoning that leads to (3) is considerably improved because GZ_2 cannot be infinite. However, from the dispersion relation for $c(z)$ we obtain

$$g_V = g_V Z_2 + \frac{1}{\pi}\int_{4\mu^2}^{\infty} \frac{\operatorname{Im} c(\xi)}{\xi}\, \mathrm{d}\xi,$$

or

$$Z_2 = 1 - \frac{1}{\pi}\int_{4\mu^2}^{\infty} \frac{\operatorname{Im} \gamma(\xi)}{\xi}\, \mathrm{d}\xi. \tag{5}$$

In the case of quantum electrodynamics, it has been shown by Källén [6]

(7) R. P. Feynman and M. Gell-Mann: *Phys. Rev.*, **109**, 193 (1958). That a divergence-free strangeness-nonconserving axial vector current is ruled out experimentally has been shown by Goldberger and Treiman (*Phys. Rev.*, **110**, 1478 (1958)).

that $Z_2 = 0$. So it seems probable that the numerator in (4), and unless $g_A = 0$ also the denominator, vanish.

However, there is some reason to hope that an approximate evaluation of (4), roughly corresponding to the use of a high energy cut-off at some places in the theory, gives a result that makes physical sense. For instance, the approximate evaluation of the numerator in (4) by FEDERBUSH, GOLDBERGER and TREIMAN ([8]) in the divergence-free case gives $\simeq 1$ and not $\simeq 0$. Furthermore it is known that manipulations based on field equations and coupling terms may possibly lead to contradictions ([6]) that show that these manipulations are not justifiable unless a cut-off is introduced. Of course, in this latter case new contradictions ([9]) may arise, but the rule one should apparently follow is not to feed back the high energy behaviour of some matrix element into the formalism in order to check the high energy limit of a different, or possibly the same, matrix element. The optimal expectation with respect to approximate evaluations of (4) in the mentioned case where both numerator and denominator vanish might be that a neglect of many-particle intermediate states corresponds formally to the removal of a common factor zero.

In any case, (4) and (5) are correct in a perturbation expansion with cut-off. In order to prove this, we first give a simplified version of Källén's argument ([5]) leading to $\lim_{\xi \to -\infty} c(\xi) = \lim_{\xi \to -\infty} a(\xi) = GZ_2$, provided all renormalization constants were finite. We have in a standard way, with explicit use of (2) in the original or extended form,

$$p \,|\, V_\mu(y) \,|\, n\rangle = \overline{U}(p) \iint \mathrm{d}x\,\mathrm{d}x' \exp[ipx - inx'] \overrightarrow{Di} \quad |\, T\psi_p(x) V_\mu(y) \overline{\psi}_n(x') \,|\, \rangle \overleftarrow{Di}_x U(n) -$$

$$= \overline{U}(p) \Big[GZ_2 \int \mathrm{d}x \exp[ipx] \overrightarrow{Di}_x \langle |\, T\psi_p(x)\, \overline{\psi}_p(y) \,|\, \rangle \gamma_\mu \cdot$$

$$\cdot \int \langle |\, T(\psi_n(y)\, \overline{\psi}_n(x') \,|\, \rangle \overleftarrow{Di}_{x'} \exp[-ix'n]\, \mathrm{d}x' +$$

$$+ \iint \mathrm{d}x\,\mathrm{d}x' \exp[ipx - inx'] \overrightarrow{Di}_x \langle |\, T\psi_p(x) V_\mu(y) \psi_n(x') \,|\, \rangle_{\mathrm{conn}} \overleftarrow{Di}_{x'} \Big] U(n) .$$

Since

$$\int \mathrm{d}x \exp[ipx] \overrightarrow{Di}_x \langle |\, T\psi_p(x)\, \overline{\psi}_p(y) \,|\, \rangle = i \exp[ipx] , \quad \text{if } \boldsymbol{p} = M \ ([10]),$$

([8]) P. FEDERBUSH, M. L. GOLDBERGER and S. B. TREIMAN: *Electromagnetic structure of the nucleon* (*Phys. Rev.*, **112**, 642 (1958)).

([9]) See *e.g.* I. YA. POMERANČUK, V. V. SUDOKOV and K. A. TER-MARTIROSYAN: *Phys. Rev.*, **103**, 784 (1956), and also some unpublished work by W. THIRRING.

([10]) This is meant as $\overline{U}(p)(\boldsymbol{p} - M) = 0$, of course.

and $= iZ_2^{-1} \exp[ipy]$ if $p^2 \to \infty$ we obtain for the square bracket with $y = 0$

$$a) \qquad iG\gamma_\mu S_F'(n) \qquad \text{if } p^2 \to \infty$$

$$b) \qquad -iGS_F'(p)\gamma_\mu \qquad \text{if } n^2 \to \infty$$

$$c) \qquad G\gamma_\mu Z_2 \qquad \text{if } \boldsymbol{p} = M,\ \boldsymbol{n} = M,\ (p-n)^2 \to -\infty$$

provided the second term in the square bracket vanishes in all these limits. This, however, is the case at least in a perturbation theory with a cut-off that leads to finite renormalization constants. Namely, the connected part of the vacuum expectation value consists of Feynman integrals that correspond to connected graphs and therefore contain the infinite external momenta somewhere in the denominator. So these contributions vanish in the limit when one or two of the external momentum squares go to infinity provided the integrals are cut-off to make them convergent. This singling out of the complete disconnected parts corresponds to taking properly into account the « switching-on » singularities in Källén's formulation ([5]).

A partial check of the statements *a*), *b*) and *c*) independently of perturbation theory for a divergence-free $V_\mu(y)$ will be made in the Appendix.

Now the perturbation-theoretical proof of (4) and (5) is easy. Since the well known analytic property of the vertex, as well as the dispersion relations, are not invalidated if any propagator lines are regularized ([11]) and the high-energy behaviour is then given by the now finite GZ_2, (4) and (5) hold in these cases, with an analogous regularization for Z_2 as that to be employed in the calculation of $\gamma(\xi)$. Actually (5) could then be considered as a redefinition of Z_2 in the divergence-free case.

From this reasoning, it remains entirely open whether in any such approximate evaluation of the right hand side of (5) Z_2 comes out close to zero or not. However, in order to give a meaning to (4), comparable approximations in the numerator and denominator would have to be made, since otherwise (4) might give any value. Of course, these considerations do not imply that taking into account only the simplest intermediate states next to perturbation theory should give a reasonable result. Especially, the slightly awkward three-pion intermediate state in $\operatorname{Im} a(\xi)$ should be considered. Since the numerator of (4) has already been estimated by FEDERBUSH, GOLDBERGER and TREIMAN ([8]) to $\simeq 1$ it would be up to that state whether $g_T/g_A > 1$ or < 1.

([11]) Y. NAMBU: *Nuovo Cimento*, **6**, 1064 (1957) and **9**, 610 (1958); K. SYMANZIK: *Progr. Theor. Phys.*, **20**, 690 (1958).

Were its effect such as to make $a(-\xi)$ decrease with ξ increasing, in this approximation the sign would be correct.

It should be remarked that in the spirit of the present considerations (5) is the condition that the vector coupling renormalization vanishes accidentally for a non-divergence-free coupling. The estimate $\simeq 1$ for the right hand side of (5) just mentioned ([8]) was obtained under the explicit assumption of divergence-free coupling.

Of course, in the exact axiomatic theory the question whether the numerator in (4) is zero, or finite, or undefined, may be a sensible and eventually answerable one. The first alternative has been conjectured by CHEW ([12]). Since our argumentation in this paper supports his point of view only as far as electromagnetic corrections are neglected, we would not feel to be necessarily led to the « non-subtraction philosphy » of DRELL and ZACHARIASEN ([13]).

To finally illustrate the somewhat chameleonic nature of renormalization constants as far as approximations are concerned we discuss the approximate expression for the $\pi^{\pm}$-decay rate found by GOLDBERGER and TREIMAN ([14]). They obtain

$$A_\mu(0)\,|\pi^-\rangle \simeq -ik_\mu \frac{M}{\pi^2} g g_A \frac{J}{1+(g^2/4\pi)(2J/\pi)},$$

where g is the renormalized pion-nucleon coupling constant. J is an integral depending on an assumed ${}^1S_0^3$ nucleon-antinucleon scattering phase shift and diverges logarithmically in the case of zero phase shift. Now inspection of the way this formula is derived reveals that g^2J in the numerator is proportional to the lowest order pion-amplitude renormalization $Z_3{}^1 - 1$ but with an automatic cut-off, and g^2J in the denominator arises from a mass-renormalized pion self energy. So the expression can also be written

$$\langle |A_\mu(0)\,|\pi^-\rangle \simeq -ik_\mu \frac{2Mg_A}{g}(1-Z_3), \tag{6}$$

and this «Z_3» is estimated by GOLDBERGER and TREIMAN to be small compared with one.

A certain understanding of this formula can be reached in the following way: We have

$$A_\mu(0)\,\pi \quad\quad ik_\mu F(\mu^2),$$

([12]) G. F. CHEW: *The bare particle concept and nucleon electromagnetic structure*, UCRL-8194.

([13]) S. D. DRELL and F. ZACHARIASEN: *Phys. Rev.*, **111**, 1727 (1958).

([14]) M. L. GOLDBERGER and S. B. TREIMAN: *Phys. Rev.*, **110**, 1178 (1958).

with

$$k_\mu F(k^2) = -GZ_2 \int \langle | T\overline{\psi}_p(0) i\gamma_5\gamma_\mu \psi_n(0) \varphi(x) | \rangle (\overleftarrow{\Box} + \mu^2) \exp[-ikx]\,\mathrm{d}x\,.$$

Therefore

$$k^2 F(k^2) = -GZ_2(k^2-\mu^2) \int \exp[-ikx]\, i \frac{\partial}{\partial x_\mu} \langle | T\overline{\psi}_p(0) i\gamma_5\gamma_\mu \psi_n(0)\varphi(x) | \rangle \,\mathrm{d}x =$$

$$= GZ_2(k^2-\mu^2) \int \exp[ikx]\, i \frac{\partial}{\partial x_\mu} \langle | T\psi_p(x) i\gamma_5\gamma_\mu \psi_n(x)\varphi(0) | \rangle \,\mathrm{d}x$$

$$= GZ_2(k^2-\mu^2) \int \exp[ikx] \langle | T\{\overline{\psi}_p(x) i\gamma_5 \overrightarrow{D} i\psi_n(x) +$$

$$+ \overline{\psi}_p(x) \overleftarrow{D}_i i\gamma_5 \psi_n(x) + 2M\overline{\psi}_p(x) i\gamma_5 \psi_n(x)\}\varphi(0) | \rangle \,\mathrm{d}x =$$

$$= GZ_2(k^2-\mu^2) \int \exp[ikx] \langle | T\{2M_0 \overline{\psi}_p(x) i\gamma_5 \psi_n(x)$$

$$- ig\, Z_1 Z_2^{-1} \sqrt{2}[\overline{\psi}_p(x)\psi_p(x) + \overline{\psi}_n(x)\psi_n(x)]\varphi^+(x)\}\varphi(0) | \rangle \,\mathrm{d}x\,,$$

where M_0 is the bare nucleon mass. If we keep only the first term in the curly bracket and neglect the direct meson-meson coupling, we obtain

$$k^2 F(k^2) \simeq iGZ_2(k^2-\mu^2) \frac{2M_0}{g} [(2\pi)^4 (k^2-\mu_0^2) \Delta'_F(k) - iZ_3^{-1}]\, Z_1^{-1} Z_3\,,$$

where μ_0 is the bare meson mass. So we finally have

$$F \simeq \frac{2G}{g} \frac{[M_0 Z_2]}{Z_1} \left\{ \frac{[Z_3\mu_0^2]}{\mu^2} - Z_3 \right\}. \tag{7}$$

Owing to our approximation there is nothing else left: Z_1 and $M_0 Z_2$ could be related to each other, so they are to be replaced by 1 and M, respectively, and G is to be replaced by g_1. In the further approximation where $Z_3\mu_0^2 \simeq \mu^2$ (see, however, added note) (6) is obtained. This calculation is intimately related to a consideration by NORTON and WATSON [15] for pseudovector pion coupling, as is not surprising in view of the equivalence theorem.

One of the advantages of the dispersion methodological treatment of this problem seems to be not to require to decide whether pseudoscalar or pseudo-

[15] R. E. NORTON and W. K. R. WATSON: *Phys. Rev.*, **110**, 996 (1958).

vector coupling is to be used. There are, however, several possibilities: Either the question of bare couplings is meaningless at all, or only one of these couplings is not physically selfcontradictory, or both make sense and are not, or are, physically distinguishable. In the last case, the difference would lie in some parameters (possibly connected with high energy behaviour) not yet paid attention to, their investigation being presently replaced by a series of assumptions.

* * *

The author would like to thank Prof. W. HEISENBERG for his interest in this work and for useful conversations. He also would like to use this opportunity to thank Prof G. KÄLLÉN for several discussions of the switching-on procedure.

APPENDIX

For a divergence-free $V_\mu(y)$ one finds with (2) in a manner analogous to that of TAKAHASHI ([16]) by straightforward differentiation that

$$\frac{\partial}{\partial y_\mu} \langle | T\psi_p(x)\, V_\mu(y)\, \psi_n(x') | \rangle_{y=0} = \\ = G\langle | T\psi_p(x)\, \overline{\psi}_p(x') | \rangle \delta(x') - G\langle | T\psi_n(x)\, \overline{\psi}_n(x') | \rangle \delta(x) ,$$

or, in momentum space,

$$\text{(A.1)} \qquad i(p-n)_\mu V^\mu(p,n) = G(\boldsymbol{p}-m)\{S'_F(p) - S'_F(n)\}(\boldsymbol{n}-m) .$$

The approximation underlying *a*), *b*) and *c*) in the main text leads for this expression to

$$\text{(A.2)} \qquad iGZ_2(p-n)_\mu(p-m)S'_F(p)\gamma^\mu S'_F(n)(\boldsymbol{n}-m) = \\ = iGZ_2(\boldsymbol{p}-m)i\int \frac{\varrho(\varkappa)\,\mathrm{d}\varkappa}{\boldsymbol{p}-k}(\boldsymbol{p}-\boldsymbol{n})i\int \frac{\varrho(\varkappa')\,\mathrm{d}\varkappa'}{\boldsymbol{n}-k'}(\boldsymbol{n}-m) .$$

If

$$p^2 \to \infty , \qquad \int \frac{\varrho(\varkappa)}{\boldsymbol{p}-k}\,\mathrm{d}\varkappa \to \frac{\boldsymbol{p}}{p^2} Z_2^{-1} ,$$

and we get from (A.2) $-G\boldsymbol{p}S'_F(n)(\boldsymbol{n}-m)$ in accordance with (A.1).

([16]) Y. TAKAHASHI: *Nuovo Cimento*, **6**, 371 (1957).

$n^2 \to \infty$ is similarly treated. Even the case $p^2 \to \infty$, $n^2 \to \infty$ checks. When $\boldsymbol{p} = M$, $\boldsymbol{n} = M$ we get zero from (A.1) as well as from (A.2), independently of $(p - n)^2$, and therefore also for $(p - n)^2 \to -\infty$.

Notes added in proof.

a) The author learnt that formula (4) was also known to M. L. GOLDBERGER (private communication).

b) The replacement of $Z_3\mu_0^2$ by μ^2 in formula (7) is not justifiable in a simple way. For instance, the quadratic divergence of μ_0^2 is only compensated with the help of the disconnected part of the contribution that was previously dropped entirely. Therefore, it is the form of (6) (proportionality to $g_A M/g$) rather than the numerical factor than can be interpreted in the way outlined in the paper.

RIASSUNTO (*)

Si propone, e si dimostra in teoria delle perturbazioni con cut-off, una formula che dà il rapporto g_A/g_V nel decadimento β ove si postuli l'eguaglianza delle corrispondenti costanti d'accoppiamento nude, purchè si trascurino le interazioni elettromagnetiche. Si discutono i fondamenti fisici di una formula di questo tipo e si illustrano confrontandoli con recenti lavori di GOLDBERGER e TREIMAN sul decadimento π-μ.

(*) *Traduzione a cura della Redazione.*

IL NUOVO CIMENTO Vol. XI, N. 2 16 Gennaio 1959

A System of Coupled Oscillators as a Functional Model of Neuronal Assemblies (*).

V. Braitenberg, E. R. Caianiello, F. Lauria and N. Onesto

Scuola di Perfezionamento in Fisica Teorica e Nucleare, Sezione di Cibernetica - Napoli

(ricevuto il 21 Novembre 1958)

Summary. — Proposal of a model which promises to share with the living nervous system the properties of *economy*, capacity to recognize *similarity*, character of *wholeness* (Gestalt).

1. – We wish to present here in a purely qualitative and non-mathematical form, some points which we have come to believe relevant to the problems posed by the interpretation of nervous functions. Quantitative analyses are in progress along these lines and will be reported in due time; the very fact that they appear feasible encourages us to put forth this preliminary account of our work, in the hope of provoking thus already some discussion and criticism.

We wish to emphasize that we do not by any means regard the following as a complete picture of what actually goes on in a brain. We are concerned here with a problem of quite different nature: that of deciding, first of all, which is a convenient starting « level » for an investigation of nervous functions. We take as such the consideration not of single neurons, but rather of assemblies of relatively large numbers of them. This level of description has the advantage of linking up with the physics of many-body systems, and, more generally, of quantized interacting fields, which is in some respects well advanced, and offers both suggestive analogies with physiological situations and well established mathematical methods of approach.

(*) The research reported in this document has been sponsored in part by the European Office of the Air Research and Development Command, United States Air Force.

We shall outline in the following the basic principles on which a theory can be founded accordingly and models built to imitate the functions of the nervous system. Sheer imitation of single neurons and their interconnection and grouping will not fail to exhibit properties of living nervous systems, but is of limited theoretical interest in itself, since it is evident that any substantial progress will require a good grasp of the physical and mathematical principles involved.

2. – We shall now discuss these ideas in greater detail, speaking, for the sake of clarity, only in terms of a concrete realization, say an electronic or mechanical model. While we rather believe that such a model, if skillfully built, will exhibit the behaviour predicted for it, the degree to which it will apply to the functional interpretation of the nervous system is of course debatable. Improved versions of working models would have their own uses, though quite apart from physiology-this being not the least interesting aspect of the question.

3. – We notice first that some of the main requirements to be met are the following:

a) *Economy i.e.* the problem of keeping the number of distinct functional elements low, while handling very large numbers of functional patterns.

b) Recognition of « *similarity of shape* »; this does not correspond to any clear cut mathematical concept now in existence, but emerges clearly from animal experiments as one of the most important principles by which vast numbers of objectively different images are recognized by the brain as belonging to the same class (*e.g.* all the different ways of writing the letter A).

c) The principle of « *wholeness* » or « *Gestalt* » which states that a system is more than the sum of its constituent parts, and implies that the response to the sum of two images need not be equal to the sum of the responses to each individual image.

We envisage models which are intended to overcome these difficulties, as described in the following.

4. – In an array, which for simplicity we imagine two-dimensional and so large that boundary effects may be neglected, we dispose a number of active elements, for short « oscillators », thus characterized:

a) they are capable of sustained oscillation of prescribed wave forms;

b) each oscillator is coupled with a number of oscillators of the same array by a variable coupling.

One way of realizing our model is then to impose that:

1) different *inputs* to this organ are represented by changes in the coupling constants in different sets of points of the array;

2) different *outputs* are provided by different frequency spectra of the total oscillation of the array, which we may read *e.g.* by means of frequency analysis.

5. – This criterion has been chosen for the purposes of this discussion, as providing the most simple example of the process of signal transfer between input and output; other choices are of course possible: crystal physics, to quote just one instance, offers examples of similar behaviour. Gestalt is essential and enters naturally into the picture, because the modes of a system of coupled oscillators are typical of the system as a whole, and are quite different from the modes of the single free oscillators. The same regular behaviour is to be expected also if one starts, say, from an entirely random assembly of coupled oscillators: randomness has, so to say, order in its laws.

Signal transfer occurs therefore, speaking mathematically, as a (Fourier) transformation between configuration space (input) and momentum space (output). The array, with no signal being received, will oscillate, as a whole, in the fundamental mode; a signal alters the couplings, so that the whole changes its mode of oscillation, going—in quantum mechanical language—into some excited state.

We are willing to believe that some features of the electroencephalogram may be interpreted in analogy to this model. Thus, for instance, the alpha-pattern would indicate the fundamental mode of the unperturbed (occipital) cortex; its disappearance upon reception of a signal (for normal subjects) would denote the breakdown of the fundamental mode and the appearance of the higher frequencies of the excited states, which have of course smaller amplitudes.

6. – A theory of the connection between successive arrays is beyond the scope of this report; we just mentioned here that it does not appear to offer any additional difficulties, because an array, by its very structure, acts as a dispersive medium, *i.e.* as a frequency analyzer. The same array, or a very similar one, can convert a frequency received from an other array into a sharply localized positional stimulus, *i.e.* perform the transformation back from momentum space (input) into configuration space (output, and then input of still other arrays). We prefer to postpone the discussion of this and many similar questions to the time when our mathematical study, being completed, will permit exact quantitative statements. We are contented, here, with having given the indication of one plausible transfer mechanism.

7. – It is interesting to see how this model meets the difficulties raised in Sect. 3, typical of many more points which can, and in part have, been raised, and thus far answered with similar arguments.

a) *Economy.* Since the coupling constants can be varied within wide ranges of values, we may obtain practically any number of different frequency spectra representing the output corresponding to a very large number of different input patterns. Each possible input configuration determines a particular mode of oscillation of the whole array, and this can in turn be detected with the desired precision through frequency analysis.

b) *Similarity.* The complexity of the psychological concept of similarity of shape becomes apparent if one considers all the properties of figures which enter into it without completely determining it, such as: the « weight » of a figure (*e.g.* the total amount of ink in a printed character), continuity or discontinuity, orientation, topological class, « geometrical similarity » with standard figures, possibility of perspective transformation into standard figures, pattern of curvature of lines, such as successions of concavities and convexities, angularities etc. It is characteristic for the performance of living nervous systems that they apply some degree of tolerance to each of these components of similarity (*e.g.* an almost closed handwritten « o » is very similar to a closed one, even if they belong to quite different topological classes, a slightly tilted character is still immediately read while one rotated 180 degrees is not, etc.), arriving at the recognition of similarity between two figures through the summation of these partial similarities.

There is good reason to believe that the model described above may be able to recognize similarities between figures in quite the same manner, *i.e.* taking into account many features pertaining to different abstract categories of « similarity ». If the output is Fourier analyzed automatically, it may be sufficient to limit the expression to the first n terms, or to certain sets of terms, in order to obtain a many-to-one relation between input patterns and output patterns apt to embody the criterion of similarity.

c) *Gestalt.* The fact that the input acts as a whole on the output, or, as defined above, the non-additivity of the individual outputs corresponding to two inputs, can be regarded as a corollary of the well known property of systems of coupled oscillators, in which the action of any oscillating unit on the oscillation of the whole array is dependent on the coupling and on the states of all other units. It may be noted that this interdependence can be enhanced if the couplings of each oscillator are extended beyond the immediately neighbouring oscillators.

8. – *Model with memory.* A model with memory can be obtained from the organ described above, quite clearly, if the coupling constants between any

two oscillators are taken as functions of all the past states of the two oscillators. The input-output relation would then acquire the basic property of « reintegration » as defined by the psychologists, *i.e.* the response to a certain pattern can be obtained from the organ if only parts of the pattern are presented at the input, provided that the whole pattern has occurred often enough in the history of the organ, and its parts have therefore become *associated*.

It is curious to note that this mechanism would eventually undergo « senile degeneration », in the sense that, with increasing age, it would tend more and more to refer new facts to old ones and progressively lose its capacity to make new memory traces.

RIASSUNTO

Proposta di un modello che promette di realizzare le proprietà di *economia* di parti, capacità di riconoscere *somiglianze*, carattere di « *Gestalt* », tipiche dei sistemi nervosi viventi.

On the Maximal Energy and Intensity of the Electrons Accelerated by the Microtron.

F. Porreca

Istituto di Fisica dell'Università - Napoli

(ricevuto il 20 Ottobre 1958)

Summary. — Keeping in account the electron's acceleration time in a microtron operating with $a = 2$ and $b = 1$ and the pulse duration of the magnetron, the maximal values of the energy and the intensity of the accelerated beam are established.

The increase of the orbital energy and the intensity H of the related magnetic field of the microtron are known to be represented by the equations

$$(1) \qquad H = \frac{2\pi\nu m_0 c}{e}\frac{1}{a-b} \qquad \text{and} \qquad e\Delta V_0 = m_0c^2\frac{b}{a-b},$$

where ΔV_0 is the peak voltage at the accelerating cavity's gap, the value m_0c^2 being 0.511 MeV.

As shown by these equations, the energy of the accelerated electrons is higher, the greater the « b » and the lower the « $a - b$ » are, where « a » and « b » are proportionality factors between the period T_1 of the first orbit, and the ΔT increase from one orbit to the following one, and the τ period of radio frequency, respectively:

$$(2) \qquad T_1 = a\tau\,, \qquad \Delta T = b\tau\,.$$

In order to obtain a peak voltage ΔV_0 at the cavity's gap, the cavity has to be energized with a peak power P as given by $P = \Delta V_0^2/2R$, where R is the cavity's impedance, which takes into consideration also the load due to the electron beam ([1,2]).

([1]) H. F. Kaiser: *Journ. Franklin Inst.*, **257**, 89 (1954).

([2]) P. A. Redhead, H. Le Caine and W. J. Henderson: *Can. Journ. Res.*, A **28**, 73 (1950).

In these conditions, which are considered to be the best, the estimate R value being about $0.5 \cdot 10^3\ \Omega$, peak energies of $\sim 10^5$ W must be reached in the cavity, so as to obtain a peak ΔV_0 of about 10^5 V; consequently, the peak energy which is distributed by the magnetron through the transmission line should be at least the double, in view of the well known fact of the absorption of energy by the stabilising resistive load connected in series to the resonator along the wave guide.

The impossibility of finding on the market such a high powered magnetron (> 2 MW peak) and the even greater difficulty in building a microwave resonator which may be able to operate without trouble with a peak axial electric field of less than 10^6 V/cm, precludes the possibility of selecting « b » > 1, the only operating way of the microtron at high energies being thus limited to $b = 1$. As to the possible values of the parameter « a », we must consider that the final electron energy to be reached in the microtron is proportional to Hr, if r is the last orbit radius. Therefore, with a given diameter of the magnet, the highest energy is obtained by operating with the highest field H. From $b = 1$ and eq. (1) we obtain $a = 2$ [3]. In this way, the orbital energy increase of the particles is ~ 0.5 MeV, while n MeV is the increase obtained after $2n$ orbits.

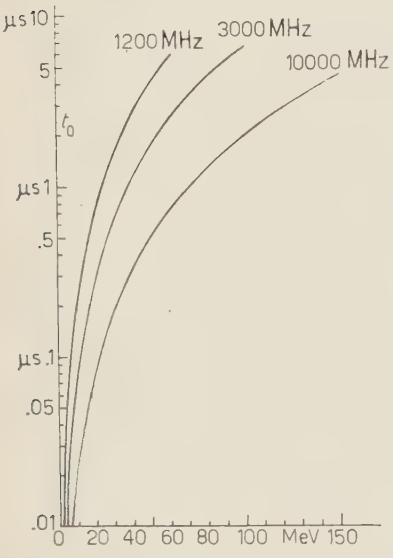

Fig. 1.

A final total acceleration time $t_0 = n(2n+3)\tau$ should be necessary to reach the final energy of n MeV.

It is obvious that this time t_0 should not exceed the pulse duration T of the magnetron; for the operation of the machine this time must thus be practically $n(2n+3) \ll T$. Moreover, from eq. (1) we have decided to operate at a very high radio frequency, for a given « a » and « b ». The choice is thus practically limited to the available magnetrons with a frequency of 1200 MHz, 3000 MHz and 10000 MHz.

Fig. 1 shows the definite accelerating time vs. the energy reached by the electrons.

For a given duration T of the magnetron pulse, there is an energy maximum value of the electrons, which may be known from the point abscissae of the crossing line $T = \text{const}$, with the curve corresponding to the operating frequency (Table I).

Thus, for a given frequency ν and a pulse duration T, only an electron pulse of this utmost maximal energy will hit the target.

It is evident, as it will readily show, that the finite accelerating time t_0 must be very *short*, in comparison to the magnetron pulse duration T, for

[3] C. Henderson, F. F. Heymann and R. E. Jennings: *Proc. Phys. Soc.*, B **66**, 654 (1953).

the increase of the beam's intensity. Of course, the pulse frequency of the magnetron modulator acts also for the proportional increase of the electron beam.

TABLE I.

T	1200 MHz	3000 MHz	10000 MHz
1 μs	24 MeV	37 MeV	70 MeV
2 μs	34 MeV	54 MeV	99 MeV
3 μs	42 MeV	67 MeV	123 MeV
4 μs	48 MeV	78 MeV	141 MeV
5 μs	54 MeV	86 MeV	158 MeV

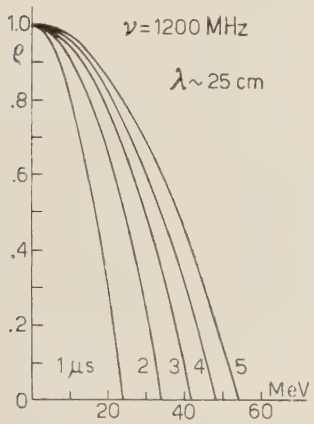

Fig. 2*a*.

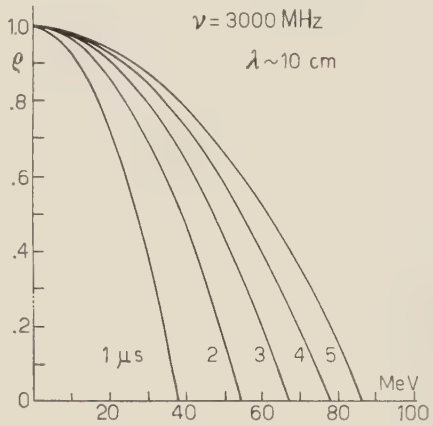

Fig. 2*b*.

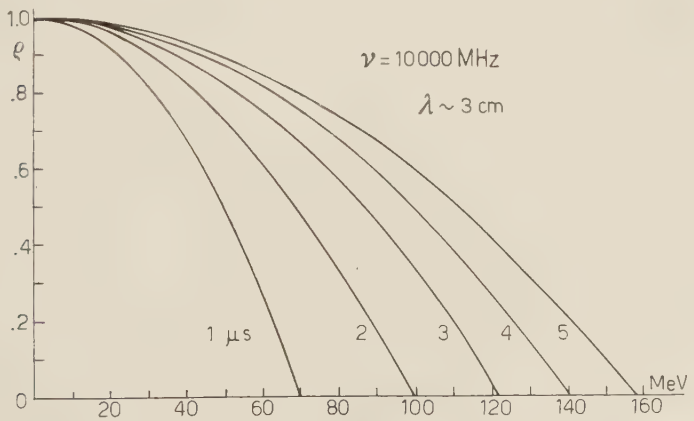

Fig. 2*c*.

It is convenient therefore to introduce an « efficiency coefficient » of the machine as a ratio between the number N_a of the accelerated electrons leaving the

machine during a pulse of the magnetron, and the number N_r of the electrons leaving the cavity during the same time:

$$\varrho = \frac{N_r}{N_r} .$$

(Of course, this ratio is the same as the one of the corresponding intensity).

From the previous relations, we may give by simply making further re-arrangements, a convenient expression of ϱ in terms of τ, T and n:

$$\varrho = \frac{T - (2n+3)n\tau}{T} = 1 - \frac{(2n+3)n\tau}{T} .$$

The last equation shows that ϱ $(0 < \varrho < 1)$ is increasing, going to unity, as T is getting more and more bigger than τ.

The curves of Fig. 2 show the equation $\varrho = \varrho(n)$ for a proper set of the available radio frequency and of the pulse duration T, from 1 μs to 5 μs.

It may be observed that the actual value T of the magnetrons which are presently available, does not exceed 3 μs.

RIASSUNTO

Tenendo conto del tempo di accelerazione degli elettroni e della durata degli impulsi del magnetron, si stabiliscono i valori massimi dell'energia e dell'intensità degli elettroni accelerati.

LETTERE ALLA REDAZIONE

(La responsabilità scientifica degli scritti inseriti in questa rubrica è completamente lasciata dalla Direzione del periodico ai singoli autori).

Meson Mass Spectrum.

K. M. GUGGENHEIMER

Department of Natural Philosophy - The University of Glasgow, Glasgow

(ricevuto il 15 Luglio 1958)

Extended particles can possess an angular momentum l as well as an intrinsic spin s. The energy can be expected to be a function of $l(l+1)$ and of $s(s+1)$, and may assume the simple form

$$(1) \qquad E/c^2 = a\big(l(l+1) + s(s+1)\big)\, \mathrm{m_e}\,.$$

The lightest meson is the μ-meson with mass $m = 207\ \mathrm{m_e}$. One can attribute to it the quantum numbers $l=1$ and $s=\frac{1}{2}$. Then one obtains

$$(2) \qquad a = 207/2.75 = 75.27\,.$$

The mass values calculated according to equations (1) and (2) are assembled in Table I.

The calculated masses are compared with observed values. The well established masses of the μ-; K-; Λ-; Σ- and Ξ-mesons are underlined. They fall into a narrow domain of the scheme of Table I, with $s < l \leqslant 5$; $s \leqslant \frac{5}{2}$.

TABLE I. – *Meson masses as multiples of the electron rest mass* m_e.

s \ $l=$		1	2	3	4	5	6
$\frac{1}{2}$	calc.	207	508	960	1562	2315	3217
	obs.	207	520	966	1550	2327	3220
		$\underline{\pi}$	$\underline{\zeta}$	$\underline{\mathrm{K}}$		$\underline{\Sigma}$	
$\frac{3}{2}$	calc.		733	1186	1788	2540	3445
	obs.		738	1180	(1836)	2583	3450
					$\underline{\mathrm{p}}$	$\underline{\Xi}$	
$\frac{5}{2}$	calc.			1562	2161	2917	
	obs.			1550	2181	2950	
					$\underline{\Lambda}$		
$\frac{7}{2}$	calc.				2692		
	obs.				2700		

The mass of about 525 m_e has been measured recently by ALIHANIAN *et al.* [1] for 21 K^- particles, and a similar value $m = 520\ m_e$ (ζ-meson) has been found by DANIEL and PERKINS [2], but further confirmation would be desirable.

The mass 750 m_e has been observed by FRIEDLANDER *et al.* [3].

Three cases of $m = 1180\ m_e$ were reported by MENON and O'CEALLAIGH [4].

FRETTER *et al.* [5] reported particles with $m = 738$; 1180; 1550 and 2950 m_e, and a group of particles with $m = 1783\ m_e$ which it is difficult to distinguish from protons, but which compare very well with the calculated value 1788 m_e in the present scheme.

BONETTI *et al.* [6] found several cases of $m = 2700\ m_e$.

A case with $m = 2860\ m_e$ or 2940 m_e was described by KING *et al.* [7].

Further evidence for the calculated mass values $< 3000\ m_e$ can be found, *e.g.*, in the survey by BRIDGE [8].

Two rare events with $m = 3220\ m_e$ and $m = 3450\ m_e$ have been measured by EISENBERG [9] and by ANNIS *et al.* [10] respectively. These two empirical values agree remarkably well with calculated values in Table I.

The calculated mass 960 m_e is equal to the sum of the rest masses of two μ-mesons and two π-mesons. A fermion of mass about 960 m_e can emit a neutrino or an electron and be transformed into this complex of two π-mesons and two π-mesons, and one can understand that this complex can disintegrate in various ways. Emission of an electron by K-mesons has been observed by FRIEDLANDER [11] and others.

The mass $m = 1562\ m_e$ occurs twice in the scheme of Table I, namely, for $l = 4$; $s = \frac{1}{2}$, and for $l = 3$; $s = \frac{5}{2}$. Moreover, if one subtracts the mass 273 m_e of the π-meson from the proton mass, one obtains $1836 - 273 = 1563\ m_e$.

The binding of a π-meson to a particle with mass 1562 m_e may lead to a system of exceptional stability owing to the possibility of resonance between two states of binding.

FOWLER *et al.* [12] found tracks corresponding to particles of initial mass about 1500 m_e and of the final mass of a proton. A particle with mass 1562 m_e could possibly capture a π-meson by resonance during flight and continue as a proton, but there should be side tracks from a decaying particle of mass 1562 at rest.

The π-meson is a boson and could be composed of two fermions, *e.g.*, a pair of electrons bound in a state with $l = 1$. Extending equation (1) to this case, one could expect

$$(3) \quad E/c^2 = a\big(l(l+1) + 2s(s+1)\big)\, m_e\,.$$

With $l = 1$ and $s = \frac{1}{2}$ one obtains $m = 263\ m_e$. The mass of the neutral μ-meson is 264 m_e.

The simple scheme of equation (1) is at least relevant to the interpretation of all known meson masses. All mass values are obtained by introducing a single constant, and there is evidence for all calculated masses with $s < l \leqslant 6$; $s + l \leqslant 15/2$.

(1) A. I. ALIHANIAN, N. V. ŠOSTAKOVIČ, A. T. DADAIAN, V. N. FEDOROV and B. N. DERIAGIN: *Journ. Exp. Theor. Phys.*, **4**, 817 (1957).

(2) R. R. DANIEL and D. H. PERKINS: *Proc. Roy. Soc.*, A **221**, 351 (1954).

(3) M. W. FRIEDLANDER, D. KEEFE, M. G. K. MENON, R. W. H. JOHNSTON, C. O'CEALLAIGH and A. KERNAN: *Phil. Mag.*, **46**, 144 (1955).

(4) M. G. K. MENON and C. O'CEALLAIGH: *Proc. Roy. Soc.*, A **221**, 292 (1954).

(5) W. B. FRETTER, E. W. FRIESEN and A. LAGARRIGUE: *Suppl. Nuovo Cimento*, **4**, 569 (1956).

(6) A. BONETTI, R. LEVI-SETTI, B. LOCATELLI and G. TOMASINI: *Suppl. Nuovo Cimento*, **12**, 292 (1954).

(7) D. D. KING, N. SEEMAN and M. M. SHAPIRO: *Phys. Rev.*, **92**, 838 (1953).

(8) H. S. BRIDGE: *Progress in Cosmic Ray Physics*, **3**, 145 (1956).

(9) Y. EISENBERG: *Suppl. Nuovo Cimento*, **4**, 484 (1956).

(10) M. ANNIS F. H. HARMON and R. D. SARD: *Nuovo Cimento*, **6**, 1155 (1957).

(11) M. W. FRIEDLANDER, D. KEEFE, M. G K. MENON and L. VAN ROSSUM: *Phil. Mag.*, **45**, 1043 (1954).

(12) P. H. FOWLER and D. H. PERKINS: *Suppl. Nuovo Cimento*, **4**, 487 (1956).

IL NUOVO CIMENTO Vol. XI, N. 2 16 Gennaio 1959

On the Mass of Elementary Particles.

A. Carrelli

Istituto di Fisica dell'Università - Napoli

(ricevuto il 1° Agosto 1958)

In a recent paper, Fröhlich (1), referring to a similar publication by Nambu (2), dwells once more on the fundamental problem following which a modern theory on elementary particles should be able to give theoretically the value of their masses. In other words the problem not yet defined of auto-value for masses would seem the same as the set and solved problem of auto-value for energies.

An empirical formula could similarly be found corresponding to the well-known formulae of spectroscopy. The number of the masses of the particles that have been so far determined is rather noticeable and therefore an attempt might be made to discover, at least empirically, a « Balmer formula » pending the discovery of a theory capable of explaining it.

The first remark that must be made in this regard is that this is possible if the characteristic mass of elementary particles does not receive an appreciable contribution from the energy pertaining to the field; this means that the only admissible contribution is the one due to the coupling with the electromagnetic field. It has been proved (3) that this contribution (when the electronic mass is used as unit) can have a value of not more than a few dozen units.

This result might also be expressed in a different way, by saying, for instance, that a difference of about 10 units from the experimental value of the masses (that are expressed in electronic units) is admissible for the values that may be obtained from any whatever empirical relation that might be suggested.

There is also another observation that may be made in connection with these masses: Fröhlich does not consider among them the meson π, the proton and the neutron. In this way the mesons π, K and the hyperons are considered as different from n and p and from the meson μ (that, after all, is for other reasons already clearly distinguished from the meson π).

The fundamental position which is the starting point, is that of considering as fundamental mass the mass of the electron M_e, considering the other M as multiples of this mass M_e by means of the number 137, thus we have $M = N \cdot 137\, M_e$. An attempt is made to give an empirical expression of N. The Table of Fröhlich is reproduced.

(1) H. Fröhlich: *Nucl. Phys.*, **7**, 148 (1958).

(2) Y. Nambu: *Progr. Theor. Phys.*, 595 **7**, (1952).

(3) A. Petermann: *Helv. Phys. Acta*, **27**, 441 (1954); R. O. Feymann and G. Sperzmann: *Phys. Rev.*, **94**, 506 (1954).

The masses considered are 5 and, as it appears, these can be given with satisfactory approximation (also taking into account the more modern values of $1/\alpha$ and of the masses) by giving N the values 2, 7, 16, 17 and 19.

Fröhlich suggests an empirical formula for N; he makes a distinction between bosons and nucleons, that is between μ, K and Λ, Σ, Ξ, and he considers that the nucleonic number n is 0 for the first two and 1 for the others; this means that he does not take into consideration the antiparticles for which n should be equal to -1. He obtains a number j from the nucleonic number n on the strenght of the relation $n(n+1) = j(j-1)$ $(j \geqslant 0)$. This relation, if $n=0$, gives for j the values 0 and 1, and for $n=1$ the value $j=2$. Therefore the formula proposed by Fröhlich for N is the following:

$$N = (j+1)(j+2) + j^2 + \tfrac{1}{2}nm(m+1)\,. \qquad m = 0, 1, \ldots j.$$

From this formula the five values of N may be obtained according to the positions selected.

It must be noted however that in this way the existence of other particles is excluded from the empirical formula. Therefore it does not have the character of Balmer's formula inasmuch as the number of masses it yields is limited in relation to the masses that have already been found.

But another remark can be made referring to the suggested formula; for the antiparticles in fact the value $n = -1$ must be set, and with such a value for n, j appears equal to 0 and 1 and so for N the values 2, 7 and 6 are obtained; the value 6 is missing from the Table.

	π^+	π^0	K	Λ	Σ^+	Σ^-	Ξ
M	273	264	966	2 180	2 331	2 341	2 590
M_0	274		959	2 190	2 329		2 603
$M_0/137$	2		7	16	17		19
E	-1	-10	$+7$	-12	$+2$	$+12$	-13

It is to be noticed therefore that the problem cannot be considered as having attained its final conclusion; perhaps it would be interesting to make some other attempt over and above that made by Fröhlich, that might supply, among the many possible ones, a formula capable of foreseeing both the already known masses as well as the others. The suggested formula is the following:

$$N = (j+1)(j+2) + j^2 + 2\sum_{1}^{j}(-1)^n \cdot \frac{(n+1)j(j-1)(j-2)\ldots(j-n-1)[(2n)^2-(2n-1)^2]}{n(n+2)!}\,.$$

This gives for $j = 0, 1, 2, 3, 4$ the values 2, 7, 16, 17, 19, but does not limit the particles to those that are known, and moreover for $j = 5, 6, 7$ it foresees particles having N equal to 22,6; 28,5; 36,9; in other words it effectively considers the possibility of a spectrum of particles.

IL NUOVO CIMENTO Vol. XI, N. 2 16 Gennaio 1959

An Experimental and Indirect Method for Determining the High Atmosphere's Density.

C. Casci and V. Giavotto

Istituto di Motori per Aeromobili, Politecnico - Milano

(ricevuto il 26 Novembre 1958)

1. – Introduction.

To day it is a fact of everybody's experience that high atmosphere drag, which is very weak but acts continually, gradually dissipates the total energy of an artificial satellite; for that satellite's orbit becomes closer and closer to the Earth's surface, until the satellite itself is burned by the friction of denser atmospheric layers.

Therefore we speak of satellite lifetime, which is the duration of a satellite's orbit.

Moreover, it is obvious that lifetime computations are especially useful for design purposes; they make possible to foresee the applications of a satellite, and to estimate the duration needed for the energy sources that feed its instrumentation. However, all these computations, are affected by uncertainty, owing to lack of information on the high atmosphere's density.

This paper provides values for the high atmosphere's density, and presents the method by which such values have been calculated, using, as data, observed lifetimes of satellites already fallen down. It is clear that said results are approximate, owing to the approximation of the available data; for instance, lifetimes are known with the approximation of one day. Moreover, these results are valuable only for heights greater than 130 km above Earth's surface, because variations of atmospheric density under such height would not produce any sensible variations on artificial satellites' lifetime. Besides, under that height, density is known from experimental results.

For the above reasons, and for the particular method employed, values of atmospheric density are obtained, which have more technical than scientific interest, because their worth is surer for computing satellite lifetimes, than as geophysical data.

2. – Atmospheric density.

As now, atmospheric density is known up to the height of 220 km, as a result of rocket exploration [1,2].

(1) The Rocket Panel: *Phys. Rev.*, **88**, 1027 (1952).

(2) H. E. Newell jr.: *High Altitude Rocket Research* (New York, 1953).

Above that height, curves of atmospheric density vs. altitude have been derived, which are results of simple extrapolation, or of some particular theory ([3,4]).

At the altitudes interesting artificial satellite lifetimes, atmospheric density may be expressed by an exponential formula ([4,5]), of the following type:

$$\varrho = k \exp\left[-h/c\right], \tag{1}$$

where: ϱ is density, h altitude, k and c two constants. For these constants the values most commonly accepted are ([1,4]):

$$k = 7.7 \cdot 10^{-10} \text{ g/cm}^3, \qquad c = 23.3 \text{ km}.$$

Once accepted this very simple relation between density and altitude, the problem of computing atmospheric density is reduced to the calculation of the two constants k and c.

3. – Lifetime computation.

The computation of artificial satellite lifetime is, by its nature, an approximate computation; for its purposes, above mentioned, it is not necessary to bring approximation too close; for instance, an approximation of 1% may generally be accepted.

Therefore, some helpful semplification can be used, whether in the definition of the problem, or in numerical computation development.

We will not speak about numerical approximated methods, which, moreover, are not typical of these calculations, but we mention the main simplifying hypotheses, used in defining the problem. They are:

a) atmospheric density can be expressed by an exponential formula;

b) drag at extremely low densities can be expressed by the classical formula of aerodynamics, where drag coefficient is regarded as constant;

c) satellite mouvement is regarded as a perturbed Keplerian motion, where perturbances are considered small; *i.e.*, time derivatives of the five elliptic parameters defining the obsculating ellipse are considered small, in comparison with the time derivative of the sixth, defining the satellite's position on its orbit; among perturbations, the effect of the Earth's rotation is taken into account (*).

Equation (2) determines the lifetime of a satellite which travels an elliptic orbit, whose inclination on the Earth's equator has the value i ([6]); in this equation, unlike

([3]) N. V. PETERSEN: *Journ. Amer. Rocket Soc.*, **26** (1956).

([4]) I. G. HENRY: *Journ. Amer. Rocket Soc.*, **27** (1957).

([5]) L. SEDOV: *The Sputniks*. Lecture at the IX Congress of IAF (Amsterdam, August 1958).

(*) Not every author takes into account the effect of the Earth's rotation on lifetimes; this effect may reach 30 % in the case of equatorial near-circular orbits, as the writers have shown in another paper ([6]).

([6]) C. CASCI and V. GIAVOTTO: *Sul tempo di vita dei satelliti artificiali*. Paper presented at IX Congress of IAF (Amsterdam, August 1958).

other authors ([3,4,7,8]), we take into account the Earth's rotation (*).

$$(2) \qquad t_v = \frac{\pi\sqrt{K}}{2H} \int_{a_f}^{a_0} \frac{\mathrm{d}a}{\sqrt{a} \int_{a(1-\varepsilon)}^{a} \frac{\exp\left[-(r-R)/c\right]\left[K\left((2/r)-(1/a)\right) - 2\Omega\cos i\sqrt{Ka(1-\varepsilon)^2}\right]}{\sqrt{\left((a\varepsilon)^2-(a-r)^2\right)/\left(r(2a-r)\right)}}\,\mathrm{d}r}.$$

Computation of Eq. (2) has been programmed and carried out on high speed digital computer CRC 102 A/P, existing at the « Centro di Calcoli Numerici » of the Politecnico di Milano. However, we must notice that the interior integral of Eq. (2) is an improper integral; therefore it became necessary to find a particular change of variable, able to remove singularities, in order to make use of numerical methods of integration (see Appendix).

Such a change of variable transforms Eq. (2) into (3) (*):

$$(3) \qquad t_v = \frac{\pi\sqrt{K}}{H} \int_{u_f}^{u_0} \frac{\mathrm{d}u}{u^2 \int_{-\pi/2}^{\pi/2} \exp\left[-\frac{u^2\varepsilon}{c}(\sin y - X)\right] \sqrt{1-\varepsilon^2\sin^2 y}\left[K\frac{1-\varepsilon\sin y}{u^2(1+\varepsilon\sin y)} - \Psi(u)\right]\mathrm{d}y}$$

where, expanding ([6]):

$$(4) \qquad H = kS/m\,.$$

4. – Method for determining the atmospheric density.

The problem of determining the atmospheric density is now reduced to the calculation of the two constants k and c of Eq. (1).

Once known the lifetime t_v of a satellite, its mass m and its front area S, and initial characteristics of its orbit, Eq. (3) constitutes a relation between the constants k and c.

Considering available data, it has been realized that the surest data are those yelded by Sputnik I. In fact, lifetime, initial characteristics of the orbit, and the m/S ratio of Sputnik I are known with good accuracy; on the contrary, m/S of other satellites already fallen down is not so exactly known, whether they have a non-spherical shape (therefore a non-constant S), or their weight and dimensions are not exactly known.

Therefore, the lifetime of Sputnik I has been used in a first equation involving k and c; for a second equation, atmospheric density at a certain altitude h, measured by means of rocket probes, was chosen.

(*) For. nomenclature in Eqs. (2) and (3) see explanation at the end of the paper.

([7]) E. SÄNGER: *Interavia*, **4** (1949).

([8]) N. V. PETERSEN: *Summary of proposed methods for determining satellite's lifetimes.* Rendiconti del VII Congresso Internazionale Astronautico, Roma: Associazione Italiana Razzi (Settembre 1956).

Having put:

$$\bar{\varrho} = (\bar{h}) \,, \tag{5}$$

the second equation is obtained from Eq. (1):

$$\bar{\varrho} = k \exp\left[-\bar{h}/c\right] , \tag{6}$$

whence:

$$k = \bar{\varrho} \exp\left[\bar{h}/c\right] . \tag{7}$$

By introducing Eq. (4) and (7) into Eq. (3) we obtain one equation in the only unknown c:

$$\frac{m}{S} \frac{\pi\sqrt{\overline{K}}}{\bar{\varrho} \exp\left[\bar{h}/c\right]} \cdot \tag{8}$$

$$\cdot \int_{u_f}^{u_0} \frac{\mathrm{d}u}{u^2 \int_{-\pi/2}^{\pi/2} \exp\left[-\frac{u^2\varepsilon}{c}(\sin y - X)\right] \sqrt{1-\varepsilon^2 \sin^2 y} \left[K \frac{1-\varepsilon \sin y}{u^2(1+\varepsilon \sin y)} - \Psi(u)\right] \mathrm{d}y} - t_v = 0 .$$

Equations (7) and (8) give the solution of the problem.

5. – Numerical solution of the problem.

Equation (8) may be written in the symbolic form:

$$f(c) = 0 \,. \tag{9}$$

Owing to its complexity, Eq. (8) had to be processed in CRC 102 A/P digital computer.

Having the program for computing $f(c)$, already tested (*), we used this program as a sub-routine, in the program of Eq. (9).

The numerical method chosen consisted of a cyclic step: we take two values of the unknown c, c_1 and c_2, so that the solution is certainly between them; *viz.*:

$$f(c_1) f(c_2) < 0 \,, \tag{10}$$

then $f(c_3)$ is reckoned, where:

$$c_3 = \frac{c_1 + c_2}{2} \,.$$

Hence:

if $f(c_1) f(c_3) < 0$ we replace c_2 with c_3;

if $f(c_1) f(c_3) > 0$ we replace c_1 with c_3;

and we go on.

(*) Cfr. diagram in Fig. 8 of ref. ([6]).

We have chosen this particular method, because it converges with a rapidity non dependent on the kind of the function $f(c)$, hence it permits to foresee with accuracy computing time.

6. – Results.

The data to introduce into Eq. (8) are:
Sputnik I:

lifetime	$t_v = 92$ days ,
ratio of mass to front area	$m/S = 317$ kg/m² .

Density experimentally measured (from [1]):

height of measure	$\bar{h} = 150$ km ,
density	$\bar{\varrho} = 3.404 \cdot 10^{-5}$ kg/m³ .

The computation of the constants, using Eq. (7) and (8), gives:

$$c = 17.38 \text{ km} ,$$
$$k = 1.906 \cdot 10^{-5} \text{ kg/m}^3 .$$

High atmosphere densities, calculated with the above values of k and c, are shown in Fig. 1, plotted versus the altitude, in a logarithmic scale.

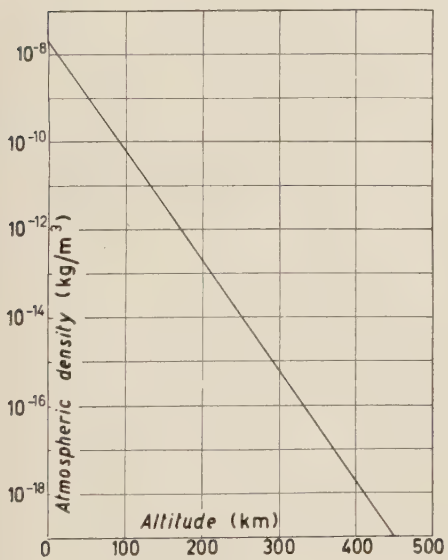

Fig. 1.

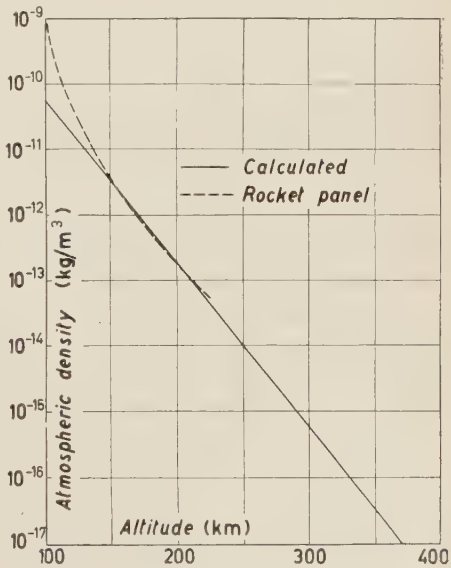

Fig. 2.

Fig. 2 shows a comparison between the densities of Fig. 1 and the densities measured, by means of rocket probes, up to the height of 220 km. It can be seen that a good agreement exists between the two curves, from 130 to 220 km.

7. – Appendix.

To remove singularities from the following definite integral:

$$\text{(A.1)} \qquad \int_{a(1-\varepsilon)}^{a(1+\varepsilon)} \frac{\exp\left[-(r-R)/c\right]\left[K((2/r)-(1/a))-2\Omega\cos i\sqrt{Ka(1-\varepsilon^2)}\right]}{\sqrt{((a\varepsilon)^2-(a-r)^2)/(r(2a-r))}}\,\mathrm{d}r\,,$$

of Eq. (2), we define:

$$r = \varepsilon a x + a\,,$$

$$\Psi(a) = 2\Omega\cos i\sqrt{Ka(1-\varepsilon^2)}\,,$$

$$X = \frac{1}{\varepsilon}\left(\frac{R}{a}-1\right).$$

Hence, integral (A.1) becomes:

$$\text{(A.2)} \qquad a\int_{-1}^{1} \frac{\exp\left[-(a\varepsilon/c)(x-X)\right]\left[K(1-\varepsilon x)/(a(1+\varepsilon x))-\Psi(a)\right]}{\sqrt{(1-x^2)/(1-\varepsilon^2x^2)}}\,\mathrm{d}x\,.$$

Having stated: $x = \sin y$, by introducing (A.2) in Eq. (2), we obtain:

$$\text{(A.3)} \qquad t_v = \frac{\pi\sqrt{K}}{2H}\int_{a_f}^{a_0} \frac{\mathrm{d}a}{a^{\frac{3}{2}}\int_{-\pi/2}^{\pi/2}\exp\left[-\frac{a\varepsilon}{c}(\sin y - X)\right]\sqrt{1-\varepsilon^2\sin^2 y}\left[K\,\frac{1-\varepsilon\sin y}{a(1+\varepsilon\sin y)}-\Psi(a)\right]\mathrm{d}y}\,.$$

At last, by defining $a = u^2$, we have the final expression:

$$\text{(A.4)} \quad t_v = \frac{\pi\sqrt{K}}{H}\int_{u_f}^{u_0} \frac{\mathrm{d}u}{u^2\int_{-\pi/2}^{\pi/2}\exp\left[-\frac{u^2\varepsilon}{c}(\sin y - X)\right]\sqrt{1-\varepsilon^2\sin^2 y}\left[K\,\frac{1-\varepsilon\sin y}{u^2(1+\varepsilon\sin y)}-\Psi(u)\right]\mathrm{d}y}$$

where:

$$u_0 = \sqrt{a_0}\,,$$

$$u_f = \sqrt{a_f}\,,$$

$$\Psi(u) = 2\Omega u\cos i\sqrt{K(1-\varepsilon^2)}\,,$$

$$X = \frac{1}{\varepsilon}\left(\frac{R}{u^2}-1\right).$$

8. – Nomenclature.

ϱ = atmospheric density;
k, c = constants defining atmospheric density;
h = altitude above Earth's surface;
k_g = universal gravitational constant;
M = Earth's mass;
K = const $= k_g M$;
H = const $= \frac{1}{2} C_r m/S$;
C_r = drag coefficient;
m = satellite's mass;
S = satellite's front area;
a = semi-major axis of obsculating ellipse;
a_0 = initial value of a;
a_f = final value of a;
ε = eccentricity of obsculating ellipse;
r = altitude above Earth's center;
R = mean radius of Earth;
Ω = angular velocity of Earth;
i = inclination of orbit on equator;
u = variable of integration $= \sqrt{a}$;
u_0 = $\sqrt{a_0}$;
u_f = $\sqrt{a_f}$;
$\Psi(a)$ = function representing effect of Earth's rotation;
x = variable of integration $= \dfrac{1}{\varepsilon}\left(\dfrac{r}{a} - 1\right)$;
y = variable of integration = $\arcsin x$;
X = constant $= \dfrac{1}{\varepsilon}\left(\dfrac{R}{a} - 1\right)$.

IL NUOVO CIMENTO Vol. XI, N. 2 16 Gennaio 1959

Über eine Verallgemeinerung der Grundformel der Raketendynamik.

N. St. Kalitzin

Bulgarische Akademie der Wissenschaften - Sofia

(ricevuto il 28 Novembre 1958)

Die Grundformel der Raketendynamik, welche von Tziolkovsky gegeben ist, lautet

$$v = q \ln \frac{m_0}{m} . \tag{1}$$

Hierbei bedeutet m_0 die Anfangsmasse der Rakete, wenn die Geschwindigkeit der Rakete $v = 0$ ist, m ist die zu der Geschwindigkeit $\boldsymbol{v}$ gehörige Raketenmasse. q ist die Geschwindigkeit der von der Rakete zurückgeschleuderten Teilchen. Formel (1) gilt unter der Voraussetzung, daß q während der Bewegung konstant bleibe und die Rakete sich geradlinig im freien Raume (unter «freiem Raum» versteht man nach Tziolkovsky einen Raum ohne Atmosphäre und ohne Gravitationskräfte) bewege.

Es wäre wünschenswert die Grundformel (1) für beliebige krummlinige Bewegung der Rakete und für veränderliche Geschwindigkeit $\boldsymbol{q}$ der weggeschleuderten Teilchen, wobei auch der Winkel zwischen $\boldsymbol{v}$ und $\boldsymbol{q}$ eine beliebige veränderliche Größe sein kann, zu verallgemeinern. Außerdem verlangen die in letzter Zeit viel diskutierten «Ionenraketen» eine Verallgemeinerung der Formel (1) für relativistische Geschwindigkeiten $\boldsymbol{q}$.

Wir wollen zunächst die Formel (1) für nichtrelativistische Geschwindigkeiten $\boldsymbol{q}$ verallgemeinern. Zu diesem Zweck gehen wir von der Grundformel der Mechanik eines Massenpunktes mit veränderlicher Masse aus, welche Formel von Meschtchersky herrührt

$$\boldsymbol{F} - m \frac{\mathrm{d}\boldsymbol{v}}{\mathrm{d}t} + \frac{\mathrm{d}m}{\mathrm{d}t} (\boldsymbol{v} - \boldsymbol{a}) , \tag{2}$$

$\boldsymbol{F}$-die Kraft.

m ist die Masse des Massenpunktes, $\boldsymbol{v}$ seine Geschwindigkeit, $\boldsymbol{a}$ die Geschwindigkeit des Massenzuwachses $\mathrm{d}m$. Wir führen in (2) die relative Geschwindigkeit

$$\boldsymbol{q} = \boldsymbol{a} - \boldsymbol{v} , \tag{3}$$

ein. Wenn wir $\boldsymbol{F} = 0$ und (3) in (2) einsetzen, so ergibt sich

$$\frac{\mathrm{d}m}{m}\boldsymbol{q} = \mathrm{d}\boldsymbol{v} \,. \tag{4}$$

Wir multiplizieren (4) skalar mit $\boldsymbol{v}$

$$\frac{\mathrm{d}m}{m}\boldsymbol{qv} = \boldsymbol{v}\,\mathrm{d}\boldsymbol{v} \,. \tag{5}$$

Das Integral von (5) lautet

$$\ln\frac{m}{m_0} = \int_{\boldsymbol{v}_0}^{\boldsymbol{v}} \frac{\boldsymbol{v}\,\mathrm{d}\boldsymbol{v}}{\boldsymbol{qv}} \,. \tag{6}$$

Hier ist $\boldsymbol{qv}$ als Funktion von $\boldsymbol{v}$ aufzufassen. Wenn wir in (6)

$$\boldsymbol{qv} = q\cdot v\cdot\cos\alpha \,, \qquad \boldsymbol{v}\,\mathrm{d}\boldsymbol{v} = v\,\mathrm{d}v \,,$$

und $\boldsymbol{v}_0 = 0$ einsetzen, (q ist die Größe der relativen Geschwindigkeit, α der Winkel zwischen $\boldsymbol{v}$ und $\boldsymbol{q}$), so ergibt sich

$$\ln\frac{m}{m_0} = \int_0^v \frac{\mathrm{d}v}{q\cos\alpha} = \int_0^v \frac{\mathrm{d}v}{q_v} \,. \tag{7}$$

Dabei bedeutet q_v die Projektion von $\boldsymbol{q}$ auf die Richtung von $\boldsymbol{v}$. q_v ist hier als Funktion von v aufzufassen. Formel (7) stellt die gesuchte Verallgemeinerung der Formel (1) für den Fall einer beliebigen krummlinigen Bewegung der Rakete dar, wobei die Geschwindigkeit q_v veränderlich ist. Wenn wir in (7) $q_v = -q = \mathrm{const}$ einsetzen, so ergibt sich unmittelbar die Formel (1) von Tziolkovsky.

Die Verallgemeinerung der Gleichung (7) für relativistische Geschwindigkeiten $\boldsymbol{q}$ läßt sich folgendermaßen durchführen. Wir haben in [1] für relativistische Geschwindigkeiten der Rakete und der von ihr zurückgeschleuderten Teilchen die Formel gefunden

$$\ln\frac{m}{m_0} = \int_{\boldsymbol{v}_0}^{\boldsymbol{v}} \frac{\boldsymbol{v}\,\mathrm{d}\boldsymbol{v}}{\boldsymbol{qv}\,(1 - v^2/c^2)} \,. \tag{8}$$

Für nichtrelativistische Geschwindigkeiten der Rakete ($\boldsymbol{q}$ bleibt relativistisch) erhalten wir aus (8)

$$\ln\frac{m}{m_0} = \int_{\boldsymbol{v}_0}^{\boldsymbol{v}} \frac{\boldsymbol{v}\,\mathrm{d}\boldsymbol{v}}{\boldsymbol{qv}} \,, \tag{9}$$

d. h. die Formel (6). Also gilt Formel (7) auch für relativistische Geschwindigkeiten $\boldsymbol{q}$ der zurückgeschleuderten Teilchen. Formel (7) kann von Bedeutung sein auch für die Ionenraketen.

[1] Nikola St. Kalitzin: *Nuovo Cimento*, **8**, 843 (1958).

Effective Range Theory in Nucleon-Alpha Scattering (*).

G. Pisent and C. Villi

Istituto di Fisica dell'Università - Trieste
Istituto Nazionale di Fisica Nucleare - Sottosezione di Trieste

(ricevuto il 13 Dicembre 1958)

The interest in accurate analyses of the nucleon-α scattering data has been revived by recent attempts to explain the experimental phaseshifts in terms of two-body nuclear potentials containing a spin-orbit term. A simple method for testing the accuracy of the low energy data, and the consistency of the analyses so far carried out [1], is provided by the effective range theory. The aim of this note is to evaluate the scattering length and the effective range for the nucleon-α scattering up to states of orbital angular momentum $L=1$. The extension of the method to higher angular momenta is straightforward. The results of this investigation encourage the belief that a systematic application of the theory may be profitable in yielding information about the nucleon-α potential relating the energy variation of the phaseshifts to fundamental interactions.

Calling M_0 the reduced mass of the nucleon-α assembly and k the momentum (+) of the incident nucleon in the center-of-mass system, the scattering length and the effective range for the state of orbital angular momentum L and total angular momentum $J=L\pm\frac{1}{2}$ will be indicated by $a_{L,J}(k_0)$ and $r_{L,2J}(k_0)$ respectively, where $\eta=2M_0e^2/k=k_0/k$. For $L=0$ $[a_{0,\pm1}(k_0)\equiv a_0(k_0),\ r_{0,\mp1}(k_0)\equiv r_0(k_0)]$ the effective range equations for the scattering of protons by α-particles are given by

$$F_0(k, \operatorname{ctg}\delta_0, \eta) = -a_0^{-1}(k_0) + \tfrac{1}{2}r_0(k_0)k^2\,, \tag{1}$$

where δ_0 is the S-wave phaseshift, and

$$F_0(k, \operatorname{ctg}\delta_0, \eta) = k[C^2(\eta)\operatorname{ctg}\delta_0 + 2\eta Q_0(\eta)]\,, \tag{2a}$$

(*) This research has been sponsored by the Wright Air Development Center of the Air Research and Development Command, United Air Force, through its European Office, under Contract NO AF 61 (052)-164.

(+) A system of units where $\hbar=c=1$ is used.

(1) For references to earlier literature see the review article *The scattering of nucleons by alpha-particles*, by P. E. Hodgson: *Adv. in Phys.*, **7**, 1 (1958).

the functions $C^2(\eta)$ and $Q_0(\eta)$ being defined as

$$C^2(\eta) = 2\pi\eta\,(\exp[2\pi\eta] - 1)^{-1}\,, \tag{2b}$$

$$Q_0(\eta) = \sum_{n=1}^{\infty} (\eta^2/n)\,(n^2 + \eta^2)^{-1} - \ln\eta - \ln\gamma\,, \tag{2c}$$

where $\ln\gamma = 0.577\,2$ is the Euler-Mascheroni constant. For $L=1$ the effective range equations are

$$F_1(k, \operatorname{ctg}\delta_J, \eta) = a_{1,2J}^{-3}(k_0) - r_{1,2J}^{-1}(k_0)k^2\,, \tag{3}$$

where

$$F_1(k, \operatorname{ctg}\delta_J, \eta) = k^3\{(1+\eta^2)C^2(\eta)\operatorname{ctg}\delta_J + 2\eta[Q_1(\eta) - 2] + 2\eta^3 Q_1(\eta)\}\,. \tag{4a}$$

the function $Q_1(\eta)$ being defined as

$$Q_1(\eta) = \sum_{n=1}^{\infty} (2n + 4 + \eta^2)[n^3 + 4n^2 + n(4+\eta^2)]^{-1} - 2(4+\eta^2)^{-1} - \ln\eta - \ln\gamma\,. \tag{4b}$$

The effective range equations for the scattering of neutrons by α-particles are obtained from eqs. (1), (2), (3) and (4) at the limit for $\eta = k_0 = 0$.

The values of $a_{L,2J}$ and $r_{L,2J}$ have been determined for the proton-α scattering using the Chritchfield and Dodder phaseshifts [2], and for the neutron-α scattering using the results obtained by Seagrave [3] and by Clementel and Villi [4]. In both cases the effective range prescription of linearity of $F_L(k, \operatorname{cot}\delta_J, \eta)$ as a function of the incident energy is fulfilled up to $E \simeq 7$ MeV for $L=0$ and up to $E \simeq (3 \div 4)$ MeV for $L=1$, $J=\frac{3}{2}$ (Fig. 1). The linearity of $F_1(k, \operatorname{cot}\delta_{\frac{1}{2}}, \eta)$, as a function of k^2, is consistent with the data for $J=\frac{1}{2}$, but not sufficiently determined for fixing unambiguously the values of $r_{1,1}$ and $a_{1,1}$. The values of the effective range and of the scattering length for $L=0$, $J=\frac{3}{2}$ are listed in Table I.

Table I. – *Effective range $r_{L,2J}$ and scattering length $a_{L,2J}$ for proton-α ($k_0 = 0.0555\cdot 10^{13}$ cm^{-1}) scattering and for neutron-α scattering ($k_0=0$) in the S and $P_{\frac{3}{2}}$ state.*

State	Proton-α	Neutron-α
$L=0$	$a_0(k_0) = (5.35 \pm 0.9)\cdot 10^{-13}$ cm $r_0(k_0) = (1.16 \pm 0.6)\cdot 10^{-13}$ cm	$a_0(0) = (2.43 \pm 0.01)\cdot 10^{-13}$ cm $r_0(0) = (1.88 \pm 0.04)\cdot 10^{-13}$ cm
$L=1,\ J=\frac{3}{2}$	$a_{1,3}(k_0) = (3.66 \pm 0.04)\cdot 10^{-13}$ cm $r_{1,3}(k_0) = (3.88 \pm 0.10)\cdot 10^{-13}$ cm	$a_{1,3}(0) = (4.11 \pm 0.05)\cdot 10^{-13}$ cm $r_{1,3}(0) = (2.78 \pm 0.50)\cdot 10^{-13}$ cm

The equivalent scattering length $a_0^*(k_0)$ concerning the pure nuclear interaction, derived from $a_0(k_0)$, is found to have a value close to $a_0(0)$, namely

$$a_0^*(k_0) = (2.65 \pm 0.06)\cdot 10^{-13}\ \text{cm}\,.$$

[2] C. L. Chritchfield and D. C. Dodder: *Phys. Rev.*, **76**, 602 (1949).
[3] J. D. Seagrave: *Phys. Rev.*, **92**, 1222 (1953).
[4] E. Clementel and C. Villi: *Nuovo Cimento*, **2**, 1121 (1955).

The value of $a_0(0)$ can also be derived on the basis of the rigid sphere approximation, because $R_0 = -\delta_0/k = a_0(k_0)$, where R_0 is the channel radius for the S state inter-

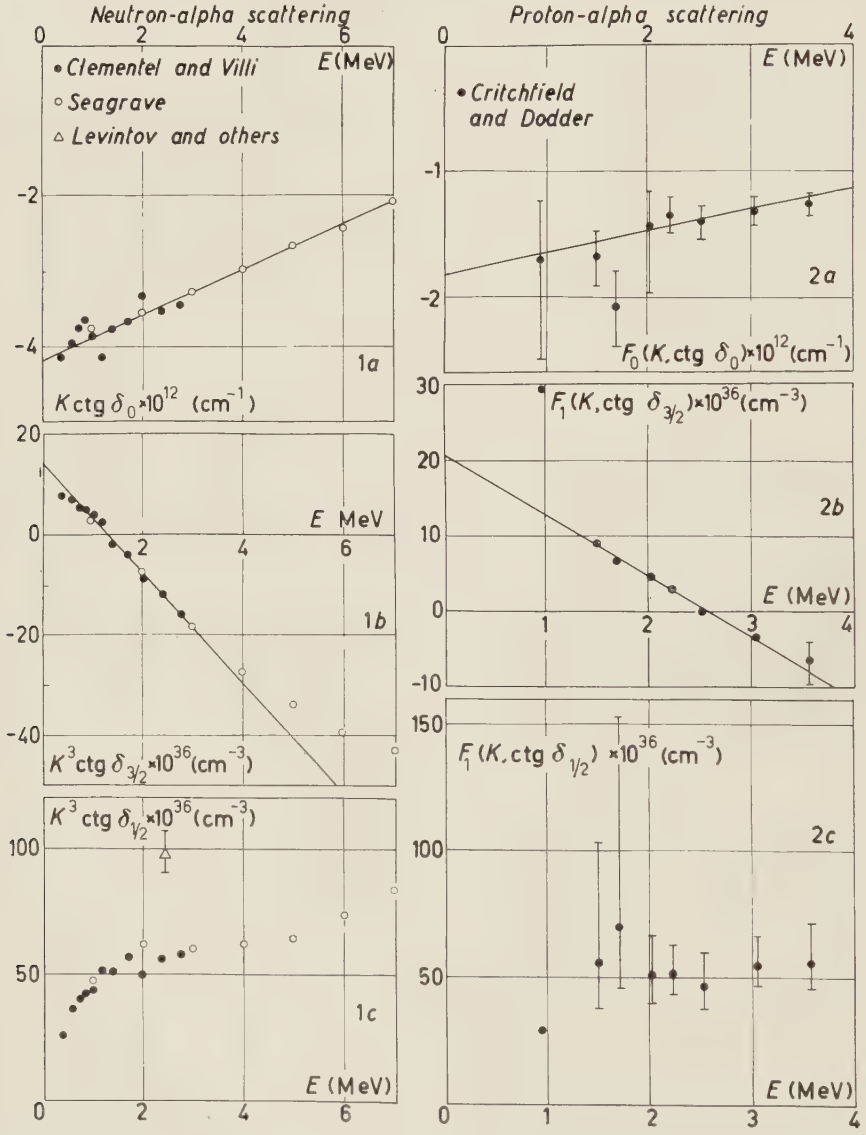

Fig. 1. – Effective range plot for nucleon-α scattering. The values of the effective range and the scattering length, derived from Fig. 1 (a, b) and Fig. 2 (a, b), are listed in Table I. From Fig. 1c and 2c it is seen that the available data do not fix the values of $r_{1,1}$ and $a_{1,1}$. The value of $F_1(k, \cot \delta_{\frac{1}{2}}, 0) \equiv k^3 \cot \delta_{\frac{1}{2}}$, calculated at $E = 2.45$ MeV using the $\delta_{\frac{1}{2}}$ chosen by LEVINTOV *et al.* [6], is in disagreement with all analyses so far carried out [3,4]. No definite conclusion about this discrepancy can be drawn from the analysis of the data until the stability of $\delta_{\frac{1}{2}}$ against small D wave perturbations is carefully investigated. From the above results it is clear that the constraints on the problem of the phaseshift determination, imposed by the effective range theory, allow the determination of the energy dependence of the phaseshifts up to about $E \simeq 4$ MeV on the basis of the experimental knowledge of the differential cross-section and polarization at two energies only.

action. The values of the effective range parameters, derived from the interaction in the $P_{\frac{3}{2}}$ state, are consistent with a resonant scattering from the compound nucleus ^{5}He at $E=1.30$ MeV ($k_0=0$) and from the compound nucleus ^{5}Li at $E=2.83$ MeV ($k_0=0.055\,5\cdot10^{13}$ cm^{-1}). The phaseshifts used to evaluate $a_{L,2J}$ and $r_{L,2J}$ (Table I) and the behaviour of $F_1(k, \cot\delta_J, \eta)$, plotted in Fig. 1 as a function of the incident energy E, belong to the inverted doublet. As is well known, it is a peculiarity of the single channel reactions that the phaseshifts $\delta_{\frac{1}{2}}$ and $\delta_{\frac{3}{2}}$ of the inverted doublet are related to those $(\delta_{\frac{1}{2}}^+, \delta_{\frac{3}{2}}^+)$ of the normal doublet by the equation $\delta_{\frac{1}{2}}-\delta_{\frac{3}{2}}=\delta_{\frac{3}{2}}^+-\delta_{\frac{1}{2}}^+$. The function $F_1(k, \cot\delta_{\frac{1}{2}}, \eta)$, plotted in Fig. 2, has

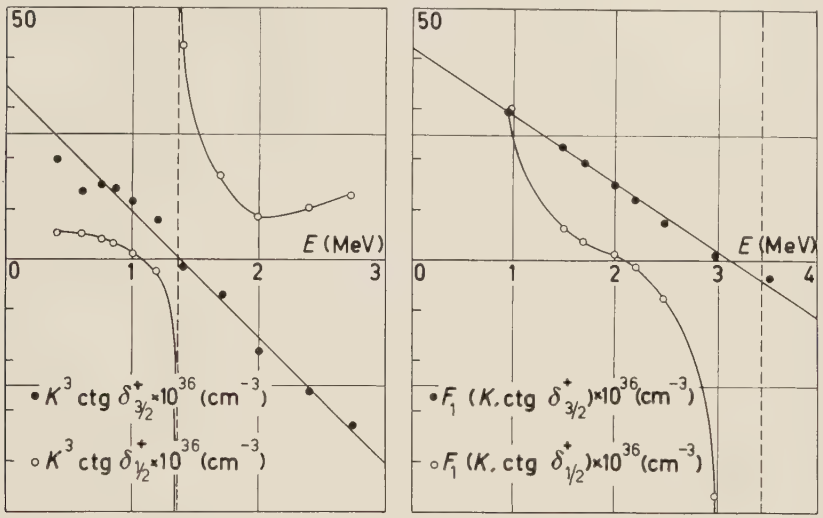

Fig. 2. – Effective range plot of the normal P doublet for the nucleon-α scattering. The infinite jump of the function $F_1(k, \cot\delta_{\frac{1}{2}}^+, \eta)\equiv F_1(k, \cot\delta_{\frac{1}{2}}^+)$ and $F_1(k, \cot\delta_{\frac{1}{2}}^+, 0)\equiv k^3\cot\delta_{\frac{1}{2}}^+$ shows that the continuity of $\delta_{\frac{1}{2}}^+$, as a function of the scattering energy E, is incompatible with the linearity prescription of the effective range theory. Since the validity of the effective range equations can be justified, by inspection of the effective range integral, at least up to $E\simeq 4$ MeV, the solution $\delta_{\frac{1}{2}}^+$, and consequently the associated solution $\delta_{\frac{3}{2}}^+$, although implied by the mathematics of the problem, must be ruled out as physically meaningless [see note (5)].

been evaluated using the phaseshifts for the normal doublet, calculated by Clementel and Villi (4) ($\eta=k_0=0$) and by Critchfield and Dodder (2) ($k_0=0.055\,45\cdot10^{13}$ cm^{-1}). The spectacular deviation of $F_1(k, \cot\delta_{\frac{1}{2}}^+, \eta)$ and $F_1(k, \cot\delta_{\frac{1}{2}}^+, 0)$ from the linearity prescription of the effective range theory is sufficient by itself for concluding, independently of polarization measurements, that the normal doublet is an unphysical solution of the phaseshift equations (5).

(5) As has been already emphasized in ref. (4), the normal and the inverted doublets correspond to the well known Fermi-Yang ambiguity in the elastic scattering of pions by protons. The preceding discussion can be readily extended to this case by regarding $\delta_0\equiv\alpha_3$, $\delta_{\frac{1}{2}}\equiv\alpha_{31}$, $\delta_{\frac{3}{2}}\equiv\alpha_{33}$ as the S and P wave phaseshifts for the isobaric spin $T=\frac{3}{2}$. The behaviour of $k^3\cot\alpha_{31}$ as a function of k^2, calculated in terms of the Yang phaseshifts, deviates grossly from the linearity prescription of the effective range theory. This is an alternative argument for ruling out the Yang set without resorting to polarization measurements or even to comparison with spin-flip dispersion relations

From the above considerations it appears that the crucial point for a quantitative understanding of the nucleon-α elastic scattering process lies in the $P_{\frac{1}{2}}$ state interaction. This interaction has been examined in the light of recent polarization measurements, performed by Russian Authors [6]. The value of the function $F_1(k, \cot \delta_{\frac{1}{2}}, 0)$, evaluated at $E = 2.45$ MeV with their choice of $\delta_{\frac{1}{2}}$, falls clearly outside the general trend of $k^3 \cot \delta_{\frac{1}{2}}$, derived from the analyses of Seagrave [3] and Clementel and Villi [4]. To understand this puzzling result it is convenient to express the polarization of the recoiling neutron in a more feasible way than the one adopted by LEVINTOV *et al.* [6] Be $\sigma(\theta)$ the differential cross-section for a neutron elastically scattered by an α-particle and $f(\theta)$ the corresponding scattering amplitude. Calling $P(\theta)$ the polarization of the recoiling neutron, the quantity $\sigma(\theta)P(\theta)$ is defined as

$$\sigma(\theta)P(\theta) = \text{Trace}\,[f^*(\theta)\boldsymbol{\sigma}f(\theta)] = k^2 \sin\theta \sum_{n=0}^{n_{\max}} B_n(k) P_n(\cos\theta)\,. \tag{5}$$

Introducing two vectors $\boldsymbol{a}_L$ and $\boldsymbol{b}_L$ defined in terms of phaseshifts as

$$\boldsymbol{a}_L = (L+1)\exp[2i\delta^L_{L+\frac{1}{2}}] + L\exp[2i\delta^L_{L-\frac{1}{2}}] - (2L+1)\,, \tag{6a}$$

$$\boldsymbol{b}_L = \exp[2i\delta^L_{L+\frac{1}{2}}] - \exp[2i\delta^L_{L-\frac{1}{2}}]\,, \tag{6b}$$

the scattering amplitude, written as a matrix in spin space, reads

$$kf(\theta) = [a(\theta) + \sigma\cdot\boldsymbol{n}\,b(\theta)]\chi_N\,, \tag{7}$$

where

$$a(\theta) = \sum_L (\boldsymbol{a}_L/2i) P_L(\cos\theta)\,, \qquad b(\theta) = i\sum_L (\boldsymbol{b}_L/2i) P^1_L(\cos\theta)\,, \tag{8}$$

χ_N and $\boldsymbol{n}$ being the spin function of the neutron and the unit vector normal to the plane of scattering. Including all waves up to $L = L_{\max} = 2$ ($n_{\max} = 2L_{\max} - 1$), the expansion coefficients $B_n(k)$ read

$$\left\{\begin{aligned}
B_0(k) &= 2[(\delta_0|\delta^1_{\frac{1}{2}}) - (\delta_0|\delta^1_{\frac{1}{2}}) - (\delta^1_{\frac{1}{2}}|\delta^2_{\frac{3}{2}}) + (\delta^1_{\frac{1}{2}}|\delta^2_{\frac{5}{2}}) + 2(\delta^1_{\frac{3}{2}}|\delta^2_{\frac{5}{2}}) - 2(\delta^2_{\frac{3}{2}}|\delta^2_{\frac{3}{2}})],\\
B_1(k) &= 6[(\delta_0|\delta^2_{\frac{5}{2}}) - (\delta_0|\delta^2_{\frac{3}{2}}) + (\delta^1_{\frac{3}{2}}|\delta^1_{\frac{3}{2}}) + 2(\delta^2_{\frac{3}{2}}|\delta^2_{\frac{5}{2}})]\,,\\
B_2(k) &= 2[(\delta^1_{\frac{3}{2}}|\delta^2_{\frac{5}{2}}) + 5(\delta^1_{\frac{3}{2}}|\delta^2_{\frac{5}{2}}) - 6(\delta^1_{\frac{3}{2}}|\delta^2_{\frac{3}{2}})]\,,\\
B_3(k) &= 18(\delta^2_{\frac{1}{2}}|\delta^2_{\frac{5}{2}})\,,
\end{aligned}\right. \tag{9}$$

[W. C. DAVIDON and M. L. GOLDBERGER: *Phys. Rev.*, **104**, 1119 (1956)]. The effective range theory has been first applied to the pion-proton scattering in the $L=1$, $J=\frac{3}{2}$; $T=\frac{3}{2}$ state by K. A. BRUECKNER [*Phys. Rev.*, **87**, 1026 (1952)]. According to the preceding discussion, the scattering length a_3, determined by J. OREAR [*Nuovo Cimento*, **4**, 856 (1956)] from the low energy data of positive pions elastically scattered by protons, follows from the well known rigid sphere approximation ($a_3 = -x_3/k$) and should be interpreted as the equivalent scattering length for the pure nuclear interaction. It would be interesting to examine the low energy data concerning the scattering of positive pions by protons, by taking into account the Coulomb effects in the effective range equations.

[6] I. I. LEVINTOV, A. V. MILLER and V. N. SHAMSEV: *Sov. Phys., Journ. Exp. Theor. Phys.*, **5**, 258 (1957).

where $(x/y)=\sin x \sin y \sin(x-y)$. Assuming $\delta_{\frac{3}{2}}^2=\delta_{\frac{3}{2}}^2=0$ and calling $\delta_{\frac{3}{2}}^1=\delta_{\frac{3}{2}}$ and $\delta_{\frac{1}{2}}^1=\delta_{\frac{1}{2}}$, the expansion coefficients $B_n(k)$ of the quantity $\sigma(\theta)P(\theta)$ can be readily expressed as functions of $r_{L,2J}$ and $a_{L,2J}$. The quantity $P(\theta)$ has been plotted in Fig. 3 using the values of the effective range and the scattering length listed in Table I. The dotted curve refers to $\delta_{\frac{1}{2}}=20°\ 20'$ ([3,4]), whereas the continuous curve

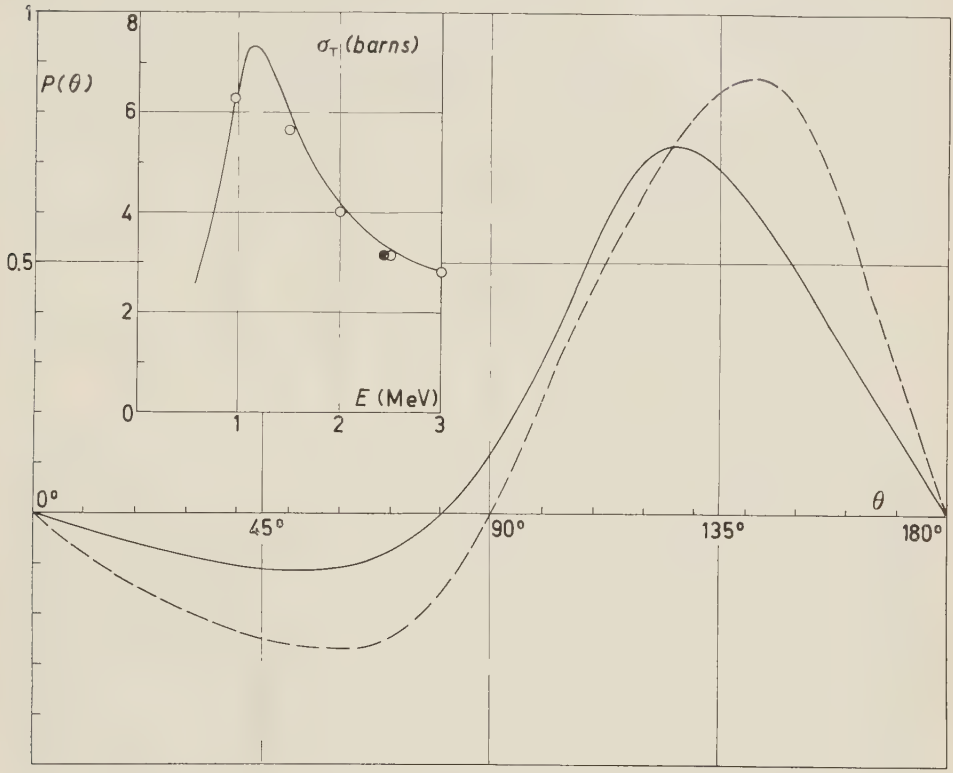

Fig. 3. – Polarization of the recoiling neutron in the C.M.S. The function $P(\theta)$ has been calculated at $E=2.45$ MeV using the values of the effective range parameters listed in Table I and assuming ([3,4]) $\delta_{\frac{1}{2}}=20°\ 20'$ (dotted curve) respectively $\delta_{\frac{1}{2}}=12°$ ([6]) (continous curve). Since the polarization measurement of Levintov *et al.* ([6]) implies $\theta=128°$, the value $\delta_{\frac{1}{2}}=12°$ appears to be only weakly supported by the experiment. The total cross-section has been computed using the effective range parameters listed in Table I and the values of $\delta_{\frac{1}{2}}$ determined in previous analyses ([3,4]) (continous curve). The points o refer to measurements carried out by J. H. Coon (unpublished, 1952), quoted by Seagrave. The point • has been evaluated using Levintov's value $\delta_{\frac{1}{2}}=12°$. Because of the insensitivity of $\sigma_T(k)$ on $\delta_{\frac{1}{2}}$, reliable information on the $P_{\frac{1}{2}}$ state interaction can be obtained from accurate measurements of $\sigma(\theta)$ at small angles, where effects due to higher harmonics could be detactable. Inspection of eqs. (9) shows that small perturbations brought about by D waves within the energy interval where the effective range theory is valid, may sensibly modify the fitting mechanism of the polarization.

refers to $\delta_{\frac{1}{2}}=12°$ ([6]). Since the polarization experiment performed by Levintov *et al.* ([6]) involves at $E=2.45$ MeV the angle $\theta=128°$ in the center-of-mass system, Fig. 3 brings to evidence that the value $\delta_{\frac{1}{2}}=12°$ is only weakly supported by the experiment.

It is worth while to point out that the available data concerning the elastic scattering of neutrons by α-particles do not allow a sufficiently accurate evaluation of the real part of the forward scattering amplitude. This is the main reason for the erratic behaviour exhibited by the functions $F_1(k, \cot \delta_{\frac{1}{2}}, \eta)$ and $F_1(k, \cot \delta_{\frac{1}{2}}, 0)$ *vs* k^2. As is shown in Fig. 3, the imaginary part of the forward scattering amplitude $\mathrm{Im}\, f(0^\circ) = (k/4\pi)\sigma_T(k)$ is only slightly dependent on $\delta_{\frac{1}{2}}$. Therefore, since $\mathrm{Re}\, f(0^\circ)$ practically depends only on the differential cross-section in the forward direction, the problem arises as to whether the conventional extrapolation at zero degrees of $\sigma(\theta)$ cuts off, or not, small contributions due to D waves (7), which may be important either to interpret the *low* energy polarization experiments or to linearize the behaviour of $k^3 \cot \delta_{\frac{1}{2}}$ as a function of k^2. So long as this point is not elucidated, the reliability of any conclusion concerning the strength of the spin-orbit interaction, derived from the analysis of the data, is in the balance. This is the case in which the theory asks the experiment to give a clear-cut answer and not a mere indication on what the energy and the angular distribution of $\sigma(\theta)$ and $P(\theta)$ may be.

* * *

The Authors are pleased to thank Prof. G. POIANI for several helpful discussions.

(7) As far as the determination of D waves is concerned, there is apparently some misunderstanding in the literature. So far, D waves have been extracted from the data by SEAGRAVE (3) for $k_0 = 0$ and for $k_0 \neq 0$ by D. C. DODDER and J. L. GAMMEL [*Phys. Rev.*, **88**, 520 (1952)], by W. E. KREGER, W. JENTSCHKE and P. C. KRUGER [*Phys. Rev.*, **93**, 837 (1954)], by T. M. PUTNAM, J. E. BROLLEY and L. ROSEN [*Phys. Rev.*, **104**, 1303 (1956)] and by K. W. BROCKMAN [*Phys. Rev.*, **102**, 391 (1956)]. In this connection it has to be stressed that in a single channel reaction there exist four distinct sets of two D phaseshifts ($D_{\frac{3}{2}}$, $D_{\frac{5}{2}}$), which are consistent with the data. This problem has been discussed by E. CLEMENTEL and C. VILLI [*Nuovo Cimento*, **5**, 1343 (1957)] in the particular case of the scattering of positive pions by protons. The same situation occurs obviously for the nucleon-α scattering. The D wave ambiguity is somewhat different from the P wave ambiguity, because two out of the four sets of D phaseshifts are associated with the normal P doublet and the remaining two are associated with the inverted one. Thus, if one rules out the normal P doublet, *there still remain two inverted P doublets each one associated with one set of D phaseshifts*, which are equally good as far as the fit of the data is concerned. Which one of these two sets of P and D waves represents a physical solution is at present unknown. A discrimination between them can be done by taking into account the constraints imposed by the effective range theory. According to this point of view, the energy dependence of the $D_{\frac{3}{2}}$ and $D_{\frac{5}{2}}$ phaseshifts, derived by previous analyses, does not appear to possess those features which should characterize a physical solution. This problem, however, deserves a further examination.

Preliminary Remarks on a Consequence of the Isobar Model of Multiple Meson Production.

H. W. Meier

Deutsche Akademie der Wissenschaften zu Berlin
Kernphysikalisches Institut Zeuthen

(ricevuto il 16 Dicembre 1958)

Recently several authors have published papers ([1-4]) about experimental tests of the different variants of the two-centres-model ([5-9]) for multiple meson production in high energy nucleon-nucleon collisions. In all these papers the determination of the Lorentz factor γ_c of the laboratory system (L-system) with respect to the centre of mass system (CM-system) of the colliding particles is an important object of investigation.

Assuming the emitting centres to be moving parallel to one another in the L-system we get from the Lorentz transformations of the energies of the two centres the relation ([2,3])

$$\gamma_c = \sqrt{\gamma_1 \gamma_2}\,, \tag{1}$$

γ_1, γ_2 being the Lorentz factors of the radiating centres in the L-system.

On the other hand from the energy conservation law in the L-system follows for the isobar model ([4]) that

$$\gamma_c = \frac{1}{2}(\gamma_1 + \gamma_2)\left(1 + \frac{3}{4}\frac{E''}{mc^2}\,n\right). \tag{2}$$

([1]) P. Ciok, T. Coghen, J. Gierula, R. Hołyński, A. Jurak, M. Mięsowicz, T. Saniewska, O. Sranisz and J. Pernegr: *Nuovo Cimento*, **8**, 166 (1958).

([2]) P. Ciok, T. Coghen, J. Gierula, R. Hołyński, A. Jurak, M. Mięsowicz, T. Saniewska and J. Pernegr: *Nuovo Cimento* (in press).

([3]) G. Cocconi: *Phys. Rev.* (in press).

([4]) J. Burmeister, K. Lanius and H. W. Meier: *Nuovo Cimento* (in press).

([5]) S. Takagi: *Progr. Theor. Phys.*, **7**, 123 (1952).

([6]) W. L. Kraushaar and L. J. Marks: *Phys. Rev.*, **93**, 326 (1954).

([7]) H. J. Bhabha: *Proc. Roy. Soc. London*, **219**, 293 (1953).

([8]) Z. Koba: *Progr. Theor. Phys.*, **17**, 288 (1957).

([9]) D. Černavskij: preprint.

In this formula $\overline{E''}$ is the mean value of the energies of the mesons in the rest systems of the radiating centres; n_s is the number of shower particles and m the nucleon mass.

From numerical calculations based on a large number of jets follows that in part the γ_c values computed with (2) are considerably smaller than the values according to (1).

In this paper we make use of the Lorentz transformations without the assumption that the emitting centres are moving parallel to one another in the L-system after the collision. Let γ' be the Lorentz factor of the two centres and ϑ' the angle between the primary direction and the directions of the centres in the CM-system. Then we have

$$\gamma_1 = \gamma_c\gamma' + \sqrt{(\gamma_c^2 - 1)(\gamma'^2 - 1)}\cos\vartheta', \tag{3a}$$

$$\gamma_2 = \gamma_c\gamma' - \sqrt{(\gamma_c^2 - 1)(\gamma'^2 - 1)}\cos\vartheta'. \tag{3b}$$

Subtracting (3b) from (3a) we get for the case $\gamma_c^2 \gg 1$

$$\cos\vartheta' = \frac{\gamma_1 - \gamma_2}{\sqrt{(\gamma_1 + \gamma_2)^2 - 4\gamma_c^2}}. \tag{4}$$

Thus knowing not only γ_1 and γ_2, but also γ_c we can calculate ϑ'. Taking the usual transformation formulae

$$\operatorname{tg}\vartheta_1 = \frac{\sin\vartheta'}{\gamma_c(K + \cos\vartheta')}, \qquad \operatorname{tg}\vartheta_2 = \frac{\sin\vartheta'}{\gamma_c(K - \cos\vartheta')}, \tag{5}$$

where

$$K = \frac{\gamma'}{\gamma_c}\sqrt{\frac{\gamma_c^2 - 1}{\gamma'^2 - 1}}. \tag{6}$$

and

$$\gamma' = \frac{\gamma_1 + \gamma_2}{2\gamma_c}, \tag{7}$$

(we have obtained the last equation by adding the two equations (3)) we get the angles ϑ_1 and ϑ_2 between the primary direction and the directions of the emitting centres in the L-system after the collision. Consequently $\Delta\vartheta = \vartheta_1 + \vartheta_2$ is the angle between the directions of the motion of the emitting centres in the L-system.

There are two difficulties in the determination of $\Delta\vartheta$. The first one is connected with the determination of γ_c. In the following we take for γ_c the values corresponding to relation (2) and study the consequence of the isobar model. The second difficulty is the determination of γ_1 and γ_2. In order to get the exact value of $\Delta\vartheta$, we have to choose the values of γ_1 and γ_2 which have been determined by taking into account the true directions of the two emitting centres in the L-system. However, these directions can be exactly determined only from the angular distribution of all produced (charged and uncharged) particles and by taking into account their momentum distribution. As a first approximation we have taken the geometrical

distribution of the charged particles relative to the primary direction (the « uncorrected » distribution). In second approximation we made use of the two geometrical distributions of the charged particles relative to the geometrical axes of the inner and diffuse cone (the « corrected » distributions). Taking these distributions we have estimated « uncorrected » and « corrected » values of γ_1 and γ_2 and have calculated $\Delta\vartheta$ (rows in the tables, marked « uncorrected » and « corrected », respectively).

We can compare the obtained values of $\Delta\vartheta$ with the values of $\Delta\vartheta_t$ estimated from the target diagram of the charged particles in order to test whether both these quantities are of the same order of magnitude or not.

In Table I are given the results of the jet Be 2 ([10]). In order to estimate the influence of different subdivisions of the inner and diffuse shower particles on the data we have studied three possible subdivisions $n_1/n_2 = 7/9$, 8/8 and 9/7 (n_1, n_2 number of shower particles of the inner and diffuse cone, respectively). The values γ_c have been computed with formula (2). The meaning of the other quantities follows from the above mentioned.

TABLE I. – *Data for the jet* Be 2.

n_1/n_2		γ_1	γ_2	γ_c	ϑ_1	ϑ_2	$\Delta\vartheta$	$\Delta\vartheta_t$
7/9	uncorrected	470	12.0	40	12′	7° 7′	7° 19′	7° 16′
	corrected	390	6.5	36	8′	7° 32′	7° 40′	
8/8	uncorrected	390	8.9	39	10′	7° 29′	7° 39′	8° 17′
	corrected	430	6.4	40	7′	7° 33′	7° 40′	
9/7	uncorrected	320	6.6	37	8′	7° 35′	7° 43′	9° 21′
	corrected	330	6.9	37	9′	7° 35′	7° 44′	

The Table II shows the results of the jet Pr 27 (*).

TABLE II. – *Data for the jet* Pr 27.

n_1/n_2		γ_1	γ_2	γ_c	ϑ_1	ϑ_2	$\Delta\vartheta$	$\Delta\vartheta_t$
9/8	uncorrected	148	12.6	26	32′	6° 23′	6° 55′	6° 58′
	corrected	151	6.4	25	16′	6° 41′	6° 57′	

*) The author thanks Dr. J. PERNEGR, Prague, for kindly sending him the angular distribution of this jet.

([10]) G. BOZOKI, G. DOMOKOS, E. FENYVES, E. GOMBOSI, K. LANIUS and H. W. MEIER: *Intern. Conf. on Mesons and Recently Discovered Particles* (Padova-Venezia, 1957).

It can be seen that the values $\Delta\vartheta$ calculated from the Lorentz transformations (3) and the γ_c formula (2) are in good agreement with the values $\Delta\vartheta_t$ corresponding to the target diagram. Furthermore, it may be seen that there is no important difference between the data from the « uncorrected » and the « corrected » distributions.

The separation of the two cones consequently leads to a geometrical effect: in the target diagram the distributions of the inner and diffuse shower particles will not be circular but elliptic. However an estimate of the ratio A/a of the large axis to the small axis of the ellipse of one cone shows that this pure geometrical effect will be dominated in most cases by the fluctuations in the angular distributions of the shower particles. An appreciable effect is expected at relatively large cone angles only. For instance, if $\vartheta_2 = 20°$ and the cone angle α of the diffuse cone is equal $60°$ we have a ratio $A/a = 1.8$ which, however, increases very quickly for increasing values of α.

* * *

The author is greatly indebted to Prof. M. Mięsowicz, Dr. J. Gierula, Dr. J. Pernegr and their co-workers, to Dr. D. Černavskij and Dr. K. Lanius for valuable discussions.

IL NUOVO CIMENTO Vol. XI, N. 2 16 Gennaio 1959

Operation at 1000 MeV of the Frascati Electronsynchrotron.

A. Alberigi, F. Amman, C. Bernardini, U. Bizzarri, G. Bologna, G. Corazza, G. Diambrini, G. Ghigo, A. Massarotti, G. P. Murtas, M. Puglisi, I. F. Quercia, R. Querzoli, G. Sacerdoti, G. Salvini, G. Sanna, P. G. Sona (*), R. Toschi and A. Turrin

Laboratori di Frascati

M. Ageno

Istituto Superiore di Sanità - Roma

E. Persico

Istituto di Fisica dell'Università - Roma

(ricevuto il 18 Febbraio 1959)

The Frascati ElectronSynchrotron has been operated at 1000 MeV on February 9th, 1959 [1].

The following data summarize the main characteristics of the machine.

— Maximum Energy (reached on February 9th): 1000 MeV.

— Maximum Energy that should be possible with the present magnet: 1200 MeV.

— Repetition rate: 20 pulses/s.

— Magnet structure: weak focusing; « C » sections opened outside.

— Peak magnetic field for 1000 MeV; 9260 gauss.

— Injector: Van de Graaff, of 2.5 MeV kinetic energy.

— Radio frequency system: a first frequency modulated cavity; a second high voltage constant frequency cavity. Both cavities are amplifier driven. Maximum voltage of the second cavity: 70 kV.

The excitation of the magnet is independent from the main supply line. Currents were strongly stabilized in amplitude and frequency (1 ‰).

The donut was built in araldite hardened with quartz, with an internal lining of thin stainless steel strips. Therefore the donut can be easily machined, and targets and electrodes can be put practically in any place. A vacuum of 10^{-6} mm Hg has been achieved.

Each part of the machine has been designed in a conservative way, and carefully tested before final assembly.

A top view of the machine is seen in Fig. 1; a cross section of the magnet and donut it given in Fig. 2.

Beam searching started in the first

(*) At present at the Laboratory CISE, Milano.

(1) Frascati group, Atti del Congresso di Palermo della Società Italiana di Fisica, Settembre 1958, in publication.

days of December and we reached 300 MeV using only the first cavity in this stage of operation.

The beam reached the maximum energy as soon as the second cavity was turned on. At present there is no phase correlation between the two cavities.

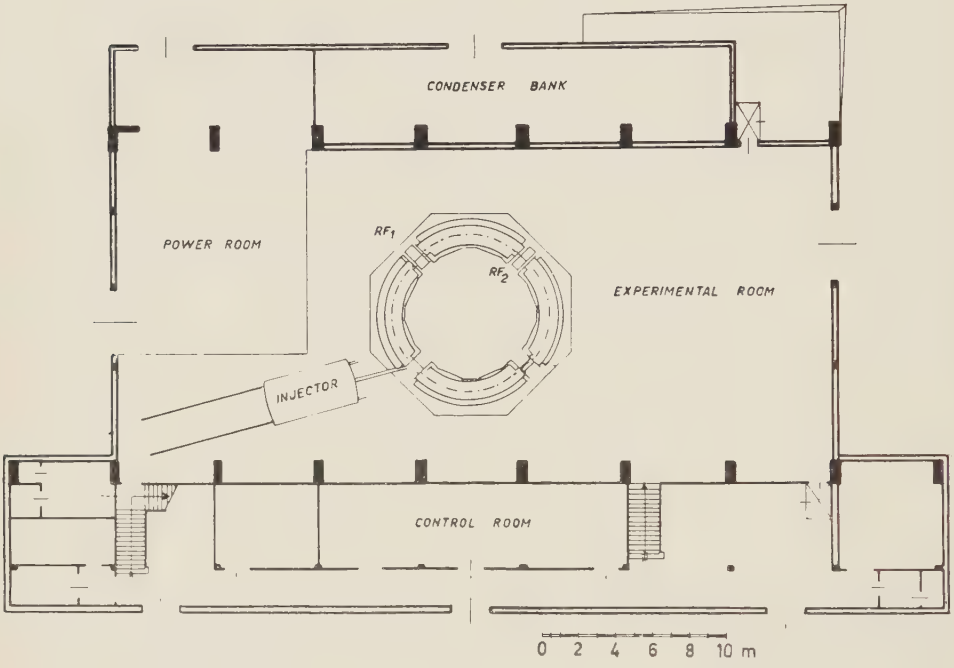

Fig. 1. - Top view of the electronsynchrotron and the experimental room.

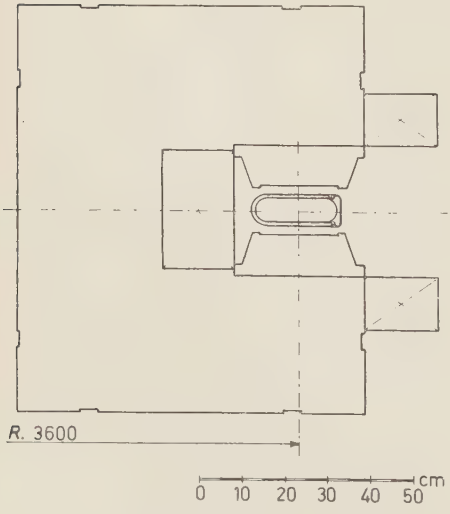

Fig. 2. – Radial section of the magnet.

The Bremsstrahlung is obtained by collision against a fixed target. A γ-ray pulse of about 1 ms duration is obtained by a suitable amplitude modulation of the second cavity at the end of the acceleration cycle. The maximum energy was estimated measuring the magnetic field at which the electrons hit the target.

The injected current is at present 3 mA for 1 μs. Preliminary measurements of γ-ray beam intensity, made with a Wilson type quantameter, give a maximum output of $8 \cdot 10^{10}$ equivalent quanta per minute and an average output of $6 \cdot 10^{10}$ Q/min.

Observation of the γ output versus the injected pulse length seems to indicate that the first cavity captures at least three turns of the injected electrons.

LIBRI RICEVUTI E RECENSIONI

G. J. DIENES and G. H. VINEYARD – *Radiation Effects in Solids*. Interscience Publishers, New York-London, 1957; pag. VIII+226.

Lo studio delle interazioni tra le radiazioni e la materia è oggi di grande attualità e ha dato origine, con i suoi molteplici aspetti a molti diversi rami di ricerca. Questo libro tratta, come gli Autori precisano nella prefazione, degli aspetti fisici delle azioni delle radiazioni sui solidi e si occupa principalmente delle sostanze inorganiche e delle radiazioni di alta energia. Si noti che vengono così lasciati da parte sia i fenomeni di carattere prevalentemente chimico, sia gli effetti di radiazioni di relativamente bassa energia, già da lungo tempo studiati, come la luminescenza.

La limitazione degli argomenti trattati appare logica e naturale quando si prenda in considerazione la natura delle interazioni studiate: sono qui esclusi i fenomeni legati alla eccitazione elettronica ed alla ionizzazione, per mettere in evidenza piuttosto le conseguenze dello spostamento di atomi dal loro posto nel reticolo. A questo fenomeno, che può essere prodotto da radiazioni di varia natura, purchè di sufficiente energia, possono essere connesse nella grande maggioranza dei casi, le modificazioni di proprietà osservate nei solidi cristallini irradiati. Tali modificazioni infatti possono essere attribuite alla formazione di difetti reticolari, ed alla loro interazione con i difetti preesistenti; allo stato attuale della teoria molti effetti vengono spiegati considerando come effetto primario della irradiazione, oltre alla ionizzazione, lo spostamento di atomi che vengono portati in posizioni interstiziali lasciando dietro di sè una « vacanza » (difetti di Frenkel). Si noti tuttavia che la teoria semplificata non basta a spiegare tutti i fenomeni osservati, per cui accanto alla formazione delle coppie vacanza-interstiziale ed a fenomeni successivi prodotti da tali difetti (annichilazione, aggregazione, blocco di dislocazioni, ecc.) sembra necessario ammettere in alcuni casi l'intervento di altri tipi di perturbazione dell'ordine reticolare (thermal spikes, displacement spikes, ecc.). È comunque chiaro che i problemi connessi con la formazione dei difetti nei solidi cristallini irradiati, con il loro effetto sulle proprietà osservabili e con la loro sparizione in opportune condizioni (per esempio in conseguenza della ricottura) presentano interesse grandissimo, sia scientifico che applicativo e che in un prossimo futuro questo campo sarà ampiamente studiato sia dai Fisici che dagli Ingegneri.

Dei due principali punti di vista su questi problemi, quello che mette in evidenza le modificazioni delle proprietà dei materiali irradiati ai fini delle applicazioni (e si basa quindi in molti casi su esperienze eseguite nel reattore in normali condizioni di lavoro) e quello che delle modificazioni di proprietà si serve piuttosto come di indici per indagare sulla struttura dei cristalli, gli Autori preferiscono il secondo. DIENES e VINEYARD, noti entrambi per importanti contributi nel campo degli effetti della irradiazione, si propongono di offrire in questo volume un quadro degli aspetti scientifici dell'argomento, illustrando le principali teorie con riferimenti critici ai risultati sperimentali

ottenuti in condizioni particolarmente semplici e controllate; di altri fenomeni, di natura più complessa ed osservati in condizioni meno esattamente definite, essi fanno cenno soltanto quando ciò appare indispensabile per la completezza.

L'esposizione chiara ed equilibrata sembra particolarmente adatta per chi voglia farsi un'idea dei fatti e delle interpretazioni, senza i più complessi dettagli della teoria e senza l'enorme massa dei risultati, spesso contrastanti che potrebbero, gli uni con gli altri, offuscare la limpidezza di una visione d'insieme. Gli Autori hanno saputo trovare un felice compromesso tra i due estremi, hanno saputo impegnarsi ove appariva opportuno, con interpretazioni e valutazioni personali e con dati numerici approssimati, senza mai perdere di vista però il rigore logico della linea fondamentale di pensiero. Il lettore si sente così guidato con sicurezza attraverso la complessità dell'argomento e non perde mai di vista quali siano i limiti di validità delle teorie e le approssimazioni raggiunte dalle esperienze.

Viene esaminata dapprima la formazione dei difetti nelle sue interpretazioni teoriche e subito dopo sono descritti gli esperimenti fondamentali che permettono di valutare l'energia di soglia necessaria per produrre uno spostamento e il numero dei difetti elementari introdotti in un cristallo, in varie condizioni.

L'influenza dei difetti sulle proprietà fisiche dei solidi è poi presa in considerazione nel quarto capitolo mentre il quinto è riservato ai fenomeni di « annealing » cioè alla sparizione e all'assestamento dei difetti che può dar luogo al ripristino più o meno completo delle condizioni originali, alla liberazione della energia accumulata ecc.

Finalmente, tra gli « argomenti speciali » dell'ultimo capitolo, troviamo la « crescita » dell'uranio per effetto di irradiazione, le modificazioni di fase prodotte in alcuni sistemi dalla stessa causa, la precipitazione da soluzioni solide, e gli effetti chimici: tutti questi soggetti sono elencati a parte, probabilmente perchè, per la complessità dei fenomeni, non appaiono agli Autori i più adatti a fornire informazioni sui difetti originariamente prodotti dalla irradiazione. In questi casi tuttavia, a detta degli Autori stessi, l'irradiazione promette di essere un potente strumento per le ricerche future.

Le alterazioni delle proprietà meccaniche sono trattate piuttosto brevemente e meriterebbero forse maggiore attenzione, specialmente se si tiene conto che Dienes è l'autore di una teoria di vasto respiro, proprio su questo argomento, di cui ancora si attende la conferma sperimentale.

Il volume, arricchito da ampia bibliografia, si presenta come un ottimo testo per scopi didattici e di informazione generale, adatto specialmente per fornire un sicuro punto di partenza per chi intenda proseguire lo studio; le teorie nella loro completezza ed i risultati sperimentali nel loro dettaglio, potranno poi essere cercati risalendo alle fonti originali o agli ampi lavori di rassegna che non mancano in questo campo.

F. A. Levi

C. Kittel – *Elementary Statistical Physics*, John Wiley and Sons, Inc., New York, 1958; 228 pagine, $ 8.

Esistono già dei buoni libri di meccanica statistica, ma mancava finora quello che veramente serve ai giovani fisici e cioè un libro dove fossero spiegati tanti aspetti della fisica più autentica, che vanno inquadrati su una base statistica.

Questo libro realizza in pieno questo scopo con una scelta di argomenti vastissima: dai più noti esempi del gas di perfetto di Fermi e di Bose, fino ai più recenti aspetti delle temperature negative, l'uso delle calcolatrici elettroniche

nei problemi di dinamica molecolare, le collisioni di particelle ad *alt*issime energie con il metodo di Fermi e così via. Gran parte del libro è devoluta ai processi irreversibili, basata ampiamente sulla teoria delle fluttuazioni e dei processi statistici, e non come una semplice esposizione delle relazioni fenomenologiche di Onsager. Tanto i problemi dell'equilibrio che i problemi fuori dell'equilibrio vengono poi trattati con un notevole uso di esercizi, e con uno stimolante ed elegante riferimento alla bibliografia essenziale. Non ci rimane che augurarci che questo ottimo libro venga presto tradotto in italiano per più arricchire il nostro patrimonio scolastico.

G. Careri

A. P. French – *Principles of Modern Physics.* John Wiley & Sons Inc. New York (1958), pp. IX + 355, $ 6.75.

Nel campo della editoria scientifica esistono oggi numerose opere che si propongono di esporre in modo semplice i più importanti fatti sperimentali studiati dai fisici negli ultimi sessanta anni, e la loro interpretazione teorica.

Il libro del Prof. French si aggiunge a questa schiera caratterizzandosi per una esposizione accurata e chiara, ricca di disegni efficacemente illustrativi. Anche i principali dispositivi sperimentali sono descritti schematicamente, e inoltre numerosi esempi e dati numerici risultano assai utili al lettore.

Alcuni importanti problemi che richiedono una trattazione matematica, non indispensabile in una prima lettura, sono trattati in appendice.

Nel trattare ciascun argomento l'autore si è preoccupato di non dimenticare la strada storicamente seguita dai fisici per giungere allo stato attuale delle nostre conoscenze. Questa caratteristica, unita alla breve ma essenziale bibliografia che correda questo volume, ne rende consigliabile la lettura non solo ai giovani che per la prima volta si avvicinano a questi argomenti, ma anche a chi voglia rapidamente richiamare nozioni studiate da tempo e purtroppo non sempre ricordate.

A. Alberigi

J. Koch, R. H. V. Dawton, M. L. Smith and W. Walcher – *Electromagnetic isotope Separators and Applications of Electromagnetically Enriched Isotopes.* North Holland Publishing Co., Amsterdam, 1958, pp. 314, 26.50 fiorini olandesi.

Questo libro è relativo ad un argomento assai particolare, ma riempie in modo egregio la mancanza di notizie che si aveva in questo campo. Tutti sapevano del grande separatore Colutron, uno di spettrometro di massa di dimensioni eccezionali che fu approntato durante la guerra a Berkeley per produrre piccole quantità di uranio 235 puro. Ma ben pochi ne conoscevano i dettagli costruttivi perchè la materia era rigorosamente soggetta a segreto. Ora questo libro raccoglie l'esperienza che si è raggiunta in questi ultimi anni con questi particolari spettrometri, tanto in relazione ai loro problemi costruttivi che alle applicazioni nelle ricerche di fisica nucleare.

Il libro è diviso in tre parti. La prima tratta dei separatori di piccola e media grandezza, quali si possono facilmente installare vicino ad una pila per studiare le proprietà dei singoli prodotti di fissione. La seconda parte tratta invece dei grandi separatori elettromagnetici in quanto tali, e dell'esperienza che si è guadagnata ultimamente nella separazione di isotopi particolarmente importanti. Infine la terza parte è un trattamento generale dei problemi fisici connessi con questa spettrometria di massa a correnti forti, con una esauriente

discussione delle difficoltà derivanti dalla carica spaziale, dalle aberrazioni ecc. Ne risulta un insieme armonico, e di autentico valore scientifico.

G. Careri

J. Kistemaker, J. Bigeleisen and A. O. C. Nier, Editors – *Proceedings of the International Symposium on Isotope Separation*, North Holland Publ. Co., Amsterdam (1958), pp. 704, 55 fiorini olandesi.

Si tratta dei rendiconti del I Congresso Internazionale su questo argomento, che si è tenuto ad Amsterdam nell'Aprile del 1957. Gli isotopi di cui si discute sono quelli stabili, e nell'insieme l'argomento è più che altro una chimico-fisica applicata, divenuta oggi importante per la necessità di produrre su base quasi industriale il deuterio e l'uranio 235.

Tra i 63 lavori presentati, solo pochi hanno un carattere generale ed introduttivo, per cui il libro è di molto valore specialmente per gli specialisti. In particolare notiamo che accanto ad aspetti classici del problema (ingegneria chimica di tipo tradizionale, calcolo delle disposizioni più adatte degli elementi per i processi di distillazione, scambio chimico e diffusione), si trovano per la prima volta trattati per esteso i processi di separazione per elettromigrazione, per via elettromagnetica e per ultracentrifugazioni. Questa ci sembra la novità di questa raccolta, che perciò raccomandiamo alle biblioteche di fisica e di ingegneria.

G. Careri

Direttore responsabile: G. POLVANI Tipografia Compositori - Bologna

Questo fascicolo è stato licenziato dai torchi il 24-II-1959